0008-7114

Caryologia

2020
Vol. 73 - n. 1

International Journal of Cytology, Cytosystematics and Cytogenetics

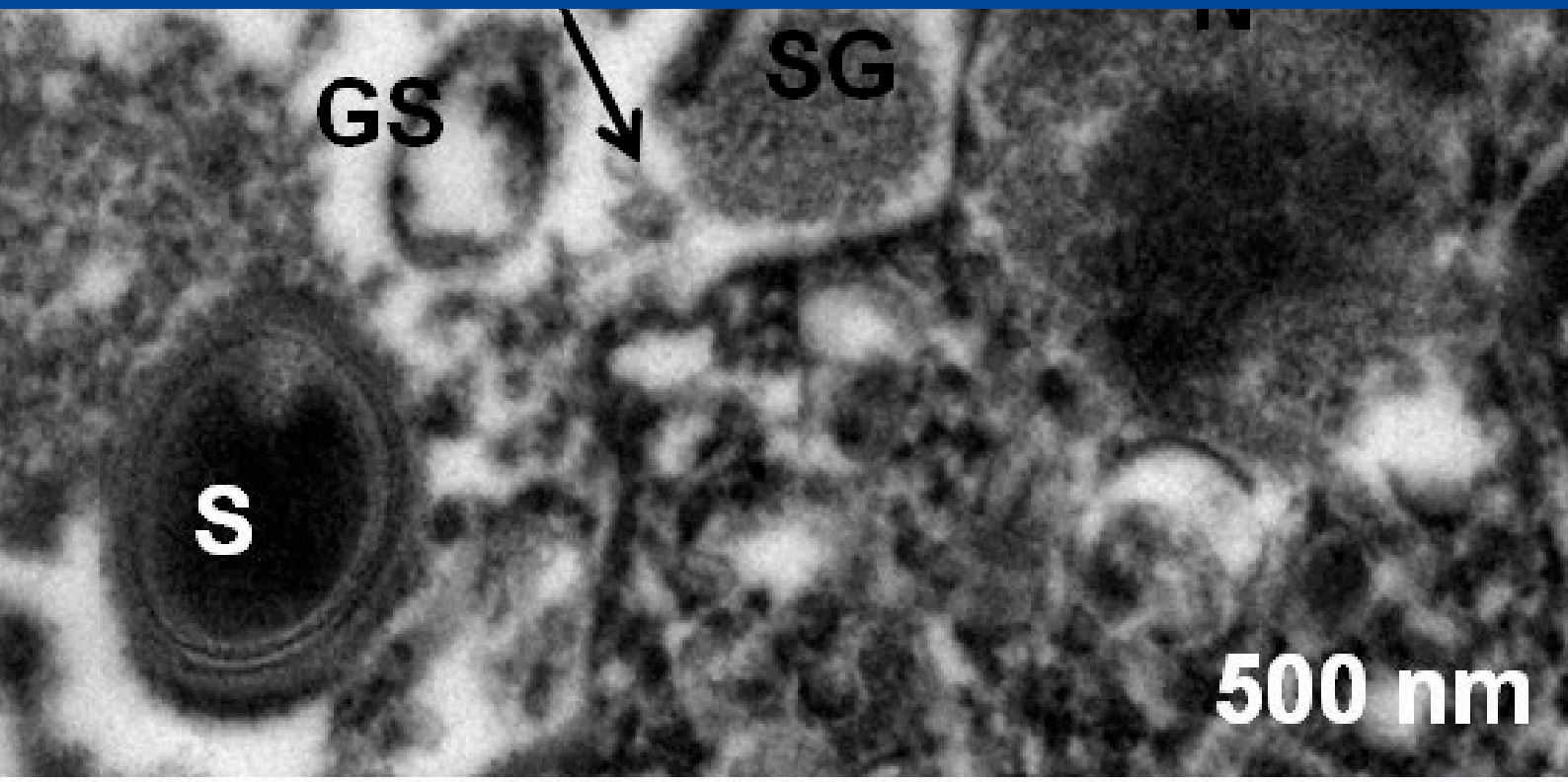

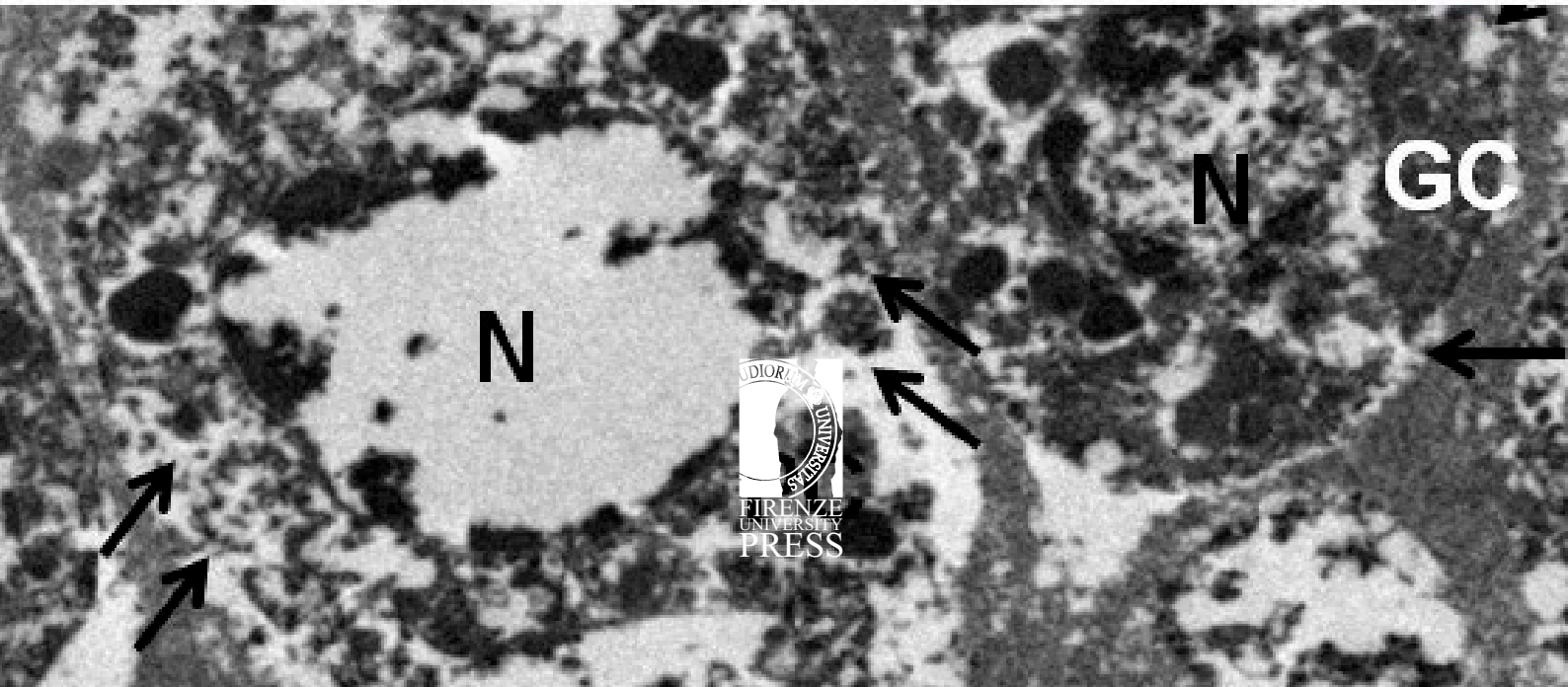

FIRENZE UNIVERSITY PRESS

Caryologia. International Journal of Cytology, Cytosystematics and Cytogenetics
Caryologia is devoted to the publication of original papers, and occasionally of reviews, about plant, animal and human karyological, cytological, cytogenetic, embryological and ultrastructural studies. Articles about the structure, the organization and the biological events relating to DNA and chromatin organization in eukaryotic cells are considered. *Caryologia* has a strong tradition in plant and animal cytosystematics and in cytotoxicology. Bioinformatics articles may be considered, but only if they have an emphasis on the relationship between the nucleus and cytoplasm and/or the structural organization of the eukaryotic cell.

Cover: figure from the article inside by Shambhavi et al. "Phagocytic events, associated lipid peroxidation and peroxidase activity in hemocytes of silkworm Bombyx mori induced by microsporidian infection". Electron microscope observations of silkworm hemocytes after microsporidian infection at the nucleus level.

Caryologia

International Journal of Cytology, Cytosystematics and Cytogenetics

Volume 73, Issue 1 - 2020

Firenze University Press

***Caryologia*. International Journal of Cytology, Cytosystematics and Cytogenetics**

Published by
Firenze University Press – University of Florence, Italy
Via Cittadella, 7 - 50144 Florence - Italy
http://www.fupress.com/caryologia

Caryologia
International Journal of Cytology, Cytosystematics and Cytogenetics

Firenze University Press
www.fupress.com/caryologia

OPEN ACCESS

Citation: S. Sadeghian, A. Hatami, M. Riasat (2020) Karyotypic investigation concerning five *Bromus* Species from several populations in Iran. *Caryologia* 73(1): 3-10. doi: 10.13128/caryologia-863

Received: April, 2019

Accepted: February, 2020

Published: May 8, 2020

Data Availability Statement: All relevant data are within the paper and its Supporting Information files.

Competing Interests: The Author(s) declare(s) no conflict of interest.

Karyotypic investigation concerning five *Bromus* Species from several populations in Iran

Sara Sadeghian, Ahmad Hatami, Mehrnaz Riasat

Research Division of Natural Resources Department, Fars Agricultural and Natural Resources Research and Education Center, AREEO, Shiraz, Iran
*Corresponding author: s.sadeghian@areeo.ac.ir

Abstract. Karyotypes of five taxa (fourteen populations) of the genus *Bromus* from different geographic origins is presented: *B. scoparius, B. japonicus*, *B. madritensis*, *B. rubens* and *B. tomentellus*. The ploidy levels were different. *B. scoparius* and *B. japonicus* were found 2n=2x=14, *B. madritensis* and *B. rubens* were found 2n=4x=28 and *B. tomentellus* were found 2n=6x=42. Detailed karyotype analysis allows us to group the different populations and to postulate relationships among them.

Keywords. *Bromus*, Chromosome, Karyology, Iran.

INTRODUCTION

The genus *Bromus* L. belongs tribe *Bromeae* and Poaceae family. The taxon includes about 160 annual and perennial species (Acedo and Liamas, 2001) distributed all over the world. *Bromus* species are distributed in temperate regions and are always exist with rangeland species (Verloove, 2012). It is an important rangeland plant species in Iran, which are placed in 6 sections; *Bromus*, *Genea*, *Nevskiella*, *Neobromus*, *Ceratochla* and *Pnigma* (Bor, 1970) (Table 1). The Genea section is the widest section of the *Bromus* genus in terms of geographic distribution (sales, 1994).

Bromus species are known as the species with various intra-specific ploidy levels and form different ecotypes with various characteristics. Hill (1965) recorded up to 112 chromosomes for *B. erectus*. Devesa *et al.* (1990) indicates the importance of cytological studies for understanding the evolution of the genus *Bromus*. Naganowas ka (1993) used genetic distances estimated based on centromeric index and total chromosome length to investigate interrelationships of several species of *Bromus*. Yang and Dunn (1997) recorded various levels of polyploidy in *B. inermis* Leyss. Martinello and Schifino-Wittmann (2003) studied 14 accessions of *Bromus auleticus*. Their accessions were all hexaploid and the high symmetry and homogeneity of the karyotypes made it difficult to detect possible intraspecific differences.

Massa *et al.* (2004) proposed a taxonomic treatment within *Bromus* sect. *Ceratochloa* of South America. Their plant materials included 28 hexaploid

(2n=6x=42) populations and 2 octaploid (2n=8x=56) populations. Oja and Laarmann (2002) also recorded different ploidy levels within species of *Bromus* (2n=14, 28, 42 and 56). Sheidai and Fadaei (2005) studied ten populations of six *Bromus* species and the species possess karyotypes varying from 2n = 2x = 14 (diploid) to 2n = 4x = 28 (tetraploid).

Mirzaie-Nodoushan *et al*. (2006a) investigated karyotypic of some *Bromus* species in Iran and indicated that populations of the species were differed in their karyotypic characteristics and ploidy levels of the populations were varied from 2n=14 to 2n=84. Mirzaie-Nodoushan *et al*. (2006b) also reported evolutionary karyotypic variation in *B. tomentellus* populations in Iran and confirmed the existence of high levels of ploidy as well as existence of dodecaploid karyotypes in the species. Sadeghian and *et al*. (2010) studied nine populations of three *Bromus* species (*B. danthoniae*, *B. sterilis* and *B. tectorum*) and reported that all species were diploid with 2n=2x=14. Artico *et al*. (2017) also reported that the chromosomal number of *B. Linnaeus* was 2n = 6x = 42.

Since the karyological information is the basic requirement of a breeding program, in this study, 14 populations of *Bromus* were surveyed for the karyological data as a part of an ongoing work on the populations.

Cytogenetic studies play an important role in determining the relationship between species especially wild and native plants and as a first step in the analysis of the phylogeny and evolution of species is relative. Considering that the species studied in different climates of southwest Iran and Fars province are abundant they are considered as the main vegetation cover of these areas. Therefore, to investigate the relationship between species, these species have been used in this study.

MATERIALS AND METHODS

Fourteen populations of five *Bromus* species: *B. tomentellus* (three populations) belong to *Pnigma* section, *B. madritensis* (two populations) and *B. rubens* (three populations) belong to *Genea* section and *B. scoparius* (three population) and *B. japonicus* (three population) belong to *Bromus* section were studied (Table 1). Voucher specimens were deposited in the Herbarium of Fars Research and Education Center for Agriculture and Natural Resources and in gene bank RIFR (Research Institute of Forest and Rangelands) of Iran.

Root tip meristems from seedling obtained by the germination of ripe seeds collected from natural populations (14 populations, representing 5 species) on wet filter paper in Petri dishes and left at 22°C temperature. When they reached 1-1.5 cm in length, rootlets were collected. The material was pretreated in %0.5 saturated α-Bromo naphthalene at 4°C for 4 h, fixed in %10 formaldehyde and chromium trioxide (1:1 volume ratio) for 16 to 20 h at 4°C. Then, the roots tips were rinsed for 3 h in distilled water. Hydrolysis was carried out with NaOH (1 Normal) at 60°C for 20-30 min (Sadeghian *et al*. 2010)) and used hematoxylin-iron for chromosome staining for 1-2 h. Squashed in a droplet of %45 acetic acid and lactic acid (10:1) (Wittmann 1965). At least, five well-spread metaphase plates from different individuals were analyzed per population. The best metaphasical

Table 1. The origin of materials used in chromosome studies of *Bromus*.

Species (population)	Section	Origin	Altitude	Herbarium code
B. japonicus (16462)	*Bromus*	Golestan, Maraveh tapeh, station	430 m	16462
B. japonicus (16525)	*Bromus*	Golestan, Gomayshan, seidabad	-15 m	16525
B. japonicus (16587)	*Bromus*	Golestan, Tooskasetan	1216 m	16587
B. madritensis (3668)	*Genea*	Fars, Shiraz, Dasht-e Arjan	2000 m	3668
B. madritensis (Arjan)	*Genea*	Fars, Shiraz rosd of Dasht-e Arjan to Tang- e Abolhayat, about Kandee village	1300 m	-
B. rubens (15169)	*Genea*	Fars, Kazeroon, kotal dokhtar	1400 m	15169
B. rubens (15317)	*Genea*	Fars, Fasa, Mianjangal	1750 m	15317
B. rubens (2125)	*Genea*	Fars, Kazeroon	530 m	2125
B. scoparius (5983)	*Bromus*	Gilan, Talesh, subatan yelagh	1800 m	5983
B. scoparius (5984)	*Bromus*	Gilan, Talesh, khotbesara, lapehkara	1800 m	5984
B. scoparius (5985)	*Bromus*	Gilan, Masal	1900 m	5985
B. tomentellus (Bavanat)	*Pnigma*	Fars, Bavanat, Simakan, Lakposhti range	2300 m	-
B. tomentellus (Simakan)	*Pnigma*	Fars, Simakan, Lakposhti range	2350 m	-
B. tomentellus (Eghlid)	*Pnigma*	Fars, Eghlid, Dozkord, Pasahlaki	2200 m	-

plates were selected and measured by Micromeasure 3.3 software (Reeves *et al*. 2000). In each mitotic metaphase (at least 5 plates) the arm's length of each chromosome was measured.

The following parameters were estimated in each metaphase plate to characterize the karyotypes numerically: long arm (LA), short arm (SA), total length (TL), relative length percentage (RL %), arm ratio (AR), centromeric index (CI) (Huziwara, 1962), value of relative chromatin (VRC). Karyotype asymmetry was estimated by three different methods namely, total form percentage (TF %) (Huziwara, 1962); difference of relative length (DRL), intra-chromosomal asymmetry index (A_1) and inter-chromosomal asymmetry index (A_2). Both indices (A_1 and A_2) (Romero Zarco, 1986) were independent to chromosome number and size. Also karyotypic evolution has been determined using the symmetry classes of Stebbins (SC) (Stebbins, 1971). Karyotype formula was determined by chromosome morphology based on centromere position according to classification of Levan (Levan *et al*. 1964). For each population, karyograms were drawn based on length of chromosome size (arranged large to small).

In order to determine the variation between populations, one-way unbalanced ANOVA was performed on normal data and parameter means were compared by Duncan's test. The principal components analysis (PCA) was performed to evaluate the contribution of each karyotypic parameter to the ordination of species. Clustering was performed using the unweighted pair group method with arithmetic (UPGMA) after calculation of Cophenetic correlation coefficient (r) to examine karyotype similarity among populations. Numerical analysis was performed using SAS ver. 6.12 (1996), JMP ver. 3.1.2 (1995) and StatistiXL ver. 1.7 (2007) softwares.

RESULTS

There was no different among basis chromosome number of the species (x=7). The somatic chromosome numbers (2n), karyotype formula and parameters for the studied species are summarized in Table 2. Two species as *B. scoparius* and *B. japonicus* were diploid, two species as *B. madritensis* and *B. rubens* were tetraploid and one species as *B. tomentellus* was hexaploid.

The studied species included metacentric (m) and sub-metacentric (sm) chromosomes regarding the chromosomal types (Table 2). Satellites were observed in one chromosomes pair in *B. scoparius* and *B. japonicus* and two chromosomes pairs in *B. madritensis* and *B. rubens* and for *B. tomentellus* species which has three chromosomes pairs having satellites (Fig 1). According to the Stebbin's bilateral table, populations of *B. rubens* (15317) included the highest value regarding the intra-chromosomal asymmetry index (0.288) and was classified as group 1B and population of *B. japonicus* (16462) included the lowest value regarding the intra-chromosomal asymmetry index (0.180) and was classified as group 1A.

The results of analysis of variance indicated that there was a significant difference (P≤1%) between the populations in terms of chromosomal traits (TL, LA,

Table 2. Karyotypic characters of different *Bromus* taxa and population.

Taxon (population)	2n	A1	A2	%TF	DRL	VRC	SC	K.F.
B. japonicus (16462(	2x=14	0.180	0.129	45.174	5.369	9.605	1A	12m+2sm
B. japonicus (16525(	2x=14	0.197	0.145	44.700	6.131	8.704	1A	14m
B. japonicus (16587)	2x=14	0.250	0.144	42.950	6.193	8.249	1A	14m
B. madritensis (3668)	4x=28	0.206	0.213	43.022	4.353	5.358	1A	28m
B. madritensis (Arjan)	4x=28	0.238	0.199	41.988	4.757	5.329	1A	28m
B. rubens (15169)	4x=28	0.252	0.241	41.486	5.583	6.114	1B	28m
B. rubens (15317)	4x=28	0.288	0.256	38.797	5.332	6.013	1B	28m
B. rubens (2125)	4x=28	0.257	0.230	39.904	5.389	6.390	1B	24m+4sm
B. scoparius (5983)	2x=14	0.233	0.116	42.493	4.722	8.166	1A	14m
B. scoparius (5984)	2x=14	0.227	0.124	42.113	5.722	7.929	1A	12m+2sm
B. scoparius (5985)	2x=14	0.214	0.126	44.062	5.479	6.866	1A	14m
B. tomentellus (Bavanat)	6x=42	0.215	0.110	42.523	1.698	6.271	1A	38m+4sm
B. tomentellus (Simakan)	6x=42	0.204	0.122	44.354	2.278	6.894	1A	42m
B. tomentellus (Eghlid)	6x=42	0.225	0.140	41.278	2.146	6.878	1A	42m

2n: Diploid chromosome numbers A_1: intrachromosome asymmetry index, A_2: interchromosome asymmetry index, TF%: total form percentage, DRL: difference of relative length, VRC: value of relative chromatin, symmetry classes (SC) of Stebbins and karyotype formula (K.F.).

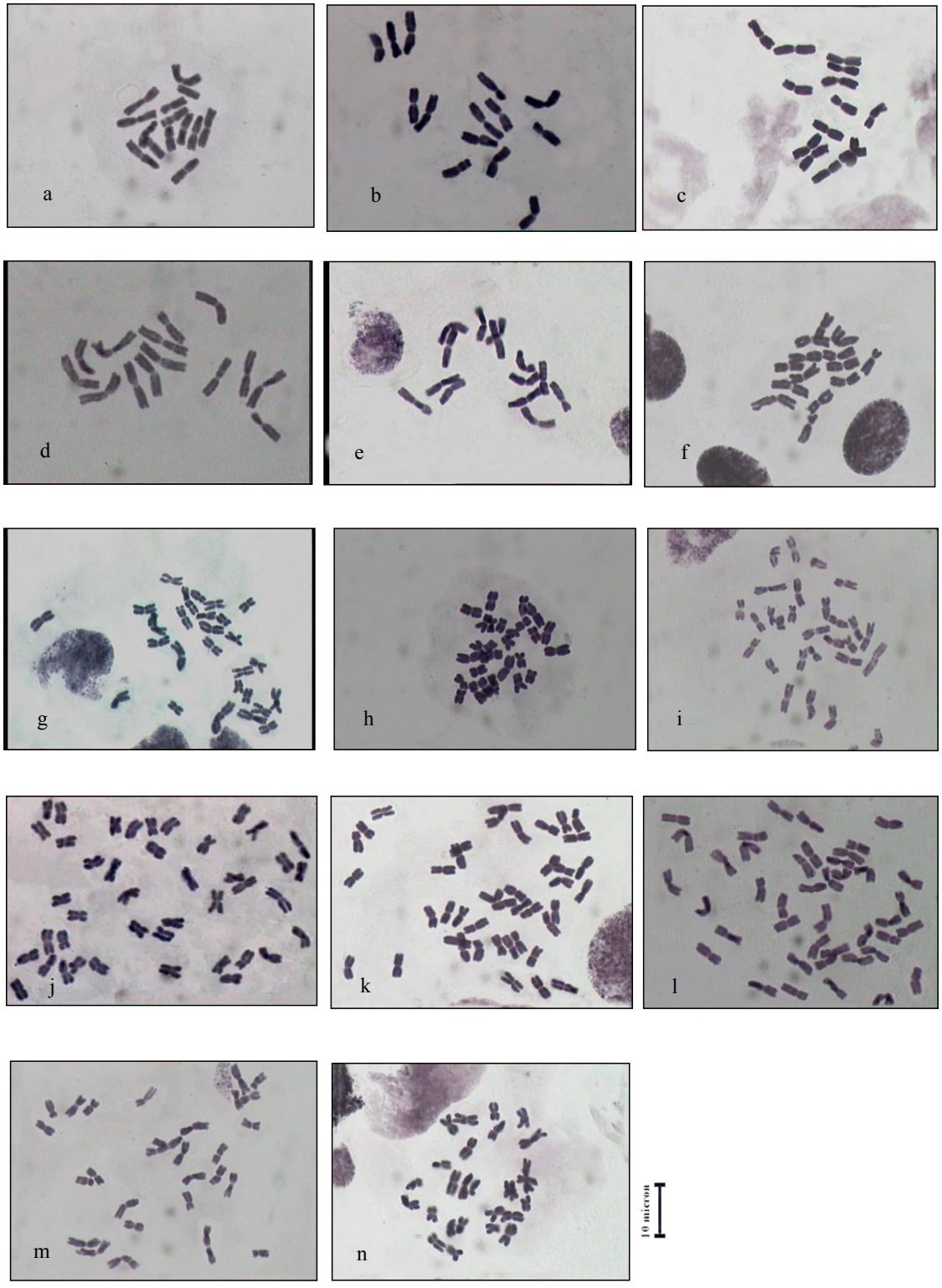

Figure 1. Representative mitotic plates of *Bromus* – (a) *B. scoparius* (5983), 2n=2x=14, (b) *B. scoparius* (5984), 2n=2x=14, (c) *B. scoparius* (5985) 2n=2x=14, (d) *B. japonicus* (16462), 2n=2x=14, (e) *B. japonicus* (16525), 2n=2x=14, (f) *B. japonicus* (16587), 2n=2x=14, (g) *B. rubens* (15169), 2n-4x=28, (h*) b. rubens* (15317), 2n=4x=28, (i) *B. rubens* (2125), 2n=4x=28, (j) *B. tomentellus* (Bavanat), 2n=6x=42, (k) *B. tomentellus* (Simakan), 2n=6x=42, (l) *B. tomentellus* (Eghlid), 2n=6x=42, (m) *B. madritensis* (3668). 2n=4x=28, (n) *B. madritensis* (Arjan), 2n=4x=28.

SA) which revealed large variations among the germplasms in regard to studied traits. Symmetry type of Stebbins (1971) and asymmetry indices of Romero-Zarco (1986) are given in Table 2.

Difference in the relative length percentage (DRL) of the highest and the smallest chromosomes varied from 6.19 in *B. japonicus* (16587) to 1.69 in *B. tomentellus* (Bavanat). According to Table 2, *B. rubens* (15317) was placed in 1B and had the highest values of intra- chromosomal asymmetry index. Similarly, high DRL value leads to more changes in the construction of chromosomes. It had the lowest TF%. The TF% and A_1 values had inverse ratio (Table 2).

The mean value of chromosome's long arm was varied from 5.27 in *B. japonicus* (16462) to 2.92 in *B. madritensis* (3668). Averages of chromosome's short arm were different from 2.24 in *B. madritensis* (Arjan) to 4.34 in *B. japonicus* (16462). The total length of the chromosome was varied from 9.61 in *B. japonicus* (16462) to 5.17 in *B. madritensis* (Arjan) and the mean value of chromosome's arm ratio was in range from 1.41 in *B. rubens* (15317) to 1.22 in *B. japonicus* (16462) (Table 3).

The results showed that the highest VRC amongst all populations was obtained for *B. japonicus* (16462) and the lowest was obtained for *B. madritensis* (Arjan). Based on intra-chromosomal asymmetry, some populations had the most asymmetrical and evolutionary karyotype. According to inter-chromosomal asymmetry, *B. rubens* (15317) had the most asymmetrical karyotype in all of the populations.

The ratio of long arm/short arm chromosomes (AR) showed a high significant difference among some species belong to different sections, while other species are not clearly distinct (Table 3). Diploid species of *B. japonicus* (16462) for instance, had the lowest AR value (1.22), the highest TF% value (45.17) and the lowest A_1 value (0.18), exhibiting the most symmetrically karyotypes, while *B. rubens* (15317) with the highest AR value (1.41), the lowest TF% value (38.80) and the highest A1 value (0.29) were introduced as the most asymmetrical karyotypes (Table 3). The pattern of variation of A_1 and A_2 values has been compared with the pattern of Stebbins' system.

The statistical comparison based on completely randomized design showed that there were significant differences among the populations for TL, LA and SA traits ($P \leq \%1$) (Table 4).

The principal component analysis (PCA) of the karyotypic parameter shows the first two principal components account for 0.81% of total variance. Component one (0.59%) put emphasized on the A_1, A_2 and DRL. While component two (0.23%) accentuates, chromosome total length, long arm length, short arm length and TF% values which had the highest coefficients of Eigen vectors (Table 5).

The diagram of the population's dispersion, based on two first components showed that the populations separated in four groups, which completely fits with the results obtained through the average grouping analysis method (Fig. 2).

The dendrogram obtained from the cytogenetic studies of 14 populations of *Bromus* indicated the for-

Table 3. Mean of chromosomes analysis of *Bromus* population.

Populations	TL	LA	SA	AR	CI	DRL	%TF	A1	A2
B. japonicus (16462)	9.61	5.27	4.34	1.22	0.46	5.37	45.17	0.18	0.13
B. japonicus (16525)	8.71	4.82	3.90	1.24	0.45	6.13	44.70	0.20	0.15
B. japonicus (16587)	8.24	4.71	3.55	1.32	0.43	6.19	42.95	0.25	0.14
B. madritensis (3668)	5.23	2.92	2.31	1.27	0.44	4.35	43.03	0.21	0.21
B. madritensis (Arjan)	5.17	2.94	2.24	1.32	0.43	4.76	41.99	0.24	0.20
B. rubens (15169)	5.91	3.38	2.54	1.33	0.42	5.58	41.49	0.25	0.24
B. rubens (15317)	5.62	3.29	2.34	1.41	0.41	5.33	38.80	0.29	0.26
B. rubens (2125)	5.97	3.42	2.55	1.35	0.42	5.39	39.90	0.26	0.23
B. scoparius (5983)	8.02	4.55	3.48	1.31	0.43	4.72	42.49	0.23	0.12
B. scoparius (5984)	7.62	4.29	3.34	1.29	0.43	5.72	42.11	0.23	0.12
B. scoparius (5985)	6.87	3.84	3.03	1.27	0.44	5.48	44.06	0.22	0.13
B. tomentellus (Bavanat)	6.08	3.42	2.67	1.28	0.43	1.69	42.52	0.22	0.11
B. tomentellus (Simakan)	6.90	3.84	3.06	1.26	0.44	2.28	44.35	0.20	0.12
B. tomentellus (Eghlid)	6.52	3.68	2.84	1.30	0.43	2.15	41.28	0.22	0.14

TL: total length of chromosome, LA: long arm, SA: short arm, AR: arm ratio, CI: centromeric index, DRL: difference of relative length, TF%: total form percentage, A_1: intra-chromosome asymmetry index, A_2: inter-chromosome asymmetry index.

Table 4. The results of variance analysis for karyotypic data based on CRD design.

S.O.V	D.F	TL	Mean of squares							
			LA	SA	AR	CI	DRL	TF	A_1	A_2
Populations	13	11.50**	2.677**	2.032**	0.014**	0.001**	10.383**	9.7ns	0.004ns	440.55**
Error	56	0.50	0.131	0.115	0.009	4.64E-04	3.987	6.869	0.002	86.161
%C.V.		2.57	0.61	0.48	0.01	5.51E-04	5.19	7.40	2.57E-03	152.93

**: Significant at 1%.

Table 5. Specific values of variance percentage and coefficients of specific vectors in analysing main components.

Name of traits	First component	Second component
SA	0.93	0.32
LA	0.87	0.44
TL	0.90	0.38
AR	0.05-	0.72
CI	0.89	-0.27
A1	0.82-	0.52
A2	-0.77	0.22
DRL	0.09	0.79
TF	0.89	-0.23
Specific values	5.28	2.07
Percentage of Variance	0.59	0.23
Cum Percentage of Variance	0.59	0.81

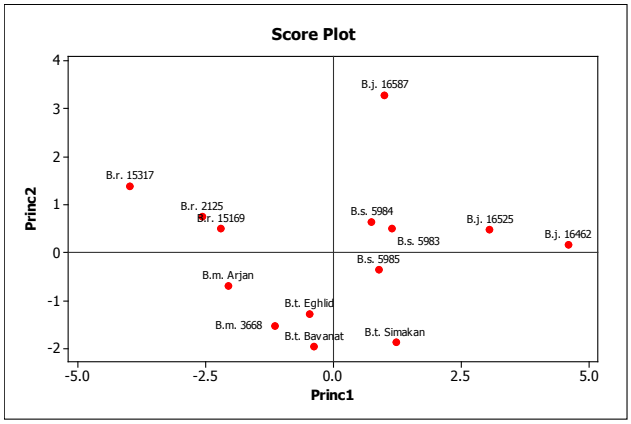

Figure 2. Scatter plot of 14 populations for the first two principals.

mation of five clusters in the Euclidean distance of 0.05. The first cluster consists of the *B. tomentellus* populations (Simakan, Eghlid and Bavanat). The populations of Bavanat and Eghlid showed the most kinship, and the population of Simakan is located in a relatively short distance to these two populations. The second cluster consists of *B. rubens* (15317) and *B. rubens* (2125) populations which showed a close kinship. The third cluster consists of the populations *B. madritensis* (3668, Arjan) and *B. rubens* (15169), the two populations of 3668 and Arjan are closely related to each other, with a relatively short distance from the population of 15169. The populations of *B. scoparius* (5983, 5984, 5985) and *B. japonicus* (16587) formed the fourth cluster. The populations of 5983 and 5984 are located close to each other with a relatively short distance from the population of 5985. The population of 5985 is located in a longer distance than the three mentioned populations. The two populations of *B. japonicus* (16462 and 16525) with a short distance from each other, formed the fifth cluster (Fig. 3).

DISCUSSION

This study reveals a detailed picture of the chromosome features in five *Bromus* species of Iran. The knowledge of chromosome numbers, karyotype evolution, ploidy level and genome size can provide additional information that not only gives further insight into the functioning of the genome, but also have considerable predictive powers.

In this genus, the basic chromosome number is x=7, as were found for fourteen populations of five species of *Bromus* (2n=2x=14, 2n=4x=28 and 2n=6x=42). This study confirmed that the *Bromus* species show great variations in the number of chromosomes. At the interspecific level, quantitative and qualitative data allowed us the differentiation of several of the taxa studied. Among species, the most variable characters were the number of "m", and "sm" chromosomes, as well as the number and position of satellites (Table 2; Fig. 1). As a result, the species also could be differentiated by the number, type and position of satellites.

This study revealed that three populations of *B. rubens* and *B. madritensis* were tetraploid (2n=4x=28) species (Table 2 and Fig. 1). This is in agreement with the results of an investigation recorded by Sheidai and Fadaei (2005). Three populations of *B. tomentellus* was the only hexaploid (2n=6x=42), but Mirzaie-Nodoushan *et al.*

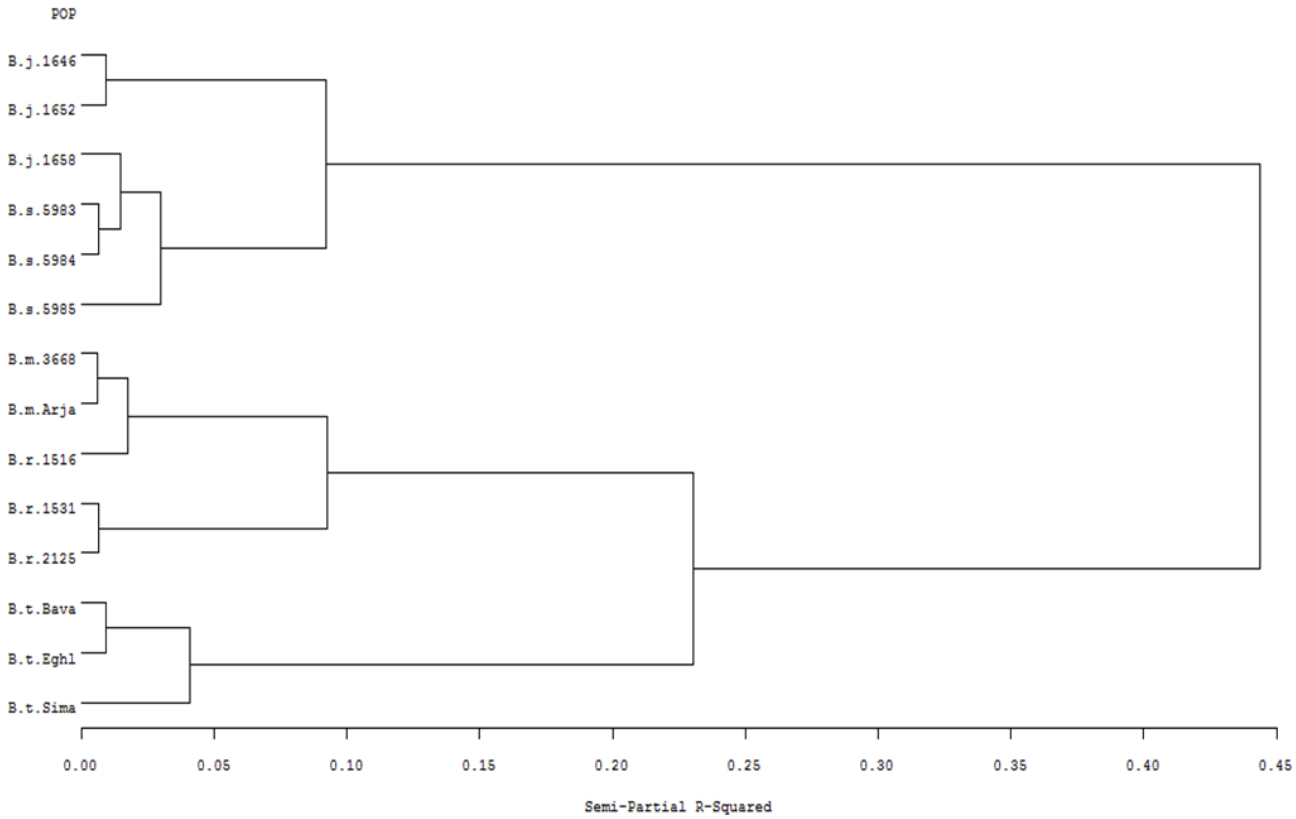

Figure 3. Dendogram of 14 populations of *Bromus* by analyzing nine karyotipic parameters using Ward 's cluster analysis method.

(2006b) recorded different ploidy levels within this species (2n=42, 70 & 84). Three populations of *B. japonicus* and *B. scoparius* species studied were diploid (2n=2x=14), supporting the earlier report of Safari *et al*. (2017). The present study confirmed that the *Bromus* species show great variations in the number of chromosomes both at inter and intra-specific levels. This kind of genetic and cytogenetic variability can confer an adaptive advantage against variable climate and other ecological elements in the region (Mirzaie-Nodoushan *et al*. 2006a).

The Duncan's test applied to the chromosome morphometric traits (LA, SA, TL, AR, DRL, TF%, A_1 and A_2) showed a highly significant difference among all examined populations of different sections (Table 3). The study revealed cytogenetic differences (P≥1%) in ANOVA for karyological data as well as the ratio of long arms to short arms among populations. So these results indicate a significant quantitative change in amount of chromatin in *Bromus* species diversification (Tables 2 and 4).

Considering the changes of intrachromosome asymmetry index (A_1) among diploid and tetraploid species, the lowest value exists in the diploid (*B. japonicus*, 16462) and the highest value exists in the tetraploid species (*B. rubens*, 15317) (Table 2).

The results of analysis of variance showed that except for A_1 and TF%, there was a significant difference (P≤1%) between genotypes in terms of chromosomal traits (LA, SA, TL, AR, DRL and A_2) which indicated large variations among the germplasms in regard to studied traits.

Cluster analysis based on chromosomal characteristics separated, the fourteen investigated populations of *Bromus* species into two major groups consistent of statistical analysis of chromosome morphometric traits (Fig. 3). The first group has eight populations of *Bromus* species (*B. madritensis, B.rubens and B. tomentellus*) which are tetraploid and hexaploid (2n=4x=28 & 2n=6x=42) and belong to *Genea* and *Pnigma* sections. The second group has six populations of *Bromus* species (*B. scoparius* and *B. japonicus*) that are diploid (2n=2x=14) and belong to *Bromus* section. Cluster analysis based on cytological data showed that the populations with the lowest metric distance may lead to use populations in crosses for inducing the highest genetic variations (Fig.3). However, grouping of the *Bromus* populations based on karyotypic data, agrees with either the taxonomic treatment of the genus *Bromus* of the same species based on morphological characters.

These genomic differences could be used for breeding purposes. In general, cytological studies of the *Bromus* species growing in Iran indicate the importance of polyploidy, chromosome structural changes, presumably quantitative changes in the amount of DNA and probably the role of growing sites in species diversification and suggest that such data may be used in the taxonomy and phylogenetic consideration of the genus (hesamzadeh and Ziaei Nasab 2010).

Acknowledgments: The authors are grateful to Mrs Ladan jowkar for drawing charts.

REFERENCES

Acedo C, Liamas F. 2001. *Variation of morphological characters of lemma and palea in the genus Bromus (Poaceae).* Ann. Bot. Fennici., 38: 1-14

Artico LL, Mazzocato AC, Ferreira JL, Carvalho CR, Clarindo WR. 2017. *Karyotype characterization and comparison of three hexaploid species of Bromus Linnaeus, 1753 (Poaceae).* Comparative Cytogenetics, 11(2):213-223.

Bor NL. 1970. *Bromus*. In: Flora Iranica, Rechinger, K.H. (Ed.). Akademische Druck-u. Verlagsanstalt, Graz, Austria, pp: 105-141.

Devesa JA, Ruiz T, Tormo R, Munoz A, Viera M.C. 1990. Contribución *al conocimiento* cariológico *de las Poaceae en Extremadura II*. Boletim Sociedade Broteriana, 63: 153-205.

Hesamzadeh SM, Ziaei Nasab M. 2010. *Cytotaxonomy of some Onobrychis (Fabaceae) species and populations in Iran.* Caryologia, 63(1):18-31.

Hill HD. 1965. *Karyology of species of Bromus, Festuca and Arrhenatherum (Gramineae)*. Bull. Torrey Bot. Club, 92: 192-197.

Huziwara Y. 1962. Karyotype analysis in some genera of Compositae. VIII. Further studies on the chromosomes of Aster. Amer. J. Bot. 49 (2): 116-119.

Levan A, Fredga K, Sandberg AA. 1964. *Nomenclature for centromic position on chromosomes*. Hereditas, 52: 201-220.

Martinello GE, Schifino-Wittmann M. 2003. *Chromosomes of Bromus auleticus Trin*. Ex Nees (Poaceae). *Genetics Mol. Biol.*., 26:369-71

Massa AN, Jensen KB, Larson SR, Hole DJ. 2004. *Morphological Variation in Bromus Section Ceratochloa Germplasm of Patagonia. Canadian J. Bot*., 82: 136–44

Mirzaie-Nodoushan H, Dehghanshoar M, Maddah-Arefi H, Asadi-Corom F. 2006a. *Karyotypic Characteristics of several Bromus species*. International Journal of Agriculture & Biology, 8(6): 717-720.

Mirzaie-Nodoushan H, Headari-Sharifabad H, Asadi-Corom F, Shariat A. 2006b. *Evolutionary karyotypic variation in Bromus tomentellus populations*. Cytologia, 71: 297-301.

Naganowaska B. 1993. *Karyotypes of five Bromus species of Genea section*. Genetica polonica, 34: 197-213.

Oja T, Laarmann H. 2002. *Comparative study of the ploidy series Bromus sterilis, B. diandrus and B. rigidus (Poaceae) based on chromosome numbers, morphology and isozymes.* Plant Biol., 4:484–91

Reeves A, Tear J. 1997-2000 Coloradostate university. from http://www.colostate.edu/Depts/Biology/micromeasure.

Romero Zarco C. 1986. *A new method for estimating Karyotype asymmetry*. Taxon, 36: 526-530.

Sadeghian S, Jafari E, Hatami A. 2010. *Cytogenetic studies in some species of Bromus L. in Iran*. Asian Journal of Biological Science 3(4): 188-194.

Safari H, Zebarjadi A.R, Kahrizi D, Jafari A.A. 2017. *Evaluation of karyotypic relationship of several species of Bromus and Genea sections from Bromus genus.* Iranian Journal of Rangelands and Forests Plant Breeding and Genetic Research 25(1): 82-96.

Sales F. 1994. *Evolutionary tendencies in some annual species of Bromus (Bromus L. sect. Genea Dum. (Poaceae)*. Botanical Journal ofthe Linnean Society, 115: 197–210.

Sheidai M, Fadaei F. 2005. *Cytogenetic syudies in some species of Bromus L. section Genea Dum*. J. Genet., 84(2): 189-194.

Stebbins GL. 1971. *Chromosomal evolution in higher plants*. Edward Arnold Publisher, London, Ltd. Pp. 216.

Verloove F. 2012. *A revision of Bromus section Ceratochloa (Pooideae, Poaceae) in Belgium*. Dumortiera, 101: 30-45.

Wittmann W. 1965. *Aceto-iron-hematoxylin-chloral hydrate for chromosome staining*. Stain Technol., 40: 161-164.

Yang G, Dunn GM. 1997. *Mitotic instabilities in tetraploid, hexaploid and octaploid Bromus inermis*. Can. J. Genet. Cytol., 19: 550-553.

Caryologia
International Journal of Cytology, Cytosystematics and Cytogenetics

Firenze University Press
www.fupress.com/caryologia

OPEN ACCESS

Citation: M. Meloni, C.A. Dettori, A. Reid, G. Bacchetta, L. Hugot, E. Conti (2020) High genetic diversity and presence of genetic structure characterise the endemics *Ruta corsica* and *Ruta lamarmorae* (Rutaceae). *Caryologia* 73(1): 11-26. doi: 10.13128/caryologia-510

Received: July, 2019

Accepted: February, 2020

Published: May 8, 2020

Data Availability Statement: All relevant data are within the paper and its Supporting Information files.

Competing Interests: The Author(s) declare(s) no conflict of interest.

High genetic diversity and presence of genetic structure characterise the endemics *Ruta corsica* and *Ruta lamarmorae* (Rutaceae)

Marilena Meloni[1], Caterina Angela Dettori[2], Andrea Reid[3], Gianluigi Bacchetta[2,4,*], Laetitia Hugot[5], Elena Conti[1]

[1] *Institute of Systematic Botany, University of Zurich, Zollikerstrase 107, 8008 Zurich, Switzerland*
[2] *Centro Conservazione Biodiversità (CCB), Dipartimento di Scienze della Vita e dell'Ambiente - Università degli Studi di Cagliari. Viale S. Ignazio da Laconi, 13 - IT-09123 Cagliari, Italy*
[3] *Department of Environmental Systems Science, ETH Zurich, Universitätstrasse 6, 8006 Zurich, Switzerland*
[4] *Banca del Germoplasma della Sardegna (BG-SAR), Hortus Botanicus Karalitanus (HBK), Università degli Studi di Cagliari. Viale Sant'Ignazio da Laconi, 9-11, IT-09123, Cagliari, Italy*
[5] *Conservatoire Botanique National de Corse, Office de l'Environnement de la Corse, Avenue Jean Nicoli, 20250 Corte, France*
* Corresponding author. E-mail: m.marilena75@gmail.com, c.angeladettori@gmail.com, areid@student.ethz.ch, bacchet@unica.it, Laetitia.Hugot@oec.fr, Elena.Conti@systbot.uzh.ch.

Abstract. Corsica and Sardinia form one of the areas with highest biodiversity in the Mediterranean and are considered one of the priority regions for conservation in Europe. In order to preserve the high levels of endemism and biological diversity at different hierarchical levels, knowledge of the evolutionary history and current genetic structure of Corso-Sardinian endemics is instrumental. Microsatellite markers were newly developed and used to study the genetic structure and taxonomic status of *Ruta corsica* and *Ruta lamarmorae*, rare endemics of Corsica and Sardinia, respectively, and previously considered a single species. Our analyses identified high levels of genetic variation within each species (P=0.883, H_e=0.543 for *R. corsica; P*=0.972, H_e=0.627 for *R. lamarmorae*). Intrinsic traits of the species (hermaphroditism, proterandry and polyploidy) and island-dependent factors (i.e. age, origin and history of the islands) might explain the detected high levels of genetic variation. We discovered differentiation between *R. corsica* and *R. lamarmorae*, and genetic structure within each species, which are consistent with the observation of low dispersal ability for both species. Our genetic results support the recent taxonomic classification of *R. corsica* and *R. lamarmorae* as separate species and suggest that they diverge at only few loci. One *R. corsica* population (SA) strongly differed from all other studied populations and appeared to be the product of hybridization between the two species in STRUCTURE analyses. Our results provide important insights for the conservation of the two rare endemics. Further genetic analyses are recommended for *R. lamarmorae* and for population SA (*R. corsica*).

Keyword. Genetic diversity, endangered species, *Ruta*, Corsica, Sardinia, microsatellite.

INTRODUCTION

The Mediterranean Basin is characterised by high species richness (10.8 species/1000 km^2, Médail and Quézel 1999) and considered one of the main "hot spots" of biodiversity in the world (Médail and Myers 2004, Thompson 2005). Additionally, this area is particularly rich in endemic taxa (about half of the approximately 25000 plant species native to this region are endemics), which are mainly concentrated in mountain chains and islands (Médail and Quézel 1997, 1999, Thompson 2005, Cañadas *et al.* 2014).

Corsica and Sardinia (Figure 1), the two largest islands of the Western Mediterranean Basin, form one of the areas with highest plant diversity in the Mediterranean and are particularly rich in endemics (Médail and Quézel 1997, Thompson 2005, Blondel *et al.* 2010). The Sardinian flora consists of 2498 taxa, with about 11.61% endemic (290 species) to the island (Conti *et al.* 2005, 2007; Bacchetta *et al.* 2012; Fenu *et al.* 2014). Corsica's flora consists of 2325 taxa, of which ca. 10% are endemics (230 species; Jeanmonod and Gamisans 2013). Both islands are considered a major glacial refugium (Médail and Diadema 2009) and together host nine of the 50 most threatened plant species occurring in Mediterranean islands (de Montmollin and Strahm 2005).

The high level of biodiversity and the number of endemics found in Corsica and Sardinia are often ascribed to their noteworthy ecosystem diversity (Bacchetta and Pontecorvo 2005) and to past geologic and paleoclimatic processes. Indeed, tectonic movements during the Tertiary (from 66 to 2.58 million years ago, MYA), the Messinian Salinity Crisis (MSC, ca. 5 MYA), the establishment of a Mediterranean climate type in the Pliocene (2-3 MYA), and climate changes associated with glacial and interglacial phases (Pleistocene: 0.01-2 MYA) have shaped the history of Mediterranean plant lineages (Hewitt 2000, Gentili *et al.* 2015, Médail and Quézel 1997, Thompson 2005).

Corsica and Sardinia are continental fragment islands belonging to a single microplate (the Corso-Sardinian (C-S) microplate; Alvarez *et al.* 1972) and are currently separated by a narrow (11 km) and shallow (less than 50 m deep) water channel through the Bonifacio Strait. The C-S microplate was attached to Southern France and Northeastern Spain until the late Oligocene (28-30 MYA), when it broke off and rafted eastward, until it collided with the Apulian microplate (i.e., the current Italian peninsula) ca. 18-20 MYA (Rosenbaum and Lister 2004, Speranza *et al.* 2002). It reached its current position in the middle of the Western Mediterranean ca. 9 MYA (Rosenbaum and Lister 2004).

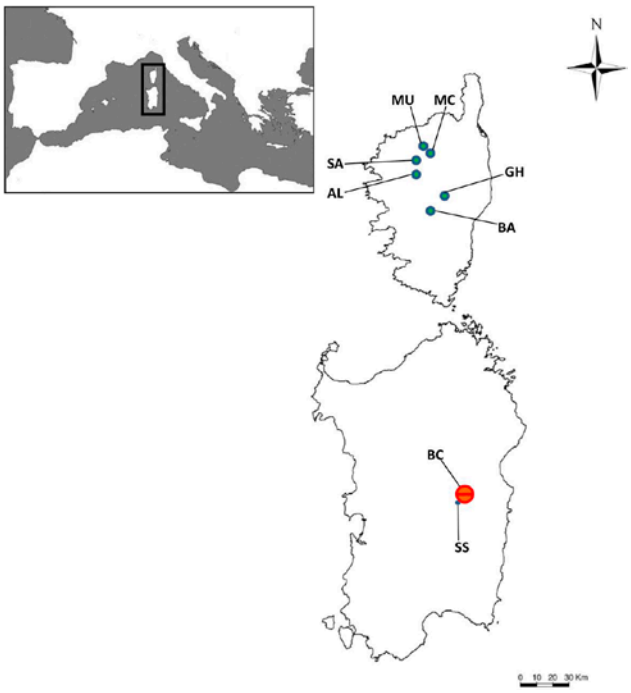

Figure 1. Localities of populations taxonomically assigned to *R. corsica* (green dots) and *R. lamarmorae* (red dot) sampled for this study. *Ruta lamarmorae* population was divided in two subpopulations. Detailed information on each population is provided in Table 1.

The separation between Corsica and Sardinia may have begun as early as 15 MYA and was complete by 9 MYA (Alvarez 1972, 1976, Cherchi and Montadert 1982, Orsini *et al.* 1980).

Species that now occur in Corsica and Sardinia could have originated in different ways: 1) they were present in the region before the split of the C-S microplate from the Iberian peninsula; 2) they reached the C-S microplate when it was temporarily connected with the Apulian microplate during the Miocene (ca.10-20 MYA, Rosenbaum *et al.* 2002); 3) they reached the C-S microplate through the land bridges that formed among Corsica, Sardinia, the Apulian plate and the African continent during the MSC (5 MYA; Hsü *et al.* 1977, Krijgsman *et al.* 1999, McKenzie 1999) or 4) during the glacial marine regressions concomitant with the glacial cycles of the Pleistocene (Thompson 2005); 5) they reached the islands via long distance dispersal at any point in time (LDD). If insular populations differentiated sufficiently from their closest relatives due to isolation and/or extinction, they gave origin to island endemics.

Although Corsica and Sardinia are one of the priority regions for conservation in Europe (Myers *et al.* 2000, Mittermeier *et al.* 2005), knowledge of the evolu-

Table 1. Description of populations of *R. corsica* and sub-populations of *R. lamarmorae* surveyed in this study.

Species	Population abbreviation	Location	Population size	Sample number	Coordinates	Altitude
R. lamarmorae	BC	Broncu Spina	~1000	30	40° 07' 34" N 9° 31' 26" E	1650m
	SS	Su Susciu	~1000	30	40° 01' 02" N 9° 19" 33" E	1620m
R. corsica	MU	Muvrella	20	8	42° 24' 0" N 8° 54 0"' E	1050m
	MC	Monte Cinto	150	16	42° 23' 0" N 8° 55' 0" E	1750m
	SA	Saltare	20	8	42° 21' 41" N 8° 52' 53"E	1180m
	GH	Ghisoni	40	23	42° 6' 37" N 9° 9' 16"E	1650m
	AL	Albertacce	120	20	42° 17' 39" N 8° 52' 44"E	1300-1500m
	BA	Bastelica	750	21	42° 0' 26" N 9° 6' 4"E	900m

tion and genetic characteristics of their endemic flora, instrumental for the long-term conservation of these species, is still poor. Some molecular phylogenetic analyses have been performed to infer when and how C-S endemics reached the two islands (Yesson *et al*. 2009, Mansion *et al*. 2008, Salvo *et al*. 2008, 2010) and few studies focused on the more recent history of these species (Bacchetta *et al*. 2008; Coppi *et al*. 2008; Mameli *et al*. 2008; Bacchetta *et al*. 2011; Garrido *et al*. 2012). Nevertheless, several questions remain unanswered, including: How did C-S endemics evolve after island colonization? What is their current genetic structure? Are Corsican and Sardinian populations of the same species genetically differentiated?

Ruta corsica DC. and *R. lamarmorae* Bacch., Brullo & Giusso are endemics of Corsica and Sardinia, respectively. The two species belong to the small genus *Ruta*, which also includes four species widely distributed in the Mediterranean *(R. angustifolia* Pers., *R. chalepensis* L., *R. montana* L., and *R. graveolens* L.) and three species endemic to the Canary Islands (*R. oreojasme* Webb & Berth, *R. pinnata* L.f. and *R. microcarpa* Svent.). *Ruta corsica* and *R. lamarmorae* exhibit some features not found in the other species of the same genus (i.e. pulvinate, subspinescent habit; green-glaucescent leaves; white to pale yellow petals) and have been interpreted by taxonomists as relictual paleo-endemics (Bacchetta et *et al*. 2006, Cardona and Contandriopoulos 1979), in other words as ancient lineages that were more widespread in the past and are now restricted to a local region (Nekola 1999, Mishler *et al*. 2014), in this case to the C-S microplate (Arrigoni 1983, Thompson 2005). They were treated as one species (i.e., *R. corsica)* until 2006, when they were split in two different taxa based on morphological (i.e., leaf shape and size of flowers, stamens and ovaries; Bacchetta *et al*. 2006) and karyological differences *(R. corsica* is diploid, *R. lamarmorae* is tetraploid; Contandriopoulos 1957, Honsell 1957). Phylogenetic analyses of chloroplast DNA sequences from only two individuals each from Corsica and Sardinia supported the separation of *R. corsica* and *R. lamarmorae*, with individuals from the two islands grouped in mutually exclusive sister clades (Salvo *et al*. 2008).

Molecular dating analyses and inference of ancestral areas of distribution for *Ruta* species suggested that the genus originated during the Eocene in Eurasia and subsequently expanded westward and southward, colonising several landmasses of the forming Mediterranean Basin (Salvo *et al*. 2010). The ancestor of the two endemics likely colonised the C-S block from the Apulian plate (i.e., the emerging Italian peninsula) during the early Miocene. The divergence between the C-S endemics and the remaining *Ruta* species apparently occurred during the middle Miocene (ca. 14 MYA). Finally, *R. corsica* diverged from *R. lamarmorae* most likely in the Pliocene (ca. 3.7 MYA), when Corsica and Sardinia had already attained their current position in the middle of the Western Mediterranean sea and were separated by the Bonifacio strait. The two islands were occasionally connected by land corridors during the MSC of the Miocene and during the glacial maxima of Pleistocene climatic oscillations (Salvo *et al*. 2010).

Given the inferred biogeographic history of *R. corsica* and *R. lamarmorae* and their current distribution in Corsica and Sardinia, respectively, these species represent an ideal case study to gain new knowledge on the genetic characteristics of the Corso-Sardinian endemic flora. The aims of the present study are thus to: (1) assess the current amount and distribution of genetic diversity for the two species, testing whether the taxonomic status of *R. corsica* and *R. lamarmorae* as separate species is warranted; and (2) use the results of genetic analyses to recommend proper conservation strategies for these species, with a particular focus on *R. lamarmorae*, recently listed as endangered according to the IUCN criteria and categories (Dettori *et al*. 2014a).

MATERIALS AND METHODS

Study species

Ruta lamarmorae was described as a species separate from *R. corsica* in 2006 (Bacchetta *et al*.). It is a small, erect, perennial shrub, 15-50 cm tall, with woody, subspinescent branches. It is characterised by bipinnate, obovate-rounded leaves, 1.5-8 cm long. The whitish, pale yellow flowers (12-13 mm in diameter) are hermaphroditic and proterandrous. The capsules, 6-7 mm long, are obtuse at the apex. As with most members of its genus, *R. lamarmorae* is tetraploid, with 2n=36 (Honsell 1957). It blooms in June-July, fruiting in August-October. It occurs mainly on siliceous substrates, at an altitude of 1500-1750 m a.s.l. *Ruta lamarmorae* is found in a single, fragmented population in the Gennargentu massif (central-eastern Sardinia). It is categorized as endangered (EN) according to the IUCN criteria (2013; Dettori *et al*. 2014a). The main threats to this species are habitat fragmentation, overgrazing and fires (Bacchetta *et al*. 2006; Dettori *et al*. 2014a).

Ruta corsica, first described in 1824 by De Candolle, shares the same habit with *R. lamarmorae* and has overall similar leaves, flowers and fruits. It differs from *R. lamarmorae* in leaf shape (obovate to cuneate-oblong), smaller flower size (8-10 mm in diameter) and fruit size and shape (7-8 mm long, with apiculate apex; Bacchetta *et al*. 2006). *Ruta corsica* is the only diploid species of the genus, with 2n=18, while the other karyotyped species are tetraploid (Contandriopoulos 1957). It blooms and fruits slightly later than *R. lamarmorae* (September-November *vs*. July-August, respectively). The species occurs at an altitude of 1000-1900 m asl, mainly on siliceous substrates, and is widespread on the main Corsican massifs with about 15 populations. It is listed as Least Concern (LC) under the French red list of threatened species (UICN, France 2013).

To date, no information is available on the mating system, the pollination biology and the mode of dispersal of the diaspores of neither of the two species.

Sample collection and DNA extraction

Plant material was collected during summer 2010 (see Table 1). Since the only existing population of *R. lamarmorae* has a scattered distribution on the Gennargentu massif, we sampled plants from the two opposite sides of the massif, in other words from the Northwestern (BC, 30 individuals) and Southwestern slopes (SS, 30 individuals; Figure 1). Because sub-populations BC and SS are large (thousands of individuals; Gianluigi Bacchetta, pers. obs.), sampling was carried out in order to minimize collection of related individuals and cover the entire occupied area. Samples of *R. corsica* were collected from a total of 96 individuals from six populations chosen in order to cover the entire distribution range of the species (see Figure 1 and Table 1 for details on each population). Leaf-tissue samples were dried and preserved in silica gel. Total genomic DNA was isolated from dried leaves using the QIAGEN® DNeasy plant mini kit, following the manufacturer's guidelines, with minor modifications. In particular, an increased volume of buffer AP1 (from 400 µl to 600 µl), buffer AP2 (from 130 µl to 200 µl) and RNase A (from 4 µl to 6 µl), as well as a longer incubation time with buffer AP1 (30 minutes) for cell lysis were applied.

Microsatellite development and genotyping

DNA isolated from one specimen of *R. lamarmorae* sampled from population BC was used by Genetic Marker Services (Brighton, UK, www.geneticmarkerservices.com) to develop an enriched library, design and test microsatellite primer pairs. Enrichment involved incubating adaptor-ligated restricted DNA with filter-bonded synthetic repeat motifs, $(AG)_{17}$, $(AC)_{17}$, $(AAC)_{10}$, $(CCG)_{10}$, $(CTG)_{10}$ and $(AAT)_{10}$. Twenty-one positive library colonies were selected for sequencing, from which 15 microsatellites were designed and tested. The primer sets were designed using PRIMER 3.0 (Rozen and Skaletsky, 2000). Each primer pair was tested for amplification ability and polymorphism on eight individuals of *R. lamarmorae* (four from BC and four from SS). Cross-species amplification was tested on four individuals of *R. corsica* and four individuals of *R. chalepensis* (another species of the same genus with wider distribution also occurring in Sardinia; Salvo *et al*. 2010). Polymerase chain reactions (PCRs) for primer screening

were performed in 25 µL and contained approximately 50 ng of DNA, 5 pmol of each unlabelled primer, 1.5 mM of $MgCl_2$, 0.2 mM of each dNTP, 1X PCR buffer and 0.5 U of SupraTherm DNA Polymerase (GeneCraft, Cologne, Germany). *In-vitro* amplifications consisted of: 60 s denaturation at 95°C, followed by 25 cycles of 95°C for 60 s, annealing at 55°C for 60 s and 72°C for 60 s, ending with a final extension at 72°C for 5 min. This first screening of microsatellites was performed on high-resolution agarose gels.

The primer pairs able to amplify polymorphic products were then used to genotype all sampled individuals via amplification with fluorescently labelled primers and separation of PCR products by capillary electrophoresis. Amplifications were performed following the two-step method described by Schuelke (2000), using ca. 20 ng of genomic DNA, 2.5 µl of 10X reaction buffer, 0.5 µl of each dNTP (10 mM), 1 µl of $MgCl_2$ (50 mM), 0.2µl of the forward primer with M13(–21) tail at the 5' end (10 µM), 0.5 µl of the reverse primer (10 µM), 0.5 µl of the fluorescently labelled M13(–21) primer (FAM, NED, VIC, PET; 10 µM) and 0.1 µl of Taq DNA polymerase (5 U/µl; Bioline GmbH, Luckenwalde, Germany) in a final volume of 25µl. Amplification reactions started with 94°C for 3 min, followed by 30 cycles of 94°C for 30 s,s 55°C for 45 s (see Table 2), and 72°C for 1 min. The fluorescently labelled M13(–21) primer was incorporated in the following eight cycles of 94°C for 30 s, 53°C for 45 s, and 72°C for 1 min, followed by a final extension step of 72°C for 5 min. Up to four PCR products of different primer sets were pooled for each individual and separated by capillary electrophoresis on an AB3130xl Genetic Analyzer. Alleles were sized against the internal size standard GeneScan™ LIZ500™ (Applied Biosystems) and scored using GeneMapper® software Version 4.0 (Applied Biosystems). The observed allele size of all genotyped individuals was decreased by 18bp in order to account for the M13(–21) universal sequence tag.

Population genetic analyses

Even though *R. lamarmorae* is known to be tetraploid (Honsell 1957), a maximum of two alleles per locus and per individual were detected in all populations, thus showing disomic inheritance. Because genetic analyses can be performed with standard population genetic tools developed for diploid organisms in tetraploid species characterised by disomic inheritance (Stift *et al.* 2008; Meloni *et al.* 2013), our analyses were conducted assuming a diploid status for *R. lamarmorae*.

We assessed genetic diversity by quantifying the number of alleles (N_A), proportion of polymorphic loci (P), number of private alleles (A_P), observed (H_o) and expected (H_e) heterozygosity for each population across loci. Populations were tested for deviations from Hardy-Weinberg (HW) equilibrium using Fisher's exact test with the Markov chain algorithm (Guo and Thompson 1992). The fixation index, F_{IS}, was estimated in order to assess departure from Hardy-Weinberg expectations due to non-random mating. Fisher's exact test was performed within each population to check for linkage disequilibrium (LD) between all different pairs of loci. These analyses were performed with the web-based Genepop (Raymond and Rousset 1995; Rousset 2008) and GenAlEx v. 6.5 (Peakall and Smouse 2012). The program BOTTLENECK (Piry *et al.* 1999) was used to detect recent genetic bottlenecks in the studied populations. Based on the observed number of alleles and the sample size of a population, the program computes the gene diversity expected under the assumption of mutation-drift equilibrium and compares it to Hardy–Weinberg gene diversity (H_e; Nei 1978) to establish whether there is a significant deficit of gene diversity resulting from a recent bottleneck. As recommended by the authors of the program, a Wilcoxon sign-rank test (Luikart *et al.* 1998) was performed using 1000 bottleneck simulation replicates under the stepwise mutation model (SMM).

FSTAT 2.9.3 (Goudet 1995) was used to estimate genetic differentiation among populations by F_{ST}. We also measured R_{ST}, an analogue of F_{ST} specific for microsatellite data, employing a stepwise mutation model (SMM, Slatkin 1995); R_{ST} was measured using the software SPAGeDi 1.4 (Hardy and Vekemans 2002). The same program was used to perform an allele-size permutation test (10000 permutations) to evaluate the contribution of stepwise mutations to the observed genetic differentiation, hence the relative suitability of F_{ST} vs. R_{ST} (Hardy *et al.* 2003). In addition, since F_{ST} can considerably underestimate differentiation when loci are highly variable (as commonly found with microsatellite markers; Hedrick 2005; Jost 2008; Meirmans and Hedrick 2011), we also calculated Jost's D_{est} (Jost 2008) using 1,000 bootstrap replicates in SMOGD (Crawford 2010).

An Analysis of Molecular Variance (AMOVA) was performed to assess the hierarchical partitioning of genetic variation among populations and species. We followed the procedure of Excoffier *et al.* (1992), Huff *et al.* (1993), Peakall *et al.* (1995), and Michalakis and Excoffier (1996) by estimating F_{ST} and using 999 random permutations of the data in GenAlEx v.6.5 (Peakall and Smouse 2012). With the same program, a Principal Coordinate Analysis (PCoA) based on a genetic distance matrix was performed to visualise genetic relatedness among individuals. To test for isolation by distance, a

Mantel test (Mantel 1967) was applied to the matrix of pairwise Nei's genetic distances (Nei 1972, 1978) and the matrix of geographical distances with 999 random permutations in GenAlEx v. 6.5 (Peakall and Smouse 2012).

Population structure was inferred using the Bayesian clustering method implemented in STRUCTURE (v. 2.3; Pritchard *et al*. 2000; Hubisz *et al*. 2009). The program uses a Markov Chain Monte Carlo (MCMC) procedure to estimate P(*X*|*K*), the posterior probability that the data fit the hypothesis of *K* clusters, and assigns individual genotypes to clusters by estimating the membership coefficient Q for each individual based on allele frequencies at unlinked loci (independent of locality information). We tested all possible values of *K* from 1 to 9; for each *K* we ran an admixture model (each individual draws some fraction of the genome from each of the *K* populations) with correlated allele frequencies 20 times with a length of burnin period of 100,000 followed by 100,000 MCMC repetitions. To identify the best *K*, we measured *Δ*K (the rate of change in the log probability of data between successive *K* values), as suggested by Evanno *et al*. (2005) and implemented in STRUCTURE HARVESTER (Earl and vonHoldt 2012). This method provides the most accurate estimate of the number of clusters *K* (Evanno *et al*. 2005), but does not allow for discrimination between K=1 and K=2. Therefore we also calculated the average posterior probability of the data for each value of *K*, Ln P(*X*|*K*), as proposed by Pritchard *et al*. (2000). After determining the most effective number of genetic groups (*K*) for our data, we ran STRUCTURE with the admixture model and default parameter settings; the inferred genetic composition of individuals was then determined using 100,000 iterations after a burnin period length of 100,000.

RESULTS

Microsatellite development and cross-species amplification

Of the 15 microsatellites newly developed for *R. lamarmorae*, 13 were suitable for genetic analyses on the target species (Table S1). Tests on cross-species amplification showed that 13 markers could be used for *R. corsica* while 11 could be amplified in the more distantly related *R. chalepensis* (Table S1).

Genetic diversity

Eleven microsatellites showing a clear amplification pattern after capillary electrophoresis on both *R. corsica* and *R. lamarmorae* were used for genotyping (Table 2). Because all studied individuals of *R. corsica* and *R. lamarmorae* were heterozygotes for the same two alleles in locus RL9, this marker was excluded from population genetic analyses. In *R. lamarmorae*, all amplified loci were polymorphic; in *R. corsica*, locus RL16 was fixed in populations SA, GH, AL, BA; population SA showed fixed alleles also at loci RL15, RL17 and RL18. The number of alleles identified across all loci ranged from 22 to 61 in *R. corsica* populations, and from 55 to 68 in the two *R. lamarmorae* sub-populations (Table 3). Private alleles were found in all populations except SA (Table 1).

All populations, except for GH, were at HW equilibrium (p>0.05). F_{IS} values were positive in the two sub-populations of *R. lamarmorae*, as well as in four out of six populations of *R. corsica* (MU, MC, GH and BA; Table 3), meaning that the departure of genotype frequencies from Hardy-Weinberg expectations was always associated with a deficit of heterozygotes. Conversely, an excess of heterozygotes was found in populations SA and AL (*R. corsica;* Table 3).

Significant linkage-disequilibrium (LD) at the 5% level was detected at one pair of loci for populations GH (RL6-RL18), AL (RL13-RL15) and MU (RL12-RL17), three loci for population BC (RL4-RL6, RL13-RL15, RL11-RL17), four loci for SA (RL4-RL12, RL4-RL13, RL11-RL13, RL12-RL13) and BA (RL6-RL11, RL12-RL15, RL13-RL15, RL15-RL18), and eight loci for SS (RL4-RL5, RL5-RL11, RL5-RL13, RL6-RL13, RL11-RL13, RL15-RL17, RL12-RL18, RL15-RL18). It was impossible to perform most of the tests for populations MU (25 out of 45 pairs of loci) and SA (30 out of 45 pairs of loci).

Gene diversity (H_e) was high in all populations, with a mean value of 0.627 for *R. lamarmorae* and 0.543 for *R. corsica;* the only population showing a relatively low value was SA (*R. corsica*), with H_e= 0.323 (Table 3).

The only population showing significant signs of a recent bottleneck was BA (*R. corsica*, p = 0.032), while all other populations were at mutation-drift equilibrium.

Genetic structure

Genetic differentiation among populations measured with F_{ST} was always statistically significant ($P < 0.05$); it was 0.086 between the two sub-populations of *R. lamarmorae* and ranged between 0.012 (MU-MC) and 0.240 (AL-SA) in *R. corsica* (Table 4). Genetic differentiation among populations across the two species ranged between 0.050 (MU-SS) and 0.212 (SA-BC). Population SA was the most differentiated, with $0.173<F_{ST}<0.240$ (Table 4). The overall genetic differentiation among populations was significant (p=0.01), with F_{ST}=0.097 for *R. corsica* and F_{ST}=0.086 for *R. lamarmorae*. Simi-

Table 2. Characteristics of 15 microsatellite markers developed in *Ruta lamarmorae*. Shown for each marker are the GenBank accession number, forward and reverse sequences of the primer pair, repeat motif, and size of the expected PCR product (bp). Primers in bold were used for genotyping; locus RL9 was excluded from statistical analyses as all genotyped individuals of *R. corsica* and *R. lamarmorae* were heterozygotes for the same two alleles.

Locus	GenBank accession no.	**Primer sequence (5'-3')**	**Repeat**	**Expected size (bp)**
RL4	KP098574	F: ACATCAGCCCTTCAACTACG R: CCTAAAGAATCAATTATAAGCAACC	$(TC)_{13}$	182
RL5	KP098575	F: TCGTAGAGCCAATCACAGGA R: GCTGCTTCATTTGCTTTGAA	$(AG)_{14}$	219
RL6	KP098576	F: CTCGATCGGGAAGAACTTACA R: ATCCAATCCCAACCCAACTT	$(GA)_{14}$	131
RL7	KP098577	F: TTGAGTGAGGAGGGTTAGGG R: TGAGACACGCCAATTTCAGA	$(GA)_{7}$	140
RL9	KP098579	F: CTTGCTCATGCCACCTTTTA R: ACCCACAAGCTCCTCCTGTA	$(GT)_{9}$	145
RL10	KP098580	F: ACATGTTGCAGAATTTGAAAGG R: TTAAAGAGGCAACAACCTGGA	$(AG)_{13}$	160
RL11	KP098581	F: GAAACGGGCTTCTTCAACAG R: GTACAGGACATGATGCAAA	$(GA)_{15}$	113
RL12	KP098582	F: CTCCGTTCGCAGAAAGACAC R: TTACGACCCACACGCAAGTA	$(GT)_{8}(GA)_{8}$	204
RL13	KP098583	F: CAACCCCATCTGTGAATCCT R: GCTTGCACTTTGGAGTTTTTG	$(TC)_{12}$	185
RL15	KP098585	F: CGCCTTTCTTACTTGAAAAGGTT R: TCAACAAGACACTGCAACCA	$(TC)_{13}$	194
RL16	KP098586	F: TTTCGTCAAAATTGACATCAGC R: TCAACAAGACACTGCAACCA	$(TG)_{7}$	170
RL17	KP098587	F: TGGAGTTTCATGTCGGATTG R: TGAGATAACCGCCTCCTACC	$(TG)_{7}$	242
RL18	KP098588	F: TCCCAACGCACAGTGAAATA R: GTGTTTCCTCGAAGCTGCTC	$(TG)_{10}$	166
RL19	KP098589	F: CGTCTTGAAATGATGTTACCTG R: CCTAACAAACAACACAAATAATAAATG	$(TC)_{16}$	225
RL20	KP098590	F: TGTTTTCGTGCAAAAATTCG R: GGACTTACCTATCCGAAAATGG	$(GT)_{19}$	246

Table 3. Genetic diversity parameters inferred from microsatellite analysis. N_A total number of alleles across loci, P proportion of polymorphic loci, A_P number of private alleles, H_o observed heterozygosity, H_e expected heterozygosity, F_{IS} fixation index; SD, standard deviation. For abbreviations of populations see Table 1.

Population	N_A	P	A_P	$H_o \pm$ SD	$H_e \pm$ SD	$F_{IS} \pm$ SD
BC	55	1	4	0.554 ± 0.082	0.614 ± 0.078	0.097 ± 0.100
SS	68	1	8	0.587 ± 0.076	0.639 ± 0.083	0.082 ± 0.027
Overall *R. lamarmorae*	123	0.967	12	0.571 ± 0.055	0.627 ± 0.056	0.109± 0.052
MU	51	1	2	0.623 ± 0.075	0.688 ± 0.072	0.094 ± 0.056
MC	55	1	3	0.578 ± 0.077	0.630 ± 0.073	0.081 ± 0.076
SA	22	0.6	0	0.350 ± 0.118	0.323 ± 0.105	-0.083 ± 0.073
GH	53	0.9	1	0.546 ± 0.082	0.593 ± 0.084	0.080 ± 0.041
AL	61	0.9	1	0.624 ± 0.085	0.624 ± 0.086	-0.001± 0.031
BA	53	0.9	3	0.497 ± 0.080	0.533 ± 0.081	0.070 ± 0.061
Overall *R. corsica*	295	0.883	10	0.536 ± 0.036	0.543 ± 0.035	0.160 ± 0.024

Table 4. Pairwise population estimates of F_{ST} (diagonal below) and D_{est} (above diagonal). All values are statistically significant (95% CI). For abbreviations of populations see Table 1.

	R. lamarmorae			*R. corsica*				
	BC	SS	MU	MC	SA	GH	AL	BA
BC		0.179	0.146	0.155	0.303	0.234	0.256	0.254
SS	0.086		0.278	0.121	0.208	0.156	0.099	0.193
MU	0.087	0.050		0.003	0.177	0.076	0.065	0.103
MC	0.102	0.065	0.012		0.179	0.048	0.060	0.077
SA	0.212	0.173	0.176	0.173		0.168	0.238	0.158
GH	0.130	0.083	0.052	0.038	0.184		0.131	0.124
AL	0.129	0.060	0.046	0.044	0.240	0.085		0.156
BA	0.160	0.136	0.092	0.071	0.213	0.088	0.122	

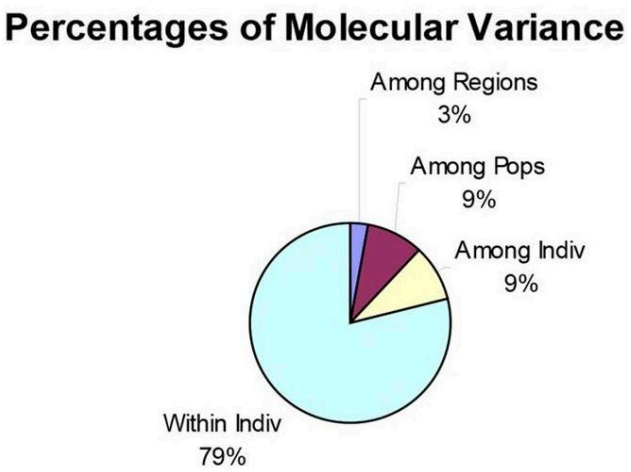

Figure 2. Analysis of Molecular Variance (AMOVA) based on ten microsatellite markers used to genotype 96 individuals taxonomically assigned to *R. corsica* (six populations) and 60 individuals taxonomically assigned to *R. lamarmorae* (one population divided in two sub-populations). The two regions considered in this analysis represent the two islands.

larly, the AMOVA (based on F_{ST}) displayed that most of genetic variation was partitioned within-population (88%), while only 9% was found among populations and 3% between islands (Figure 2). Values of R_{ST} (analogous to F_{ST}, but specific to microsatellite data; Slatkin 1995) were slightly smaller than those of F_{ST} ($0.003< R_{ST} <0.253$) (Table S2). However, observed R_{ST} values were not significantly higher than permuted R_{ST}, suggesting that stepwise mutations did not contribute to population differentiation and that F_{ST} (based on allele identity) explains genetic differentiation among populations better than R_{ST} (based on allele-size information; Hardy *et al.* 2003). Although F_{ST} is widely used as a measure of population structure, its dependency on expected heterozygosity might underestimate the genetic differentiation among populations. Higher levels of genetic differentiation among populations were detected, in fact, when the partition of diversity was based on the effective number of alleles (i.e. D_{est}, Jost 2008) rather than on the expected heterozygosity. We found D_{est}=0.179 between the two sub-populations of *R. lamarmorae*, and $0.003 <D_{est}<0.238$ for *R. corsica* (Table 4). Across populations, total D_{est} for *R. corsica* was 0.162.

The PCoA showed some genetic structure among *R. corsica* populations: while MU, MC and GH appeared strongly genetically interconnected, AL and BA overlapped only slightly, and SA was well separated from all other populations (Figure 3A). A clear genetic differentiation was also present between the two sub-populations of *R. lamarmorae* (Figure 3B). When considering both species together, population structure was still clearly present, although less marked: overall, the individuals of the two species diverged, but showed a certain degree of overlapping, populations within each species overlapped slightly more, and population SA, taxonomically assigned to *R. corsica*, remained well separated from all remaining populations (Figure 3C).

The Mantel test for correlation between genetic differentiation and geographic distances among populations was not significant (p=0.579, R^2 =0.0076).

For both *R. corsica* and *R. lamarmorae* the Ln probability of the data (Ln P($X|K$)) did not allow for discrimination between different values of K (Table S3) while, based on the ΔK statistic, the best-supported number of *a posteriori* genetic clusters was K=3 for *R. corsica* (Figure S1 A) and K=2 for *R. lamarmorae* (Figure S1 B). For K=3, populations of *R. corsica* MU, MC, GH and AL were grouped together, while SA and BA appeared genetically distinct (Figure 4A). Very little admixture seemed to occur between the two *R. lamarmorae* subpopulations for K=2 (Figure 4B). When *R. corsica* and

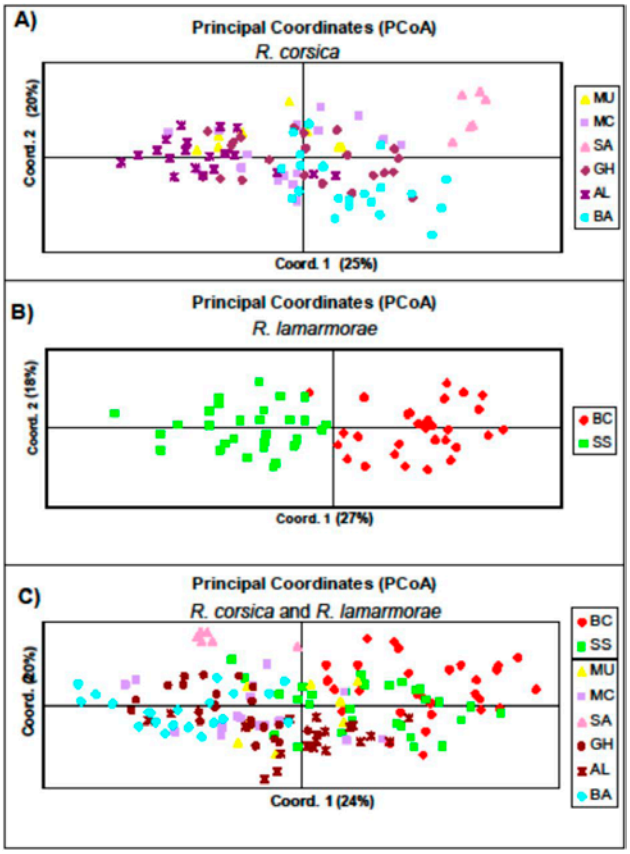

Figure 3. Principal Coordinate Analysis (PCoA) based on the multilocus genotypes of 96 individuals of *R. corsica* (A), 60 individuals of *R. lamarmorae* (B), and the two species together (C). The percentage of the total variability explained by the first two components is indicated on brackets. Each symbol represents a single plant from one of the eight studied populations. Information on each population is provided in Table 1.

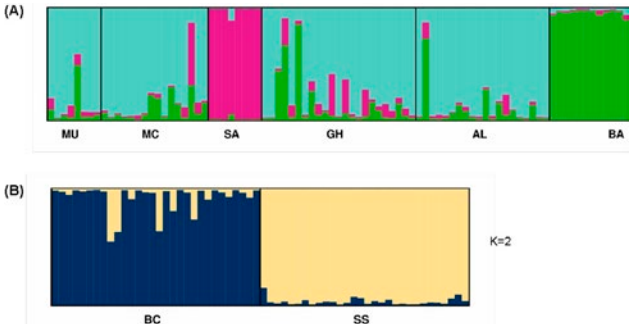

Figure 4. Proportional membership (*Q*) to clusters identified by STRUCTURE for: (A) 96 individuals from the six studied populations *of R. corsica;* (B) 60 individuals from the two studied subpopulations of *R. lamarmorae*. Colours distinguish between the different clusters identified for each of the above three scenarios. Each individual is represented by a single vertical bar and grouped by locality, indicated on the x-axis. Information on each population (locality) is provided in Table 1.

R. lamarmorae were pooled together, the most effective number of genetic groups was *K*=4 according to Pritchard's method (Pritchard *et al.* 2000, Table S3) and *K*=2 according to Evanno's method (Evanno *et al.* 2005, Figure S1 C). Figure 5 shows subfigures for *K*=4 and *K*=2; subfigures were included also for *K*=3 and 5<*K*<7, because populations subdivision was informative also for these values of *K*. For *K*=2, populations of the two species were well separated in two distinct *R. corsica* and *R. lamarmorae* clusters, except for population SA, taxonomically classified as *R. corsica*, whose individuals were genetically assigned with higher probability to populations of *R. lamarmorae* (Figure 5). Values of *K*=3 showed the separation of the two *R. lamarmorae* subpopulations, while population SA (of *R. corsica)* clustered with sub-population SS (of *R. lamarmorae;* Figure 5). For *K*=4, *R. lamarmorae* sub-populations were genetically distinct, population SA was separated from all populations, while the remaining populations of *R. corsica* formed a single cluster (Figure 5). Values of *K*=5 showed the separation of the *R. corsica* population BA (Figure 5). Values of *K*=6 and *K*=7 showed more admixture. It is notable that population SA, taxonomically assigned to *R. corsica*, remained separated from all other populations for all *K* values (Figure 5)

DISCUSSION

Microsatellite development and cross-species amplification

Most of the microsatellites developed for this study were suitable for genetic analyses on *R. lamarmorae* (13 out of 15), *R. corsica* (13 out of 15) and the more distantly related *R. chalepensis* (11 out of 15), being amplifiable and polymorphic (Table S1). Despite the difference in ploidy level between *R. corsica* (diploid) and *R. lamarmorae* (tetraploid), the high transferability of the molecular markers suggests a low divergence between the genomes of the two species.

Genetic diversity

Among the microsatellite markers developed for the present study, 11 were useful for population genetic analyses on *R. corsica* and *R. lamarmorae*. Our study revealed high levels of genetic diversity in both *R. corsica* (*P*=0.883, H_e=0.543) and *R. lamarmorae* (*P*=0.972, H_e=0.627). Even though each species is restricted to a single island (Fig-

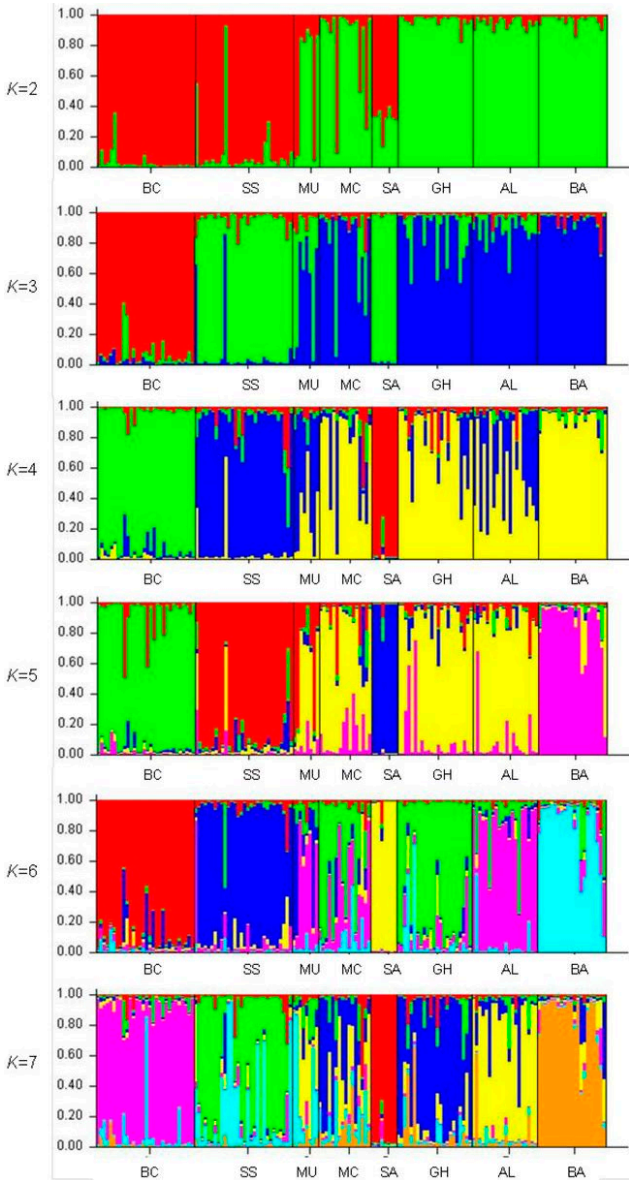

Figure 5. Proportional membership (*Q*) to clusters identified by STRUCTURE for 2<*K*<7. Colours distinguish between the different *K* clusters. All studied individuals of *R. lamarmorae* (sub-populations BC and SS: 60 individuals) and *R. corsica* (populations MU, MC, SA, GH, AL and BA: 96 individuals) are represented by vertical bars and grouped by locality, indicated on the x-axis. Information on each population (locality) is provided in Table 1.

ure 1), most populations showed fewer genetic signatures of isolation and small population size than typically expected for insular endemics (i.e., low gene diversity, high homozygosity, high LD; Ellstrand 1993, Frankham 1998, Bouzat 2010). Unexpectedly high values of genetic diversity were also found in the congener *R. oreojasme*, an endangered species endemic to the island of Gran Canaria in the Canarian archipelago (A=7.625, P=0.984, H_o=0.558, H_e=0.687; Meloni *et al.* 2015).

The occurrence of another endangered, insular endemic with high genetic diversity within the same genus suggests that *R. corsica* and *R. lamarmorae* share some intrinsic traits maintaining high levels of genetic variation with *R. oreojasme*. Hermaphroditism and proterandry, characterising all three endemics, favour outcrossing, thus increasing genetic diversity. Furthermore, polyploidy, occurring in all *Ruta* species except *R. corsica*, might also contribute to elevated genetic variation, for polyploids are usually characterised by higher genetic diversity than diploids (Soltis and Soltis 2000). Hermaphroditism, proterandry and polyploidy were associated with high levels of genetic variation also in other insular endemics outside of *Ruta* (Pérez de Paz and Caujapé-Castells 2013). Conversely, genetic analyses of *R. microcarpa*, a critically endangered species endemic to the island of La Gomera (also in the Canarian archipelago), revealed levels of genetic diversity lower than those observed in *R. corsica, R. lamarmorae* and *R. oreojasme* (H_o=0.651, H_e=0.410; Meloni *et al.* 2014). The relatively low genetic diversity found in *R. microcarpa*, resulting mainly from the almost total absence of sexual reproduction in this species (Meloni *et al.* 2015), highlights the role of outcrossing in maintaining variation within and among populations.

Despite the relatively low number of population genetic studies on C-S species, a general trend of high genetic diversity was detected in published analyses of Corsican and/or Sardinian endemics. High levels of genetic variability were found, for example, in the Sardinian *Centaurea horrida* (H_e=0.780, Mameli *et al.* 2008) and *Centaurea filiformis* (H_e=0.678, Pisanu *et al.* 2011; H_e = 0.576; Giorgio Binelli, pers. comm.), in the Corso-Sardinian *Ferula arrigonii* (P=0.92, H_w = 0.317, Dettori *et al.* 2014b), and in the Corsican *Mercurialis corsica* (Migliore *et al.* 2011).

The occurrence of high genetic diversity in several C-S species suggests that also some geographic factors (i.e., age, physical dimension, geologic origin and history of the islands) might have contributed to the genetic diversity of *R. corsica* and *R. lamarmorae* as well as of several other C-S endemics.

The complex geologic history of Corsica and Sardinia most likely influenced the evolution and current genetic diversity of their endemics in different ways. Corsica and Sardinia are considered old islands (they broke off from the Iberian peninsula as the C-S microplate ca. 30-28 MYA) and have been proposed to harbour many relictual endemics (Médail and Quézel 1999, Grill *et al.* 2007). Because they are continental fragment

islands, it has been suggested that they might have hosted the ancestors of many of their current endemic taxa before their separation from the Iberian peninsula in the Oligocene, although this hypothesis has been corroborated by molecular dating analyses only in a few cases (for example, in Araceae; Mansion *et al*. 2008). Subsequent to its split from the Iberian peninsula, the C-S microplate was temporarily connected with the Apulian microplate during the Miocene. The vicariant origin of some C-S species during the Oligocene and Miocene might have favoured relatively high levels of genetic diversity, because they did not experience the loss of genetic variation associated to LDD and founder events typical, for example, of oceanic island colonization. Furthermore, the long time-spans since colonisations (from either the Iberian peninsula in the Oligocene or the Apulian microplate in the Miocene) might have increased opportunities to accumulate genetic variation through mutation, recombination, drift and selection in CS endemics. Additionally, multiple overland migrations might have occurred while Corsica and Sardinia were connected to neighbouring continental masses via land bridges at different points in time during the Miocene and Pleistocene, thus favouring genetic exchanges also within species with limited dispersal ability, as in the case of *R. corsica* and *R. lamarmorae* (Gianluigi Bacchetta, pers. obs.).

Furthermore, the relatively stable climate characterising Corsica and Sardinia during Quaternary glacial/interglacial periods (Taberlet 1998, Grill *et al*. 2007) might also have contributed to the high genetic diversity detected in their endemics, for it allowed populations of many species to persist through several climatic cycles and accumulate genetic differences via mutation and recombination. Finally, climatic changes during the Miocene and Pleistocene might have also contributed to the high genetic variation detected in C-S species. Indeed, land bridges among Corsica, Sardinia, the Apulian plate and the African continent during the MSC (Hsü *et al*. 1977, Krijgsman *et al*. 1999, McKenzie 1999) and Quaternary glacial marine regressions (Thompson 2005) may have decreased the genetic effects of isolation by favouring genetic exchange between C-S populations and populations of the same species occurring on other land masses. Among the above mentioned island-dependent factors, the vicariant origin of the ancestor of *R. corsica* and *R. lamarmorae* following the MSC, supported by molecular dating and biogeographic analyses (Salvo *et al*. 2010), and the climatic stability of Corsica and Sardinia during Pleistocene glacial cycles might have contributed to the relatively high levels of genetic diversity detected in the two species.

Ruta lamarmorae showed slightly higher values for most diversity parameters than *R. corsica* (P=0.967, H_o=0.571, H_e=0.627 vs. P=0.83, H_o=0.536, H_e=0.543). As mentioned above, the higher ploidy of the former might explain this difference. In addition to intrinsic traits, the small size of most *R. corsica* populations (Laetitia Hugot, pers. obs.) and its scattered distribution could also explain the lower diversity found in *R. corsica*, because its populations might be more affected by inbreeding and isolation than the larger population of *R. lamarmorae* (Hamrick and Godt 1989; Ouborg *et al*. 2006).

An exception to the trend of relatively high genetic diversity found in *R. corsica* and *R. lamarmorae* is represented by population SA (taxonomically assigned to *R. corsica*), which showed some genetic erosion, being characterised by values of polymorphism, allelic diversity and heterozygosity much lower than the other populations analysed in this study (N_A =22, P=0.6, H_o=0.350, H_e=0.323, Table 3). The low genetic diversity and the presence of alleles fixed at four loci suggest that genetic drift and inbreeding strongly influenced the genetic structure of this small population (20 individuals in total; Laetitia Hugot, unpublished data; Ellstarnd *et al* 1993). They also suggest that the rate of genetic exchange between SA and other *R. corsica* populations, even the closest ones from a geographical point of view, is extremely low, and it seems unable to counteract the genetic effects of small population size.

Population genetic structure

Genetic differentiation among populations measured with F_{ST} and AMOVA (Table 4 and Figure 2 respectively) was lower than expected, when considering the low dispersal ability of *R. corsica* and *R. lamarmorae* (Gianluigi Bacchetta, unpublished data). Because F_{ST} is strongly influenced by levels of heterozygosity (Meirmans and Hedrick 2011), we cannot rule out the possibility that F_{ST} values (and AMOVA, accordingly) may simply reflect the high levels of heterozygosity detected in our study species (Table 3), and that in this case D_{est} (which is based on the effective number of alleles and thus independent of levels of heterozygosity; Jost 2008; Table 4) might better describe genetic differentiation among populations. Indeed, D_{est} values are approximately two times larger than F_{ST} values (F_{ST}=0.097, D_{est}=0.162 for *R. corsica;* F_{ST}=0.086, D_{est}=0.179 for *R. lamarmorae*), suggesting that the studied populations might be more differentiated than implied by F_{ST}. High values of heterozygosity and lower levels of F_{ST} than D_{est} were also found in the congener *R. oreojasme* (H_e= 0.687, F_{ST} = 0.097, D_{est} = 0.275; Meloni *et al*. 2015).

The differentiation among populations described by D_{est} (high for *R. lamarmorae*, relatively lower for *R. corsica;* Table 4) was supported by PCoA (Figure 3) and Bayesian analyses (Figures 4 and 5). The population structure detected in the two species (Figures 3, 4 and 5) and the absence of isolation by distance reiterates that limited gene flow probably due to low dispersal ability has played a significant role in shaping current patterns of genetic differentiation. Low dispersal ability seems to characterise particularly *R. lamarmorae*, whose sub-populations, showing the highest value of within-species D_{est} and appearing genetically well separated in PCoA and Bayesian analyses (Figures 3B and 4), are only ca. 3 km apart from each other. Analyses that included both species indicated some genetic differentiation between *R. corsica* and *R lamarmorae* (Table 4, Figures 3C and 5), lending some support to their taxonomic classification as separated species. However, some degree of admixture between them was detected. The difference in ploidy level (*R. corsica* is diploid, *R. lamarmorae* is tetraploid; Contandriopoulos 1957, Honsell 1957) and their geographic separation through the Bonifacio strait suggest that relatively low levels of admixture detected might not be the effect of gene flow between islands. Instead, this result might be better explained by the possibility that *R. corsica* and *R. lamarmorae* diverged at only few loci, probably as a consequence of low mutation rate and/or the long generation time that characterises the two species. Further analyses would be required to test this hypothesis. The high transferability of the newly developed microsatellite markers between the two species (Table S1) supports the hypothesis of low divergence.

In all genetic analyses, population SA (of *R. corsica*) strongly differed from all other studied populations (Table 4), forming a distinct group in both PCoA (Figures 3A and 3C) and STRUCTURE analyses (Figures 4 and 5). This result reinforces the conclusion that SA is more genetically isolated than the other studied populations. Because geographic distance does not explain this genetic isolation, other factors seem to affect gene flow in this population. Interestingly, in STRUCTURE analyses that included *R. corsica* and *R. lamarmorae*, population SA showed evidence of genetic admixture between the two species for K=2 (the most accurate estimate of the number of clusters obtained measuring ΔK; Evanno *et al*. 2005), was assigned to the same genetic group of *R. lamarmorae* sub-population SS for K=3, and resulted genetically differentiated from all other studied populations of both species for $4<K<7$ (Figures 5). Further genetic and karyotype studies are required to clarify the reasons of the genetic differentiation of SA. Genetic analyses on the congener *R. chalepensis*, occurring in both islands, might also help to clarify the occurrence and amount of gene flow between Corsica and Sardinia.

Conservation implications

This study provides important insights into the genetic structure of *R. corsica* and *R. lamarmorae*, with potential applications for their effective conservation. The medium to high genetic diversity characterising these endemics suggests that both species are not at high risk of extinction due to genetic factors. Nevertheless, their isolation, their very restricted distribution, the small size of *R. corsica* populations and, in the case of *R. lamarmorae*, the continued anthropogenic and environmental threats to its population (i.e., overgrazing, fires, presence of skiing infrastructures; Bacchetta *et al*. 2006) might jeopardize conservation. Moreover, mountain habitats are considered particularly sensitive to climatic change and are likely to show the effects of temperature increase earlier and more markedly than other ecosystems (Grabherr *et al*. 2000; Thuiller *et al*. 2005; Patsiou *et al*. 2014). Germination tests in *R. lamarmorae* show that an increase in winter temperatures could lead to reduced reproductive capability, because seeds may not experience the vernalization period required for germination (Bacchetta *et al*., unpublished data). We expect a similar negative effect on germination in *R. corsica*, given the close relatedness with *R. lamarmorae*, the phenotypic traits they share, and the shared ecological preference for mountain habitats. Similarly, a reduction in seed germination rate with increasing temperatures has been observed in other Sardinian taxa that occur at medium to high altitudes, including *Lamyropsis microcephala* (Mattana *et al*. 2009), *Rhamnus persicifolia* (Bacchetta et al. 2011), *Ribes multiflorum* subsp. *sandalioticum* (Mattana *et al*. 2012), and *Vitis vinifera* subsp. *sylvestris* (Orrù *et al*. 2012).

In situ conservation is essential to the long-term persistence of these two island endemics and should be aimed at preserving all extant populations, for they all carry unique alleles (a particular case is represented by population SA, whose low genetic diversity and high differentiation require further genetic analyses; Tables 3 and 4, Figures 3 and 5). For *R. lamarmorae*, seeds from sub-population BC were already collected for long-term storage at the BG-SAR (the Sardinian Germplasm Bank, University of Cagliari). Given the high differentiation detected between sub-populations BC and SS of *R. lamarmorae*, germplasm collection should be planned also from SS. Genetic studies on the eastern part of the Gennargentu massif are also advisable, because sub-populations from this area might show genetic differentiation as high as that found in the two *R. lamarmorae* sub-populations analysed here. Finally, more detailed studies

on the reproductive biology and dispersal ability of these species are fundamental for planning specific, and thus potentially successful, conservation programs and guarantee their long-term survival.

ACKNOWLEDGEMENTS

M. M. and the project were funded by the Swiss National Science Foundation (SNSF) PMPDP3_129170. Participation to a conference was funded by the Claraz Schenkung. This work is part of the doctoral thesis of C.A.D., funded by the Biodiversity Conservation Center (University of Cagliari).

DECLARATION OF INTEREST

The authors declare that they have no conflict of interest.

REFERENCES

Alvarez W. 1972. Rotation of Corsica-Sardinia microplate. Nature-Phys Sci. 235:103–105.

Alvarez W. 1976. A former continuation of Alps. Geol Soc Am Bull. 87:891–896.

Alvarez W, Cocozza T, Wezel FC. 1974. Fragmentation of alpine orogenic belt by microplate dispersal. Nature 248:309–314.

Arrigoni PV. 1983. Aspetti corologici della flora sarda. Lav Soc Ital Biogeogr. 8:81–109.

Bacchetta G, Pontecorvo CR. 2005. Contribution to the knowledge of the endemic vascular flora of Iglesiente (SW Sardinia-Italy). Candollea 60:481-501.

Bacchetta G, Brullo S, Giusso del Galdo G. 2006. *Ruta lamarmorae* (Rutaceae), a new species from Sardinia. Edinb J Bot. 63:153–160.

Bacchetta G, Coppi A, Pontecorvo C, Selvi F. 2008. Systematics, phylogenetic relationships and conservation of the taxa of *Anchusa* (Boraginaceae) endemic to Sardinia (Italy). Syst Biodivers.:161–174.

Bacchetta G, Fenu G, Mattana E. 2012. A checklist of the exclusive vascular flora of Sardinia with priority rankings for conservation. An Jardín Bot Madrid 69:61–69.

Bacchetta G, Fenu G, Mattana E, Zecca G, Grassi F, Casazza G, Minuto L. 2011. Genetic variability of the narrow endemic *Rhamnus persicifolia* Moris (Rhamnaceae) and its implications for conservation. Biochem Syst Ecol. 39:477–484.

Blondel J, Aronson J, Bodiou JY, Boeuf G. 2010. The Mediterranean region: biological diversity in space and time. 2nd ed. New York (NY): Oxford University Press.

Bouzat JL. 2010. Conservation genetics of population bottlenecks: the role of chance, selection, and history. Conserv Genet. 11:463–478.

Cañadas EM, Fenu G, Penas J, Lorite J, Mattana E, Bacchetta G. 2014. Hotspots within hotspots: endemic plant richness, environmental drivers, and implications for conservation. Biol Conserv. 170:282–291.

Cardona MA, Contandriopoulos J. 1979. Endemism and evolution in the islands of the Western Mediterranean (p. 133–169). Plants and islands. London: Academic Press.

Cherchi A, Montadert L. 1982. Oligo-Miocene rift of Sardinia and the early history of the Western Mediterranean basin. Nature 298:736–739.

Contandriopoulos J. 1957. Caryologie et localisation des espèces végétales endémiques de la Corse. Bull Soc Bot France 104:53–55.

Conti F, Abbate G, Alessandrini A, Blasi C. (eds.) 2005. An Annotated Checklist of the Italian Vascular Flora. Roma: Palombi Editori.

Conti F, Alessandrini A, Bacchetta G, Banfi E, Barberis G, Bartolucci F, Bernardo L, Bonacquisti S, Bouvet D, Bovio M., *et al.* 2007. Integrazioni alla checklist della flora vascolare italiana. Natura Vicentina 10:5–74.

Coppi A, Mengoni A, Selvi F. 2008. AFLP fingerprinting of *Anchusa* (Boraginaceae) in the Corso-Sardinian system: Genetic diversity, population differentiation and conservation priorities in an insular endemic group threatened with extinction. Biol conserv. 141:2000–2011.

Crawford NG. 2010 SMOGD: software for the measurement of genetic diversity. Mol Ecol Resour. 10:556–557.

de Montmollin B, Strahm W. (eds.) 2005. The Top 50 Mediterranean Island Plants: Wild 578 Plants at the Brink of extinction and what is needed to save them. Switzerland and Cambridge: IUCN, Gland.

Dettori CA, Murru V, Fenu G, Santo A, Bacchetta G. 2014. Schede per una Lista Rossa della Flora vascolare e crittogamica Italiana: *Ruta lamarmorae* Bacch., Brullo *et* Giusso. Inform Bot Ital. 46:142–144.

Dettori CA, Sergi S, Tamburini E, Bacchetta G. 2014b. The genetic diversity and spatial genetic structure of the Corso-Sardinian endemic *Ferula arrigonii* Bocchieri (Apiaceae). Plant Biol 16:1005–1013.

Earl DA, vonHoldt BM. 2012. STRUCTURE HARVESTER: a website and program for visualizing STRUCTURE output and implementing the Evanno method. Conserv Genet Resour. 4:359–361.

Ellstrand NC, Elam DR. 1993. Population Genetic Consequences of Small Population Size: Implications for Plant Conservation. Annu Rev Ecol Syst. 24:217–242.

Evanno G, Regnaut S, Goudet J. 2005. Detecting the number of clusters of individuals using the software STRUCTURE: a simulation study. Mol Ecol. 14:2611–2620.

Excoffier L, Smouse PE, Quattro JM. 1992 Analysis of molecular variance inferred from metric distances among DNA haplotypes: Application to human mitocondrial DNA restriction sites. Genetics 131:479–491.

Fenu G, Fois M, Cañadas EM, Bacchetta G. 2014. Using endemic-plant distribution, geology and geomorphology in biogeography: the case of Sardinia (Mediterranean Basin). Syst Biodivers. 12:181–193.

Frankham R. 1998. Inbreeding and extinction: island populations. Conserv Biol. 12:665–675.

Garrido JL, Fenu G, Mattana E, Bacchetta G. 2012. Spatial genetic structure of *Aquilegia* taxa endemic to the island of Sardinia. Ann Bot. 109:953–964.

Gentili R., Badola HK, Birks JB. 2015. Alpine biodiversity and refugia in a changing climate. Biodiversity 16:193–195.

Goudet J. 1995. Fstat version 1.2: a computer program to calculate Fstatistics. J Hered. 86:485–486.

Grabherr G, Gottfried M, Pauli H. 2000. GLORIA: a global observation research initiative in alpine environments. Mt Res Dev 20:190–192.

Grill A, Casula P, Lecis R, Menken S. 2007. Endemism in Sardinia. In:Weiss S., Ferrand N. (eds.) Phylogeography of southern European refugia. Dordrecht: Springer; p. 273–296.

Guo SW, Thompson EA. 1992. Performing the exact test of Hardy-Weinberg proportions for multiple alleles. Biometrics 48:361–372.

Hamrick JL, Godt MJW. 1989. Allozyme diversity in plant species. In: Brown HD, Clegg MT, 611 Kahler AL, Weir BS (eds.). Plant population genetics. Breeding and Germplasm Resources. Sunderland (MA): Sinauer; pp 43-63.

Hardy OJ, Charbonnel N, Fréville H, Heuertz M. 2003. Microsatellite allele sizes: a simple test to assess their significance on genetic differentiation. Genetics 163:1467–1482.

Hardy OJ, Vekemans X. 2002. SPAGeDi: a versatile computer program to analyse spatial genetic structure at the individual or population levels. Mol Ecol Notes 2:618–620.

Hedrick PW. 2005. A standardized genetic differentiation measure. Evolution 59:1633–1638.

Hewitt G. 2000. The genetic legacy of the Quaternary ice ages. Nature 405:907–913.

Honsell E. 1957. Ricerche cario-embriologiche in *Ruta corsica* DC. Delpinoa 10:141–153.

Hsü KJ, Montadert L, Bernoulli D, Cita MB, Erickson A, Garrison RE, Kidd RB, Melieres F, Muller C, Wright R. 1977. History of Mediterranean salinity crisis. Nature 267 :399–403.

Hubisz M, Falush D, Stephens M, Pritchard J. 2009. Inferring weak population structure with the assistance of sample group information. Mol Ecol Resour 9:1322–1332.

Huff DR, Peakall R, Smouse PE. 1993. RAPD variation within and among natural populations of outcrossing buffalograss [*Buchloe dactyloides* (Nutt.) Engelm.]. Theor Appl Genet. 86:927–934.

IUCN Standards and Petitions Subcommittee. 2013. Guidelines for Using the IUCN Red List 628 Categories and Criteria. Version 10. Prepared by the Standards and Petitions Subcommittee. Downloadable from http://jr.iucnredlist.org/documents/RedList-Guidelines.pdf 630

Jeanmonod D, Gamisans J. 2013. Flora Corsica. (2nd ed.) Jarnac: SBCO.

Jost L. 2008. G_{ST} and its relatives do not measure differentiation. Mol Ecol. 17:4015–4026.

Krijgsman W, Hilgen FJ, Sierro FJ, Wilson DS. 1999. Chronology, causes and progression of the Messinian salinity crisis. Nature 400:652–655.

Luikart G, Allendorf FW, Cornuet JM, Sherwin WB. 1998. Distortion of allele frequency distributions provides a test for recent population bottlenecks. J Hered. 89:238–247.

Mameli G, Filigheddu R, Binelli G, Meloni M. 2008. The genetic structure of the remnant populations of *Centaurea horrida* in Sardinia and associated islands. Ann Bot. 101:633–640.

Mansion G, Rosenbaum G, Schoenenberger J, Bacchetta G, Rosselló J, Conti E. 2008. Phylogenetic analysis informed by geological history supports multiple, sequential invasions of the Mediterranean basin by the Angiosperm family Araceae. Syst Biol. 57:269–285.

Mantel N. 1967. The detection of disease clustering and a generalized regression approach. Cancer Res 27:209–220.

Mattana E, Daws MI, Bacchetta G. 2009. Seed dormancy and germination ecology of *Lamyropsis microcephala*: a mountain endemic species of Sardinia (Italy). Seed Sci Technol. 37:491–497.

Mattana E, Pritchard HW, Porceddu M, Stuppy WH, Bacchetta G. 2012. Interchangeable effects of gibberellic acid and temperature on embryo growth, seed germination and epicotyl emergence in *Ribes multiflo-*

rum ssp. *sandalioticum* (Grossulariaceae). Plant Biol. 14:77–87.

McKenzie JA. 1999. From desert to deluge in the Mediterranean. Nature 400:613-614.

Médail F, Diadema K. 2009. Glacial refugia influence plant diversity patterns in the Mediterranean Basin. J Biogeogr 36:1333–1345.

Médail F, Myers N. 2004. Mediterranean Basin. In: Mittermeier RA, Robles Gil P, Hoffmann M, Pilgrim J, Brooks T, Mittermeier CG, Lamoreux J, da Fonseca GAB. (eds.), Hotspots revisited: Earth's Biologically Richest and Most Endangered Terrestrial Ecoregions. Monterrey, Washington, Mexico: CEMEX, Conservation International & Agrupación Sierra Madre; p. 144–147.

Médail F, Quézel P. 1997. Hot-spots analysis for conservation of plant biodiversity in the Mediterranean basin. Ann Moi Bot Gard. 84:112–127.

Médail F, Quézel P. 1999. Biodiversity hotspot in the Mediterranean basin: setting global conservation priorities. Conserv Biol. 13:1510–1513.

Meirmans PG, Hedrick PW. 2011. Assessing population structure: F_{ST} and related measures. Mol Ecol Resour 11:5–18.

Meloni M, Reid A, Caujapé-Castells J, Marrero Á, Fernández-Palacios JM, Mesa-Coelo RA, Conti E. 2013. Effects of clonality on the genetic variability of endangered rare, insular species: the case of *Ruta microcarpa* from the Canary Islands. Ecol Evol. 671 3:1569–1579.

Meloni M, Reid A, Caujapé-Castells J, Soto M, Fernández-Palacios J M, Conti E. 2015. High genetic diversity and population structure in the endangered Canarian endemic *Ruta oreojasme* (Rutaceae). Genetica 143:571–580.

Michalakis Y, Excoffier L. 1996. A generic estimation of population subdivision using distances between alleles with special reference for microsatellite loci. Genetics 142:1061–1064.

Migliore J, Baumel A, Juin M, Diadema K, Hugot L, Verlaque R, Médail F. 2011. Genetic diversity and structure of a Mediterranean endemic plant in Corsica (*Mercurialis corsica*, Euphorbiaceae). Popul Ecol. 53:573–586.

Mishler BD, Knerr N, González-Orozco CE, Thornhill AH, Laffan SW, Miller JT. 2014. Phylogenetic measures of biodiversity and neo- and paleo-endemism in Australian *Acacia*. Nat Commun. 5.

Mittermeier RA, Robles Gil P, Hoffman M, Pilgrim J, Brooks T, Mittermeier CG, Lamoreux J, da Fonseca GAB. 2005. Hotspots revisited: earth's biologically richest and most endangered terrestrial ecoregions. Chicago: University of Chicago Press.

Myers N, Mittermeier RA, Mittermeier CG, Da Fonseca GAB, Kent J. 2000. Biodiversity hotspots for conservation priorities. Nature 403:853–858.

Nei M. 1972. Genetic distance between populations. Am Nat 106:283–392.

Nei M. 1978. Estimation of average heterozygosity and genetic distance from a small number of individuals. Genetics 89:583–590.

Nekola JC. 1999. Paleorefugia and Neorefugia: The influence of colonization history on community pattern and process. Ecology 80 :2459–2473.

Orrù M, Mattana E, Pritchard WH, Bacchetta G. 2012. Thermal thresholds as predictors of seed dormancy release and germination timing: altitude-related risks from climate warming for the wild grapevine *Vitis vinifera* subsp. *sylvestris*. Ann Bot. 110:1651–1660.

Orsini J, Coulon C, Cocozza T. 1980. Le dérive cénozoique de la Corse et de la Sardaigne. Géologie Alpine 56:169–202.

Ouborg NJ, Vergeer P, Mix C. 2006. The rough edges of the conservation genetics paradigm in plants. J Ecol. 94:1233–1248.

Patsiou TS, Conti E, Zimmermann NE, Theodoridis S and Randin CF. 2014. Topo-climatic microrefugia explain the persistence of a rare endemic plant in the Alps during the last 21 millennia. Glob Change Biolo. 20:2286–2300.

Peakall R, Smouse PE. 2012. GenAlEx 6.5: genetic analysis in Excel. Population genetic software for teaching and research-an update. Bioinformatics 28:2537–2539.

Peakall R, Smouse PE, Huff DR. 1995. Evolutionary implications of allozyme and RAPD variation in diploid populations of dioecious buffalograss *Buchloe dactyloides*. Mol Ecol. 4:135–148.

Pérez de Paz J, Caijapé-Castells J. 2013. A review of the allozyme data set for the Canarian endemic flora: causes of the high genetic diversity levels and implications for conservation. Ann Bot. 111:1059–1073.

Piry S, Luikart G, Cornuet JM. 1999. Bottleneck: a computer program for detecting recent reductions in the effective population size using allele frequency data. J Hered. 90:502–503.

Pisanu S, Mameli G, Farris E, Binelli G, Filigheddu R. 2011. A natural homoploid hybrid between *Centaurea horrida* and *Centaurea filiformis* (Asteraceae) as revealed by morphological and genetic traits. Folia Geobot. 46:69–86.

Pritchard JK, Stephens M, Donnelly P. 2000. Inference of population structure using multilocus genotype data. Genetics 155:945–959.

Raymond M, Rousset F. 1995. GENEPOP (Version 1.2): population genetics software for exact tests and ecumenicism. J Hered. 86:248–249.

Rosenbaum G, Lister GS. 2004. Neogene and Quaternary rollback evolution of the Tyrrhenian Sea, the Apennines and the Sicilian Maghrebides. Tectonics 23:1.

Rosenbaum G, Lister GS, Duboz C. 2002. Reconstruction of the tectonic evolution of the western Mediterranean since the Oligocene. J Virt Expl 8:107–126.

Rousset F. 2008. Genepop'007: a complete re-implementation of the genepop software for Windows and Linux. Mol Ecol Resour 8:103–106.

Rozen S, Skaletsky H. 2000. Primer3 on the WWW for General Users and for Biologist Programmers. In: Krawetz S., Misener S. (eds.) Bioinformatics Methods and Protocols: Methods in Molecular Biology. Totowa (NJ): Humana Press; p. 365–386.

Salvo G, Bacchetta G, Ghahremaninejad F, Conti E. 2008. Phylogenetic relationships of Ruteae (Rutaceae): new evidence from the chloroplast genome and comparisons with non-molecular data. Mol Phylogenet Evol. 49:736–748.

Salvo G, Ho SYW, Rosembaum G, Ree R, Conti E. 2010. Tracing the temporal and spatial origins of island endemics in the Mediterranean Region: a case study from the *Citrus* family (*Ruta* L., Rutaceae). Syst Biol. 59:1–18.

Schuelke M. 2000. An economic method for the fluorescent labelling of PCR fragments. Nat Biotechnol 18:233–234.

Slatkin M. 1995. A measure of population subdivision based on microsatellite allele frequencies. Genetics 139:457–462.

Soltis PS, Soltis DE. 2000. The role of genetic and genomic attributes in the success of polyploids. P Natl A Sci. 97:7051–7057.

Speranza F, Villa IM, Sagnotti L, Florindo F, Cosentino D, Cipollari P, Mattei M. 2002. Age of he Corsica–Sardinia rotation and Liguro–Provençal Basin spreading: new paleomagnetic and Ar/Ar evidence. Tectonophysics 347:231–251.

Stift M, Berenos C, Kuperus P, van Tienderen PH. 2008. Segregation Models for Disomic, Tetrasomic and Intermediate Inheritance in Tetraploids: A general procedure applied to *Rorippa* (yellow cress) microsatellite data. Genetics 179:2113–2123.

Taberlet P, Fumagalli L, Wust-Saucy AG, Cosson JF. 1998. Comparative phylogeography and postglacial colonization routes in Europe. Mol Ecol. 7:453–464.

Thompson JD. 2005. Plant evolution in the Mediterranean. New York (NY): Oxford University Press.

Thuiller W, Lavorel S, Araujo MB, Sykes MT, Prentice C. 2005. Climate change threats to plant diversity in Europe. P Natl A Sci 23:8245–8250.

UICN France, FCBN, MNHN. 2012. La Liste rouge des espèces menacées en France – Chapitre Flore vasculaire de France métropolitaine : premiers résultats pour 1 000 espèces, sous-espèces et variétés. Dossier électronique.

Yesson C, Toomey NH, Culham A. 2009. Cyclamen: time, sea and speciation biogeography using a temporally calibrated phylogeny. J Biogeogr. 36:1234–1252.

Caryologia
International Journal of Cytology, Cytosystematics and Cytogenetics

Firenze University Press
www.fupress.com/caryologia

OPEN ACCESS

Citation: C. Alaca, A. Özdemir, B. Bozdağ, C. Özdemir (2020) Cytogenetic effects of C_6H_4 $(CH_3)_2$ (xylene) on meristematic cells of root tips of *Vicia faba* L. and mathematical analysis. *Caryologia* 73(1): 27-35. doi: 10.13128/caryologia-279

Received: May 31, 2019

Accepted: February 26, 2020

Published: May 8, 2020

Data Availability Statement: All relevant data are within the paper and its Supporting Information files.

Competing Interests: The Author(s) declare(s) no conflict of interest.

Cytogenetic effects of C_6H_4 $(CH_3)_2$ (xylene) on meristematic cells of root tips of *Vicia faba* L. and mathematical analysis

Cihangir Alaca[1], Ali Özdemir[1], Bahattin Bozdağ[2], Canan Özdemir[2,*]

[1] *Celal Bayar University, Science and Art Faculty, Mathematics Department, Manisa, Turkey*
[2] *Celal Bayar University, Science and Art Faculty, Biology Department, Manisa, Turkey*
*Corresponding author. E-mail: cozdemir13@gmail.com

Abstract. Xylene is a readily flammable and poisonous liquid with a chemical formula of C_6H_4 $(CH_3)_2$. It is used as raw material or auxiliary raw material in many industrial products such as dye, pencil, agricultural chemicals, rubber, fiber, glue and diaper. In this study, cytogenetic effects of xylene, on the meristematic cells of root tips of *V. faba* L. used as food have been investigated. For this purpose, the seeds of the plant have been treated with xylene solutions prepared in different concentrations for different time periods. Chromosomes at the root tips have been looked and the effect of xylene has been determined. The abnormalities as chromosome breaking, chromosome dispersion, bridge chromosome, chromosome adherence, ring chromosome have been observed. Abnormalities have been seen at each treatment depended on the time periods. In addition to these visible damages of xylene in the study, possible damages on chromosomes carrying genetic codes of living beings to future generations have been investigated and mathematical analyzes has been made. The results obtained have been evaluated statistically.

Keywords. Abnormalities, Chromosome, Mathematical analysis, Xylene.

1. INTRODUCTION

Xylene is a colorless, characteristic solvent odorous and liquid form raw material with a chemical formula of C_6H_4 $(CH_3)_2$ and molecular weight of 106.17 GR / MOL. It is formed by bonding two methyl groups to benzene and it is a readily flammable and poisonous liquid. Xylene may leak to surface, surface water or groundwater, where it may remain for months or more. Xylene is widely used industry and medical technology as a solvent, but concerns about its safety have been raised from time to time (Jenifer 1994). Health and safety authorities in most countries recommend a threshold limit value (TLV) of 100 ppm in the working environment. Xylene vapour is absorbed rapidly from the lungs, and xylen1. e liquid and vapour are absorbed slowly through the skin. Of the xylene absorbed, about 95%

is metabolised in the liver to MHA and 70 to 80% of metabolites are excreted in the urine within 24 hours. Differences are suspected between animal species, and between animals and humans, in the metabolism of, and sensitivity to, xylene (Langman 2009). There have been different studies about that the cytogenetic effects of some metals and chemical substances except to xylene on plant in literature. Various chemical substances which may be used in Medicine, Biology and Agricultural fields can affect negatively growth of both plants beside their positive effects (İnceer *et al*. 2003; Kıran and Şahin 2005). İnceer and Beyazoğlu (2000) have investigated cytogenetic effects of copper chloride on root cells of *Vicia hirsuta* (L.) S.F. Gray and they detected that this compund affects cell division negatively and also leads to chromosomel abnormalities. The researchers reported that compounds with mercury affect spindle threads during cell division in *V. faba* and *Allium cepa* L. (Leonard *et al*. 1983). Some researchers have made some investigations about the effects of heavy metal pollution on plants, resulted from different factors at environment and enterence of these elements into soil and plant (Çelik *et al*. 2004; Özdemir 2008; Özdemir *et al*. 2015; Şutan 2018).

In this study, we investigated the effects of xylene used as raw materials or auxiliary raw materials in many industrial products such as dye, pencil, agrochemicals, rubber, fibers, glue and diaper on chromosomes of *V. faba* used as food. Faba bean is one of the most important grain legumes in the world because of its multiple uses and its ability to grow over a wide range of climatic conditions (Kursheed *et al*.2018) The results of the research have been determined mathematically and the as statistical have been evaluated. For this purpose, xylene solutions have been prepared in different concentrations, and the seeds of the *V. faba* have been germinated with treatment with these solutions. Chromosomes at at the root tips have been looked and the effect of xylene has been determined.

The environment where xylene, a carcinogenic substance, is present at 100 ppm or more than 435 mg/m^3 in air is harmful to human health (Haglund *et al*. 1980). In addition to these visible damages of xylem in the study, possible damages on chromosomes carrying genetic codes of living beings to future generations have been investigated and mathematical analyzes have been made. The results obtained have been evaluated statistically.

2. MATERIAL AND METHODS

In our study, we determined the concentration of xylene by taking into consideration the application period and the level of harm to human health in the literature. The amounts given in the literature belong to the direct xylene effect of the human. We tried to determine this effect by applying on seed of *V. faba*, which commonly used by people as food. Thus, we used 10 ml / L, 10 ml / L, 12h and 24h values for the application. The seeds of *V. faba* have been treated with these concentrations of xylene during 12 and 24 hours. Then, the seeds have been has beenhed by distiled water and germinated in petri dish at 20-25 °C. The root tips obtained, have been put in 70 % ethyl alcohol after the fixation of they. Stock root tips have been stained by Feulgen method (Darlington and La Cour 1976) and have been got ready for microscopic examination. Homoligous areas have been chosen on these preparations for cytogenetic examination; the cells in these areas have been counted and the number of mitotic cells have been also detected. Chromosomel abnormalities have been tried to detected in the cells counted. Preparates has been photographed with motorized Leica DM 3000 microscope. Chromosome abnormalities detected in the study have been coded as A, B, C, D, E, F, G, H and I (Table 3). The concentrations and times of treatment have been coded as 1-4

(10 ml/L -12h): 1, (10 ml/L -24h): 2, (100 ml/L -12h): 3, (100 ml/L -24h): 4

We used following formulas for calculating the mitotic index and the percentage of total abnormalities. In this the study the cell numbers in per unit area (24x24mm) have been considered.

$$\text{Mitotic index} = \frac{\text{Number of dividing cells}}{\text{Total number of cells}} \text{ x } 100$$

$$\text{\% of total abnormalities} = \frac{\text{Number of cells with abnormal chromosome}}{\text{Total number of cells}} \text{ x } 100$$

Statistical analyses have been performed using MINITAB software package.

3. RESULTS

At the end of the study, it has been observed that different concentrations of xylene treatment on the seeds have been increased mitotic cell division at the different periods of time, compared with the control group (Figure 1). This situation has been reached on the top point at 12 hour of 100ml/L treatment. At the 12 hour

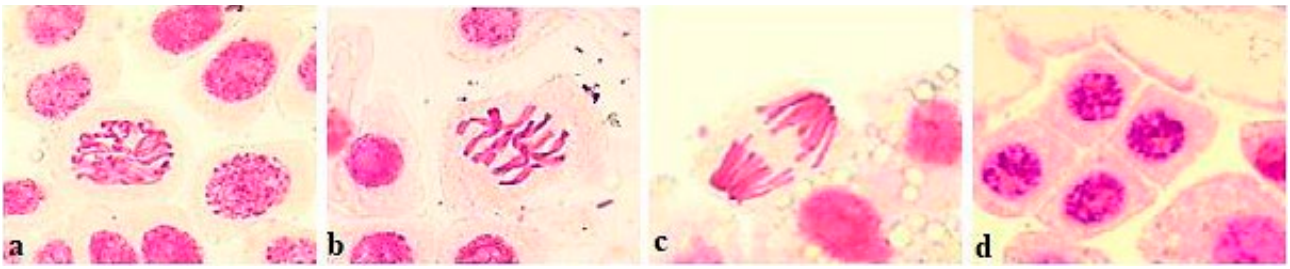

Figure 1. Photomicrographs of *V. faba* root tip meristem cells. Normal mitotic phases: (A) prophase, (B) metaphase, (C) anaphase, and (D) telophase.

Table 1. The mitotic index and total chromosome abnormalities in the root tip cells of *V. faba*.

	Control	10 ml/L		100 ml/L	
		12h	24h	12h	24h
Mitotic index (%) ± SD	12.02 ± 7.84	25.23 ± 11.12	20.02 ± 10.12	32.02 ± 17.14	27.03 ± 19.64
Total abnormalities (%)	0.00	03.13	10.21	07.05	18.03
The number of different chromosome abnormalities	0.00	2	9	6	4

S.D.- Standart Deviation, Time (h): hour.

Table 2. Number (%) of cells in each mitotic stage of *V. faba* roots treated with xylene.

Stages (%)	Control	10 ml/L		100 ml/L	
		12h	24h	12h	24h
Prophase	10.00	22.12	18.00	27.06	20.02
Metaphase	1.30	2.03	1.20	1.60	1.70
Anaphase	0.82	0.72	0.87	0.13	1.20
Telophase	0.42	0.02	0.60	1.12	2.02

Time (h): hour.

for 100ml/L of treatment, mitotic cell division has been decreased. Mitotic division increased again at the 12 and 24 hour of 100ml/L of treatment (Table 1,2). In the cells of the root tips of treated with xylene investigated seeds various chromosomel abnormalities as sticky chromosome, ring chromosome, chromosome breaking, bridge chromosome, vagrant chromosome, polar deviation, binucleated cell and scattered anaphase at different stages of mitotic division have been detected (Figure 2-8). Total abnormalities (%) has been observed high level all treatment for 24 hours of time according to 12 hours of time (Table 1-3). The number of different chromosome abnormalities have been observed the highest level at 10ml/L and 24 hour treatment time. Whereas the at least number of different chromosome abnormalities have been observed at 10ml/L and 12 hour treatment time. The chromosomel abnormalities with the highest percentage have been seen in sticky chromosome and ring chromosome. Bridge chromosomes have been seen as single, binary, triple and multiple bridge shaped in the all treatment except to control and 12h- 100ml/L treatment. Chromosome shrinking, ring chromosome and chromosome breaking have been seen all treatment times except to 10ml/L and 12 hour and control. Binucleated cell and Scattered anaphase have been seen in the all treatment except to control and 12h- 10ml/L treatment (Table 1-3; Figure 3,7)

Also, according to the statistical results derived, there is a considerable positive relation between the increase concentration of treatment and the mitotic index (%). On the other hand, there are positive relation between the time of treatment and the chromosome abnormality (%) (Table1-3).

The statistical analysis of the results are shown in Tables 1-8. According to Table 4 and 8 based on the Pearson's correlation and analysis of variance method

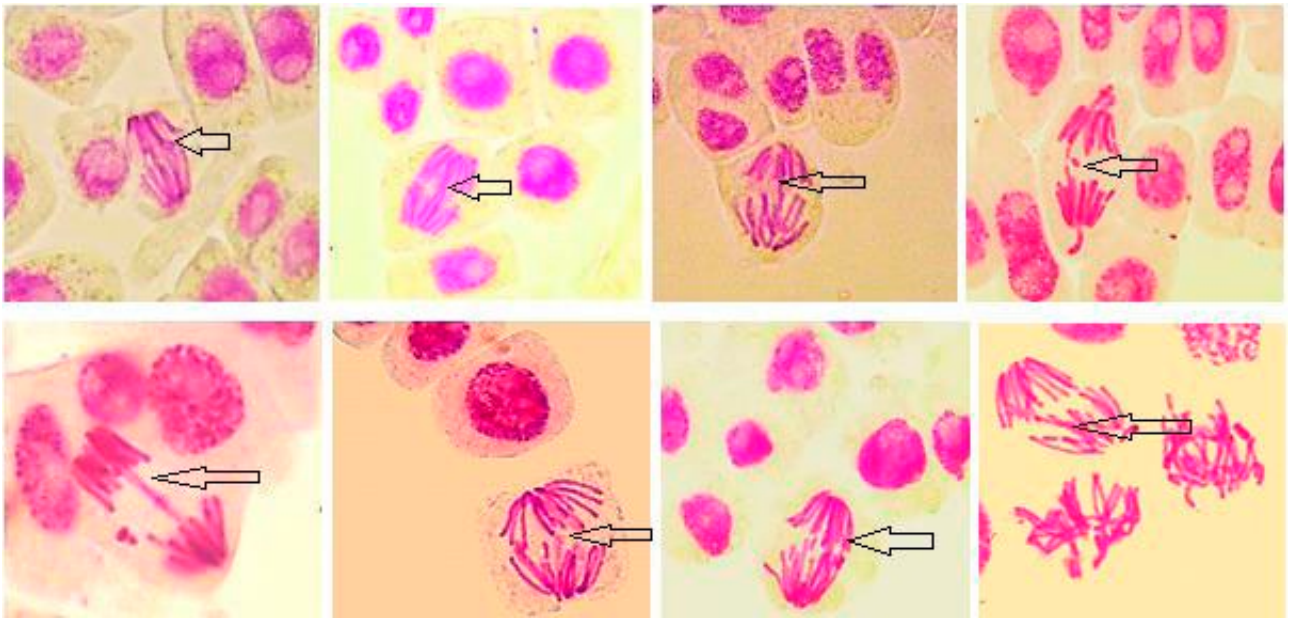

Figure 2. The xylene induced abnormalities: Anaphase bridges

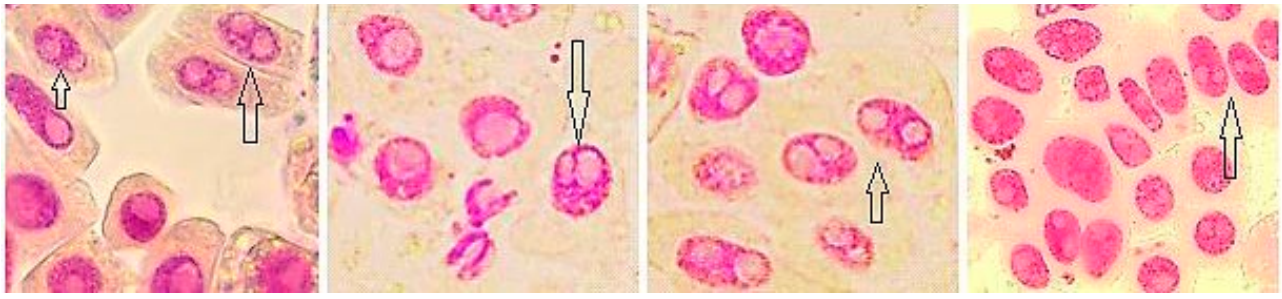

Figure 3. The xylene induced abnormalities: Binucleated cells

Table 3. The xylene induced chromosome abnormalities in the root tip cells of *V. faba.*

Chromosome abnormalities (%)		10 ml/L		100 ml/L	
		12h (1)	24h (2)	12h (3)	24h (4)
Sticky chromosome	**A**	1.30	2.30	1.50	3.20
Ring chromosome	**B**	1.30	3.20	1.20	2.10
Chromosome breaking	**C**	0.53	2.80	0.60	1.50
Bridge chromosome	**D**	0.00	1.21	1.10	4.30
Vagrant chromosome	E	0.00	0.00	1.40	3.20
Polar deviation	F	0.00	0.00	0.30	2.20
Binucleated cell	G	0.00	0.20	1.30	0.70
Scattered anaphase	**H**	0.00	0.10	0.10	0.80

Treatment time (h): hour. Abbreviations: A-H: Codes of chromosome abnormalities.
Abbreviations: 1-4 : Codes of Treatment (10 ml/L -12h): 1, (10 ml/L -24h): 2, (100 ml/L -12h): 3, (100 ml/L -24h): 4.

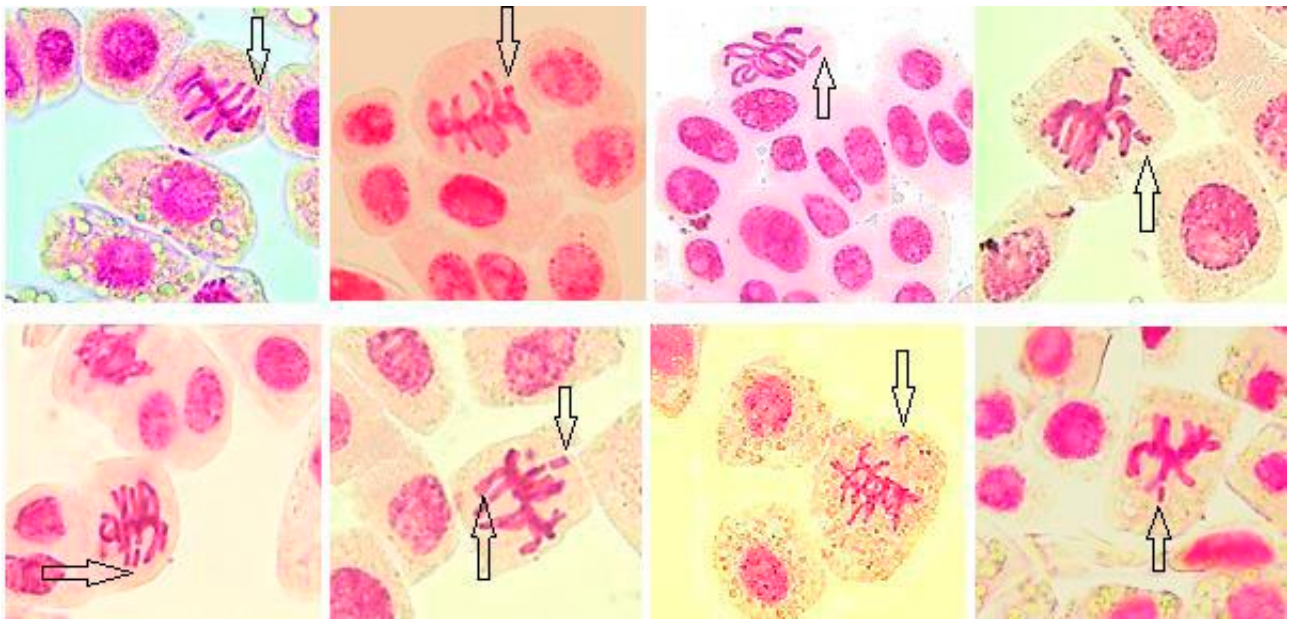

Figure 4. The xylene induced abnormalities: Chromosome breaking.

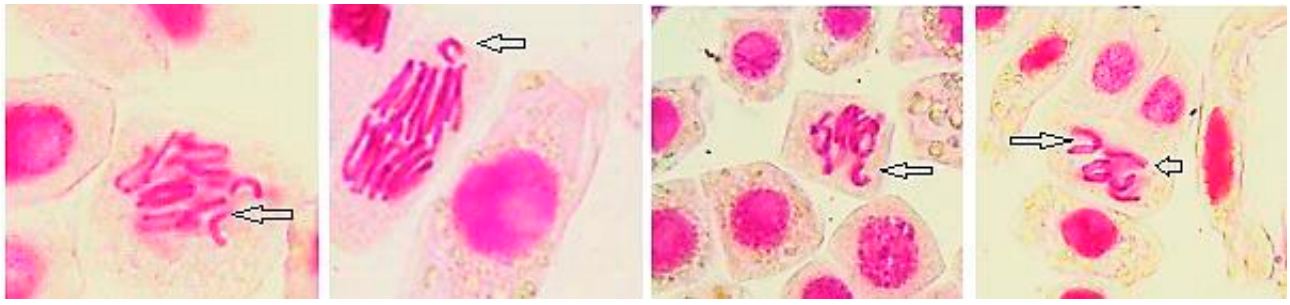

Figure 5. The xylene induced abnormalities: Vagrant chromosome.

Table 4. Pearson's correlation based on chromosome abnormalities.

	A	B	C	D	E	F	G
B	0,966 0,034*						
C	0,938 0,062	0,894 0,106					
D	0,012* 0,988	0,195 0,805	0,264 0,736				
E	0,342 0,658	0,539 0,461	0,117 0,883	0,916 0,084			
F	0,266 0,734	0,419 0,581	0,031* 0,969	0,964 0,036	0,950 0,050*		
G	0,220 0,780	0,441 0,559	0,313 0,687	0,326 0,674	0,579 0,421	0,301 0,699	
H	0,142 0,858	0,298 0,702	0,161 0,839	0,985 0,015	0,921 0,079	0,991 0,009**	0,249 0,751

* Significant at the level of P< 0.05. ** Significant at the level of P< 0.01. Abbreviations: A-I : Codes of chromosome abnormalities.

Table 5. Pearson's correlation based on chromosome abnormalities.

	1	2	3
2	0,851 0,007**		
3	0,412 0,310	0,272 0,514	
4	0,028* 0,762	0,135 0,750	0,470 0,239

* Significant at the level of P< 0.05. ** Significant at the level of P< 0.01. Abbreviations: 1-4 : Codes of Treatment.

(Correlation), there are important correlations among (A-B, D; C-F; D-F, D-H; E-F; F-H) the investigated chromosome abnormalities at levels of 0.01 and 0.05 (Table 4, 8). According to Table 5, based on the Pearson's cor-

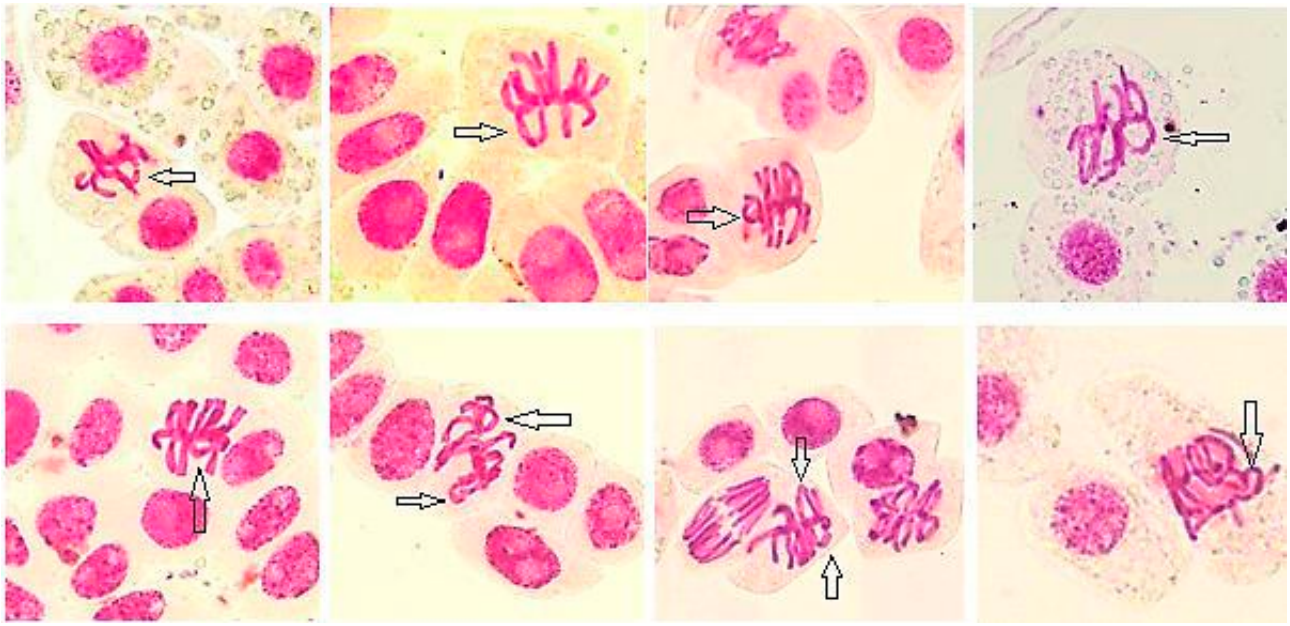

Figure 6. The xylene induced abnormalities: Ring chromosome.

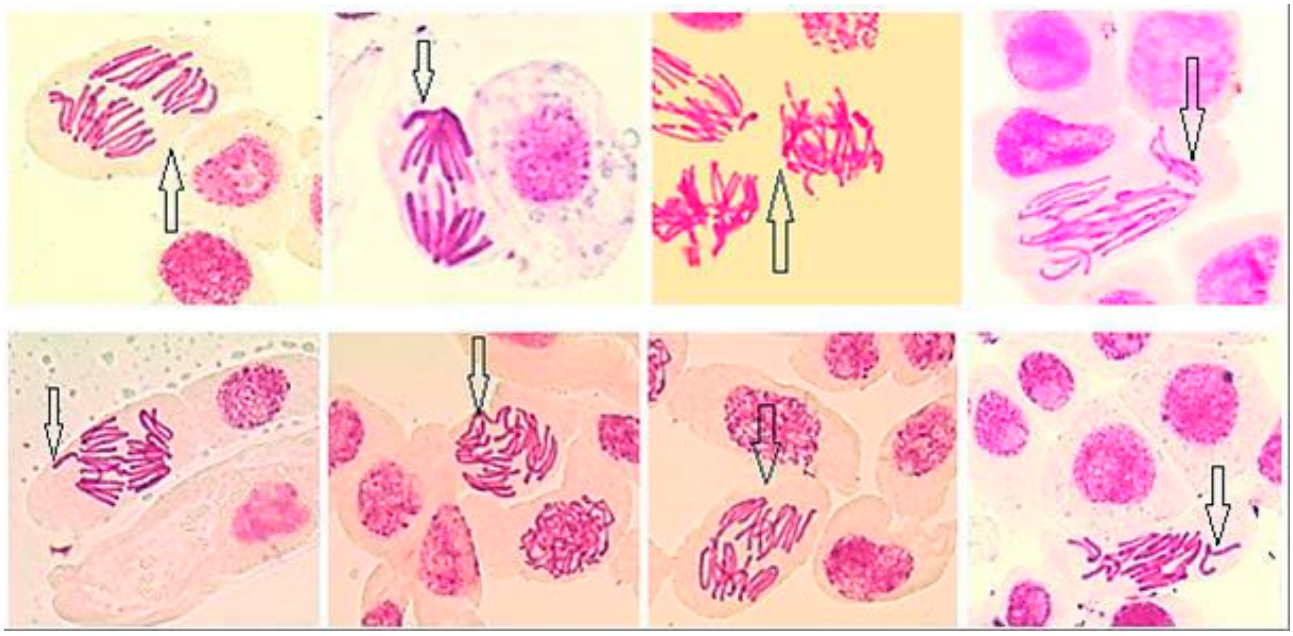

Figure 7. The xylene induced abnormalities: Polar deviation and Scattered anaphase.

relation method there are important correlations among (1-2; 1-4) the treatment time and treatment concentrations at levels of 0.01 and 0.05 According to Table 9, based on the analysis of variance method, there are important correlations among only 1-2 the treatment time and treatment concentrations at levels of 0.01.

4. DISCUSSION

In this study, we studied the cytogenetic effects of xylene on which human beings are exposed in different way on chromosome of plant. For this aim we used meristematic cells of root tips belonging to the *V. faba*

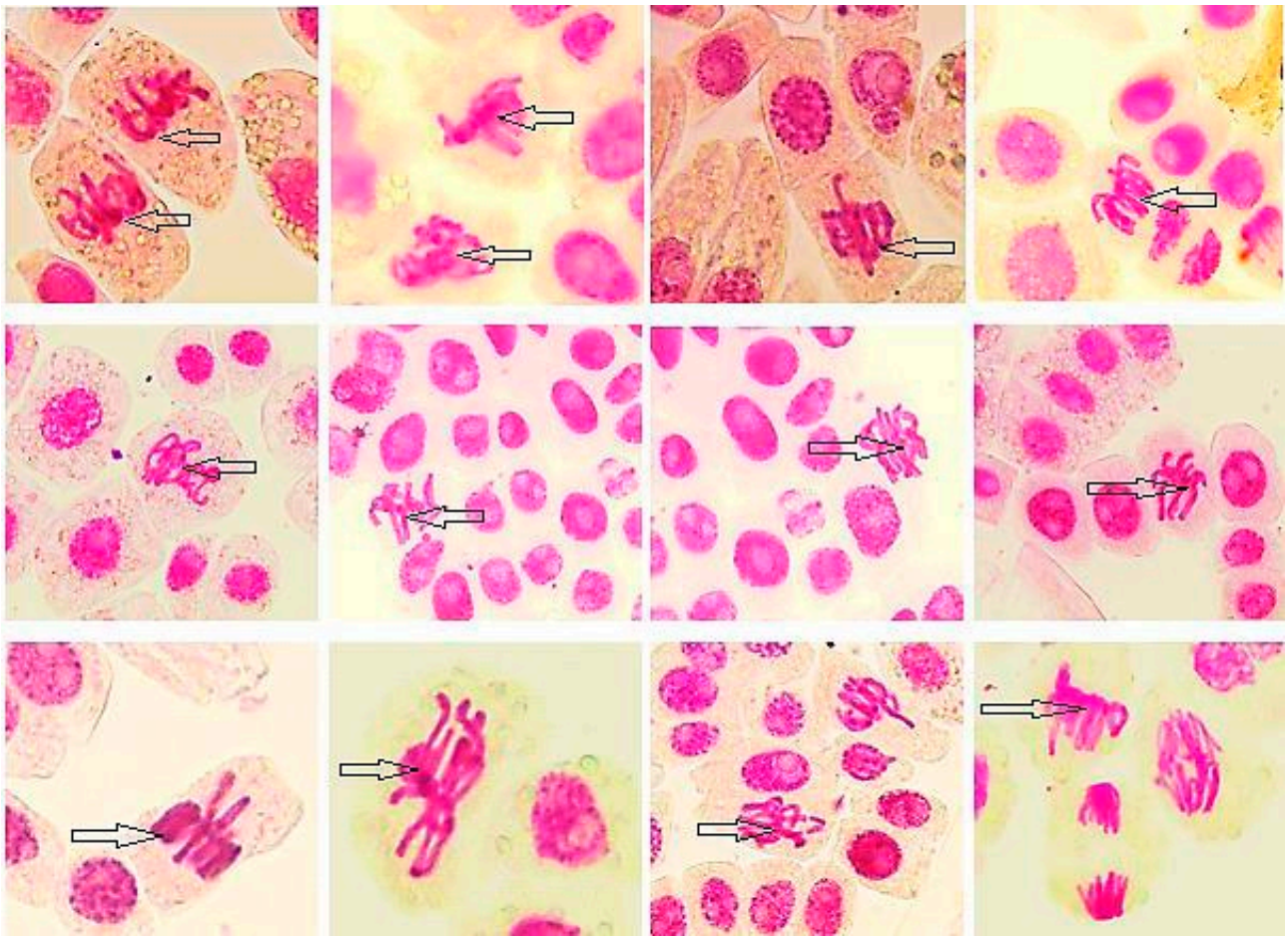

Figure 8. The xylene induced abnormalities: Sticky chromosome.

Table 6. Regression Analysis: **A** versus **B**.

The regression equation is C5 = 0,899 + 0,435 C6				
Predictor	Coef	SE Coef	T	P
Constant	0,8995	0,1588	5,66	**0,030**
C6	0,43508	0,08255	5,27	0,034
S = 0,140751; R-Sq = 93,3%; R-Sq(adj) = 89,9%				

Analysis of Variance					
Source	DF	SS	MS	F	P
Regression	1	0,55038	0,55038	27,78	0,034
Residual Error	2	0,03962	0,01981		
Total	3	0,59000			

Abbreviations: A-B : Codes of chromosome abnormalities

Table 7. Regression Analysis: **1** versus **2**.

The regression equation is C1 = - 0,065 + 0,370 C2				
Predictor	Coef	SE Coef	T	P
Constant	-0,0654	0,1645	-0,40	0,705
C2	0,36970	0,09332	3,96	0,007
S = 0,334601; R-Sq = 72,3%; R-Sq(adj) = 67,7%				

Analysis of Variance					
Source	DF	SS	MS	F	P
Regression	1	1,7570	1,7570	15,69	**0,007**
Residual Error	6	0,6717	0,1120		
Total	7	2,4288			

Abbreviations: 1-2: Codes of Treatment.

which widely used as food by humans. The researchers have pointed out that *Allim cepa* has as an advantage due to its large chromosomes, easily observed with a light microscope (Bonciua 2019). For the same reason,

Table 8. Correlation between 8 investigated chromosome abnormalities (Analysis of Variance).

	MS	F-value	Probability	Significance
A-B	0.5503	27.78	0.034	*
A-C	0.5187	14.56	0.062	NS
A-D	45.134	482.2	0.050	*
A-F	0.0418	01.15	0.734	NS
B-F	0.5120	0.430	0.581	NS
B-H	0.2580	0.190	0.702	NS
C-D	0.2370	0.150	0.736	NS
D-F	9.5300	26.47	0.036	*
D-H	9.9522	66.84	0.015	**
E-F	6.2427	18.71	0.050	*
F-H	3.3103	115.7	0.009	**
G-H	0.0624	0.130	0.751	NS

MS: Mean Square; *P<.05; **P<.01; A-H: Codes abnormalities; NS: Not Significant.

Table 9. Correlation between treatment time and concentrations (Analysis of Variance).

	MS	F-value	Probability	Significance
1-2	1,7570	15,69	**0,007**	**
1-3	0,4128	1.230	0,310	NS
1-4	0,0398	0.100	0,762	NS
2-3	0,9520	0.480	0,514	NS
2-4	0.2340	0.110	0,750	NS
3-4	0.4380	0.710	0,239	NS

MS: Mean Square; **P<.01; Abbreviations: 1-4: Codes of Treatment; NS: Not Significant.

we have used *V. faba* which has this feature in this study. We think that the results of the study are quite important. Because chromosomes are the passwords that keep the viability. We have been determined that xylene has been caused to some chromosamal abnormality on root tip cells of the plant as bridge chromosome, chromosome breaking, sticky chromosome, ring chromosome, vagrant chromosome, scattered anaphase. Similarly, the researchers investigated the cytotoxic effect of benzene and thinner, the toxic chemical used in the painting of steel furniture such as xylene. The effect were evaluated using root tip cells of *Allium cepa*. They observed Chromosomal abnormalities induced were early separation, exclusion, laggard, sticky bridge and persistent bridge (Barbhuiya *et al*. 2018). Some other the researchers reported that copper chloride has caused to some chromosamal abnormality on root tip cells of *Vicia hirsuta* (L.) Gray. According to the same researchers the most observed abnormalityes have been chromosome adherence and bridge chromosome (İnceer and Beyazoğlu 2000). In other study, it has been determined that increase of the lead (PbCl2) concentrations cell division has been decreased, several mitotic anomalies such as c mitosis, lagging chromosomes, multipolar anaphases and chromosome bridges on root tip cells of *Lens culinaris* Medik (Kıran and Şahin 2005). In another study, It has been determined that the frequency of mitotic cell division have been affected by uranium depending on the different treating time and uranium led to chromosomel abnormalities in the *V. faba* cells (Özdemir *et al*. 2008). Similarly, in our study, the mitotic division of the seed treated with xylene gradually increased in comparision to the control group. On the other hand, the chromosome abnormalities vary in parallel with the concentration while the chromosome abnormalities changes irregularly with the time periods of the treatment in our study. As a result of the study, xylene has been shown to induce cleavage in plant meristematic cells and cause abnormal cell division and chromosomel abnormalities. Statistical analysis have been performed using Analysis of Variance, Regression and Pearson Correlation tests. The differences have been evaluated with the same tests. The reason for the application of this statistical method is to see if there is a difference between the groups on the variables studied. These statistical methods have been used to test the differences between two or more groups for our investigated. The results have been taken into account in the significance evaluations at P <0.05 and P <0.01 levels. Thus, we have tried to prove and evaluate the results obtained from laboratory studies numerically. Also, according to the statistical results derived, different concentrations of xylene treatment on the seeds have been increased mitotic cell division at the different periods of time, compared with the control group. However, mitotic division of these treated seeds decreased with increasing application time. This result shows that the application time in mitotic division is important. On the other hand there is a considerable positive relation between the treatment time (hour) and the chromosome abnormality (%). As shown in the tables According to analysis of variance, regression analysis and pearson correlation tests it has been found that there have been statistically important differences at levels of 0.01P between Scattered anaphase and Polar deviation (Table 4,6,8). We can say that these chromosomal abnormalities are interrelated and trigger each other.

We did not find any detalied study on the effect of xylene on plant chromosomes except for a few studies on the effect of xylene on animal cells in our literature review (Mohtashamipur *et al*. 1985; Dean 1985; Nise 1991). In literatüre some researchers have done studies

on the health damages of xylene through various routes of exposure. The researchers indicated that xylene, an aromatic hydrocarbon, is widely used in industry and medical laboratory as a solvent and it is a flammable liquid that requires utmost care during its usage. Also researchers pointed that prolonged exposure to xylene leads to a significant amount of solvent accumulation in the adipose and muscle tissue (Rajan and Malathi 2014). Thus, we think that we are trying to close this deficiency in the literature with this study.

The researchers observed the damage of chromosome in bone marrow cells of rats after dosing with xylene (Lebowitz *et al*. (1979). Similarly Donner *et al*. (1980) exposed rats to technical-grade xylene by inhalation at 300 ppm, 6 h/day, 5 days/week for up to 18 weeks. The chromosome damage has been detected in animals examined after 9, 14 or 18 weeks exposure. The occurrence of these disorders in the chromosomes shows that this negativity will be transmitted from generation to generation. People who have been reluctantly exposed to xylene could have similar effects. Therefore, the use of this chemical in our lives should make us think.

REFERENCES

Barbhuiya S. N, Barhoi D, Datta S.K, and Giri1 S. 2018. Two Major Components of Steel Fabrication Industry, Benzene and Thinner Induce Cytotoxicity in Allium cepa L. Root Cells. Cytologia 83(2): 155–158. https://doi.org/10.1508/cytologia.83.155

Bonciu E, Firbas P, Fontanetti C. S., Jiang W, Karaismailoğlu M C, Liu D, Menicucci F, Pesnya D.S., Popescu A, Romanovsky A.V., Schiff S, Ślusarczyk J, de Souza C. P., Srivastava A., Sutan A., Papini A. 2018. An evaluation for the standardization of the Allium cepa test as cytotoxicity and genotoxicity assay. Caryologia 71(3): 191-209. https://doi.org/10.1080/00087114.2018.1503496

Celık A, Kartal A, Akdoğan A, Kaska Y. 2004. Determining the heavy metal pollution in Denizli (T*ü*rkey) by using Robinio pseudo-acacia L. Environmental International 1-8.

Darlıngton C.D, La Cour F. 1976. The Handling of Chromosomes. Allen and Unwin De Flora S, Bennıcellı C, Bagnasco M. 1994. Genotoxicity of Mercury Compounds. A Review. Mutat Res. 317: 57-79.

Dean 1985. Recent findings on the genetic toxicology of benzene, tolüene, xylenes and phenols. Mutation Res. 154: 153-181.

Donner, M., J. Maki-Paakkanen, H. Norppa, M. Sorsa and H. Vainio (1980) Genetic toxicology of xylenes. Mutation Res. 74: 171-172.

Haglund U, Lundberg I, Zech L. 1980. Chromosome aberrations and sister chromatid exchanges in Swedish paint industry workers. Scandinavian Journal of Work, Environment & Health 6(4): 291-298.

Inceer H, Beyazoğlu O. 2000. Bakır Klorür'ün Vicia hirsuta (L.) S.F. Gray Kök Ucu Hücreleri Üzerine Sitogenetik Etkileri. Turkish Journal of Biology 24: 553-559.

Inceer H, Ayaz S, Beyazoğlu O, Enturk E. 2003. Bakır klorür'ün Helianthus annuus (L.) kök ucu hücreleri üzerine sitogenetik etkileri. Turkish Journal of Biology 27: 43-46.

Kıran Y, Sahın A. 2005. The effects of the lead on the seed germination, root growth and root tip cell mitotic divisons of Lens culinaris medik. G.U. Journal of Science 18(1):17-25.

Kursheed S, Raina A, Amin Laskar R, Khan S. 2018. Effect of gamma radiation and EMS on mutation rate, their effectiveness and efficiency in faba bean (*V. faba* L.). Caryologia 1-8.

Jenifer M. Langman, 1994. Xylene: Its toxicity, measurement of exposure levels, absorption, metabolism and clearance. Journal Pathology 26(3): 301-309. Published online: 06 Jul 2009.

Lebowitz H., D. Brusick, D. Matheson, D.R. Jagannath, M. Reed, S. Goode and G. Roy 1979. Commonly used fuels and solvents evaluated in a battery of short-term bioassays. Environ. Mutagen. 1: 172-173.

Leonard A, Jacqued P, Lauverys R. 1983. Mutagenicity and Teratogenicity of Mercury Compounds. Mutat. Res. 114: 1-8

Mohtashamipur E, K. Norpoth, U. Woelke, P. Huber, 1985. Effects of ethylbenzene, toluene, and xylene on theinduction of micronuclei in bone marrow polychromatic erythrocytes of mice. Arch. Toxicol. 58: 106-109.

Nise, G., Högstedt, B., Bratt, I., Skerfving, S. 1991. Cytogenetic effects in rotogravure printers exposed to toluene (and benzene). Mutation Research/Genetic Toxicology 261(3), 217–223.

Özdemir A, Bozdağ B, Sepet H, Parlak Y, Kocabaş O, Serap E, Özdemir C. 2015. Cytogenetic effects of technetium on meristematic cells of root tips of Vicia faba L. and statistical comparison. Caryologia 68(3): 200-206.

Özdemir C, Ereeş S, Çam S. 2008. Cytogenetic Effects Of Uranium On Root Tip Cells Of Vicia faba L. Botanica Lithuanica 14(3): 155-158.

Peter Langma 2009. Rampage school shooters: A typology Aggression and Violent Behavior 14: 79-86.

Rajan S. T, Malathi N. 2014. Health hazards of xylene: a literature review. J Clin Diagn Res. 8(2): 271-274.

Şutan N. A., Uţă, G., Bărbuceanu, D. 2018. Oxidative stress and cytogenetic effects in root tip cells of Allium cepa L. induced by alcoholic extracts of Leptinotarsa decemlineata (Say). Caryologia 1-9.

Caryologia
International Journal of Cytology, Cytosystematics and Cytogenetics

Firenze University Press
www.fupress.com/caryologia

OPEN ACCESS

Citation: S. Siddiqui, S. Al-Rumman (2020) Clethodim induced pollen sterility and meiotic abnormalities in vegetable crop *Pisum sativum* L.. *Caryologia* 73(1): 37-44. doi: 10.13128/caryologia-269

Received: May 25, 2019

Accepted: February 23, 2020

Published: May 8, 2020

Data Availability Statement: All relevant data are within the paper and its Supporting Information files.

Competing Interests: The Author(s) declare(s) no conflict of interest.

Clethodim induced pollen sterility and meiotic abnormalities in vegetable crop *Pisum sativum* L.

Sazada Siddiqui*, Sulaiman Al-Rumman

Department of Biology, College of Science, King Khalid University, Abha 61413, Saudi Arabia
*Corresponding author. E-mail: sasdeky@kku.edu.sa

Abstract. Pesticides are highly noxious materials.Their poisonousness might not be unequivocally precise to the target entities but can unfavorably disturb various procedures in the non-target host plants. In the present study, the effect of application of clethodim on pollen sterility and meiotic anomalies of *Pisum sativum* L are studied. *Pisum sativum* L seeds are treated with different concentrations of clethodim varying from 0.01%, 0.02%, 0.03%, and 0.04% for exposure time of 1 hour and their effect on pollen sterility and chromosomal anomalies were investigated. The outcomes reveal that treatment of clethodim on *Pisum sativum* L seeds induces pollen sterility (PS) and chromosomal anomalies (CA) in a dose-dependent manner. Also in clethodim treated seeds, an elevation in the proportion of abnormal meiotic phases were observed which was time and concentration dependent. Secondary association (SeA), precociuos separation (PS), clumped nuclei (CNu) were reported in metaphase I & II, stickiness (Stc), bridges (Br) and laggards (Lg) in anaphase I & II. The results of the present study reveal that frequently used herbicide clethodim has a substantial cytotoxic effect on meiotic cells of *Pisum sativum* L.

Keywords. Herbicide, Clethodim, Pollen sterility, Meiotic abnormality, *Pisum sativum* L.

INTRODUCTION

The application of herbicides has led to an alteration in the phytosociological properties of weeds and to a choice of biotypes resilient to herbicides. In addition, it also causes effects in the health of humans and environment although they are categorized as an extremely efficient means in the regulation of weeds. According to He *et al*. (2012), all over the world, the most applied chemical materials are the herbicides. In the 90's, the worldwide pesticide sales continued to stay moderately persistent, amongst 270 to 300 billion american dollars, 79% of this amount is related to herbicides. Amongst the three foremost groups of pesticides i.e. herbicides, fungicides and insecticides; herbicides have taken the top slot since 2007 (Zhang *et al*. 2011). In order to upsurge agricultural output, the application of herbicides for regulating weeds is the most widely used practice in worldwide agriculture. Nevertheless, when these chemical substances are applied in an unrestrained

way, they can influence and disturb other organisms, particularly aquatic creatures (Nwani *et al*. 2011; Van Bruggen *et al*. 2018).

Earlier reports have shown that much of the noxious effects of herbicides on plants and animals were inadequately explored (Chevreuil *et al*. 1996; Kim and Feagley 1998; Abdel-Rahman *et al*. 1999). As a result of the absence of evidences about the effect of herbicides in the biotic environments, they can also epitomize a setback to health of human beings (Munger *et al*. 1997; Gorell *et al*. 1998). The influence of pesticide in the environments is determined by its noxiousness, concentration and dispersion manner (Van der Werf 1996). The mutagenic effects of the herbicides can result from several reactions within the organism, as a direct action of the compound on the nuclear DNA; incorporation in the DNA during cell replication; interference in the activity of the mitotic or meiotic division, resulting in incorrect division of the cell (Timbrell 1999). A few herbicides affect directly the elongation, cell differentiation and cell division of plants.

Herbicide clethodim falls into the cyclohexanedione oxime class. From post-emergence, clethodim is active as an herbicide against various species of grass weeds mostly in sunflower, soybean, cotton and other broad-leaved plants (Edwards 2005). Earlier studies have emphasized the adverse effects of the herbicides on plant physiology and cytogenetics. Maleic hydrazide (MH) is one of the few herbicides which prevents the synthesis of proteins and nucleic acids (Siddiqui *et al*. 2008). Mutagenic action of glyphosate, alachor and maleic hydrazide has been reported by Siddiqui *et al*. (2012), diclofop-methyl and lindane has been stated by Anila and Ditika (2013) and anilofos has been described by Arzu *et al*. (2014) on root tip cells of plant.

Pisum sativum L, (Fabaceae) is a plant useful in the manure production, ayurvedic medications and food (Davies *et al*. 1985). It is one of the most used leguminous plant and is a source of protein. There are no studies available in the literature which have assessed the adverse effects of clethodim on *Pisum sativum* L, a potential multipurpose crop. In the current investigation, we have assessed the noxious consequences of clethodim on meiotic cells of *Pisum sativum* L.

MATERIALS AND METHODS

Seeds and chemical

Pisum sativum L seeds, variety ARKIL were obtained from the Indian Council of Agricultural Research - Bbhoj Krishi Vigyan Kendra, Near Village Naktara, P. O. Bankhedi, NH-86 Ext., Raisen Sagar Road, Bhopal, India.

Clethodim herbicide was obtained from the Delta Chemical Company based in Riyadh, Saudi Arabia.

Treatment of Pisum sativum L with clethodim

Healthy and even sized seeds of *Pisum sativum* L were taken and submerged for 6 hours in double distilled water of pH 6.7. In a glass beaker of 250 mL, seeds of *Pisum sativum* L were immersed for 1 hour in 150 mL clethodim solutions of various concentrations (0.01, 0.02, 0.03 and 0.04%). The seeds were shaken frequently for providing ample air to the seeds. For eliminating any remaining amount of clethodim, the treated seeds were properly cleaned with double distilled water. For control, a set of seeds were submerged in distilled water. In order to eradicate any remaining chemical sticking to the seed coat, the seeds were cleaned with tap water. Each set of seeds comprising of 10 seeds per pot were seeded in pots having a height of 24 cm and width of 17 cm. The entire experiment was repeated thrice under similar conditions.

Pollen grain analysis

For experiments related to pollen grains, flower buds of similar age were collected from treated plants and control group. They were fixed in 70% alcohol. For identifying pollen sterility as well as fertility, pollens were stained with 1% propionocarmine. Pollens having uniform size and shape which were stained dark purple in colour and filled with nuclei and cytoplasm were considered as fertile whereas pollen grains which were stained pale yellow colour or colourless, having irregular size and shape and without nuclei and cytoplasm were defined as sterile. Pollen sterility was calculated as the ratio of non viable pollen grains to the total number of pollens and expressed in percentage.

$$\text{No. of sterile pollen grains} = \frac{\text{No. of non viable pollen grains}}{\text{Total no. of pollen grains}} \times 100$$

Meiotic analysis

To assess the effect on meiotic cells, flower buds of similar size were fixed in 1:3 acetic acid saturated with iron and absolute alcohol for 24 hours and than passed to 70% alcohol. The meiotic cell preparations were prepared by traditional acetocarmine squash technique (Man-

Table 1. Percentage of meiotic abnormality in metaphase I & II and anaphase I & II plate of *Pisum sativum* L in PMCS exposed to different concentrations of clethodim for 1 hour.

(%)	Concentration time	Treatment PMC cells	Total		Metaphase I/II (Mean ±S.E)		Anaphase I/II (Mean ±S.E)		
			Sec. asso.	Pre.sep.	Clumped nuclei	Stickiness	Bridges	Laggards	Total anomalies
	1 h								
0.00		110	0.0 ± 0.00	0.0 ± 0.00	0.0 ± 0.0	0.0 ± 0.0	0.0 ± 0.0	0.0 ± 0.0	00.0 ± 0.0
0.01		125	1.5 ± 0.34	2.6 ± 0.29	3.5 ± 0.2	1.8 ± 0.3	2.4 ± 0.4	1.4 ± 0.2	13.2 ± 1.73
0.02		115	2.8 ± 1.20	3.8 ± 0.93	4.6 ± 0.9	2.2 ± 0.7	3.1 ± 0.7	2.8 ± 0.6	19.3 ± 5.03
0.03		128	3.2 ± 1.70	4.2 ± 1.04	$6.4^{\$}$ ± 1.3	3.5 ± 1.2	3.8 ± 0.3	3.4 ± 1.2	24.5 ± 7.34
0.04		130	$6.5^{\#}$ ± 2.80	$6.1^{\$}$ ± 2.1	$7.4^{\$}$ ± 2.4	$6.7^{¥\#}$ ± 2.0	$6.5^{\#}$ ± 2.7	$6.2^{\$\#}$ ± 2.1	$39.4^{\$}$ ± 14.1

$p \leq 0.05$; $^{\$}p \leq 0.01$; $^{¥}p \leq 0.001$ compared to control. Data are mean of three replicates ± SE; 0.0 = Control group.

ton 1950). By squashing the anther in an acetocarmine stain, slides were prepared. In normal butnyl alcohol (NBA) series, permanent slides were made and they were mounted in Canada balsam and than dried up at 45°C.

Statistical analysis

Statistical analysis was performed employing one way ANOVA test using GPIS software 1.13 (GRAPHPAD, California, USA) to detect the significance of differences of variables. All values are expressed as mean ± SE.

RESULTS

The occurrence of pollen sterility and meiotic chromosomal abnormalities were listed in (Figs 1, 2 and Table 1). It is clear from the results that clethodim was proficient in inducing pollen sterility and different types of meiotic chromosomal abnormalities such as secondary association (SeA) (Fig. 2, A and B), precociuos separation (PS) (Fig. 2, C and D), and clumped nuclei (CNu) (Fig. 2, E and F) in metaphase I & II and stickiness (Stc) (Fig. 2, G and H), bridges (Br) (Fig. 2, I and J) and laggards (Lg) (Fig. 2, K and L) in anaphase I & II.

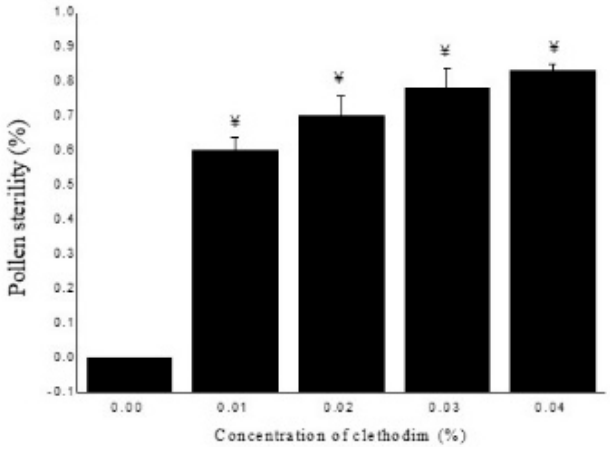

Figure 1. Pollen sterilty of *Pisum sativum* L PMCS exposed to different concentrations of clethodim for 1 hour. $^{¥}p \leq 0.001$ compared to control. Data are mean of three replicates ± SE; 0.0 = Control group.

Effect of clethodim on pollen sterility of Pisum sativum L.

The observation reveals that the percentage of pollen mother cells (PMCS) showing pollen sterility increased with increase in concentrations of clethodim at different exposure times and was null in control (Fig. 1). A lower percentage of pollen sterility were observed at 0.01% concentration which was 60% at one hour and it was highly significant (p>0.001) when compared to control. In addition, at highest concentration high increase in pollen sterility were reported which reached 83% at one hour in clethodim treated PMCS.

Pollen sterility is a sign of disturbance in reproductive process which was observed in clethodim treated pollen mother cells of *Pisum sativum* L at 1 hour (Fig. 1). The increase in the ratio of sterile pollen grains in the clethodim treated groups as the dose increases might be due to their toxic effects on pollen grains.

Effect of clethodim treatment on chromosomal aberration (CA) of Pisum sativum L

Cytological analysis also documented numerous anomalies in the PMCS of clethodim treated plants at one hour, as shown in Table 1. Different types of CA such as SeA, PS, and CNu were noticed in metaphase I & II and Stc, Br and Lg were observed in anaphase I &

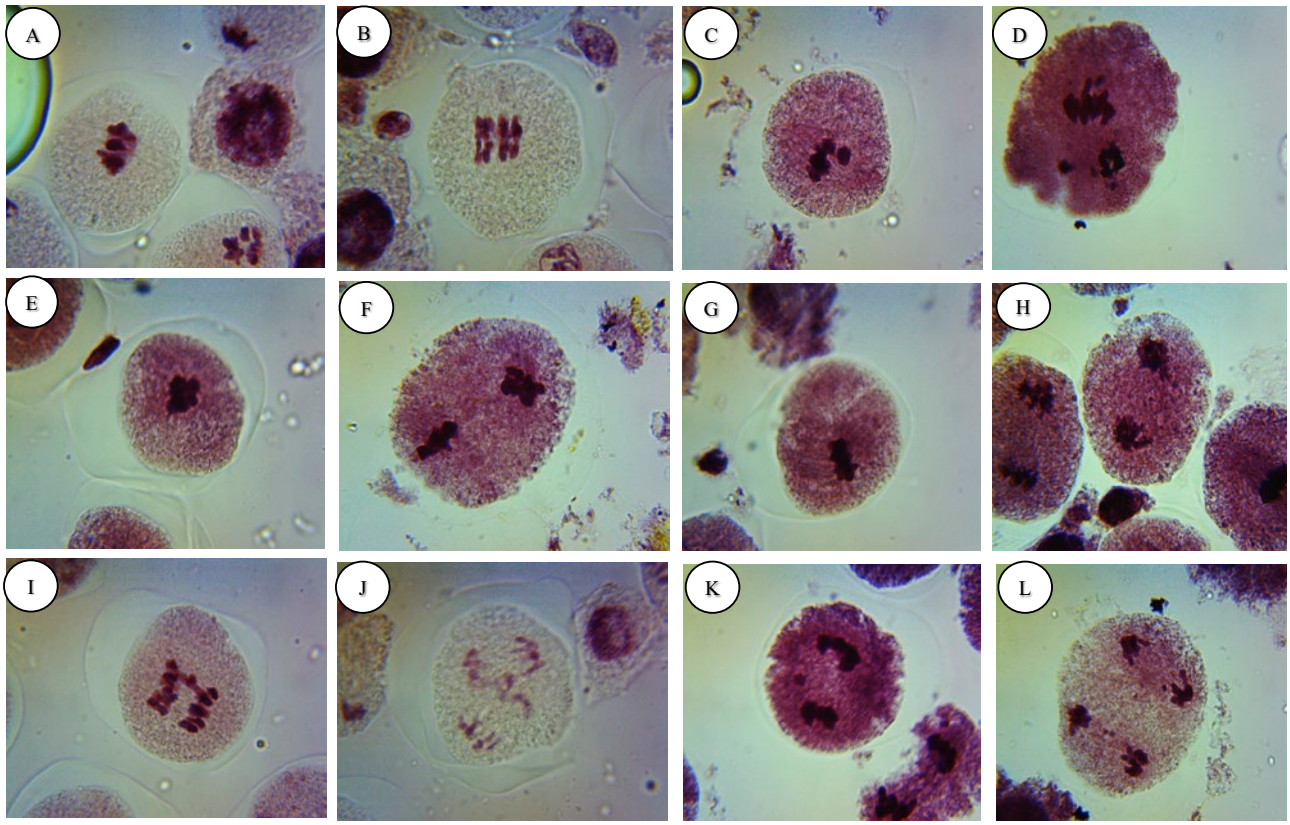

Figure 2. (A-L) Meiotic aberrations induced by clethodim in *Pisum sativum* L PMCS. (A-B) Secondary association; (C-D) Precocious separation; (E-F) Clumped nuclei at Metaphase I & II, (G-H) Sticky chromosome; (I-J) Bridges; (K-L) Laggards at Anaphase I & II in PMCS in *Pisum sativum* L.

II (Table 1 and Fig. 2). Cytological investigations clearly revealed that the level of CAs gradually increased along with increasing concentrations of clethodim at one hour. Studies of different stages of meiotic division shows that almost all the stages of division were affected to a certain extent.

The percentage of formation of SeA, PS, and CNu in metaphase I & II were reported maximum in 0.04% (6.5% - significant $p \leq 0.05$, 6.1% - very significant $p \leq 0.01$ and 7.4% - very significant $p \leq 0.01$) as compared to control, at one hour and reported minimum in 0.01% (1.5%, 2.6% and 3.5%) at one hour of clethodim treated plants.

The percentage of formation of Stc, Br, and Lg in anaphase I & II were reported maximum in 0.04% (6.7% - very significant $p \leq 0.01$ and significant $p \leq 0.05$, 6.5% - significant $p \leq 0.05$ and 6.2% - very significant $p \leq 0.01$) as compared to control at one hour and reported minimum in 0.01% (1.8%, 2.4% and 1.4%) at one hour of clethodim treated plants.

Increased incidence of CAs were in the following order for 1 hour clethodim treatment: CNu > Stc > BR = SeA > Lg > PS.

DISCUSSION

In the present study, the occurrence of laggards and bridges in anaphase I & II were strictly correlated with sterility. Similar finding were reported by Liang *et al.* (1967) on sorghum by Atrazine treatment which affected meiotic stability. Çalli (2008) reported that the Equation Pro (22.5% Famoxadone+30% Cymoxanil) fungicide instigates abnormalities in the meiosis of pollen grains and thus resulting in pollen sterility. Dubey *et al.* (1977) reported a decrease in viability of about 60% in the pollen of eggplants, indicated by the joint effect of a dinitro herbicide and two organophosphate insecticides. Fungicide propiconazole produced damaging effects on pollen tube development and pollen germination of *Tradescantia virginiana* (He *et al.* 1995). Rana and Swaminathan (1964) and Ramanna (1974) found that any deviance in cytokinesis or karyokineses could generate non-viable microspores. Sinha and Godward (1969;1972) found that translocations were liable for reduced pollen fertility. In *H.orientalis*, tube growth and *in vitro* pollen germination was disturbed and affected by the herbicide

Quizalofop-p-ethyl (QPE) treatments. Especially, the maximum QPE concentration instigated alterations in the morphological attributes of *H. orientalis*. Pollen germination is decreased by three times by utmost vigorous QPE application. Within the pollen tube morphological anomalies were also detected (Deveci *et al*. 2017).

Pisum sativum L and *Allium cepa* L are generally used in order to check the genotoxicity and cytotoxicity of several chemicals (Bonciu *et al*. 2018 a and b; Siddiqui 2018). Previous works have revealed that herbicides have mutagenic effect on *Pisum sativum* L and *Allium cepa* L (Siddiqui *et al*. 2008; Rosculet *et al*. 2019). Cytological abnormalities in plants can be a useful monitoring method for the recognition of chemicals present in the environment that might cause a genetic threat. In the current study, we found numerous kinds of chromosomal irregularities such as SeA, PS, CNu in metaphase I & II, Lg, Br, and Stc in anaphase I & II in *Pisum sativum* L after treatments with clethodim of one hour.

The prevalence of secondary association has been found in treated plants. Incidence of secondary association is a regular attribute occurring primarily because of the existence of more than two homologous chromosomes. In the course of secondary pairing, there is a debate on the participation of homologous chromosomes amongst the researchers. Hirayoshi (1957) differed with the postulation that contemplates the participation of homologous chromosome in secondary association and after investigating thorough outcomes in *Zizanieae* and *Oryzeae* offered the inference that secondary association might be an incidence effective under physico and bio-chemical effects and has got no relation to the exact homology of chromosomes.

Secondary pairing within bivalents is well thought to be a sign of polyploid attribute of a species as found in Kidney bean (Girjesh and Nitu, 2014), *Ocimum* (Mukherjee and Datta 2005), *Uraria picta* (Bhattacharya and Datta 2010). As per Stebbins (1950), secondary association may be contemplated to be a phenomenon that illustrates the polyploid attribute of a species but detailed phylogenetic estimations may not be framed from this since secondary pairing within bivalents is substantially altered by further chromosomal alterations.

In the present study, the occurrence of precocious movement also appeared enhanced with rising clethodim concentations. Precocious separations were formed due to unstable spindle process or inactivation of spindle formation and interrupted homology for pairing of chromosomes that might lead to the precocious motion of chromosomes (Umar and Singh 2003). It might also be attributed due to the occurrence of breakage of chromosomes or because of the heavy metals breaching the protein moiety of the nucleoprotein backbone.

In the current study, the prevalence of clumped nuclei also get boosted with rising clethodim concentations. Because of the turbulences at the cytochemical level, clumped nuclei were created. Clumping of the chromosomes can occur with regular arrangement at metaphase and separation may result in the creation of bridges. Some types of gene mutations that cause incorrect coding of some non-histone proteins involved in chromosomal organization can lead to chromosomal clumping. There is a possibility that the mutagen reacts with the available histone proteins and results in an alteration in the surface property of the chromosomes because of incorrect folding of DNA and hence causing the chromosomes to stick or clump (Grant 1978).

Stickiness was also reported with increase in the clethodim concentrations. Stickiness could occur because of incomplete detachment of the nuclear proteins and changes in their design of association or because of incomplete detachment of the nucleoproteins and amendment in their design of association or because of depolymerization of nucleic acids instigated by clethodim treatment. Stickiness might result from disorders in cytochemical balance reaction (Dewitte *et al*. 2010; Rosculet *et al*. 2019). Depolymerisation of nucleic acids due to herbicidal treatment or by incomplete detachment of nucleoproteins (Kaufman *et al*. 1955) or by the limited separation of nucleoprotein variation in their design of organization (Evans 1962) may cause stickness.

Numerous bridges were formed in anaphase I & II in the treated plants. Bridges were probably created by breaking and combination of chromosomes bridges which augmented with the treatment of clethodim. Formation of chromosomal bridges could occur because of the chromosomal stickiness and consequent failure of free anaphase division or because of inversion of chromosome fragments or irregular translocation (Gomurgen 2000). Rosculet *et al*. (2019) reported that the origin of bridges were mainly because of the merger amongst broken chromosomes.

The laggards noticed within the current investigation could be due to the failure of the movement of chromosomes or because of the deferred termination of stickiness of the ends of chromosomes. Lagging of chromosomes might occur because of the interruption of the motion of bivalents towards equatorial plate at metaphase I. The utmost regular occurence was the lagging of single univalent (Zeyad *et al*. 2019). Barthelmess (1957) reported that more than one lagging chromosomes in meiosis might occur because of the interruption of the prometaphase motion of chromosomes supplemented by

union of the centromeric to the adjoining inner surface of plasma. Bridges and laggards might have been formed because of deferred terminalisation of stickiness of the ends of chromosomes (Kaur and Grover 1985). Creation of micronuclei at telophase I is caused by laggards. Generation of micronuclei at telophase II is caused by laggards or acentric fragments and thus it results in the alteration in numeral and size of pollen grains ensuing from mother cells.

As reported in previous findings, our outcomes suggest the possibility of these chemicals to instigate meiotic anomalies (Namrata and Alka 2014; Das *et al*. 2018). The chromosomal abnormalities caused by these herbicides might be because of their impeding effect on spindle proteins and their capability to instigate swap over of sister chromatids (Tartar *et al*. 2006; Siddiqui *et al*. 2009). Previous investigations have revealed that free radicals might be the reason for genomic uncertainty in cells. Damages in DNA, disarray in the cytoskeleton and disproportion in energy metabolism might result in chromosomal anomalies as reactive oxygen species are extremely unstable (Siddiqui *et al*. 2012; Siddiqui 2015).

Due to genetic and physiological disarrays, numerous types of meiotic abnormalities might have been created. It has become clear from the above findings that clethodim used in the current work is probably capable of instigating several types of chromosomal anomalies.

CONCLUSION

Within the experimental settings applied in the current work, clethodim displayed a sturdy genotoxic effect on *Pisum sativum* L. It is obligatory to do additional research work on the attribute of the harvests resulting from seeds and plants subjected to these chemicals in relation to their nutritive worth and their vulnerability to acclimatize with diseases. Additionally, it is significant to note that the pesticide preparations encompassing these active constituents may or may not have a parallel effect on the plant cells. Regarding this, supplementary researches are essential to evaluate their outcome on biological procedures.

ACKNOWLEDGMENTS

We are grateful to Deanship of Scientific Research at King Khalid University, Abha, Kingdom of Saudi Arabia for providing technical and administrative support.

DECLARATION

The authors declare no conflict of interest.

FUNDING

The authors (Sazada Siddiqui and Suleiman Al-Rumman) extend their appreciation to the Deanship of Scientific Research at King Khalid University for funding this work through research groups program under grant number R.G.P.1/49/39.

REFRENCES

Abdel-Rahmam AR, Wauchope RD, Truman CC, Dowler CC. 1999. Runoff and leaching of atrazine and alachlor on a sandy soil as affected by application in sprinkler irrigation. J of Environ Sci and Health-B: Pesti and Food Cont. 34:381–396.

Anila MD, Ditika K. 2013. Cytotoxic and genotoxic potency screening of two pesticides on *Allium cepa* L. Proc Tech. 8:9–26.

Arzu O, Dilek A, Yasin E, Sevim FE. 2014. Potential cytotoxic effect of anilofos by using *Allium cepa* assay. Cytotechnology. 67:783–791.

Barthelmess A. 1957. Chemish induzierte multipalare Mitosen. Protoplasma. 48:546–561.

Bhattacharya A, Datta AK. 2010. Secondary chromosome associations in *Uraria picta* (Jacq.) DC. (Family: Leguminosae). Cytologia. 75:37–40.

Bonciu E, Roşculete E, Olaru AL, Roşculete CA. 2018[a]. Evaluation of the mitodepressive effect, chromosomal aberrations and nuclear abnormalities induced by urea fertilization in the meristematic tissues of *Allium cepa* L. Caryologia. 71(4):350-356.

Bonciu E, Firbas P, Fontanetti CS, Wusheng J, Karaismailoğlu MC, Donghua Liu, Menicucci F, Pesnya DS, Popescu A, Romanovsky AV, Schiff S, Ślusarczyk J, de Souza CP, Srivastava A, Sutan A, Papini A. 2018[b]. An evaluation for the standardization of the *Allium cepa* test as cytotoxicity and genotoxicity assay. Caryologia. 71(3):191-209.

Çalli İÖ. 2008. Effects of fungicide on meiosis of tomato (*Lycopericon esculentum* Mill.). Bangladesh J Bot. 37(2):121–125.

Chevreuil M, Garmouma M, Teil MJ, Chesterikoff A. 1996. Occurrence of organochlorines (PCBs, pesticides) and herbicides (triazines, phenylureas) in the atmosphere and in the follout from urban and rural stations of Paris area. Science of the Environ. 182:25–37.

Das A, Dutta S, Nag S, Mandal S. 2018. Effect of acephate pesticide on meiosis in onion (*Allium cepa*). Inter J of Agri. 10(6):5456 –5459.

Davies DR, Berry GJ, Heath MC, Dawkins TCK. 1985. Pea (*Pisum sativum* L.). In: Summerfield RJ, Roberts EH (Eds.). Grain legume crops. Williams Collins (London). p. 147–198.

Deveci A, Aksoy O, Al G. 2017. Investigation of the effects of quizalofop-P-ethyl on pollen germination of *Hyacinthus orientalis* L. Caryologia. 70:77–81.

Dewitte A, Eeckhaut T, Van Huylenbroeck J, Van Bockstaele E. 2010. Meiotic aberrations during 2n pollen formation in Begonia. Heredity. 104:215–23.

Dubey PS, Shrivastava A, Shevade A. 1977. Pesticidal toxicity bioassay with pollen damage. Environ. Poll. 13(3):169–171.

Edwards D. 2005. Reregistration Eligibility Decision (RED) for Sethoxydim. United States Environmental Protection Agency. p. 1–27.

Evans HJ. 1962. Chromosome aberrations induced by ionizing radiations. Int Rev Cytol. 13:221–232.

Girjesh K, Nitu C. 2014. Secondary chromosomal association in kidney bean (*Phaseolus vulgaris* L.). Jordan J Biol Sci. 7(1):71–74.

Gomurgen AN. 2000. Cytological effect of the herbicide 2,4-D isooctylester 48% on root mitosis of *Allium cepa*. Cytologia. 65:383–388.

Gorell JM, Jhonson CC, Rybicki, BA, Peterson EL, Richardson RJ. 1998. The Risk of Parkinson's disease with exposure to pesticides, farming, well water, and rural living. Neurology. 50(5):1346 –1350.

Grant WF. 1978. Chromosome aberrations in plant as a monitoring system. Environ Health Per. 27:37–43.

He H, YuJ, Chen G, Li W, He J, Li H. 2012. Acute toxicity of butachlor and atrazine to freshwater green alga *Scenedesmus obliquus* and cladoceran *Daphnia carinata*. Ecotox Environ Saf. 80:91–96.

He Y, Wetzstein HY, Palevitz BA. 1995. The effects of a triazole fungicide, propiconazole, on pollen germination, tube growth and cytoskeletal distribution in *Tradescantia virginiana*. Sex Plant Reprod. 8:210–216.

Hirayoshi I. 1957. The chromosomal relationships in Oryzeae and Zizanieae. Cytologia Supp. Vol Proc Int Genet Symposia. 1956:293–297.

Kaufman BP, McDonald MR, Bernstein MH. 1955. Cytochemical studies of changes induced in cellular materials by ionizing radiations. Ann N Y Acad Sci. 59:553–566.

Kaur P, Grover IS. 1985. Cytological effects of some organophosphorus pesticides. II. Meiotic effects. Cytologia. 50:199–211.

Kim JH, Feagley SE. 1998. Adsorption and leaching of trifluralin, metolachlor, and metribuzin in a commerce soil. Journal of Environmental Science and Health-B: Pest and Food Conta. New York. 33:529–546.

Liang GH, Feltner KC, Liang YYS, Morril JM. 1967. Cytogenetic effects and responses of agronomic characters on grain sorghum following atrazine application. Crop Sci. 7(3):245–248.

Manton I. 1950. Problems of cytology and evolution in the Pteridophyta. Cambridge: Cambridge University Press; p. 316.

Mukherjee M, Datta AK. 2005. Secondary chromosome associations in *Ocimum basilicum* L and *Ocimum tenuiflorum* L. Cytologia. 70:149–152.

Munger R, Isacson P, Hu S, Burns T, Hanson J, Lynch CF, Cherryholmes K, Vandorpe P, Hausler JrWJ. 1997. Intrauterine growth retardation in Iowa communities with herbicides- contaminated drinking water supplies. Environ Health Persp. 105:308–314.

Namrata S, Alka S. 2014. Biomonitoring of genotoxic effect of glyphosate and pendimethalin in *Vigna mungo* populations. Cytologia. 79(2):173–180.

Nwani CD, Nagpure NS, Kumar R, Kushwaha B, Kumar P, Lakra, WS. 2011. Mutagenic and genotoxic assessment of atrazine-based herbicide to freshwater fish *Channa puntatus* (Bloch) using micronucleus test and single cell gel electrophoresis. Envir Toxic and Pharm. 31:314–322.

Ramanna MS. 1974. The origin of unreduced microspores due to aberrant cytokinesis in meiocytes of potato and its genetic significance. Euphytica. 23:20–30.

Rana SR, Swaminathan MS. 1964. Cytological aspects of pollen sterility. Recent Advances in Palynology. p. 276-304. National Botanical garden, Lucknow.

Rosculete CA, Bonciu E, Rosculete E, and Olaru LA. 2019. Article determination of the environmental pollution potential of some herbicides by the assessment of cytotoxic and genotoxic effects on *Allium cepa*. Int J Environ Res Public Health 16: 75.

Siddiqui S, Khan SS, Meghvansi MK, Nazoora SA. 2008. Mutagenic effect of herbicide maleic hydrazide on seed germination and radicle length on *Trigonella foenum-graecum*. Indian J Appl Pure Biol. 23:103–106.

Siddiqui S, Meghvansi MK, Khan SS. 2012. Glyphosate, alachor and maleic hydrazide have genotoxic effect on *Trigonella foenum-graecum* L. Bull Environ Contam Toxicol. 88:659–665.

Siddiqui S, Meghvansi MK, Wani MA, Jabee F. 2009. Evaluating cadmium toxicity to the root meristem of *Pisum sativum* L. Acta Physiol Plant. 31:531–536.

Siddiqui S. 2015. DNA damage in Cicer plant grown on soil polluted with heavy metals. J of King Saud University – Sci. 27:217–223.

Siddiqui S. 2018. Cytotoxicity induced by aluminum sulfate in cells of root meristem of *Pisum sativum* cv. Arikil. Bangladesh J Bot. 47(2):219–226.

Sinha SSN, Godward MBE. 1969. Radiation studies in *Lens culinaris*. Mitosis type of aberration and their elimination in root and shoot apical meristem. J Cytol Genet. 3:80–91.

Sinha SSN, Godward MBE. 1972. Radiation studies in *Lens culinaris*. Meiosis: abnormalities induced due to gamma radiation and its consequences. Cytologia. 37:685–695.

Stebbins GL. 1950. Variation and Evolution in Plants. Columbia Univ Press. New York.

Tartar G, Kaymak F, Muranli FDG. 2006. Genotoxic effects of Avenoxan on *Allium cepa* L. and *Allium sativum* L. Caryologia. 59:241–247.

Timbrell JA. Introduction to Toxicology. 2. Ed. Estados Unidos: Taylor & Francis, 1999. p.167.

Umar G, Singh V. 2003. Comparative analysis of meiotic abnormalities induced by gamma rays and EMS in Barley. J Indian Bot Soc. 82:19–22.

Van Bruggen AHC, He MM, Shin K, Mai V, Jeong KC, Finckh MR, Morris JG Jr. 2018. Environmental and health effects of the herbicide glyphosate. Sci. of the Total Environ. 616–617:255–268.

Van der Werf HMG. 1996. Assessing the impact of pesticides on the environment. Agric Ecosyst Environ. 60:81–96.

Zeyad MT, Kumarb M, Malika A. 2019. Mutagenicity, genotoxicity and oxidative stress induced by pesticide industry wastewater using bacterial and plant bioassays. Biotech Reports. 24: e00389.

Zhang W, Jiang F, Ou J. 2011. Global pesticide consumption and pollution: with Chinas as a focus. Proceedings of the Inter Acad of Ecol and Envir Scies. 1(2):125–144.

Caryologia
International Journal of Cytology, Cytosystematics and Cytogenetics

Firenze University Press
www.fupress.com/caryologia

OPEN ACCESS

Citation: B. Huri Gölge, F. Vardar (2020) Temporal Analysis of Al-Induced Programmed Cell Death in Barley (*Hordeum vulgare* L.) Roots. *Caryologia* 73(1): 45-55. doi: 10.13128/caryologia-185

Received: March 8, 2019

Accepted: November 2, 2019

Published: May 8, 2020

Data Availability Statement: All relevant data are within the paper and its Supporting Information files.

Competing Interests: The Author(s) declare(s) no conflict of interest.

Temporal Analysis of Al-Induced Programmed Cell Death in Barley (*Hordeum vulgare* L.) Roots

Büşra Huri Gölge, Filiz Vardar*

Marmara University, Faculty of Arts and Sciences, Department of Biology, Göztepe, 34722, İstanbul, Turkey
*Corresponding author. E-mail: filiz.vardar@gmail.com

Abstract. Aluminum (Al) is the third most elements found in the earth crust and Al toxicity is one of the most dangerous toxicants in terms of plants. As soil acidity increases due to a number of environmental factors, Al becomes soluble and transforms into toxic forms. In the present study, barley (*Hordeum vulgare* L.) roots were exposed to 100 µM $AlCl_3$ solution for short (1/2, 1, 2, 3, 4, 5, 6 and 7 h) and long (24, 48, 72 and 96 h) term to reveal time dependent programmed cell death evidences. At the end of time periods, Al^{+3} accumulations, loss of plasma membrane integrity and lipid peroxidation increased time dependently. On the other hand, increase in caspase-1 like enzyme activities were observed in Al toxicity beginning from ½ h. Similar to apoptosis seen in animals, cytochrome c release from mitochondria to cytoplasm was also determined quantitatively. As a result of our research, increase of cytochrome c release from mitochondria to cytoplasm was time dependent which is one of the indicators of programmed cell death. Finally, under Al stress, genomic DNA fragmentation was measured by Flow Cytometry, and it was determined that DNA fragmentation was visible at first hours, but it was more significant after long term application in barley roots. In conclusion; the presented study highlights the adverse effects of Al on barley roots and importance of clarifying the relationship between Al toxicity and time dependent programmed cell death mechanism.

Keywords. Aluminum, caspase-1 like activity, cytochrome c, DNA fragmentation, lipid peroxidation, programmed cell death.

INTRODUCTION

Aluminum (Al), as an abiotic stress factor, exists as third most abundant mineral forming 8% in earth's crust (Matsumoto 2000; Abate *et al.* 2013). It has been known that Al is the primary limiting factor on plant growth and development in acidic soils. Considering the 67% of the world's potential arable lands are acid soil, most of the agronomic plants are face to Al toxicity (Kochian *et al.* 2004; Abate *et al.* 2013; Ma *et al.* 2014). Non-toxic Al appears as insoluble aluminosilicates or oxides, but when soil pH decreases (pH<5) Al solubilized into reactive and phytotoxic forms being in a range of 10–100 µM (Matsumoto 2000; Ciamporova 2002; Vardar and Ünal 2007). Several

researches revealed that Al adversely affects the plant within a few minutes even at low micro-molar doses; as a result of this Al is considered as major constraint for crop yield (Vitorello *et al*. 2005; Abate *et al*. 2013).

Considering the whole plant, root apex (root cap, meristem and elongation zone) is the first target organ and accumulates more Al (Matsumoto 2000; Vardar *et al*. 2006). Several studies prove that Al induce morphological, biochemical and physiological alterations. Besides, it is a genotoxic agent leading adverse effects on DNA structure and function. Moreover, Al toxicity decreases mitotic index and causes chromosome aberrations (Frantzios *et al*. 2000; Vardar *et al*. 2011). Recent works also revealed that Al also adversely affects DNA methylation and polymorphism on LTR retrotransposons suggesting these alterations may be a defense mechanism to Al stress (Guo *et al*. 2018; Taşpınar *et al*. 2018).

There is a close relation to Al toxicity and ROS (reactive oxygen species) production triggering oxidative damage in the cell. Over accumulation of ROS cause damage on lipid, protein, carbohydrate, photosynthetic pigments and DNA leading to programmed cell death (PCD) (Darko *et al*. 2004; Sharma and Dubey 2007; Gupta *et al*. 2013).

PCD is considered as an alternative adaptive mechanism in plants to enable the survival of whole organism under extreme environmental stresses (Jackson and Armstrong 1999; Drew *et al*. 2000; Vardar *et al*. 2018). PCD is a genetically regulated cell suicide process and coordinated by specific proteases and nucleases (Wang *et al*. 2011; Vardar and Ünal 2012; Wituszyńska and Karpiński 2013; Petrov *et al*. 2015). It has been identified by common characteristics in eukaryotes such as cell shrinkage, vacuolization, cytochrome c release, specific protease activation, chromatin condensation, DNA fragmentation and finally breakdown of the cell (Vardar and Ünal 2008; Papini *et al*. 2011; Wang *et al*. 2012; Poor *et al*. 2013). There are several researches concerning abiotic stress induced PCD in plants, but Al stress-induced PCD is still need to be investigated to clarify its toxicity and tolerance mechanism. Even if there are a few research on temporal occurrence of Al-induced PCD (Vardar *et al*. 2015; 2016), more detailed time dependent analyses are of the essence. Therefore, we designed a detailed analysis addressing Al-induced PCD in the course of short and long term exposure in *Hordeum vulgare* roots.

MATERIAL AND METHODS

Plant material

The seeds of barley (*Hordeum vulgare* L. cv Çetin 2000) which were obtained from The Field Crops Central Research Institute (Ankara, Turkey) were sterilized with 1% sodium hypochloride solution for 10 min. After rinsing, seeds were placed on moistened filter paper in petri dishes for germination. The petri dishes were kept in a plant growth room with fluorescent tubes giving an irradiance of 5000 lux (day/night 16/8 respectively), temperature of 23 ± 2 °C, and relative humidity 45–50% for 48 h. The barley seedlings which reached 0.5-1 cm root elongation were immersed in 100 µM $AlCl_3$ (pH 4.5) with different time intervals. In the present study the exposure time designed in two groups: short (½, 1, 2, 3, 4, 5, 6 and 7 h) and long time (24, 48, 72 and 96 h) exposure. Distilled water was used for the control group. Fifty seeds were used for each experimental group. All of the analyses were assessed with three replicates for statistical validity. Analysis of variance of all the experimental data was performed with SPSS 13.0 computer program. Student t- test was used to determine the statistical significance of differences among the means at $P < 0.05$.

Determination of Al uptake

Al^{+3} ion uptake in control and treated roots was assessed by hematoxylin staining method (Ownby 1993). The intact barley roots were stained with solution containing 0.2% (w/v) hematoxylin and 0.02% (w/v) KIO_3 for 15 min in dark. Then the roots were washed with distilled water and 10 root tips (1 cm) immersed in 4 mL 1N HCl (v/v) for 1 h. After immersion, HCl solution was measured at 490 nm spectrophotometrically.

Determination of loss of plasma membrane integrity

The loss of plasma membrane integrity in control and treated roots was detected by Evans blue staining method (Pandey *et al*. 2013). The intact barley roots were stained with 0.25% (w/v) Evans blue solution for 30 min. After rinsing in distilled water for 10 min, 10 root tips (1 cm) were homogenized in 1 mL of 1% (w/v) sodium dodecyl sulphate (SDS) solution. After centrifugation at 13500 rpm for 10 min, the supernatant was measured at 600 nm spectrophotometrically.

Determination of lipid peroxidation

Lipid peroxidation was measured by the amount of malondialdehyde (MDA) produced after reaction with thiobarbituric acid (TBA) (Cakmak and Horst 1991). The

control and treated roots (0.4 g) were homogenized in 2 mL 0.1% (w/v) trichloroacetic acid (TCA). After centrifugation at 12000 g for 20 min, the supernatants (0.5 mL) were added on 0.6% (w/v) TBA in 20% (w/v) TCA (2 mL) and boiled at 95 °C for 30 min. The mixture was transferred to ice immediately. After color change the samples centrifuged at 12000 g for 10 min. Absorbance of the TBA-reactive substance was determined as TBA-MDA complex at 532 and 600 nm.

Determination of caspase-1 like activities

Control and $AlCl_3$ treated root tips (0.3 g) were ground in ice-cold mortar with 1 mL extraction buffer (50 mM HEPES-KOH – pH 7, 10% sucrose, 0.1% CHAPS, 5 mM DTT, and 1 mM EDTA) according to Lombardi *et al*. (2007). The homogenates were transferred on ice for 10 min and centrifuged at 14000 rpm (+4 °C) for 10 min. Protein concentration was determined by Nano photometer. For determination of caspase-1 activity, ENZO's Caspase-1/ICE Colorimetric Protease Activity Assay Kit was used. According to manufacturer's instructions, equal amounts of protein extracts were incubated at 37 °C for 90 min with p-NA (p-nitroaniline)-labeled substrates YVAD. The caspase-1 like activity was measured at 400 nm and calculated according to the standard curve. Comparison of the absorbance of p-NA from an apoptotic sample with an un-induced control allows determination of the fold increase in caspase activity.

Determination of cytochrome c release

Control and $AlCl_3$ treated root tips (0.2 g) were ground in ice-cold mortar with 3 mL 0.1 M phosphate buffer saline (PBS, pH 7.7). The homogenates were centrifuged (+4°C) for 15 min and the supernatant re-centrifuged at 16000 rpm for 15 min. After centrifugation, supernatant was collected as cytoplasmic phase and pellet is collected as mitochondrial phase. The pellet was re-suspended with 200 µL PBS (Huang *et al*. 2014). For determination of cytochrome c (cyt c) release, MyBioSource's Plant Cyt C ELISA Kit was used. According to manufacturer's instructions, both cytoplasmic and mitochondrial phases were incubated with HRP-conjugated reactive at 37°C for 60 min. After rinsing with washing solution, chromogen A and B solution were added and incubated at 37°C for 15 min. Along with stop solution, cytochrome c was measured at 450 nm and calculated according to the standard curve.

Determination of DNA fragmentation

DNA fragmentation was analyzed by flow cytometry in control and Al treated roots. For this purpose, *CyStain® UV Precise P* kit special for plants was used. The nuclei were isolated from 6 root tips by careful slicing with a razor blade in 0.4 mL Nuclei Extraction Buffer. The extract was collected with micropipette and stained with 1.6 mL DAPI in a micro centrifuge tube. The tubes were transferred on ice for 1-2 min and then filtered to test tubes. The DNA fragmentation of nuclei was analyzed with flow cytometry (Sysmex).

RESULTS

To determine the temporal effects of Al, the barley roots were exposed to 100 µM $AlCl_3$ (pH 4.5) for short (0, ½, 1, 2, 3, 4, 5, 6 and 7 h) and long (24, 48, 72 and 96 h) time points. After Al exposure Al^{+3} ion uptake, loss of plasma membrane integrity, lipid peroxidation, caspase-1 like activities, cytochrome c release and DNA fragmentation were analyzed in relation to time dependent programmed cell death (PCD) occurrence.

According to hematoxylin analysis Al^{+3} ion uptake increased by 8.7%, 30.4% and 73.9% at ½, 1 and 2 h, respectively. Ongoing times Al uptake raised by about 1.5 fold up to 5 h, 1.8 fold at 6 h and 2.1 fold at 7 h (Fig. 1a). After long term exposure, Al uptake increased exponentially by 4.6, 7.5, 11.3 and 12.1 fold at 24, 48, 72 and 96 h, respectively (Fig. 1b).

Evans blue analysis is frequently used to determine the loss of plasma membrane integrity. It has been known that the dye can penetrate through ruptured membranes and stains the damaged cells. In this respect after Al exposure plasma membrane rupture determined in barley root cells time dependently. Based on our results the dye uptake increased by 25.3%, 34.6%, 46.7%, 74.7%, 72%, 78.7%, 94.7% and 97.3% from ½ to 7 h respectively (Fig. 2a). After long time Al exposure Evans blue uptake increased progressively. It was increased by 2.4, 3.5, 4 and 4.3 fold at 24, 48, 72 and 96 h, respectively (Fig. 2b).

Under oxidative stress conditions, over production of reactive oxygen species (ROS) cause lipid peroxidation. After Al exposure MDA content one of the end product of lipid peroxidation showed an increment even at ½ h and it raised 6-7 fold up to 7 h (Fig. 3a). The increment showed 7.5, 9.7, 8.1 and 6-fold increase at 24, 48, 72 and 96 h, respectively. Although the MDA content was highest at 48 h, it decreased at 72 and 96 h with regard to 48 h (Fig. 3b).

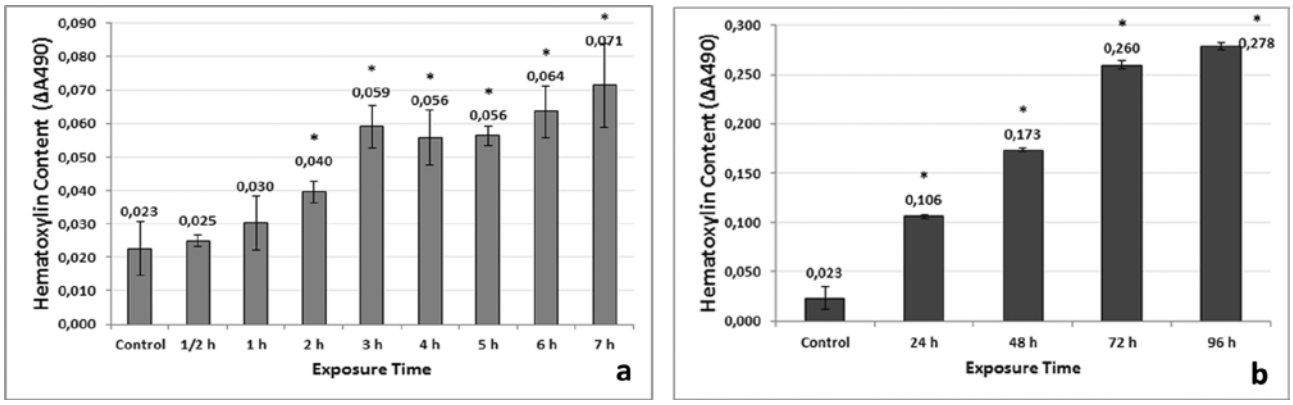

Figure 1. Hematoxylin content of control and 100 μM $AlCl_3$ treated barley roots at short (a) and long (b) time points. The data with (*) are significantly different from the control at $P < 0.05$ level.

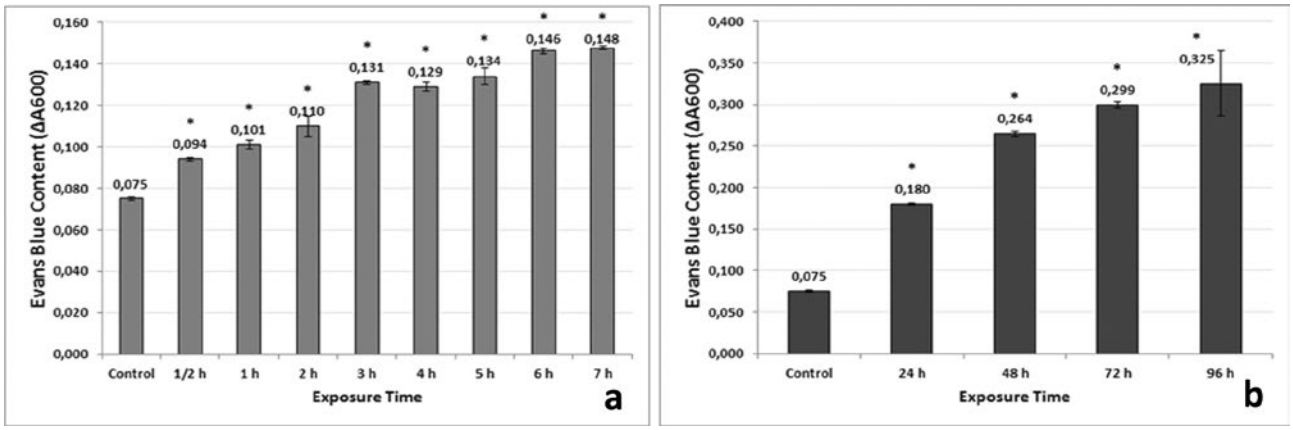

Figure 2. Evans blue uptake of control and 100 μM $AlCl_3$ treated barley roots at short (a) and long (b) time points. The data with (*) are significantly different from the control at $P < 0.05$ level.

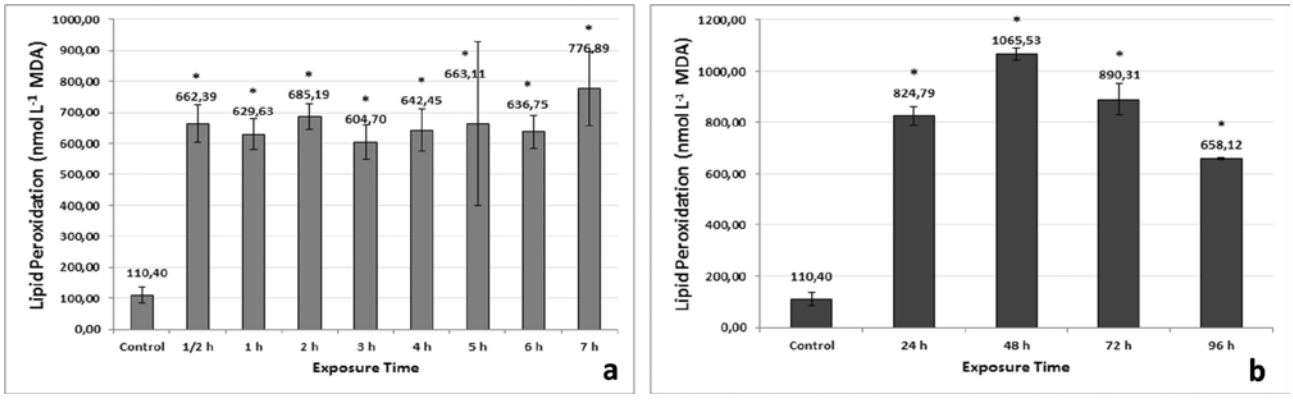

Figure 3. Lipid peroxidation of control and 100 μM $AlCl_3$ treated barley roots at short (a) and long (b) time points. The data with (*) are significantly different from the control at $P < 0.05$ level.

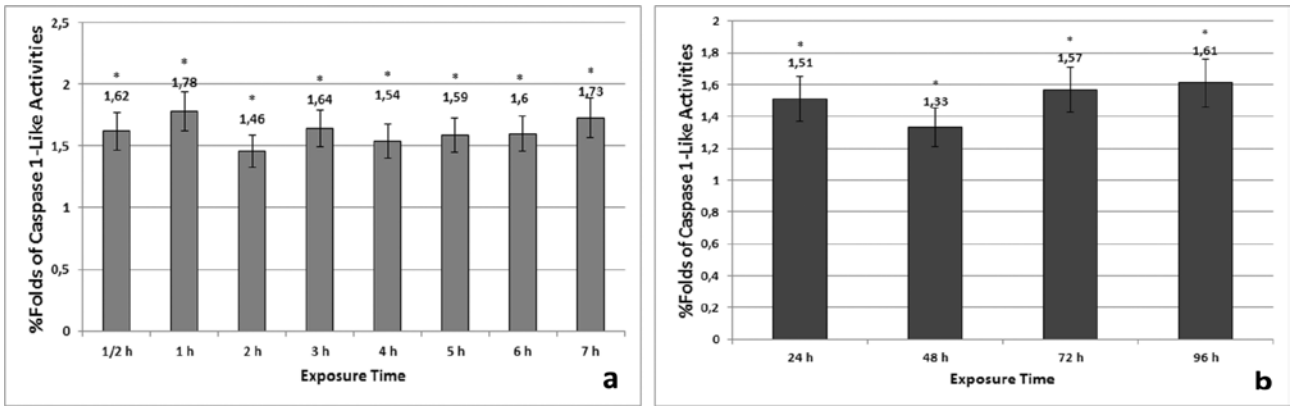

Figure 4. % fold caspase-1 like activities of control and 100 µM $AlCl_3$ treated barley roots at short (a) and long (b) time points. The data with (*) are significantly different from the control at $P < 0.05$ level.

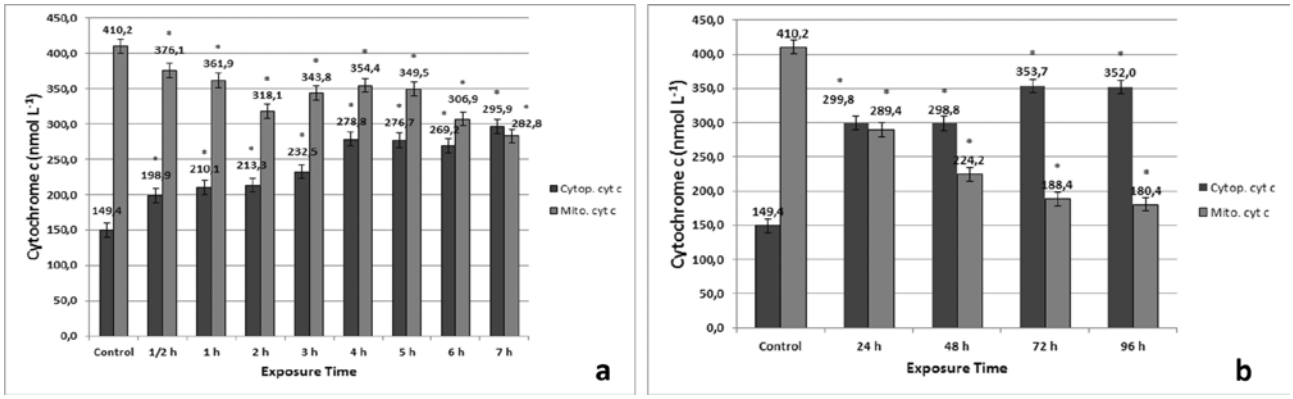

Figure 5. Cytochrome c level in mitochondria and cytoplasm of control and 100 µM $AlCl_3$ treated barley roots at short (a) and long (b) time points. The data with (*) are significantly different from the control at $P < 0.05$ level.

Although there are no functional homologs of animal caspases, there are true caspase-like activities in plants during PCD. Although the results of caspase-1 like activities showed fluctuations between exposure groups, Al caused increase both at short and long time points. The increased activities were among 1.33 – 1.78 than that of control (Fig. 4a, b).

It has been known that cyt c is released from inner mitochondrial membrane to cytoplasm during PCD. In barley roots, after Al exposure cyt c release started from ½ h and increased exponentially. It was 33.1% in ½ h, 40.6% in 1 h, 42.8% in 2 h, 55.6% in 3 h, 86.6% in 4 h, 85.2% in 5 h, 80.2% in 6 h and 98.1% in 7 h (Fig. 5a). After long term exposure it increased about 2 fold in 24 and 48 h, and about 2.4 fold in 72 and 96 h (Fig. 5b).

DNA fragmentation is one of the significant markers of PCD and flow cytometry is one of the analyses that used. The fragmented DNA can be seen as peaks at the left of G1 in the histogram. After the data analysis, the cell rate of having fragmented DNA was 23.7%, 17.3%, 31.4%, 37.1%, 15.0%, 37.8%, 25.1% and 30.6% between ½ - 7h, respectively (Fig. 6). At long term exposure DNA fragmentation rate was more significant. It was 63.7%, 49.6%, 62.6% and 64.4% between 24-96 h, respectively (Fig. 7). According to the flow cytometry Al caused DNA fragmentation both in short and long term exposure.

DISCUSSION

Al toxicity is one of the major inhibitors of plant growth and development in acidic soils (Abate *et al*. 2013; Ma *et al*. 2014). Although multiple studies have been performed in understanding physiological and molecular mechanism of Al toxicity and tolerance in the last few decades, there is limited studies concerning time dependent occurrence of Al-induced PCD. Therefore, we

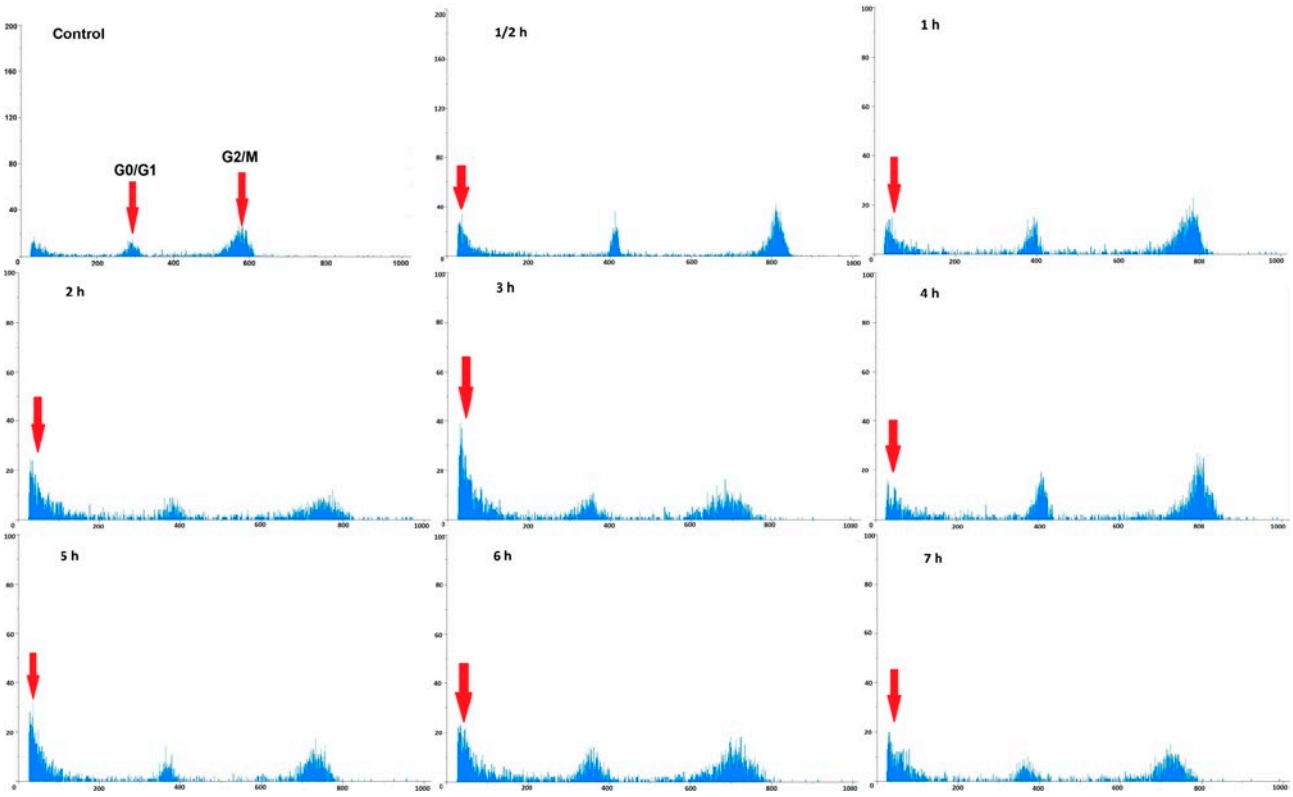

Figure 6. DNA fragmentation of control and 100 µM $AlCl_3$ treated barley roots at short term exposure. (x) axis denotes cell counts and (y) axis denotes fluorescence intensity.

determined the temporal effects of Al correlating with Al^{+3} ion uptake, loss of plasma membrane integrity, lipid peroxidation, caspase-1 like activities, cyt c release and DNA fragmentation in relation to PCD.

Al toxicity adversely affects the cellular processes due to the strong and rapid interactions of Al with apoplasmic and symplasmic targets. It has been widely known that Al accumulates more in root apex and strongly binds to negative charged materials such as cell walls and membranes (Matsumoto 2000). Several researches revealed that primer cellular responses to detrimental effects of Al could arise within second to minutes along with Al penetration (Kochian *et al.* 2005; Singh *et al.* 2017). Based on our Al^{+3} ion uptake results, Al penetrated into root apex beginning from ½ h and increased on the advancing hours. Although the Al uptake was very slight (8.7%) at the beginning, its impact was very severe in barley roots. Considering the loss of plasma membrane integrity and lipid peroxidation, the toxicity was very significant even at ½ h Al exposure. Al uptake increased gradually depending on time and at the same time loss of plasma membrane integrity enhanced. Considering the sharp increase of MDA even at ½ h suggests that Al is not detrimental on only plasma membrane. It's also very injurious on whole cellular membrane system including organelles. Although MDA content rose sharply up to 48 h, the reduction of MDA at 72 and 96 h may be related to increased generation of the other end product aldehydes such as 4-HNE.

According to general consensus Al induces oxidative stress as an abiotic stress factor in plants (Matsumoto 2000). Whereas Al is not a transition element, it catalyzes formation of ROS inducing oxidative stress (Gupta *et al.* 2013). Over-accumulation of ROS induces damage of biological molecules such as proteins, DNA and lipids. Membrane lipids are the more significant targets of ROS and culminate in lipid peroxidation eventually affecting normal cellular functions such as reduction in membrane fluidity, increase in phospholipid exchange, leakage of membrane and membrane rupture. Besides lipid peroxidation is considered as one of the hallmarks of PCD (Gill and Tuteja 2010; Woo *et al.* 2013; Nath and Lu 2015). Moreover, it has been reported that Al induces swollen mitochondria with several vacuoles, disrupted plasma membrane, and nuclear deformations following

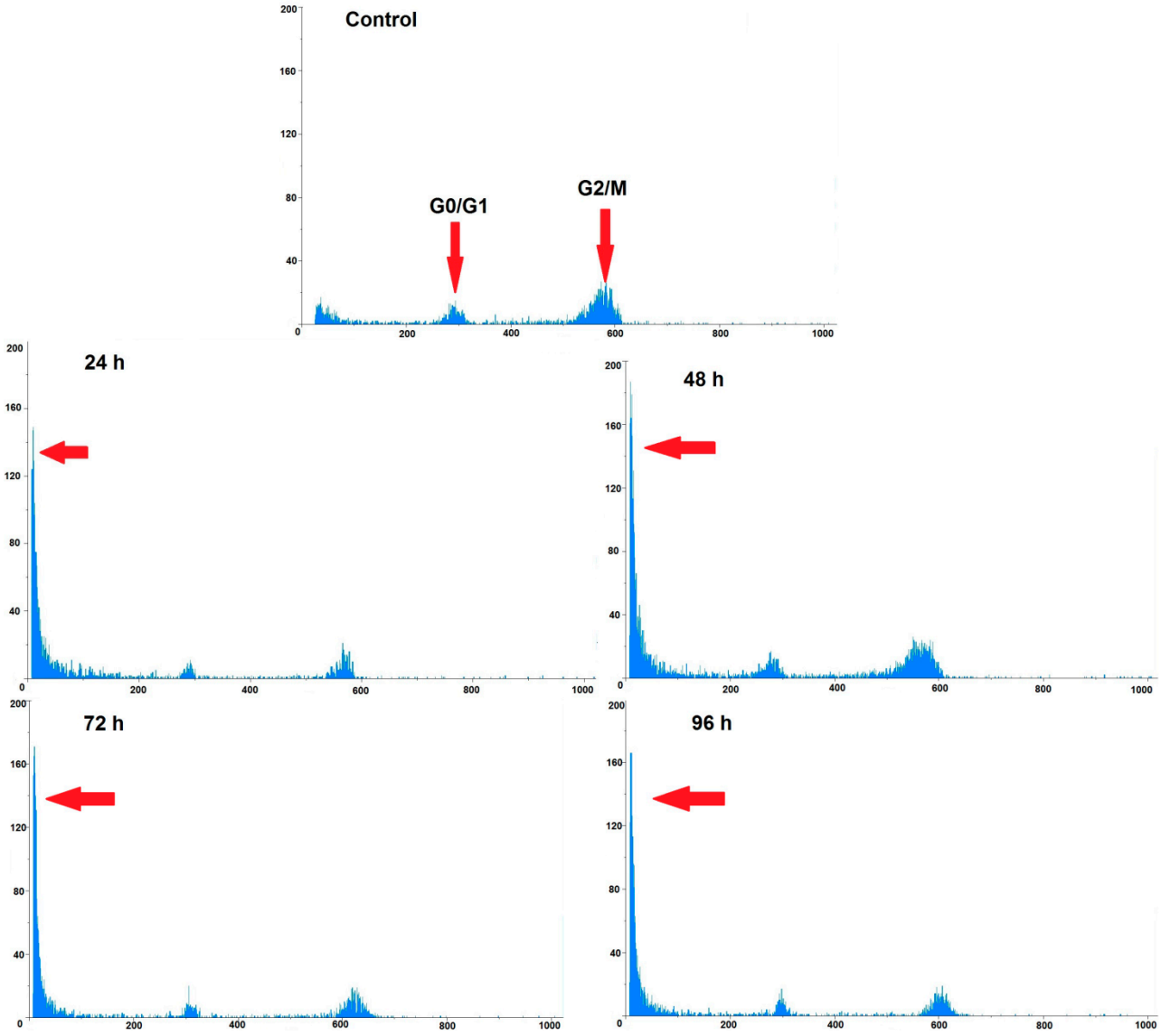

Figure 7. DNA fragmentation of control and 100 µM $AlCl_3$ treated barley roots at long term exposure. (x) axis denotes cell counts and (y) axis denotes fluorescence intensity.

the mitochondrial pathway of PCD (Gupta *et al.* 2013; Singh *et al.* 2017).

There is a close relation to ROS triggered cyt c release from the inner mitochondrial membrane to cytoplasm constituting mitochondrial pathway of PCD. ROS provokes the cardiolipin oxidation in mitochondrial inner membrane weakening the bonds of cyt c. ROS also triggers the Ca^{2+} transition as a secondary signal from ER to mitochondria reducing the mitochondrial membrane potential (ΔΨm). After ΔΨm decrease, cyt c released to intra-membrane space translocate to the cytoplasm from the mitochondrial permeability transition pores (MPTP) in the outer mitochondrial membrane (Ott *et al.* 2007; Williams *et al.* 2014). In PCD cyt c release stimulates caspase-like activities resulting in execution of PCD (Li and Xing 2010; Petrov *et al.* 2015; Gunawardena and McCabe 2015).

Huang *et al.* (2014) indicated that Al-induced ROS accumulation and PCD is closely related. According to their results 100 µM $AlCl_3$ caused increase in MPTP opening, reduction of ΔΨm, cyt c translocation to cytoplasm and caspase 3-like activity subsequent to ROS accumulation in *Arachis hypogaea* roots. It has been concluded that Al induced PCD is mediated by ROS

related cascade of cellular events resulting in mitochondrial alterations and caspase like activities. Simultaneously, Zhan *et al*. (2014) established the relation between ROS accumulation and mitochondrial alterations during Al-induced PCD in *Arachis hypogaea*. The researchers reported that increase in mitochondrial ROS induced reduction of mitochondrial Ca concentration, opening of MPTP, collapse of ΔΨm and cyt c release were more extensively in Al sensitive cultivar depending on Al concentration. Similarly, in the present study Al application caused cyt c release to the cytoplasm depending on time. The best of our knowledge all of the researches subjecting cyt c release were qualitative analysis and no report has been published of quantitative analysis of cyt c release during PCD in plants except our study.

In addition to alterations of mitochondria several researchers reported caspase like activities induced by ROS increase and cyt c release after Al application (Li and Xing 2011; Huang *et al*. 2014; Aytürk and Vardar 2015; Yao *et al*. 2016). Caspases are cysteine proteases initiating and amplifying PCD and cleave their cellular substrates at certain aspartic acid residues (McIlwain *et al*. 2013). Whereas there are no functional homologs of caspases in plants, caspase-like activities have been elucidated. According to recent reports, vacuolar Processing Enzymes (VPEs) belonging to cysteine protease family cleave synthetic caspase-1 substrate YVAD (Tyr-Val-Ala-Asp) in plants (Hatsugai *et al*. 2004; Cai *et al*. 2014; Rocha *et al*. 2017). Besides synthetic caspase-1 inhibitor (ac-YVAD-CHO) blocks VPE activation (Sexton *et al*. 2007; Misas-Villamil *et al*. 2013). Kariya *et al*. (2013; 2018) reported Al-induced dose dependent VPE activity at transcriptional level in *Nicotiana tabacum*. The researchers also indicated that the presence of VPE inhibitor (Ac-YVAD-CHO) suppressed PCD symptoms. Aytürk and Vardar (2015) revealed that short term Al toxicity also increased caspase-3, -8 and -9 like activities which are responsible for DNA fragmentation and initiation of apoptosis in animal systems in rye, barley, oat and triticale roots. Similar to the stated studies, Al application caused caspase-1 like activity from ½ h to 96 h in barley roots. Although it has been reported that Al toxicity induces different caspase like activities, using specific caspase-1 substrate is more accurate approach because VPE specific to plants has caspase-1 like activity.

DNA fragmentation which is one of the important signatures of PCD originates from internucleosomal DNA cleavage by specific proteases and nucleases. In light and electron microscopy fragmented DNA can be seen as a compact mass at the periphery of the nucleus (Vardar and Ünal 2012). DNA fragmentation can also be analyzed by TUNEL reaction, comet assay, laddering on the agarose gel and flow cytometry (Tripathi *et al*. 2016).

Flow cytometry is based on DNA staining with a florescence dye and analyze of the cell cycle (Shen *et al*. 2017). In the histogram of flow cytometry, the first peak indicates G0/G1 cycle and the second peak indicates G2/M. During cell death DNA was cleaved into oligonucleosomal fragments. As a result of this, DNA content decreases in apoptotic cells and fragmented DNA accumulates at the left of G0/G1 peak (Yamamada *et al*. 2006).

Vardar *et al*. (2015; 2016) revealed DNA fragmentation using comet assay and agarose gel electrophoresis under Al stress in early hours in wheat, rye, barley, oat and triticale. According to our results the accumulation of fragmented DNA was also visible after short term Al application. The fluctuation in the rate of cells having fragmented DNA may suggest a recovery effort in short term exposure. However the rate of dying cells is up to 50% and DNA fragmentation is more severe in long term exposure. As distinct from the previous results, we put forward the long term effect of Al on DNA fragmentation. Although there are several studies concerning DNA fragmentation revealed by flow cytometry during senescence (Yamada *et al*. 2003; 2006), there is no study available during abiotic stress as well as Al stress. However, Jaskowiak *et al*. (2018) examined the effect of Al on the cell cycle of barley roots by flow cytometry. The researchers revealed that the DNA replication and mitotic index reduced, but G2/M phase increased. Besides

In conclusion; Al caused loss of plasma membrane integrity, lipid peroxidation, cyt c release, caspase-1 like activity and DNA fragmentation which are characteristic features of PCD. Although Al uptake, plasma membrane integrity, lipid peroxidation, cyt c release increased time dependently, caspase-1 like enzyme begun to activate at ½ h and did not represented very wide difference during short or long term Al application. Moreover, DNA fragmentation was progressive at long term exposure during Al-induced PCD.

ACKNOWLEDGEMENT

This work was supported by the Research Foundation of Marmara University (BAPKO) under grant FEN-C-YLP-091116-0501 and FEN-E-090517-0270.

CONFLICT OF INTEREST

The authors declare that they have no conflict interest.

REFERENCES

Abate E, Hussien S, Laing M, Mengistu F. 2013. Aluminum toxicity tolerance in cereals: Mechanisms, genetic control and breeding methods. Afr J Agr Res. 8:711-722.

Aytürk Ö, Vardar F. 2015. Aluminum induced caspase-like activities in some Gramineae species. Adv Food Sci. 37:71-75.

Cai YM, Yu J, Gallois P. 2014. Endoplasmic reticulum stress-induced PCD and caspase-like activities involved. Front Plant Sci. 5:41.

Cakmak I, Horst JH. 1991. Effects of aluminum on lipid peroxidation, superoxide dismutase, catalase, and peroxidase activities in root tips of soybean (*Glycine max*). Physiol Plant. 83:463–468.

Ciamporova M. 2002. Morphological and structural responses of plant roots to aluminum at organ, tissue and cellular levels. Biol Plant. 45:161–171.

Darko E, Ambrus H, Stefanovits-Bányai E, Fodor J, Bakos F, Barnabás B. 2004. Aluminium toxicity, Al tolerance and oxidative stress in an Al-sensitive wheat genotype and in Al-tolerant lines developed by in vitro microspore selection. Plant Sci. 166:583–591.

Drew MC, He CJ, Morgan PW. 2000. Programmed cell death and aerenchyma formation in roots. Trends Plant Sci. 5:123–127.

Frantzios G, Galatis B, Apostolakos P. 2000. Aluminum effects on microtubule organization in dividing root tip cells of *Triticum turgidum*. I. Mitotic cells. New Phytol. 145:211–224.

Gill SS, Tuteja N. 2010. Reactive oxygen species and antioxidant machinery in abiotic stress tolerance in crop plants. Plant Physiol Biochem. 48:909–930.

Gunawardena AH, McCabe PF. 2015. Plant Programmed Cell Death, Springer.

Guo P, Qi YP, Cai YT, Yang TY, Yang LT, Huang ZR, Chen LS. 2018. Aluminum effects on photosynthesis, reactive oxygen species and methylglyoxal detoxification in two *Citrus* species differing in aluminum tolerance. Tree Physiol. 00:1–18.

Gupta N, Gaurav SS, Kumar A. 2013. Molecular basis of aluminium toxicity in plants: A review. Am J Plant Sci. 4:21–37.

Hatsugai N, Kuroyanagi M, Yamada K, Meshi T, Tsuda S, Kondo M, Nishimura M, Hara-Nishimura I. 2004. A plant vacuolar protease, VPE, mediates virus-induced hypersensitive cell death. Science. 305:855–858.

Huang WJ, Oo TL, He HY, Wang AQ, Zhan J, Li CZ, Wei SQ, He LF. 2014. Aluminum induced rapidly mitochondria dependent programmed cell death in Al sensitive peanut root tips. Bot Stud. 55:67–78.

Jackson MB, Armstrong W. 1999. Formation of aerenchyma and the processes of plant ventilation in relation to soil flooding and submergence. Plant Biol. 1:274–287.

Jaskowiak J, Tkaczyk O, Slota, Kwasniewska, J, Szarejko I. 2018. Analysis of aluminum toxicity in *Hordeum vulgare* roots with an emphasis on DNA integrity and cell cycle. PLOS One. 13:e0193156.

Kariya K, Demiral T, Sasaki T, Tsuchiya Y, Turkan I, Sano T, Yamamoto Y. 2013. A novel mechanism of aluminium-induced cell death involving vacuolar processing enzyme and vacuolar collapse in tobacco cell line BY-2. J Inorg Biochem. 128:196–201.

Kariya K, Tsuchiya Y, Sasaki T, Yamamoto Y. 2018. Aluminium-induced cell death requires upregulation of NtVPE1 gene coding vacuolar processing enzyme in tobacco (*Nicotiana tabacum* L.). J Inorg Biochem. 181:152–161

Kochian LV, Hoekenga OA, Pineros MA. 2004. How do crop plants tolerate acid soils? Mechanisms of aluminum tolerance and phosphorous efficiency. Ann Rev Plant Biol. 55:459–493.

Kochian LV, Piñeros MA, Hoekenga OA. 2005. The physiology, genetics and molecular biology of plant aluminum resistance and toxicity. Plant Soil. 274:175–195.

Li Z, Xing D. 2011. Mechanistic study of mitochondria dependent programmed cell death induced by aluminum phytotoxicity using fluorescence techniques. J Exp Bot. 62:331–343.

Lombardi L, Ceccarelli N, Picciarelli P, Lorenzi R. 2007. Caspase-like proteases involvement in programmed cell death of *Phaseolus coccineus* suspensor. Plant Sci. 172:573–578.

Ma JF, Chen ZC, Shen RF. 2014. Molecular mechanism of Al tolerance in Gramineous plants. Plant Soil. 381:1–12.

Matsumoto H. 2000. Cell biology of aluminum toxicity and tolerance in higher plants. Int Rev Cytol. 200:1–47.

McIlwain DR, Berger T, Mak TW. 2013. Caspase functions in cell death and disease. Cold Spring Harb Pers Biol. 5:a008656.

Misas-Villamil JC, Toenges G, Kolodziejek I, Sadaghiani AM, Kaschani F, Colby T, Bogyo M, van der Hoorn RAI. 2013. Activity profiling of vacuolar processing enzymes reveals a role for VPE during oomycete infection. Plant J. 73:689–700.

Nath K, Lu Y. 2015. A Paradigm of reactive oxygen species and programmed cell death in plants. J Cell Sci Ther. 6.

Ott M, Gogvadze V, Orrenius S, Zhivotovsky B. 2007. Mitochondria, oxidative stress, and cell death. Apoptosis. 12:913–922.

Ownby JD. 1993. Mechanisms of reaction of hematoxylin with aluminium-treated wheat roots. Physiol Plant. 87:371–380.

Pandey P, Srivastava RK, Dubey RS. 2013. Salicylic acid alleviates aluminum toxicity in rice seedlings better the magnesium and calcium by reducing aluminum uptake, suppressing oxidative damage and increasing antioxidative defense. Ecotoxicology. 22:656–670.

Papini A, Mosti S, Milocani E, Tani G, Di Falco P, Brighigna L. 2011. Megasporogenesis and programmed cell death in *Tillandsia* (Bromeliaceae). Protoplasma. 248:651–662.

Petrov V, Hille J, Mueller-Roeber B, Gechev TS. 2015. ROS mediated abiotic stress-induced programmed cell death in plants. Front Plant Sci. 6:69.

Poor P, Kovacs J, Szopko D, Tari I. 2013. Ethylene signaling in salt stress- and salicylic acid-induced programmed cell death in tomato suspension cells. Protoplasma. 250:273–284.

Rocha GL, Fernandez JH, Oliveira AEA, Fernandes KVS. 2017. Programmed cell death-related proteases in plants. In Tech, Croatica.

Sexton KB, Witte MD, Blum G, Bogyo M. 2007. Design of cell-permeable fluorescent activity-based probes for the lysosomal cysteine protease asparaginyl endopeptidase (AEP)/legumain. Bioorgan Med Chem Lett. 17:649–653.

Sharma P, Dubey RS. 2007. Involvement of oxidative stress and role of antioxidative defense system in growing rice seedlings exposed to toxic concentrations of aluminum. Plant Cell Rep. 26:2027–2038.

Shen Y, Vignali P, Wang R. 2017. Rapid profiling cell cycle by flow cytometry using concurrent staining of DNA and mitotic markers. Bio-protocol. 7.

Singh S, Tripathi DK, Singh S, Sharma S, Dubey NK, Chauhan DK, Vaculík M. 2017. Toxicity of aluminium on various levels of plant cells and organism: A review. Environ Exp Bot. 137:177–193.

Taşpınar MS, Aydin M, Sigmaz B, Yagci S, Arslan E, Agar G. 2018. Aluminum-induced changes on DNA damage, DNA methylation and LTR retrotransposon polymorphism in maize. Arab J Sci Eng. 43:123–131.

Tripathi AK, Pareek A, Singla-Pareek SL. 2016. TUNEL assay to assess extent of DNA fragmentation and programmed cell death in root cells under various stress conditions. Plant Physiol. 7.

Vardar F, Arıcan E, Gözükırmızı N. 2006. Effects of aluminum on in vitro root growth and seed germination of tobacco (*Nicotiana tabacum* L.). Adv Food Sci. 28:85–88.

Vardar F, Ünal M. 2007. Aluminum toxicity and resistance in higher plants. Adv Mol Biol. 1:1–12.

Vardar F, Ünal M. 2008. Proteolytic enzymes in plant programmed cell death. Turk J Sci Rev. 1:65–78.

Vardar F, İsmailoğlu I, İnan D, Ünal M. 2011. Determination of stress responses induced by aluminum in maize (*Zea mays* L. Karadeniz Yıldızı). Acta Biol Hung. 62:156–170.

Vardar F, Ünal M. 2012. Ultrastructural aspects and programmed cell death in the tapetal cells of *Lathyrus undulatus* Boiss. Acta Biol Hung. 63:56–70.

Vardar F, Akgül N, Aytürk Ö, Aydın Y. 2015. Assessment of aluminum induced genotoxicity with comet assay in wheat, rye and triticale roots. Fresen Environ Bull. 37:3352–3358.

Vardar F, Çabuk E, Aytürk Ö, Aydın Y. 2016. Determination of aluminum induced programmed cell death characterized by DNA fragmentation in Gramineae species. Caryologia. 69:111–115.

Vardar F, Yanık F, Çetinbaş-Genç A, Kurtuluş G. 2018. Aluminum-induced toxicity and programmed cell death in plants In:Advances in Health and Natural Sciences Yuksel B, Karagül MS (eds), chapter 10, Nova Book USA.

Vitorello VA, Capaldi FRC, Stefanuto VA. 2005. Recent advances in aluminum toxicity and resistance in higher plants. Brazil J Plant Physiol. 17:129–143.

Wang J, Li X, Liu Y, Zhao X, Chen C, Tian F. 2011. MEK/ERK inhibitor U0126 enhanced salt stress-induced programmed cell death in *Thellungiella halophila* suspension-cultured cells. Plant Growth Regul. 63:207–216.

Wang GP, Zhang ZH, Kong DJ, Liu QX, Zhao GL. 2012. Programmed cell death is responsible for replaceable bud senescence in chestnut (*Castanea mollissima* BL.). Plant Cell Rep. 31:1603–1610.

Williams B, Verchot J, Dickman MB. 2014. When supply does not meet demand-ER stress and plant programmed cell death. Front Plant Sci. 5:211.

Wituszyńska W, Karpiński S. 2013. Programmed cell death as a response to high light, UV and drought stress in plants In:Vahdati K, Leslie C (eds) Abiotic stress plant responses and applications in agriculture. InTech, Croatica.

Woo HR, Kim HJ, Nam HG, Lim PO. 2013. Plant leaf senescence and death - regulation by multiple layers of control and implications for aging in general. J Cell Sci. 126:4823–4833.

Yamamada T, Takatsu Y, Manabe T, Kasumi M, Marubashi W. 2003. Suppressive effect of trehalose on apoptotic cell death leading to petal senescence in ethylene-insensitive flowers of gladiolus. Plant Sci. 164:213–221.

Yamamada T, Takatsu Y, Kasumi M, Ichimura K, van Doorn WG. 2006. Nuclear fragmentation and DNA

degradation during programmed cell death in petals of morning glory (*Ipomea nil*). Planta. 224:1279–1290.

Yao, S; Huang, W; Pan, C; Zhan, J; He, LF. (2016). Caspase-like proteases regulate aluminum-induced programmed cell death in peanut. Plant Cell Tissue and Organ Culture, 127 (3), 691-703.

Zhan, J; Li, W; He, HY; Li, CZ; He, LF. (2014). Mitochondrial alterations during Al-induced PCD in peanut root tips. Plant Physiology and Biochemistry, 75, 105-113

Caryologia
International Journal of Cytology, Cytosystematics and Cytogenetics

Firenze University Press
www.fupress.com/caryologia

OPEN ACCESS

Citation: S. Mehri, H. Shirafkanajirlou, I. Kolbadi (2020) Genetic diversity, population structure and chromosome numbers in medicinal plant species *Stellaria media* L. VILL.. *Caryologia* 73(1): 57-65. doi: 10.13128/caryologia-680

Received: July, 2019

Accepted: October, 2019

Published: May 8, 2020

Data Availability Statement: All relevant data are within the paper and its Supporting Information files.

Competing Interests: The Author(s) declare(s) no conflict of interest.

Genetic diversity, population structure and chromosome numbers in medicinal plant species *Stellaria media* L. VILL.

Shahram Mehri*, Hassan Shirafkanajirlou, Iman Kolbadi

Department of Agronomy and Plant Breeding, ParsAbad Moghan Branch, Islamic Azad University, ParsAbad Moghan, Iran
*Corresponding author. E-mail: sh.mehri2000@gmail.com

Abstract. *Stellaria media* L. VILL., is known under the name of chickweed, it is an annual plant in the family Caryophyllaceae. *Stellaria media* is distributed in the all regions of Iran and has been introduced to many habitats of the world. *S. pallida* is very similar to *S. media.* This plant is considered to be as a herbal remedy and is used in folk medicine. *Stellaria media* is edible and nutritious. In the present study, we used morphological and ISSR data for this species. For this, 43 morphological characteristics, including 16 qualitative and 26 quantitative. AMOVA and Gst analyses showed that the populations of this species are genetically differentiated. Nm analysis revealed very low value of genetic diversity among the studied population and mantel test indicated isolation by distance occurred among them. The present study showed that the studied populations of *S. media* are differentiated in morphological characteristics and genetic content. In general, species relationships obtained from morphological and molecular data were largely congruent.

Keywords. Genetic diversity, ISSR, Morphology, Species relationship, *Stellaria media*.

INTRODUCTION

The family Caryophyllaceae comprised about 81 genera and 2600 species (Bittrich 1993; Ullah *et al*. 2019a). *Stellaria* L. (Caryophyllaceae, Alsinoideae) includes both annual and perennial herbaceous plants that are widely distributed in the temperate zones of Europe and Asia (Lu and Rabeler 2001; Keshavarzi and Esfandani –Bozchaloyi, 2014a, 2014b; Ullah *et al*. 2019b, 2019c) and about 120 species with worldwide distribution, mainly in the north temperate zone (Morton 2005; Ullah *et al*., 2018a, 2018b).

In Flora Iranica this genus has 9 species and divided into 2 sections: sect. *Pseudalsine* Boiss. consist of one species *S. alsinoides* Boiss. & Buhse and sect. *Stellaria* with six species: *S. holostea* L., *S. persica* Boiss., *S. graminea* L., *S. nemorum* L., *S. media* (L.) Vill., *S. pallida* (Dumort.) Pire (Rechinger 1988). Main center of diversification for *Stellaria* is Eurasia, with a center of distribution in the mountains of E. central Asia. Some species are also cosmopolitan (Bittrich 1993; Ullah *et al*. 2018c).

There are limited chromosome records for *Stellaria* in the world. Basic Chromosome numbers of x=10, 11, 12 and 13 have been reported for the genus (Federov 1969; Moore 1973; Goldblatt 1981). *Stellaria media*, chickweed, are annual and with slender stems, they have hairs on one side of the stem. The leaves are linear or oval, smooth or minutely, 13 to 17 × 1.5 to 7 mm. Flowers are hermaphrodite and petals are white with 5 deeply. Sepals prominently 4 to 6-nerved, 4 to 7 mm. Stigmas are 3 and the stamens are 3. *Stellaria media* common in waste places, open areas, lawns, meadows, and widely distributed to temperate regions of Europe, Asia and Northern America.

Stellaria media is edible and nutritious and has a history of herbal use and medicinal properties. This species has been used as to soothe severe itchiness even where all other remedies have failed (Slavokhotova *et al*. 2011). it is considered for rheumatic pains, skin diseases, and period pain as well as for bronchitis and arthritis (Slavokhotova *et al*. 2011). *Stellaria media* possess significant chemicals known as saponins, which can be cause saponin poisoning in cattle (Haragan 1991).

There are many studies which are on taxonomy, pollen morphology, phylogeny, seed micromorphology, anatomy, trichome and cytology of *stellaria* species (Esfandani-Bozchaloyi and Keshavarzi 2014; Keshavarzi and Esfandani-Bozchaloyi 2014 a, b; Ullah *et al*. 2018a, 2018b, 2018c). However, genetic diversity of *stellaria* species have been reported in a few studies (Verkleij *et al*. 1980; Chinnappa and Morton 1984), also outcrossing or inbreeding, genetic structure, genetic variability within/between populations and ecological adaptation on *Stellaria* of Iran have not been investigated yet.

According to Ellis and Burke (2007) genetic diversity are essential in the adaptability and survival of population, because it is as a way for adapt to changing environments in populations. The adapt of the population to the changing environment will depend on the presence of the genetic diversity. Large populations have higher genetic diversity due to more to maintain genetic material and small populations have the loss of diversity which is called genetic drift. Mating or inbreeding between individuals with similar genetic occur in small population sizes, thus decreasing genetic diversity and finally we have more common alleles.

Hence, the used of markers will depend on the type of the species. We have been used DNA marker based techniques such as Inter-Simple Sequence Repeats (ISSRs), due to easy, highly reproducible, stable and useful in species delimitation, gene tagging, gene flow, breeding programs and evolutionary biology (Ellis and Burke 2007; Esfandani-Bozchaloyi *et al*. 2018a, 2018b, 2018c). Therefore, we studied morphological and molecular study of 11 geographical populations of *S. media* for the first time in Iran.

MATERIALS AND METHODS

Morphological studies

85 plant sample were selected from eleven populations located in three provinces of Iran. Identification of species *Stellaria media* were based on the descriptions provided by Flora Iranica (Rechinger 1988). The sampling sites and herbarium number are provided in Table 1, Figure 1. Vouchers were deposited at the herbarium of Islamic Azad University, Science and Research Branch, Tehran, Iran (IAUH).

DNA extraction

Fresh leaves of 85 individuals following a modified CTAB protocol. The quality was checked on a 1 % agarose

Table 1. Location addresses and ecological characters of the *Stellaria media*

Population	Locality	Latitude	Longitude	Altitude (m)	Voucher no.
1	Guilan, Road to Sangar	37°06' 57"	49°11'06"	47	IAUH 201600
2	Guilan, Bandar Anzali, Pine artificial woodland	37°27'34"	49°42'40"	-25	IAUH 201701
3	Guilan, Loleman	37°28'59"	49°33'45"	-29	IAUH 201702
4	Guilan, Siahkal, Sangar	37°09'08"	49°55'02"	27	IAUH 201603
5	Guilan, Gole rodbar river	37°10'05"	49°56'38"	15	IAUH 201604
6	Guilan , Sheytan kouh hill side	37°12'04"	50°03'12"	9	IAUH 201605
7	Guilan , Lahijan , Highlands of Sheytan Kouh	37°11'52"	50°03'17"	159	IAUH 201606
8	Guilan, Bandar Anzali, Road side	37°27'48"	49°22'30"	-11	IAUH 201707
9	Mazandaran, Chalos Neamat abad	36°49'02"	50°52'20"	-16	IAUH 201608
10	Mazandaran, Shirodi Ring Road	36°51'10"	50°32'11"	-18	IAUH 201709
11	Mazandaran, Noshahr	36°35'04"	51°35'14"	-20	IAUH 201710

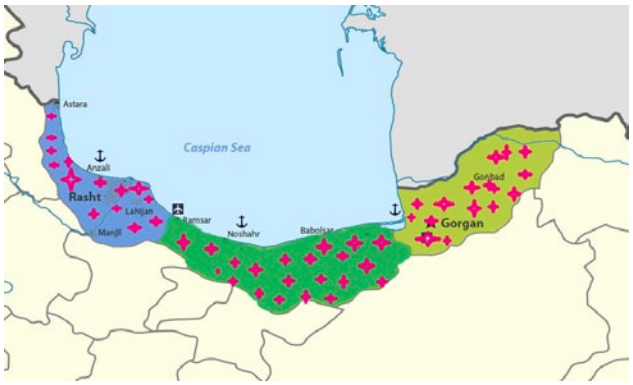

Figure 1. Distribution map of the studied populations.

gel and spectrophotometry. A set of ten primers; (GG) 5GT, (AA) 7GT, (AAA) 5Gt, UBC 234, (GG) 7AT, (AG) 7G, UBC 825, UBC 823, (GG) 5T and (GC) 8GG were used for ISSR analysis. PCR were carried out in 25 µl reactions containing 20 ng of template DNA, 0.3 mM dNTPs, 1µM primers, 1.0 µl of 20 ×PCR buffer (Cinnagen, Iran),1.8 mM of MgCl2, and 5 units of Taq polymerase (Cinnagen, Iran).

The amplification was carried out, with programmed as initial pre-denaturation at 95°C for 5 min followed by 36 cycles of denaturation at 94°C for 45 s, annealing at temperature (52-55°C) for 40 s, and extension at 72°C for 1min. A final 5 min extension at 72°C followed the completion of 38 cycles.

Karyological study

For somatic chromosome study, the seeds were soaked for 24 hours in running water and germinated in the laboratory (ca. 21°-24°). The root tips were cut between 9-11 AM and pretreated in 0.002M 8- hydroxyquinoline (4hours) and fixed in a cold mixture of ethanol and acetic acid (3:1) for 24 hours. Root tips were macerated in 1N HCl for 10 minutes (Cold Hydrolysis) at room temperature. The slides were staining in 2% Fe-acetocarmin for 10 hours.

Data analyses

Morphological studies

For morphological studies 43 morphological characters including 16 qualitative and 26 quantitative characters were studied following the protocols of (Ashfaq *et al*. 2019; Attar *et al*. 2019; Gul *et al*. 2019a; Gul *et al*. 2019b; Kandemir *et al*. 2019; Shah *et al*. 2018a, 2018b; Zaman *et al*. 2019) (Table 2).

Table 2. List of selected characters and their codes in morphological studies.

No.	Characters	Numerical code
1	Plant height	mm
2	Length of basal leaves	mm
3	Width of basal leaves	mm
4	Length of stem leaves	mm
5	Width of stem leaves	mm
6	Bract length	mm
7	Width bract	mm
8	Length pedicel	mm
9	Number of seeds per capsule	
10	Number of flowers per inflorescence	
11	Number of calyx	
12	Length calyx	mm
13	Width calyx	mm
14	Number of petal	
15	petal length	mm
16	Petal width	mm
17	Cleft size of petals	mm
18	Inter node length	mm
19	Number of stamen	
20	Number of stigma	
21	Capsule length	mm
22	Seed length	mm
23	Seed width	mm
24	Cleft size of capsule	mm
25	Number suture capsules	
26	Veins number sepals	
27	Growth period	0-annual 1- perennial
28	Bract apex	0-acute 1- narrow 2-absence
29	State of stem	0-unbranched 1-branched
30	State of stem strength	0-thin 1- strong
31	Hairs of stem	1-unilateral hair 2-multilateral hair
32	Cross-section of stem	0-round1- rectangular 2-elliptical
33	Shape of basal leaves	0-linear 1- linear-lanceolate
34	Basal leaves apex	0-acute 1- narrow
35	Basal leaves petiole	0-absence 1- presence
36	Hair of basal leaves petiole	0-absence 1- presence
37	Shape caulin leaves	0- linear 1- linear-lanceolate
38	Caulin leaves apex	0- acute 1- narrow
39	Caulin leaves petiole	0-absence 1- presence
40	Hair of caulin leaves petiole	0-absence 1- presence
41	Hair of caulin leaves margin	0-absence 1- presence
42	Hair of caulin leaves lamina	0-absence 1- presence
43	Shape of bract	0-linear 1- linear-lanceolate

Morphological traits were standardized (Mean = 0, Variance = 1) and used to estimate Euclidean distance for ordination analyses (Podani 2000). PCA (Principal components analysis) biplot and MDS (Multidimensional scaling) were applied for grouping and identify the most variable morphological traits of among the populations (Podani 2000). We used from PAST version 2.17 (Hammer *et al.* 2012) for multivariate statistical analyses.

Molecular analyses

ISSR bands scored as present (1) or absent (0). Genetic polymorphism was determined by genetic diversity parameters: Shannon information index (I), percentage of polymorphism, the number of effective alleles and Nei's gene diversity (H) (Freeland *et al.* 2011). Neighbor-Net networking was used for Nei's genetic identity among studied populations (Huson and Bryant 2006; Weising *et al.* 2005). We used from PAST ver. 2.17 (Hammer *et al.* 2012), SplitsTree4 V4.13.1 (2013) and DARwin ver. 5 (2012) software for analysis data.

For AMOVA (Analysis of molecular variance) we used of GenAlex 6.4 software (Peakall and Smouse 2006; Meirmans and Van Tienderen 2004) that was determined Genetic differentiation of the species and Nei·s Gst analysis in GenoDive ver.2 (2013) (Hedrick 2005; Jost 2008) were used to revealed genetic distance of the species.

First data were scored as dominant markers (ISSR) so we used from STRUCTURE analysis for estimate the parameters that related to gene flow among studied population. Burn-in = 10000, and 10 runs were performed for relationship between Genetic structure and distance of geographical. Maximum likelihood method and Bayesian Information Criterion (BIC) was studied by structure analysis (Falush *et al.* 2007; Evanno *et al.* 2005; Meirmans 2012). Gene flow was determined by Calculating Nm from Gst by PopGene ver. 1.32 (1997). (Pritchard *et al.* 2000).

RESULTS

In this study 11 populations of *Stellaria media* were selected from northern regions of Iran. Genetic diversity parameters revealed that the highest percent of genetic polymorphism (48.89%) and gene diversity (0.179) exist in Guilan, Bandar Anzali, (population No.5), while the lowest amount of genetic polymorphism (13.33%) showed in population Guilan, Road side Bandar Anzali (No.8) Table 3.

Table 3. Genetic diversity parameters in the studied populations. (N = number of samples, Ne = number of effective alleles, I= Shannon's information index, He = gene diversity, UHe = unbiased gene diversity, P%= percentage of polymorphism, populations).

Pop	N	Na	Ne	I	He	uHe	%P
pop1	6.000	0.633	1.136	0.120	0.080	0.087	23.33%
pop2	8.000	0.644	1.119	0.121	0.077	0.083	25.56%
pop3	23.000	0.756	1.140	0.138	0.088	0.090	32.22%
pop4	5.000	0.511	1.123	0.109	0.073	0.081	20.00%
pop5	10.000	1.011	1.312	0.265	0.179	0.188	48.89%
pop6	6.000	0.944	1.279	0.231	0.158	0.172	40.00%
pop7	5.000	0.533	1.118	0.101	0.068	0.075	18.89%
pop8	4.000	0.422	1.099	0.078	0.054	0.061	13.33%
pop9	6.000	0.678	1.140	0.120	0.081	0.089	21.11%
pop10	6.000	0.922	1.260	0.227	0.152	0.166	42.22%
pop11	6.000	0.878	1.217	0.198	0.130	0.142	40.00%

AMOVA test showed that, 40% of total genetic diversity was within population and 60% was among population. Hedrick standardized fixation index makes of genetic distance among the studied populations. We have moderate level for AMOVA produced after 999 permutations (G'st = 0.515, P = 0.001) and Hedrick differentiation index (D-est = 0.331, P = 0.001). Our results showed that the populations of *S. media* are differentiated from each other.

Populations genetic affinity

Neighbor-Net network and Nj tree revealed identity results but here only Neighbor-Net network is discussed (Figure 2). In the network showed that the populations 1 and 4, as well as populations 7 and 8 show are placed close to each other and they have closer genetic affinity. The populations 3 and 5, 6, 11 are differentiated from the other populations.

The studied specimen in MDS plot revealed that they were stay in different groups, which this results were in agreement with the AMOVA results (Figure 3). The relationship between altitude distance and genetic distance by Mantel test after 5000 permutations makes significant in these populations (r = 0.38, P = 0.001). We have isolation in *Stellaria media* occurred that we have low amount of gene flow due to geographically more distant of populations.

Populations genetic structure

The result carried out on STRUCTURE analyses by Evanno test which makes a peak at k = 9 (Figure 4). Fur-

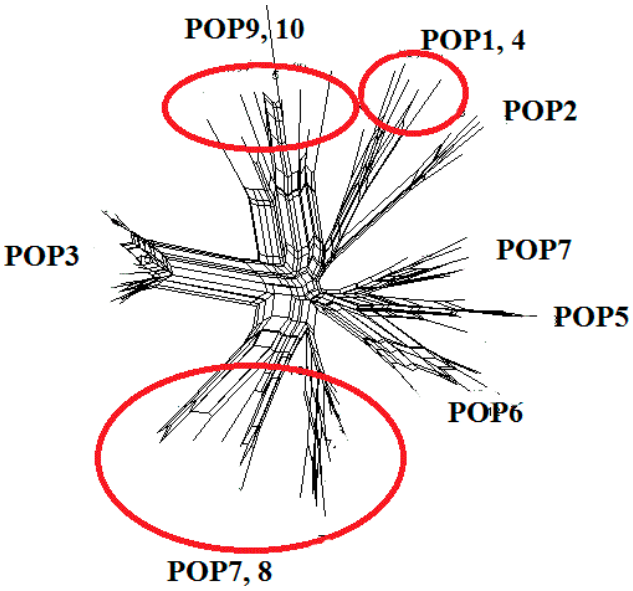

Figure 2. Neighbor-Net network of populations in *S. media* based on ISSR data.

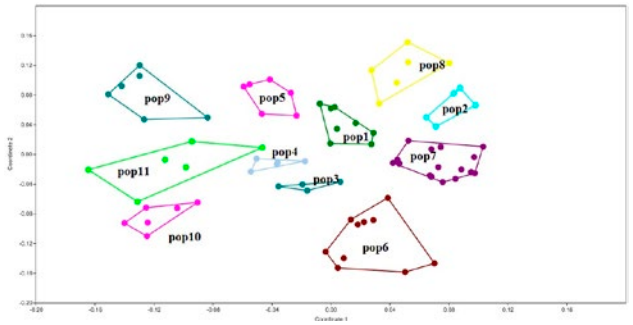

Figure 3. MDS plot of populations in *S. media* based on ISSR data.

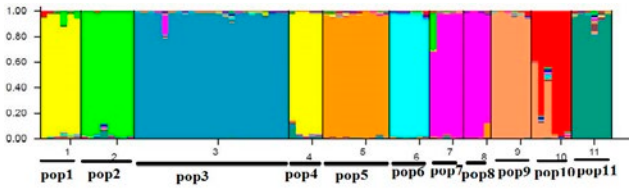

Figure 4. STRUCTURE plot of *S. media* populations based on k = 9 of ISSR data.

thermore, STRUCTURE analyses shown genetic identity between populations 1 and 4 (similarly colored), populations 7 and 8, like populations 9-10. But also it indicated genetic difference of populations 3 and 5 (differently colored), likes 6 and 11.

The results of Reticulogram (Figure 5), indicated some of shared alleles that is based on the least square

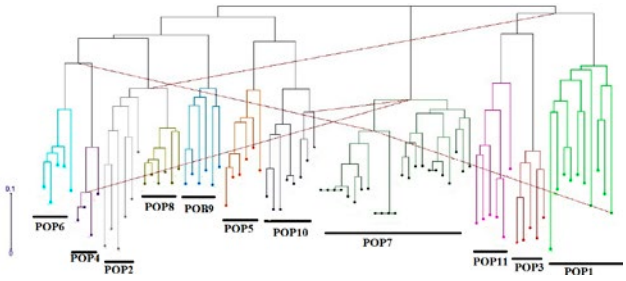

Figure 5. Reticulogram of *S. media* populations based on least square method analysis of ISSR data. (Population numbers are according to Table 1.

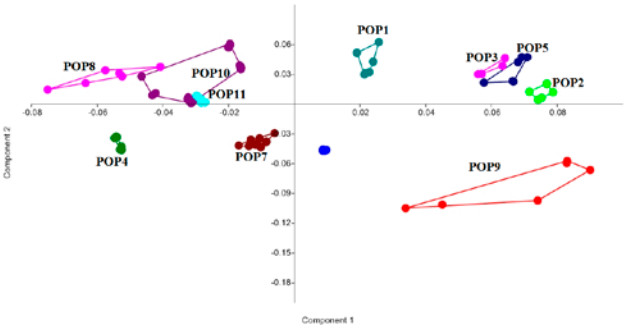

Figure 6. PCA plot of *S. media* populations based on morphological characters.

method among populations 10 and 4, 6 and between 7 and 4 and 10, also between 3, 11, 1 and 2 and 8. The mean Nm = 0.29 that is very low level of genetic diversity and supports genetic stratification as showed by STRUCTURE analyses and K-Means. Nm result agreed with population assignment test and cannot showed gene flow among these populations. In total ten ISSR primers produced 90 bands, fragment size ranged from 100 to 2800 bp.

Morphometric analyses

ANOVA test for 85 plant specimen were examined from 11 populations. Our results indicated significant difference in compare with the studied populations ($P < 0.05$). Ordination plot and other analyses produced similar result among populations (Figure 6). Our result revealed that among of the studied populations exist of morphological divergence and this divergence was due to quantitative traits. For example, length of stem leaves character separated population No. 9, but the populations 3 and 5 separated from the other populations due to character calyx length.

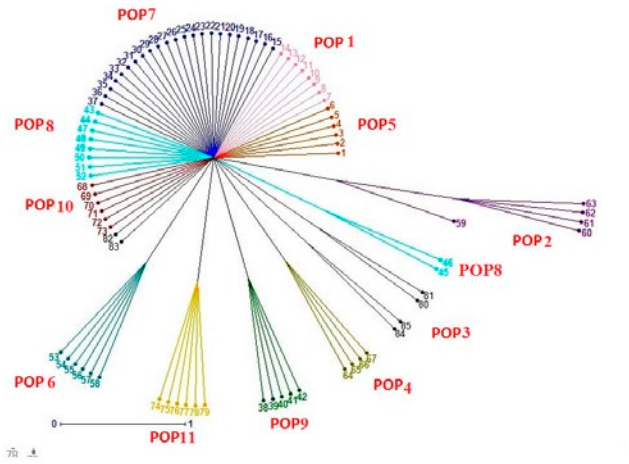

Figure 7. Consensus tree of morphological and molecular data in *S. media* populations.

We performed for both morphological and ISSR data a consensus tree (Figure 7). It indicated that some population are differenced from other population based on both morphological and molecular characters.

Karyological characteristics

In this study three populations of *S. media* show a tetraploid level, 2n=40 (Figure 8a), six populations show a tetraploid level, 2n=42 (Figure. 8b) and two populations show a tetraploid level, 2n=44 (Figure. 8c) is in accordance with previous report (Morton 2005; Runemark 1996). There are high morphological variations in populations of *S. media* so that in some references subspecies have been defined for these taxa. The results show that such variations have chromosome number differences in Iran as most morphological variations were considered from different parts of Iran for this study.

In *S. media* have been reported 2n=28, 36, 40, 42 and 44 from Eurasia with 2n=40 predominating (Federov 1974; Löve and Löve 1975; Moore 1973). This species shows a high phenotypic plasticity and genotypic flexibility.

DISCUSSION

According to Çalişkan (2012) genetic diversity provides information about adapt to changing environments, understanding of positive influence in the conservation of endangered species, hybridization and gene flow among the populations. This study evaluates on the use of Inter simple sequence repeats markers for compare gene flow and relationships within the population of *S. media* in Iran. Verkleij, *et al* (1980) showed that Amylases isoenzymes could be successfully applied to assess interpopulational variation in *Stellaria media*.

S. media has many medicinal properties and distributed in our country, however, we provided information on current taxonomic, molecular study and geographical distance. The present study indicated data about gene flow and genetic structure in some part of Iran. Chickweed can any time of the year at all germinate and flower. System pollination is mainly self-pollinating, but sometimes can occur cross-pollination by flies and insects.

According to Chater and Heywood (1993) *Stellaria media* widespread weedy species and it is the accepted name. There are three subspecies;1- subsp. *media,* 2- subsp. *Cupaniana* and 3- subsp. *postii* but some people showed that subsp. *cupaniana* (Sinha 1965; Scholte 1978) and subsp. *postii* (Sinha 1965) should be included in *S. neglecta*. According to Fedorov (1969) chromosome numbers that have been reported for *S. media* included 2n = 24, 28, 36, 38, 40, 42 and 44 from many parts of the world. However, chromosome numbers 2n =40, 42 and 44 are the most commonly reported and this species revealed a high degree of genotypic variation that is highly correlated with its reproductive (Freeland *et al.* 2011; Verkleij unpublished).

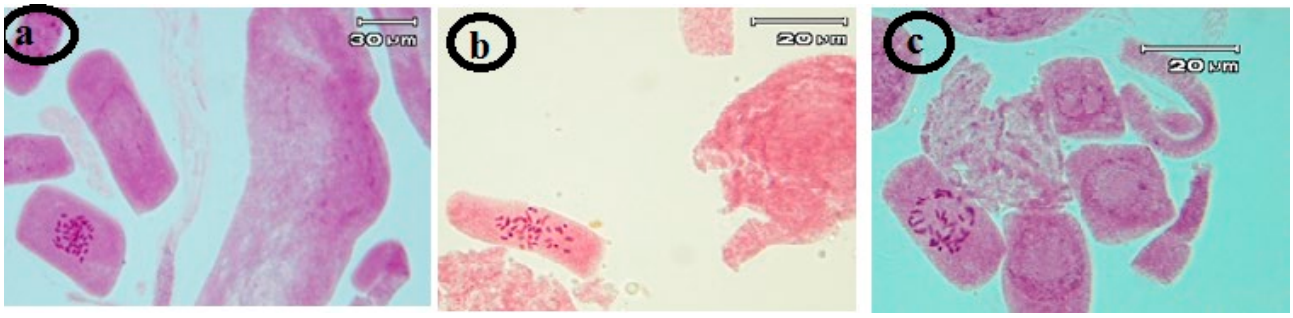

Figure 8. Micrographs of chromosomes of root tips in studied species. a) *S. media* (2n=40), b) *S. media* (2n=42), c) *S. media* (2n=44).

S. media is annual, characterized by the presence of five sepals and petals which are usually bifid; (Whitehead and Sinha 1967). Generally, within family Caryophyllaceae diversity of morphological features makes taxa complicated to be delineated and identified (Whitehead and Sinha 1967). *S. media* is occurring on abandoned fields and commonly sensitive to disturbance of its habitat. Between *S. pallida* and *S. media* there are crossing barrier and they are self-pollinating (Peterson 1936), this happened due to presence of polyploidy in *S. media* (2n=40-44) while observed the diploidy of *S. pallida* (2n = 22) (Scholte 1978; Slatkin 1993; Jolivet and Bernasconi 2007). Therefore, breeding systems plays role important in low level of gene flow in *S. media* (Hutchison and Templeton 1999; Medrano and Herrera 2008).

Our results provided that the seed morphologies of *Stellaria media* and *S. pallida* are similar. Seed coat cells are rounded polygonal and V-shaped margin. Based on these characters, we decided that *Stellaria media* could be differenced from *S. pallida*. Seed coat morphology observed of 18 species of *Stellaria* by Chen (2010). They stated that there are differences between *Myosoton* and *Stellaria*.

Rani *et al*. (2012) have studied some stem and leaf anatomical features through the pharmacognostical study for quality control of *Stellaria media*. Arora and Sharma (2012) did pharmacognostic and phytochemical studies of *Stellaria media* and showed the presence of epidermis, palisade cells, trichomes and vascular bundles in leaf.

CONFLICT OF INTERESTS

The authors have not declared any conflict of interest.

REFERENCES

Ashfaq S, Ahmad M, Zafar M, Sultana S, Bahadur S, Ullah F, Zaman W, Ahmed SN, Nazish M. 2019. Foliar micromorphology of Convolvulaceous species with special emphasis on trichome diversity from the arid zone of Pakistan. Flora: Morphology, Distribution, Functional Ecology of Plants 255: 110-124.

Arora D, Sharma A. 2012. Pharmacognostic and Phytochemical Studies of *Stellaria media* Linn. Journal of Pharmacological sciences and researches 4(5): 1819-1822.

Attar F, Esfandani-Bozchaloyi S, Mirtadzadini M, Ullah F, Zaman W. 2019. Foliar and stem epidermal anatomy of the tribe Cynoglosseae (Boraginaceae) and their taxonomic significance. Microsc Res Tech. 82: 786-802.

Bittrich V. 1993. Caryophyllaceae. in kubitzki, K. Rohwer, J., Bittrich, V. (eds.) The families and genera of vascular plant. Vol. 2, Magnoliid, Hamamelid and caryophyllid families. Springer, Berlin, pp. 112: 206-236.

Blackburn KB, Morton JK. 1957. The incidence of polyploidy in the Caryophyllaceae of Britain and Portugal. New Phytologist 56: 344-351.

Chater AO, Heywood VH. 1993. *Stellaria*. In: Tutin, T.G., Burges, N.A., Chater, A.O., Edmondson, J.R., Moore, D.M., Valentine, D.H., Walters, S.M. & Webb, D.A. (eds), *Flora Europaea* (ed. 2) 1: 161–164. (Cambridge University Press: Cambridge).

Chinnappa CC, Morton JK. 1984. Studies on the Stellaria longipes Complex (Caryophyllaceae). Systematic Botany 9(1): 60-73.

Chen X.B, Yu M, Liu QR. 2010. Micromorphological characteristics and systematical significance of seed coat of *Stellaria* L. from northern China. Journal of Beijing Normal University, Natural Science 46(1): 56–62. [In Chinese]

Çalişkan M. 2012. Genetic diversity in plants. InTech. Chapters published under CC BY 3.0 license.110: 33-39.

Ellis JR., Burke JM. 2007. EST-SSRs as a resource for population genetic analyses. Heredity 99: 125-132.

Evanno G, Regnaut S. Goudet J. 2005. Detecting the number of clusters of individuals using the software STRUCTURE: a simulation study. Mol. Ecol. 14: 2611-2620.

Esfandani-Bozchaloyi S, Keshavarzi M, 2014. Micro- and macromorphological study of *Stellaria* (*Caryophyllaceae*) and its closest relatives in Iran. Phytologia Balcanica 20(2): 179-197.

Keshavarzi M., Esfandani-Bozchaloyi S. 2014a Leaf and Stem Comparative Anatomical Analysis of Three Genera of Alsinoideae (Caryophyllaceae), Iran. J. Bot. 20 (1): 71-79. DOI: http://dx.doi.org/10.22092/ijb.2014.6158.

Keshavarzi M., Esfandani-Bozchaloyi S. 2014b. Chromosome Numbers for Some *Stellaria* L. (Caryophyllaceae) Species and Related Taxa Iran, Iran. J. Bot. 20(1): 36-40. DOI: http://dx.doi.org/10.22092/ijb.2014.6155

Esfandani-Bozchaloyi S, Sheidai M, Keshavarzi M, Noormohammadi Z. 2018a. Species Relationship and Population Structure Analysis In *Geranium* Subg. *Robertium* (Picard) Rouy With The Use of ISSR Molecular Markers. Act Bot Hung 60(1-2): 47-65.

Esfandani-Bozchaloyi S, Sheidai M, Keshavarzi M, Noormohammadi Z. 2018b. Species Identification and

Population Structure Analysis In *Geranium* Subg. *Geranium* (Geraniaceae). Hacquetia 17(2): 235-246. DOI: 10.1515/hacq-2018-0007

Esfandani-Bozchaloyi S, Sheidai M, Keshavarzi M, Noormohammadi Z. 2018c. Morphometric and ISSR-analysis of local populations of *Geranium molle* L. from the southern coast of the Caspian Sea. Cytology and genetics 52: 309-321.

Esfandani-Bozchaloyi S, Sheidai M. 2018d. Molecular diversity and genetic relationships among *Geranium pusillum* and *G. pyrenaicum* with inter simple sequence repeat (ISSR) regions, Caryologia 4: 1-14. DOI: 10.1080/00087114.2018.1503500

Falush D, Stephens M, Pritchard .J.K. 2007. Inference of population structure using multilocus genotype data: dominant markers and null alleles. Mol. Ecol. Notes. 7: 574-578.

Freeland JR, Kirk H, Peterson S.D. 2011. Molecular Ecology, 2nd Ed. Wiley-Blackwell, Chichester, 65: 464-467.

Federov AA. 1974. Chromosome numbers of flowering plants. Reprint by Otto Koeltz Science Pubs. Koenigstein, Germany. 33: 926-936.

Federov ANA. 1969. Chromosome numbers of flowering plants. Leningrad 11: 927-934.

Goldblatt p. 1981. Index to plant chromosome numbers, 1975-1978. Missouri Botanical Garden Monographs in systematic Botany 5: 543-553.

Gadella TWJ. 1977. Diploid Ranunculus ficaria L. in the Netherlands. Proceedings of the Koninklijke Nederlandse Akademie van Wetenschappen C 60: 80-82.

Gul S, Ahmad M, Zafar M, Bahadur S, Sultana S, Begum N, Shah SN, Zaman W, Ullah F, Ayaz A, Hanif U. 2019a. Taxonomic study of subfamily Nepetoideae (Lamiaceae) by polynomorphological approach. Microsc Res Tech. 22: 1-11. DOI: 10.1002/jemt.23249.

Gul S, Ahmad M, Zafar M, Bahadur S, Celep F, Sultana S, Ayaz A. 2019b. Taxonomic significance of foliar epidermal morphology in Lamiaceae from Pakistan. Microsc. Res. Tech. 33: 1-22. DOI: 10.1002/jemt.23316

Hammer Ø, Harper Dat. Ryan PD. 2012. PAST: Paleontological Statistics software package for education and data analysis. Palaeontologia Electronica 4: 1-9.

Haragan PD. 1991. Weeds of Kentucky and adjacent states: A field guide. The University Press of Kentucky. Lexington, Kentucky, 44: 278-282.

Hedrick PW. 2005. A standardized genetic differentiation measure. Evolution 59: 1633-1638.

Huson DH, Bryant D. 2006. Application of Phylogenetic Networks in Evolutionary Studies. Mol. Biol. Evol. 23: 254-267.

Hutchison DW, Templeton AR. 1999. Correlation of pairwise genetic and geographic distance measures: inferring the relative influences of gene flow and drift on the distribution of genetic variability. Evolution 53:1898–1914.

Jolivet C, Bernasconi G. 2007. Within/between population crosses reveal genetic basis for pollen competitive ability in *Silene latifolia* (Caryophyllaceae). J. Evol. Biol. 20:1361-1374.

Jost L. 2008. GST and its relatives do not measure differentiation. Mol. Ecol. 17: 4015–4026.

Kandemir N, Çelik A, Ullah F, Shah SN, Zaman W. 2019. Foliar epidermal anatomical characteristics of taxa of *Iris* subg. *Scorpiris* Spach (Iridaceae) from Turkey. Microsc Res Tech. 82: 764-774.

Lu DQ, Rabeler RK. 2001. Myosoton. *In*: Wu, Z.Y. & Raven, P.H. (Eds.) *Flora of China, vol. 6.* Science Press, Beijing; Missouri Botanical Garden Press, St. Louis, 31:38-44

Löve A, Löve D. 1975. Cytotaxonomical atlas of the Arctic flora. Cramer, Vaduz. 13:588-598

Medrano M, Herrera CM. 2008. Geographical structuring of genetic diversity across the whole distribution range of *Narcissus longispathus*, a habitat-specialist, Mediterranean narrow endemic. Annal. Bot. 102: 183–194.

Meirmans PG, Van Tienderen PH. 2004. GENOTYPE and GENODIVE: two programs for the analysis of genetic diversity of asexual organisms. Mol. Ecol. Notes. 4:792–794.

Meirmans PG. 2012. AMOVA-based clustering of population genetic data. J. Heredity. 103: 744–750.

Moore RJ. 1973. Index to plant chromosome numbers 1967-19'7 l. Utrecht, Netherlands, International Bureau for Plant Taxonomy and Nomenclature. 12: 539-540

Morton JK. 2005. *Stellaria* L. *In:* Flora of North America Editorial Committee (Eds.) *Flora of* North America North of Mexico, vol 5. Oxford University Press, New York, 55: 96-114.

Peakall R, Smouse PE. 2006. GENALEX 6: genetic analysis in Excel. Population genetic software for teaching and research. Mol. Ecol. Notes. 6: 288-295.

Podani J. 2000. Introduction to the Exploration of Multivariate Data. Backhuyes, Leiden, 34: 407-443.

Pritchard JK, Stephens M, Donnelly P. 2000. Inference of population structure using multilocus genotype Data. Genetics. 155: 945-959.

Rechinger KH. 1988. *Stellaria* L. In Rechinger, K. H. (ed), Flora Iranica no. 163: 60-76. Akad. Druckund Verlagsanstalt.

Runemark H. 1996. Mediterranean chromosome number reports 6(590- 678). Flora Mediterranea 6: 223-243.

Rani N, Vasudeva N, Kumar Sharma S. 2012. Pharmacognostical and quality control parameters of *Stellaria* media Linn. Asian Pacific Journal of Tropical Disease 22:84-S86.

Slatkin M. 1993. Isolation by distance in equilibrium and non-equilibrium populations. Evolution. 47: 264 – 279.

Scholte GAM. 1978. Biosystematic studies in the collective species Stellaria media (L.) Vill. –I. Proceedings of the Koninklijke Nederlandse Akademie van WetenschappenC 81: 442–456.

Shah SN, Ahamd M, Zafar M, Zaman W. 2018a. A light and scanning electron microscopic diagnosis of leaf epidermal morphology and its systematic implications in Dryopteridaceae: Investigating 12 Pakistani taxa. Micron 111: 36-49.

Shah SN, Ahmad M, Zafar M, Razzaq A, Malik K, Rashid N, Ullah F, Iqbal M, Zaman W. 2018b. Foliar epidermal micromorphology and its taxonomic implications in some selected species of Athyriaceae. Microsc Res Tech 81: 902-913.

Slavokhotova AA, Odintsova TI, Rogozhin EA, Musolyamov AK, Andreev YA, Grishin EV, *et al.* 2011. Isolation, molecular cloning and antimicrobial activity of novel defensins from common chickweed (*Stellaria media* L.) seeds. Biochimie. 93:450-56.

Ullah F, Nasar Shah S, Zaman W, Zafar M, Ahmad M, Ayaz A, Sohail A, Saqib S. 2019a. Using palynomorphological characteristics for the identification of species of Alsinoideae (Caryophyllaceae): a systematic approach. Grana 58: 174-184.

Ullah F, Papini A, Shah SN, Zaman W, Sohail A, Iqbal M. 2019b. Seed micromorphology and its taxonomic evidence in subfamily Alsinoideae (Caryophyllaceae). Microsc Res Tech. 82: 250-259.

Ullah F, Zaman W, Papini A, Zafar M, Shah SN, Ahmad M, Saqib S, Gul S, Sohail A. 2019c. Using multiple microscopic techniques for the comparative systematic of Spergula fallax and Spergula arvensis (Caryophyllaceae). Microsc Res Tech. 82: 352-360.

Ullah F, Shah SN, Zaman W, Ali C, Gul S, Saqib S, Ali A. 2018a. Traditional knowledge of medicinal herbs among indigenous communities in Maidan Valley, Lower Dir, Pakistan. Bull Env Pharmacol Life Sci 7: 11-23.

Ullah F, Zafar M, Ahmad M, Dilbar S, Shah S N, Sohail A, Zaman W, Iqbal M, Bahadur S, Tariq A. 2018b. Pollen morphology of subfamily Caryophylloideae (Caryophyllaceae) and its taxonomic significance. Microsc Res Tech. 81: 704-715. doi.org/10.1002/jemt.23026.

Ullah F, Zafar M, Ahmad M, Shah SN, Razzaq A, Sohail A, Zaman W, Çelik A, Ayaz A, Sultana S. 2018c. A systematic approach to the investigation of foliar epidermal anatomy of subfamily Caryophylloideae (Caryophyllaceae). Flora 22:246-256.

Verkleij JAC. de Boer AM. Lugtenborg TF. 1980. On the Eeogeneties of *Stellaria media (L.)* Viii. and *Stellaria pallida* (Dnm.) Pire from Abandoned Arable Field. Oecologia (Berl.) 46: 354-359.

Weising K, Nybom H, Wolff K, Kahl G. 2005. DNA Fingerprinting in Plants. Principles, Methods, and Applications. 2nd ed. CRC Press, Boca Rayton, 22:472-481.

Zaman W, Shah SN, Ullah F, Ayaz A, Ahmad M, Ali A, 2019. Systematic approach to the correct identification of *Asplenium dalhousiae* (Aspleniaceae) with their medicinal uses. Microsc Res Tech. 82: 459-465.

Caryologia
International Journal of Cytology, Cytosystematics and Cytogenetics

Firenze University Press
www.fupress.com/caryologia

OPEN ACCESS

Citation: E. Mitrenina, M. Skaptsov, M. Kutsev, A. Kuznetsov, H. Ikeda, A. Erst (2020) A new diploid cytotype of *Agrimonia pilosa* (Rosaceae). *Caryologia* 73(1): 67-73. doi: 10.13128/caryologia-170

Received: February 19, 2019

Accepted: February 23, 2020

Published: May 8, 2020

Data Availability Statement: All relevant data are within the paper and its Supporting Information files.

Competing Interests: The Author(s) declare(s) no conflict of interest.

A new diploid cytotype of *Agrimonia pilosa* (Rosaceae)

Elizaveta Mitrenina[1], Mikhail Skaptsov[2], Maksim Kutsev[2], Alexander Kuznetsov[1], Hiroshi Ikeda[3], Andrey Erst[1,4,*]

[1] *Laboratory of Herbarium, National Research Tomsk State University, Tomsk, Russia*
[2] *South-Siberian Botanical Garden, Altai State University, Barnaul, Russia*
[3] *The University Museum, The University of Tokyo, Tokyo, Japan*
[4] *Laboratory of Herbarium, Central Siberian Botanical Garden, Siberian Branch of the Russian Academy of Sciences, Novosibirsk, Russia*
*Corresponding author. E-mail: erst_andrew@yahoo.com

Abstract. A new diploid cytotype of *Agrimonia pilosa* Ledebour (Rosaceae) collected in China has been revealed. Karyotype formula is $2n = 2x = 16 = 14m + 2sm$. Previously, chromosome numbers in *A. pilosa* established by other researchers were $2n = 28$; 56; 70 with basic chromosome number $x = 7$. All the other members of genus *Agrimonia* Linnaeus have the same basic chromosome number. In the meanwhile, some members of fam. Rosaceae have different basic chromosome numbers: $x = 8$ (e.g., in genera *Amygdalus* L., *Aphanes* L., Cerasus Mill., etc.), $x = 9$ (e.g., in genera *Adenostoma* Hook. & Arn., *Chamaebatia* Benth., etc.), $x = 17$ (e.g., in genera *Amelanchier* Medik., *Chaenomeles* Lindl., etc.). We suppose that the new basic chromosome number $x = 8$ was revealed in *Agrimonia pilosa* collected in China.

Keywords. *Agrimonia pilosa* Ledebour, Rosaceae, chromosomes, karyotype, new cytotype, flora of China.

1. INTRODUCTION

Genus *Agrimonia* Linnaeus (fam. *Rosaceae*, subfam. *Rosoideae*) comprises 15 to 25 species and some naturally occurring hybrids distributed mainly in temperate regions throughout Europe, Asia, North America, Central America, the West Indies, southern South America, and the Southern Africa (Li *et al*. 2003; Chung 2008; Kline and Sørensen 2008; Angelo and Boufford 2012). The genus belongs to the tribe *Sanguisorbeae* DC divided into two subtribes – *Agrimoniinae* J. Presl and *Sanguisorbeae* Torr. & A. Gray. The first subtribe, along with genus *Agrimonia*, includes genera *Aremonia* Neck. ex Nestl., *Hagenia* J. F. Gmel., *Leucosidea* Eckl. & Zeyh., *Spenceria* Trimen (Potter *et al*. 2007). Last four genera are monotypic endemics (Chung 2008; Chung *et al*. 2012). Species of the subtribe display basic chromosome number $x = 7$ and different levels of ploidy ($2x$, $4x$, $6x$, $8x$, $10x$, $12x$) correlating with geographic distribution patterns (Chung 2008; Rice *et al*. 2015).

Several species in *Agrimonia* (e.g., *A. pilosa*, *A. eupatoria*) are used for medicinal purposes. They have been reported to possess antibacterial (Muruzović *et al.* 2016), antiviral (Kwon *et al.* 2005), antitumor (Miyamoto *et al.* 1987; Tang *et al.* 2017), diuretic (Giachetti 1986) and antidiabetes properties (Swanston-Flatt *et al.* 1990; Kuczmannová *et al.* 2016), antioxidant (Chen and Kang 2014; Muruzović *et al.* 2016), immunomodulating (Bukovsky and Blanarik 1994), hepatoprotective (Park *et al.*, 2004) and other effects.

In flora of China, the genus comprises following species: *Agrimonia coreana* Nakai, *Agrimonia eupatoria* Linnaeus subsp. *asiatica* (Juzepczuk) Skalický, *Agrimonia nipponica* Koidzumi var. *occidentalis* Skalický ex J. E., *Agrimonia pilosa* Ledebour (*Agrimonia pilosa* var. *pilosa* and *Agrimonia pilosa* var. *nepalensis* (D. Don) Nakai) (Li *et al.*, 2003).

In the current study, karyotype analysis of *A. pilosa* collected in China (Figure 1) has been conducted. A new diploid cytotype $2n = 16$ and a new probable basic chromosome number $x = 8$ for the genus *Agrimonia* L. were revealed.

Combination of chromosome investigation with morphological methods, molecular genetics methods and scanning electron microscopy gives possibility to obtain essential data to reach conclusions on plants systematics and phylogeny.

Figure 1. *Agrimonia pilosa* Ledebour (Beijing, China).

2. MATERIALS AND METHODS

Seeds of *A. pilosa* for cytological study and herbarium specimens were collected in China, Beijing, Yun Xiu Gu Forest park, Rocky ledges (40°60'N; 117°41'E, 22 July 2016; collectors: Erst A.S., Erst T.V., Lian L., Bing L., Shi C) and were collected in Russia, West Sibiria, Tomsk, southern edge of the city, inundation meadow (56°47'N; 85°03'E, 1 Sep. 2017; collector: Mitrenina E. Yu.). All herbarium materials are deposited in Novosibirsk (NS).

2.1. Karyotype analysis

Mitotic metaphase chromosomes in root tips of seedlings were studied. Seeds were grown at Petri dishes with wet sand at room temperature after cold stratification at 3–4° C during 4 months. Newly formed roots about 1.0–1.5 cm long were pretreated in a 0.2% colchicine solution during 2 hours at room temperature. Fixation was carried out in a mixture of absolute ethanol and glacial acetic acid (3 : 1). Root tips were stained in 1% aceto-haematoxylin, and the squashing method was employed for investigating of karyotype (Smirnov 1968).

Chromosomes were counted in 127 mitotic cells of 5 *A. pilosa* seedlings collected in China and in 25 mitotic cells of 5 *A. pilosa* seedlings collected in Russia. Mitotic metaphase chromosome plates were observed by microscope Primo Star (Carl Zeiss, Germany) and photographed by microscope AxioImager A.1 (Carl Zeiss, Germany) with software AxioVision 4.7 (Carl Zeiss, Germany) and CCD-camera AxioCam MRc5 (Carl Zeiss, Germany) at 1000× magnification at Laboratory for Ecology, Genetics and Environmental Protection ("Ecogene") of National Research Tomsk State University. For karyotyping, the software KaryoType (Altinordu *et al.* 2016) was used, and for figures, the software Adobe Photoshop CS5 (Adobe Systems, USA) and Inkscape 0.92 (USA) was used. The measurements were performed on 10 metaphase plates. For analysis of karyotype, the nomenclature of Levan, Fredgam, and Sandberg (1964) has been used.

2.2. Flow cytometry

Flow cytometry with propidium iodide (PI) staining was implemented to determine relative DNA content. At least 10 seeds from each plant were taken for this study. Each seed was analysed separately. Seed buffer (Matzk *et al*. 2001) was used for nuclei extraction. Seeds was squashed by porcelain pestle and chopped with a sharp razor blade in the nuclei extraction buffer. The samples were filtered through 50-μm nylon membrane into a sample tube. Flow cytometry with Partec CyFlow PA revealed the data on isolated nuclei fluorescence (Partec, GmbH) using the laser 532 nm wavelength, while logarithmic fluorescence data representation (logarithmic scale) was used to record the signals. To calculate the mean of peak, at least 1000 nuclei peaks with less than 2.5% CV indicator values were used. The final data did not exceed the DNA content of the mean sample by more than 3% (Kubešová *et al*. 2010). As an external standard was used *Euryops chrysanthemoides* (DC.) B. Nord, 2C = 2.70 pg, and internal standard *Glycine max* 'Polanka', 2C = 2.50 pg (Doležel *et al*. 1994; Skaptsov *et al*. 2016). We used the Statistica 8.0 software (StatSoft Inc.), Flowing Software 2.5.1 (Turku Centre for Biotechnology) and CyView software for the flow cytometer data analysis (Partec, GmbH), and for the analysis of our results. The possible effect of secondary metabolites on the binding of the intercalating dye was evaluated by co-grinding in a nuclei extraction buffer of the samples and *Allium fistulosum* L. leaves. The resulting preparation was investigated three times within 10 minutes. In the absence of variations in the average values of the detection channels of the *A. fistulosum* peak, it was believed that no effect was detected.

Flow cytometry performed at the Laboratory of Bioengineering of South-Siberian Botanical Garden, Altai State University.

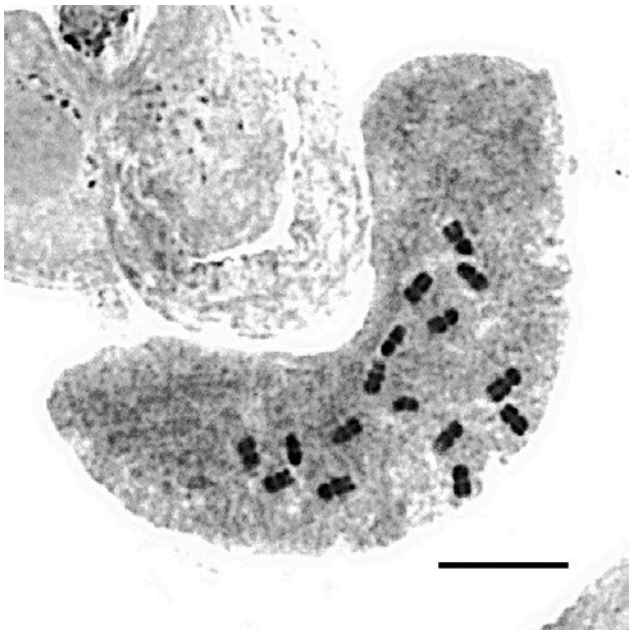

Figure 2. Mitotic metaphase chromosomes of *Agrimonia pilosa* Ledebour (Beijing, China), 2*n* = 16. Scale bar = 10 μm.

3. RESULTS

Karyotype analysis of *A. pilosa* collected in China, Beijing has been conducted. All 127 investigated cells in 5 seedlings had diploid chromosome number 2*n* = 16 (Figure 2). By the software KaryoType (Altinordu *et al*. 2016) morphometric chromosome analysis (total chromosome length, short and long chromosome arms length, arm ratio) has been conducted (Table 1). Chromosome length ranged from 1.87 ± 0.17 μm to 2.14 ± 0.18 μm. Arm ratio varied from 1.03 to 1.81. Chromosomes were classified into two groups: seven pairs with median centromeric position (metacentric chromo-

Table 1. Karyotype parameters of *Agrimonia pilosa* Ledebour, China (2*n* = 16).

Chromosome pair	Total length, μm, ± SD	Long arm, μm, ± SD	Short arm, μm, ± SD	Arms ratio (long/short)	Chromosome type
1	2.14 ± 0.18	1.29 ± 0.12	0.85 ± 0.07	1.52	m
2	2.10 ± 0.24	1.10 ± 0.11	1.00 ± 0.13	1.10	m
3	2.04 ± 0.23	1.12 ± 0.13	0.92 ± 0.12	1.22	m
4	2.02 ± 0.24	1.15 ± 0.26	0.87 ± 0.11	1.32	m
5	1.95 ± 0.29	1.06 ± 0.17	0.89 ± 0.13	1.19	m
6	1.88 ± 0.17	1.05 ± 0.22	0.83 ± 0.08	1.27	m
7	1.87 ± 0.17	0.95 ± 0.08	0.92 ± 0.09	1.03	m
8	2.11 ± 0.27	1.36 ± 0.17	0.75 ± 0.10	1.81	sm

Notes: m – metacentric chromosome; sm – submetacentric chromosome; ± SD – mean length ± standard deviation.

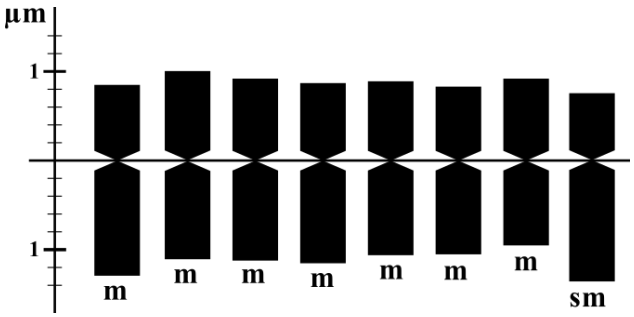

Figure 3. Idiogram of *Agrimonia pilosa* Ledebour (Beijing, China), $2n = 16$. m – metacentric chromosome, sm – submetacentric chromosome.

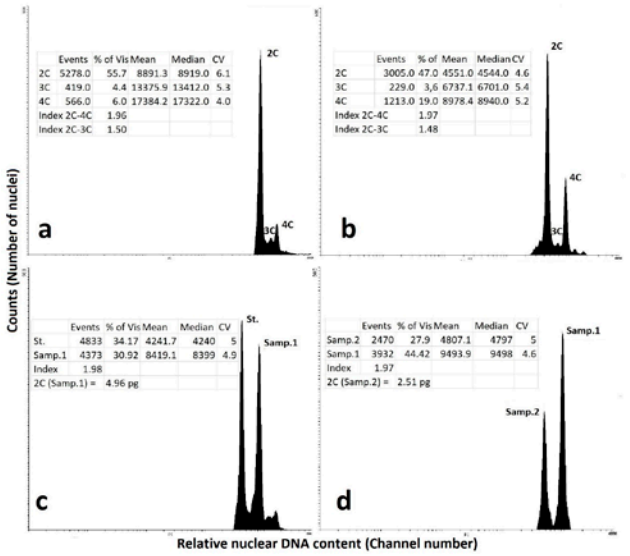

Figure 4. Flow cytometry histograms: **a** – *Agrimonia pilosa* (Tomsk, Russia); **b** – *Agrimonia pilosa* (Beijing, China); **c** – *Agrimonia pilosa* (Tomsk, Russia), Samp. 1 with internal standard (*Glycine max* (L.) Merr.), St.; **d** – *Agrimonia pilosa* (Tomsk, Russia), Samp. 1 with *Agrimonia pilosa* (Beijing, China), Samp. 2.

somes, m; arm ratio 1–1.7), and one pair with sub-median centromeric position (submetacentric chromosomes, sm; arm ratio 1.7–3.0). Some metacentric pairs were low-differentiated. They had almost equal length and arm ratio. Karyotype formula is $2n = 2x = 16 = 14m + 2sm$ (Figure 3). Karyotype asymmetry degree (Stebbins 1971): 1A. Secondary constrictions in 1–2 metaphase chromosome pairs were revealed. Nucleolus number observed in mitotic interphase were 1–2 per cell.

Chromosome counting in *A. pilosa* collected in Russia, Tomsk has revealed typical octaploidic cytotype for the species: $2n = 8x = 56$. By the flow cytometry method, we have found out relative DNA content in two agrimonies: 2C = 2.51 pg in *A. pilosa* (China) with $2n = 16$, and 2C = 4.96 pg in *A. pilosa* (Russia) with $2n = 56$ (Figure 4).

4. DISCUSSION

According to the data of Chromosome Counts Database (Rice *et al.* 2015), Index to Plant Chromosome Numbers and other learned treatise (Iwatsubo *et al.* 1993; Chung 2008; Angelo and Boufford 2012; Kumar *et al.* 2014), diploid chromosome numbers in *Agrimonia* are known as 28; 42; 56; 70 и 84 (Table 2). The basic chromosome number in the genus $x = 7$. Currently, within *Agrimonia* only polyploids have been reported. As long as the lowest ploidy levels reported among species of *Agrimonia* are tetraploids, the lineage appears to have an ancient origin where diploids have gone extinct (Chung 2008). Such a basic chromosome number is common for many members of fam. *Rosaceae* (e.g., genera *Geum* L., *Potentilla* L., *Rosa* L., etc.). At the same time, there are other basic chromosome numbers in *Rosaceae*: $x = 8$ (e.g., in genera *Amygdalus* L., *Aphanes* L., *Cerasus* Mill., *Exochorda* Lindl, *Padus* Mill., *Prunus* L.), $x = 9$ (e.g., in genera *Adenostoma* Hook. & Arn., *Chamaebatia* Benth., *Holodiscus* Maxim.), $x = 17$ (e.g., in genera *Amelanchier* Medik., *Chaenomeles* Lindl., *Kageneckia* Ruiz & Pav.) (Rice *et al.* 2015). Conventionally, subfamily classification was based on a combination of basic chromosome numbers and fruit types (Chung *et al.* 2012). Other genera belonging to subtribe *Agrimoniinae*,

Table 2. Chromosome numbers in the genus *Agrimonia* L. (Chung 2008; Angelo and Boufford 2012; Rice *et al.* 2015).

Species	Chromosome numbers
Agrimonia coreana Nakai	24; 28
Agrimonia eupatoria L.	28; 42; 56; 70; 84
Agrimonia grandis Andrz. ex C. A. Mey.	42
Agrimonia gryposepala Wallroth	56
Agrimonia incisa Torr. & A. Gray	28
Agrimonia japonica (Miq.) Koidz.	56
Agrimonia nipponica Koidz.	28
Agrimonia parviflora Aiton	28
Agrimonia pilosa Ledeb.	28; 56; 70
Agrimonia x *nipponica-pilosa* Murata	42
Agrimonia procera Wallr.	56
Agrimonia pubescens Wallroth	28
Agrimonia repens L.	28
Agrimonia rostellata Wallroth	28
Agrimonia striata Michx.	28; 56

disregarding *Agrimonia*, have following chromosome numbers and ploidy: *Aremonia* – $2n = 5x = 35$ and $2n = 6x = 42$, *Hagenia* – $2n = 6x = 42$, *Leucosidea* and *Spenceria* – $2n = 2x = 14$ (Ikeda *et al*. 2006; Chung *et al*. 2012; Rice *et al*. 2015).

Previously, a karyotype of *A. pilosa* var. *japonica* was examined by Iwatsubo *et al*. (1993). All studied plants had $2n = 56$. Chromosomes at metaphase ranged 1.2–2.5 μm in length and 1.0–2.5 in arm ratio. These were classified into two groups: 21 metacentric pairs, and seven submetacentric pairs. One submetacentric pair had a satellite on the short arm. According to other scientific data, somatic chromosome number of *A. pilosa* are $2n = 28$ and $2n = 70$ (Table 2).

We had revealed a new diploid cytotype in *A. pilosa* collected in China with $2n = 16$. Apparently, these plants exhibit diploid karyotype and new basic chromosome number $x = 8$ for the genus and subtribe. That chromosome number $2n = 16$ was determined in all 127 investigated root meristematic cells. We suppose there were no B chromosomes for diploid cytotype $2n = 14$. Dysploidy arising from chromosomes fusions (Escudero *et al*. 2014) is also unlikely, having our data on chromosomes length and morphology are relevant to the results previously obtained on *A. pilosa* with $2n = 56$ by Iwatsubo *et al*. (1993). We suppose that a haploidization of genome took place in *A. pilosa* specimen collected in China. According to classification developed by Kimber and Riley (1963), this event relates to aneupolyhaploidia, that is haploidization of polyploid form associated with aneuploidy.

In addition to karyotype`s divergence from typical polyploid *A. pilosa* with $2n = 56$, the investigated herbarium specimen exhibits reduced dimensions, fruits, and seeds. This corresponds with the revealed less ploidy level of the plant because polyploidy is followed by «gigas»-effect (Ramsey and Ramsey 2014). We do not exclude the possibility that this specimen could be related to a new taxon.

Our flow cytometry studies revealed that C-values in two investigated *A. pilosa* differ at a factor of two, approximately. This result was unexpected to us due to the fact that the number of chromosomes didn`t correlate with relative DNA content in two examined agrimonies. Unfortunately, we had no *A. pilosa* specimen with chromosome number $2n = 28$ to determine relative DNA content and to compare it with data obtained.

The sizes of the monoploid genome were found to be equal 1Cx = 1.25 pg for samples with $2n = 16$, and 1Cx = 0.62 pg for samples with $2n = 56$ which indicates a significantly more ancient origin of diploid populations, according to the genome downsizing theory (Leitch, Bennett 2004). Due to other studies reports, DNA loss in polyploid series is usually at the level of 15.4% (Zenil-Fergusson *et al*. 2016), whereas in our case, such a significant decrease may indicate complex molecular-genetic processes and DNA loss during the evolution of the *Agrimonia pilosa* genome. Studies of many eukaryotic genomes show that noncoding regions of DNA can be lost in the polyploidization process (Shaked *et al*. 2001). Some cytological studies show a loss of heterochromatin, whole chromosomes or their segments after polyploidization (Gustafson and Bennett 1982; Song *et al*. 1995; Chen and Ni 2006; Xiong *et al*. 2011). Thus, our study is correlated with the idea that the reduction of the genome is a frequent biological phenomenon.

More detailed investigation of the herbarium specimen of *A. pilosa* collected in China by molecular cytogenetics and molecular genetics methods with morphological analysis can elucidate the problem of evolution of the genus *Agrimonia*.

DISCLOSURE STATEMENT

No potential conflict of interest was reported by the author.

FUNDING

The research was supported by the Scientific Programme AAAA-A17-117012610055-3 of the Central Siberian Botanical Garden, of SB RAS (field trip), "The Tomsk State University competitiveness improvement programme" under Grant No 8.1.09.2018 (karyotyping works); state assignment of the Altay State University under Grant No FZMW-2020-0003 (genome size works). We would like to thank the reviewers for their valuable comments and suggestions. Authors are grateful to Roman Annenkov for preparing Figures 2 and 3.

REFERENCES

Angelo R, Boufford DE. 2012. Atlas of the flora of New England: Rosaceae. Phytoneuron. 81:1–56.

Altinordu F, Peruzzi L, Yu Y, He X. 2016. A tool for the analysis of chromosomes: KaryoType. Taxon. 65(3):586–592.

Bukovsky M, Blanarik P. 1994. Immunomodulative effects of ethanolic-aqueous extracts of Herba agrimoniae, Flos chamomillae and Flos calendulae cum calyce. Farm Obz. 63(4):149–156.

Chen L, Kang YH. 2014. Antioxidant activities of *Agrimonia pilosa* Ledeb: in vitro comparative activities of its different fractions. Korean J Plant Res. 27(6):642–649.

Chen ZJ, Ni Z. 2006. Mechanisms of genomic rearrangements and gene expression changes in plant polyploids. Bioessays. 28:240–252.

Chung KS. 2008. A systematic study of genus *Agrimonia* (Rosaceae). Doctoral Dissertation. University of Oklahoma, Norman.

Chung, KS, Hoang N, Elisens W, Un Oh B. 2012. Phylogenetic implication of seed coat sculpturing in subtribe Agrimoniinae (Rosaceae). Korean J Pl Taxon. 42(4):247–252.

Escudero M, Martín-Bravo S, Mayrose I, Fernández-Mazuecos M, Fiz-Palacios O, Hipp AL, Pimentel M, Jiménez-Mejías P, Valcárcel V, Vargas P *et al*. 2014. Karyotypic changes through dysploidy persist longer over evolutionary time than polyploid changes. PLoS ONE. 9(1):e85266.

Doležel J, Doleželova M, Novak FJ. 1994. Flow cytometric estimation of nuclear DNA amount in diploid bananas (*Musa acuminata* and *M. balbisiana*). Biol Plant. 36:351–357.

Giachetti D, Taddei E, Taddei I. 1986. Diuretic and urisurica of *Agrimonia eupatoria* L. Boll Soc Ital Biol Sper. 62(6):705–711.

Gustafson JP, Bennett MD. 1982. The effect of telomeric heterochromatin from *Secale cereale* on Triticale (x Triticosecale). I. The influence of the loss of several blocks of telomeric heterochromatin on early endosperm development and kernel characteristics at maturity. Can J Genet Cytol. 24:83–92.

Ikeda H, Hand K, Wu SK, Ohba H. 2006. A Revision of the genus *Spenceria* Trimen (Rosaceae). J Jpn Bot. 81(3):154–167.

Iwatsubo Y, Mishima M, Naruhashi N. 1993. Chromosome studies of Japanese *Agrimonia* (Rosaceae). Cytologia. 58:453–461.

Kimber G, Riley R. 2011. The relationships of the diploid progenitors of hexaploid wheat. Can J Genet Cytol. 5:83–88.

Kline GJ, Sørensen P. 2008. A Revision of *Agrimonia* (Rosaceae) in North and Central

America. Brittonia. 60(1):11–33.

Kubešová M, Moravcová L, Suda J, Jarošík V, Pyšek P. 2010. Naturalized plants have smaller genomes than their non-invading relatives: a flow cytometric analysis of the Czech alien flora. Preslia. 82:81–96.

Kuczmannová A, Balažová A, Račanská E, Kameníková M, Fialová S, Majerník J, Nagy M, Gál P, Mučaji P. 2016. *Agrimonia eupatoria* L. and *Cynara carduncu*lus L. Water infusions: comparison of anti-diabetic activities. Molecules. 21(5):564.

Kumar P, Rana PK, Himshikha, Singhal VK, Gupta RC. 2014. Chromosome numbers, characterization of chromosomal pairing during meiosis, origin and natural propagation in polyploidy cytotypes (4*x*, 5*x* and 6*x*) of *Agrimonia eupatoria* L. (Rosaceae) in Northwest Himalayas (India). Protoplasma. 251(4):781–795.

Kwon DH, Kwon HY, Kim HJ, Chang EJ, Kim MB, Yoon SK, Song EY, Yoon DY, Lee YH, Choi IS *et al*. 2005. Inhibition of hepatitis B virus by an aqueous extract of *Agrimonia eupatoria* L. Phytother Res. 19:355–358.

Leitch IJ, Bennett MD. 2004. Genome downsizing in polyploid plants. Biol J Linn Soc. 82(4):651–663.

Levan A, Fredgam K, Sandberg A. 1964. Nomenclature for centrometric position of chromosomes. Hereditas. 52:201–220.

Li CL, Ikeda H, Ohba H. 2003. *Agrimonia* L. In: Wu ZY, Raven PH, Hong DY, editors. Flora of China. Rosaceae, Vol. 9. Beijing, China: Science Press, pp. 384–387.

Matzk F, Meister A, Brutovská R, Schubert I. 2001. Reconstruction of reproductive diversity in *Hypericum preforatum* L. opens novel strategies to manage apomixis. Plant J. 26(3):275–282.

Miyamoto K, Kishi N, Koshiura R. 1987. Antitumor effect of agrimoniin, a tannin of *Agrimonia pilosa* Ledeb., on transplantable rodent tumors. Jpn J Pharmacol. 43(2):187–195.

Muruzović MŽ, Mladenović KG, Stefanović OD, Vasić SM, Čomić LR. 2016. Extracts of *Agrimonia eupatoria* L. as sources of biologically active compounds and evaluation of their antioxidant, antimicrobial, and antibiofilm activities. J Food Drug Anal. 24(3):539–547.

Park EJ, Oh H, Kang TH, Sohn DH, Kim YC. 2004. An isocoumarin with hepatoprotective activity in Hep G2 and primary hepatocytes from *Agrimonia pilosa*. Arch Pharm Res. 27(9):944–946.

Potter D, Eriksson T, Evans RC, Oh S, Smedmark JEE, Morgan DR, Kerr M, Robertson KR, Arsenault M, Dickinson TA *et al*. 2007. Phylogeny and classification of Rosaceae. Pl Syst Evol. 266(1–2):5–43.

Ramsey J, Ramsey TS. 2014. Ecological studies of polyploidy in the 100 years following its discovery. Philos Trans R Soc Lond B Biol Sci. 369(1648):1–20.

Rice A, Glick L, Abadi Sh, Einhorn M, Kopelman NM, Salman-Minkov A, Mayzel J, Chay O, Mayrose I. 2015. The Chromosome Counts Database (CCDB) – a community resource of plant chromosome numbers. New Phytol. 206(1):19–26.

Shaked H, Kashkush K, Ozkan H, Feldman M, Levy AA. 2001. Sequence elimination and cytosine methylation

are rapid and reproducible responses of the genome to wide hybridization and allopolyploidy in wheat. Plant Cell. 13:1749–1759.

Skaptsov MV, Smirnov SV, Kutsev MG, Shmakov AI. 2016. Problems of a standardization in plant flow cytometry. Turczaninowia. 19(3):120–122.

Smirnov YA. 1968. Uskorennyi metod issledovaniya somaticheskykh khromosom plodovykh [Accelerated method for studying somatic chromosomes in fruit trees, in Russian]. Tsitologia 10(12):1601–1602.

Song K, Lu P, Tang K, Osborn CT. 1995. Rapid genome change in synthetic polyploids of Brassica and its implications for polyploid evolution. Proc Natl Acad Sci USA. 92:7719–7723.

Stebbins GL. 1971. Chromosomal evolution in higher plants. London: Arnold.

Swanston-Flatt S, Day C, Bailey C. 1990. Traditional plant treatments for diabetes. Studies in normal and streptozotocin diabetic mice. Diabetologia. 33:462–464.

Tang L, Fu L, Lu Ch, Hou X, Shan W, Zhan Zh. 2017. New cytotoxic phloroglucinol derivatives from *Agrimonia pilosa*. Fitoterapia. 118:69–72.

Xiong Z, Gaeta RT, Pires JC. 2011. Homoeologous shuffling and chromosome compensation maintain genome balance in resynthesized allopolyploid *Brassica napus*. Proc Natl Acad Sci USA. 108:7908–7913.

Zenil-Ferguson R, Ponciano JM, Burleigh JG. 2016. Evaluating the role of genome downsizing and size thresholds from genome size distributions in angiosperms. Am J Bot.103 (7):1175–1186.

Caryologia
International Journal of Cytology, Cytosystematics and Cytogenetics

Firenze University Press
www.fupress.com/caryologia

OPEN ACCESS

Citation: I. Petrescu, I. Sarac, E. Bonciu, E. Madosa, C.A. Rosculete, M. Butnariu (2020) Study regarding the cytotoxic potential of cadmium and zinc in meristematic tissues of basil (*Ocimum basilicum* L.). *Caryologia* 73(1): 75-81. doi: 10.13128/caryologia-138

Received: January 9, 2019

Accepted: February 23, 2020

Published: May 8, 2020

Data Availability Statement: All relevant data are within the paper and its Supporting Information files.

Competing Interests: The Author(s) declare(s) no conflict of interest.

Study regarding the cytotoxic potential of cadmium and zinc in meristematic tissues of basil (*Ocimum basilicum* L.)

Irina Petrescu[1], Ioan Sarac[1], Elena Bonciu[2], Emilian Madosa[1], Catalin Aurelian Rosculete[2,*], Monica Butnariu[1]

[1] *Banat's University of Agricultural Science and Veterinary Medicine "Regele Mihai I al României" Timisoara, Romania*
[2] *University of Craiova, Faculty of Agronomy, Craiova, Romania*
*Corresponding author. E-mail: catalin_rosculete@yahoo.com

Abstract. The cytogenetic study on the meristematic tissues of basil (*Ocimum basilicum* L.) aimed to evaluate some cytotoxic effects induced by two heavy metals (cadmium - Cd and zinc - Zn) applied in three different concentrations: 10, 50 and 100 ppm. Cytogenetic tests reveal a decrease of the mitotic index and the occurrence of various chromosomal aberrations following heavy metal treatments. The cell division was significantly affected, especially in the case of Cd treatment, which showed the highest degree of toxicity in all variants compared to control variant. Instead, Zn has a lower degree of toxicity but only at concentrations of 50 ppm and 100 ppm. Types of chromosomal aberrations were relatively varied, being randomly distributed and concentration dependent, for both Cd and Zn. Were observed cells with large nucleus and disorganized-looking; interphases with pyknotic nucleus; cells with laggard chromosomes, pyknotic and sticky chromosomes, as well as cells with telophase bridge. The results reveal that Cd (at all tested concentrations) and Zn in concentrations higher than 10 ppm exhibit significant cytotoxic potential to *Ocimum basilicum* L. as a result of the effects reported in cell divisions of the meristematic tissues. We can also appreciate that the *Ocimum basilicum* L. species could be used as a test plant to determine the degree of soil pollution with heavy metals.

Keywords. Basil, cadmium, chromosomal aberrations, mitodepresive, zinc.

INTRODUCTION

Basil (*Ocimum basilicum* L.) is an herbaceous, annual and aromatic plant belonging to the *Lamiaceae* family. Basil is currently grown in many other parts of the world. Due to medical and culinary properties, as well as the spiritual and symbolic connotations that have been in the culture of the Romanian people since ancient times, basil is one of the most appreciated aromatic plants in Romania, along with rosemary, mint and sage. The basil is used as a seasonal functional food, being used both in tea and fresh salads, due to its health benefits. Functional foods have an important contribution to improving the quality of life (Butnariu and Caunii, 2013).

Basil is a plant used not only in the food industry but also in the pharmaceutical and perfume industry. For example, from a pharmaceutical point of view, the basil may be used as a nutritional supplement or therapeutic drug to protect against aspirin-induced gastric ulcers, a common problem resulting from the use of aspirin (Abd El-Ghffar *et al*., 2018).

Heavy metals are identifiable components in the environment, occurring in significant concentrations and under natural conditions. In the 21st century, the metaliferic loading of air, water, soils, and consequently of plants, animals and the human body became an urgent concern for nature pollution.

The aim of this study was to determine how the basil (*Ocimum basilicum* L.) responded to increasing Cd and Zn concentrations in terms of changes in cellular activity and especially in chromosomes structure. The vegetal meristematic tissues that are used for testing the effects of chemicals on chromosomes should be easy to obtain and less expensive and from this point of view, the basil can be suitable.

MATERIALS AND METHODS

Plant material

Dry seeds of *Ocimum basilicum* L. belong to the Genovese variety was placed in glass Petri dishes on filter paper. Three treatment variants with 4 replicates were performed for each of the heavy metals experienced (Cd and Zn). Solutions for the treatment of seeds have been obtained by dissolving the respective amounts of heavy metals in distilled water. Equal volumes of the different concentrations of cadmium nitrate $Cd(NO3)_2$ and zinc nitrate $Zn(NO3)_2$ solutions (10, 50 and 100 ppm), respectively were administered while the control was treated with distilled water. These concentrations have been established taking into account that basil is an aromatic and medicinal herbaceous plant that reacts easily to any stressful environmental factor, being easily contaminated with heavy metals during growth. The seeds (in the amount of 100 seeds per every variant) were germinated in climatic chamber (model Binder KBF 720, Binder manufacturer, USA), at 22°C. After 72 hours, the basil roots that grew to a length of 1-1.5 cm were cut and processed for microscopic preparation.

Microscopic preparations

The biological material were fixed with a mixture of absolute ethyl alcohol and glacial acetic acid in a volume ratio of 3:1 for 24 hours at 6°C in the refrigerator, followed by hydrolysis with 1 N hydrochloric acid for 5 minutes at room temperature. The stage of the meristematic roots staining was performed using the Feulgen-Rossenbeck method (Baik *et al.* 2017; Rosculete CA *et al.* 2019). Colouring was achieved in a basic fuchsine solution, in concentration of 10%. The microscopic slides were prepared using the squash technique (Asita Okorie *et al.* 2017).

Five slides for each variant were analysed for calculating the mitotic index and the chromosomal aberration frequency. The same slides used to calculate the mitotic index were studied to identify the chromosomal aberration. All slides were examined using a Kruss microscope with digital camera (Kruss manufacturer Hamburg, Germany).

Statistical analyses

Statistical analysis was done using MS Excel 2007. The data obtained were analysed to determine the effects of Cd and Zn treatments on the mitotic activity to *Ocimum basilicum* L. The mean and standard error (SE) were calculated for the mitotic index (MI) and differences between treatment means were compared using the LSD-test at probability level of 0.05% (Botu and Botu, 1997) after ANOVA analysis.

The mitotic index (MI) was calculated according to Balog (1982):

$$MI\ (\%) = \frac{\text{Total number of cells in division}}{\text{Total number of analysed cells}} \times 100$$

The index of the chromosomal aberrations (CA) and the percentage of germination (G) were also calculated:

$$CA\ (\%) = \frac{\text{Total number of aberrant cells}}{\text{Total number of cells in division}} \times 100$$

$$G\ (\%) = \frac{\text{Germinated seed}}{\text{Total seed}} \times 100$$

RESULTS

The heavy metals have differently influenced seed germination and root length to *Ocimum basilicum* L. as can be seen in Table 1. The inhibitory effect on germination is evident to the highest concentration of heavy

Table 1. Influence of cadmium and zinc on the seeds germination and root length to *Ocimum basilicum* L.

Variants	Germination (%)	Root length (X ± SE) (cm)
V1 (Control)	93.33	2.26±0.37
V2/Cd/10 ppm	80.00	1.16±0.19
V3/Cd/50 ppm	56.66	0.26±0.04
V4/Cd/100 ppm	23.31	0.21±0.04
V2/Zn/10 ppm	93.33	1.28±0.13
V3/Zn/50 ppm	74.11	1.18±0.19
V4/Zn/100 ppm	70.00	0.65±0.09

metals (V4/100 ppm) at which the germination percentage was 23.33% for Cd and 70.00% for Zn. Also the concentration of 50 ppm, both to Cd and Zn, inhibited the germination of basil seeds in the proportion of 56.66% (Cd) and 74.11% respectively (Zn).

The highest germination percentage was recorded to V2/Zn/10 ppm variant (93.33%, percentage equal to that of the untreated control).

As for the increase in length of the roots, the highest values were recorded in the variants with the lowest concentrations of heavy metals: V2/Zn/10 ppm (1.28 ± 0.13 cm) respectively V2/Cd/10 ppm (1.16 ± 0.19 cm). The most powerful inhibitory effect was found in the V4/Cd/100 ppm variant, where the average length of the roots was 0.21 ± 0.04 cm, compared to the control (2.26 ± 0.37).

Table 2 presents the results of the effects of Cd and Zn on the mitotic index and the cell division phases to *Ocimum basilicum* L. A significant reduction (p=0.05) of the mitotic index compared to the control was observed in all treatment variants.

Mitotic index value decreased with the increase concentration of heavy metal solutions. Thus, the intensity of mitotic activity was decreasing in order of treatment with Cd to Zn treatment. The higher mitodepresive effect was found in the treatment of Cd at the concentration of 100 ppm, when MI was 9.23%, i.e. 79.8% lower mitotic activity compared to control variant. However, in all variants treated with Cd, there was a significant decrease in the mitotic index compared to the control (10.26% - V3/50 ppm and 12.64% - V2/10 ppm).

In case of the Zn-treated variants, the decrease in the mitotic index was also correlated with the increase in the concentration of heavy metal, but the strongest mitodepresive effect compared to the control was found only at the concentration of 100 ppm (V4 - 17.29% and 50 ppm (V3 - 29.14%). In low concentrations (10 ppm), Zn did not negatively influence the values of the mitotic index as compared to control variant.

From point of view of the cell distribution on mitotic phases, the highest percentage was registered by prophase, followed by telophase, metaphase and anaphases in all the analysed variants, including the control.

Frequency of cells in prophase ranged from 73.47-85.61% for Cd-treated variants and 75.54-84.11% for Zn-treated variants. The frequency of cells in metaphase ranged from 7.33% (V4/Zn/100 ppm) to 10.29% (V2/Cd/10 ppm). On the other hand, the frequency of cells in anaphase stage ranged from 1.58% (V4/Cd/100 ppm) to 4.82% (V3/Zn/50 ppm). The smallest values of the mitotic index of telophase compared to control were recorded at the highest concentrations of heavy metals: 3.70% (V4/Cd/100 ppm) and 6.54% (V4/Zn/100 ppm) respectively.

Heavy metals tested induced a high number of mitotic aberrations when compared with control. The increase of mitotic aberrations was dependent on the increasing treatment concentrations (Table 3). The types of chromosomal aberrations identified in meristematic

Table 2. Mitotic index (%) and the cell division phases (%) to *Ocimum basilicum* L. treated with different concentrations of cadmium and zinc nitrate.

Variants	TCN	MI ± SE %	MI_P %	MI_M %	MI_A %	MI_T %
V1 (Control)	500	45.82±0.68	75.35	6.35	1.93	16.37
V2/Cd/10 ppm	500	12.64±0.42*	73.47	10.29	1.86	14.38
V3/Cd/50 ppm	500	10.26±0.35*	78.36	9.74	1.64	10.26
V4/Cd/100 ppm	500	9.23±0.34*	85.61	9.11	1.58	3.70
V2/Zn/10 ppm	500	43.61±0.63	76.28	7.46	2.01	14.25
V3/Zn/50 ppm	500	29.14±0.60*	75.54	9.22	4.82	10.42
V4/Zn/100 ppm	500	17.29±0.58*	84.11	7.33	2.02	6.54

TCN = Total cells number; MI = Mitotic index; MI_P = Mitotic index of Prophase; MI_M = Mitotic index of Metaphase; MI_A = Mitotic index of Anaphase; MI_T = Mitotic index of Telophase; SE = Standard error; * Significant at level 5% (p=0.05).

Table 3. Type and percentage of mitotic aberrations induced by cadmium and zinc on the meristematic roots to *Ocimum basilicum* L.

Variants	Mitotic aberrations (%)					Total aberrations (%)
	PN	PC	L	S	B	
V1 (Control)	0	0	0	1.05	0	1.05
V2/Cd/10 ppm	4.03	5.27	3.89	5.09	1.23	19.51*
V3/Cd/50 ppm	6.21	8.63	4.03	7.26	1.58	27.71*
V4/Cd/100 ppm	8.15	12.86	6.23	10.04	2.42	39.70*
V2/Zn/10 ppm	0	1.04	1.53	2.01	0	4.58
V3/Zn/50 ppm	3.05	1.01	2.03	2.34	0.89	9.32
V4/Zn/100 ppm	2.84	2.63	3.82	4.01	1.21	14.51

PN = Pyknotic Nucleus; PC = Pyknotic Chromosomes; L = Laggards; S = Stickiness; B = Bridges; * Significant at level 5% (p=0.05).

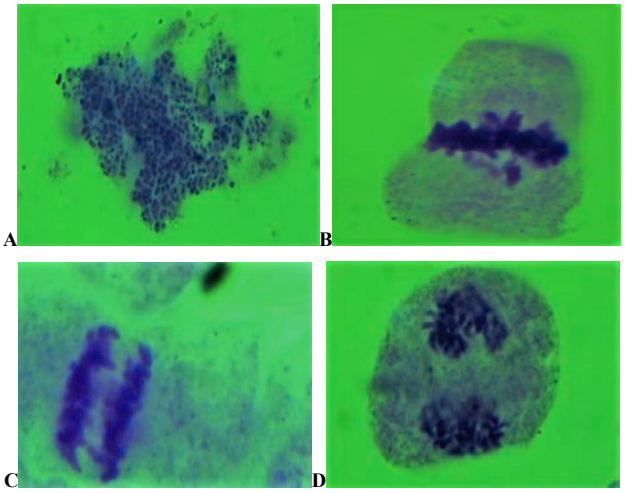

Figure 1. Some chromosomal aberrations identified in meristematic cells of *Ocimum basilicum* L. exposed to Cd and Zn: pyknosis (A); sticky metaphase whit laggards chromosomes (B); bridges (C); disturbed telophase whit pyknotic chromosomes (D).

cells of *Ocimum basilicum* L. were interphases with pyknotic nucleus; pyknotic and sticky chromosomes, cells with laggard chromosomes, as well as cells with telophase bridge.

The most common types of chromosomal aberrations were stickiness and pyknosis while the least frequent were bridges. Compared with the control variant, total chromosomal aberration rate recorded insignificant values for all variant exposed to Zn, from 4.58% (V2/Zn/10 ppm) to 14.51% (V4/Zn/100 ppm). On the other hand, in all variants exposed to Cd treatment total chromosomal aberration recorded significantly positive values from 19.51% (V2/Cd/10 ppm) to 39.70% (V4/Cd/100 ppm) respectively.

DISCUSSION

The contamination of soil and water by heavy metals is a major environmental problem. In this regard it presents an ecotoxicology risk for food chains because of strongly toxic properties of these elements for all human beings (Lassoued *et al.* 2014; Bonciu *et al.* 2018; Coroian *et al.* 2017; Puia *et al.* 2019). Understanding the phenomenon of bioaccumulation of heavy metals in living substance is of extremely complex. This contamination can have very long-term effects (Bilal *et al.* 2014; Lassoued *et al.* 2014; Bonciu *et al.* 2018).

Heavy metal pollution is one of the most serious problems of industrialization, who affects significantly soil and biodiversity and its impact continues to increase (Bae *et al.* 2016), due to these metals' non-biodegradability and high toxicity (Chul Kong, 2013). Generally, heavy metals are dangerous because they tend to bioaccumulate and can cause altered physiological and metabolic processes to plants or disturbing the metabolism of essential elements (Petrescu *et al.* 2015; Sarac *et al.* 2015; Wójcik and Tukiendorf 2014; Butnariu 2012; Mohanpuria *et al.* 2007; Dong *et al.* 2006).

In our experiment, the seed germination of *Ocimum basilicum* L. was heavily affected by the concentration of heavy metals, especially by Cd, which exhibited the highest degree of toxicity. Instead, zinc recorded a lower degree of toxicity and only at concentrations of 50 ppm and 100 ppm. The inhibition of seed germination with increasing concentration of Cd has been found also in other plants: *Vigna radiata* (Maheswari *et al.* 2017); *Triticum aestivum* (Guilherme *et al.* 2015); *Suaeda salsa* (Liu *et al.* 2012); *Spartiana alterniflora* (Mrozek and Funicelli, 1982), etc.

We can appreciate that the highest toxicity in basil seed germination as well as the increase in length of meristematic roots was induced by Cd at the concentration of 100 ppm. In other authors' opinion, at low concentrations Cd is not toxic to plants, but at higher concentrations it is toxic and preferentially accumulates in the meristematic and elongation root zones (Xu *et al.* 2009; Karcz and Kurtyka, 2007). The heavy metals can disturb the nucleolar cycle. Indirect immunofluorescence detects nucleolar material and their movement into the cytoplasm following heavy metal stress (Liu *et al.* 2016).

The length roots of *Ocimum basilicum* L. was influenced differently from one heavy metal to another and from one concentration to the other, the most power-

ful inhibitory effect being found at the highest Cd concentrations. Results suggest that Cd is highly toxic and can affect the metabolism of meristematic roots. Similar results have been reported by Gharebaghi *et al*. (2017) to two basil species (*Ocimum basilicum* L. and *Ocimum basilicum* var. *Purpurescens*).

Cytogenetic tests on *Ocimum basilicum* L. show a decrease of the mitotic index following heavy metal treatments. The mitodepresive effect of cadmium was obvious even at the lowest concentration (10 ppm). The other authors results showed that Cd causes irregularities in mitotic activity to *Pisum sativum* (Fusconi *et al*. 2007) and *Allium sativum* (Xu *et al*. 2009) and can induce increased frequency of the chromosomal aberrations to *Allium cepa* (1.5 times more than in control group), while mitotic index was significantly decreased (Evseeva *et al*. 2001). To *Allium cepa*, Cd affected the spindle and decreased anaphase and telophase stages while the metaphase stage was increased.

In the presence of certain external stimuli, the cellular progress can be blocked in one of the phases of the cell cycle or cell division, and their action is called mitoinhibition. Mitogens act to overcome intracellular braking mechanisms that block cell cycle progression, and their action is called mitostimulatory. Any deviation from the orderly and directed progression of the cell cycle, and respectively, of mitosis and cytokinesis, is reflected in a state of cytotoxicity and genotoxicity (Bonciu *et al*. 2018; Rosculete E *et al*. 2019) and some chromosomes variation (Bouziane *et al*. 2019).

Some research shows that the electron energy loss spectroscopy (EELS) and electron spectroscopic imaging (ESI) are good methods for identifying sites of localization of heavy metals at the sub-cellular level in cell organelles, cytoplasm or cell walls and clarifying the process involved in their uptake, transport and deposition or detoxification in plant cells (Liu and Kottke 2003, 2004).

The results of previous investigations indicate that heavy metals including Cd and Zn at excessive concentration can disturb cell division process and induce CA comprising c-mitosis and lagging chromosomes, anaphase bridges, and chromosome stickiness in the root tips of *A. cepa* (Liu *et al*. 1995). During mitosis, metal ions can interfere with the proper positioning of nucleolar organizing regions on chromosomes. Under metal stress, an obviously toxic phenomenon appears in nucleoli of root tips of *A. cepa* (Bonciu *et al*. 2018).

The results of this study highlight the strong cytotoxic effect of Cd to *Ocimum basilicum* L. even at low concentrations of 10 and 50 ppm. The most common types of chromosomal aberrations were stickiness; sticky chromosomes can lead, in opinion of some authors, to cell death (Singh, 2015; Karaismailoğlu, 2017). In most cases the percentages of abnormal mitotic phases were seen to increase with increasing concentration, this result being recorded in other studies also (Samanta and Bandyopadhyay, 2012; Verma *et al*. 2016; Şuţan *et al*. 2018).

The cytotoxicity effect of Zn occurred only at concentrations higher than 10 ppm. In low concentrations, Zn did not negatively influence the values of the mitotic index, the percentage of chromosome aberrations being insignificant.

Of the two heavy metals tested, Cd showed the highest degree of cytotoxicity and inhibits normal growth to *Ocimum basilicum* L. The results also suggest that basil may be used for bio-greening of soil, since it absorbs the heavy metals and synthesizes them in the cells. Besides, the decontamination of soils polluted with heavy metals through phytoremediation is one of the cheapest and simplest methods, and from this point of view, the cultivation of basil involves very low costs.

REFERENCES

Abd El-Ghffar EA, Al-Sayed E, Shehata SM, Eldahshan OA, Efferth T. 2018. The protective role of *Ocimum basilicum* L. (Basil) against aspirin-induced gastric ulcer in mice: Impact on oxidative stress, inflammation, motor deficits and anxiety-like behaviour. Food Funct. 9(8):4457-4468.

Asita Okorie A, Moramang S, Rants'o T, Magama S. 2017. Modulation of mutagen-induced genotoxicity by vitamin C and medicinal plants in *Allium cepa* L. Caryologia. 70(2):151-165.

Bae J, Benoit DL, Watson AK. 2016. Effect of heavy metals on seed germination and seedling growth of common ragweed and roadside ground cover legumes. Environ Pollut. 213(1):112-118.

Baik N, Maamri F, Bandou H. 2017. Karyological study and meiotic analysis of four species of *Aegilops* (*Poaceae*) in Algeria. Caryologia. 70(4):324-337

Balog C. 1982. The mitotic index in diploid and triploid *Allium* roots. Cytologia. 47(3/4):689-697.

Bilal E, Guenolé–Bilal I, Bounahkla M, Iatan LE, Machado de Mello F, Doumas M, Tahri M, Gallice F, Graillot D, Piegay H, Lassoued N. 2014. The freshwater mussels are a good bioindicator for monitoring the water pollution by heavy metal (The Saint– Victor–sur–Loire Lake, France). Banat¢s Journal of Biotechnology. V(10):5-11.

Bonciu E, Firbas P, Fontanetti CS, Wusheng J, Karaismailoğlu MC, Liu D, Menicucci F, Pesnya DS,

Popescu A, Romanovsky AV, Schiff S, Ślusarczyk J, De Souza CP, Srivastava A, Sutan A & Papini A. 2018. An evaluation for the standardization of the *Allium cepa* test as cytotoxicity and genotoxicity assay. Caryologia. 71(3):191-209.

Botu I, Botu M. 1997. Statistical parameters used in the evaluation of the research of fruit plants. In: Methods and techniques of research in pomiculture. Rm. Valcea (RO): Conphys Publishing. p. 213-236.

Bouziane Z, Issolah R, Tahar A. 2019. Analysis of the chromosome variation within some natural populations of subterranean clover (*Trifolium subterraneum* L., *Fabaceae*) in Algeria. Caryologia. 72(4):93-104.

Butnariu M. 2012. Vegetable Bioindicators of Heavy Metal Pollution. J Ecosys Ecograph. 2(5):e114.

Butnariu M, Caunii A. 2013. Design management of functional foods for quality of life improvement. Annals of agricultural and environmental medicine. 20(4):736-741.

Chul Kong, I. 2013. Joint effects of heavy metal binary mixtures on seed germination, root and shoot growth, bacterial bioluminescence, and gene mutation. J Environ Sci. 25(5):889-894.

Coroian A, Miresan V, Cocan D, Raducu C, Longodor AL, Pop A, Feher G, Andronie L, Marchis Z. 2017. Physical-chemical parameters and the level of heavy metals in cow milk in the Baia Mare area. Banat¢s Journal of Biotechnology. VIII(16):69-74.

Dong J, Wu FB, Zhang GP, 2006. Influence of cadmium on antioxidant capacity and four microelement concentrations in tomato seedlings (*Lycopersicon esculentum*). Chemosphere. 64(10):1659-1666.

Evseeva TI, Geras'kin SA, Khramova ES. 2001. Cytogenetic effects of separate and combined action of 232Th and Cd nitrates on *Allium cepa* root meristem cells. Tsitologiia. 43(8):803-808.

Fusconi A, Gallo C, Camusso W. 2007. Effects of cadmium on root apical meristems of *Pisum sativum* L.: cell viability, cell proliferation and microtubule pattern as suitable markers for assessment of stress pollution. Mutat Res. 632 (1-2):9-19.

Gharebaghi A, Alborzi Haghighi MH, Arouiee H. 2017. Effect of Cadmium on seed germination and earlier basil (*Ocimum basilicum* L. and *Ocimum basilicum* var. *Purpurescens*) seedling growth. Trakia J Sci. 15(1):1-4.

Guilherme de Souza MF, Habyhabanne de Oliveira M, Da Silva E. 2015. Cadmium toxicity on seed germination and seedling growth of wheat *Triticum aestivum*. Acta Sci. 37(4):499-504.

Karaismailoğlu MC. 2017. Assessments on the potential genotoxic effects of Fipronil insecticide on *Allium cepa* somatic cells. Caryologia. 70(4):378–384.

Karcz W, Kurtyka R. 2007. Effect of cadmium on growth, proton extrusion and membrane potential in maize coleoptile segments. Biol Plant. 51(4):713-719.

Lassoued N, Khelil MN, Rejeb S, Bilal E, Chaouachi M, Rejeb MN, Guenolé–Bilal I. 2014. Transfert heavy metal sewage sludge as fertilizer from soil to ray grass. Banat¢s Journal of Biotechnology. V(9):86-95.

Liu D, Jiang W, Wang W, Zhai L. 1995. Evaluation of metal ion toxicity on root tip cells by the Allium test. Israel J Plant Sci. 43:125-133.

Liu D, Kottke I. 2003. Subcellular localization of chromium and nickel in root cells of Allium cepa by EELS and ESI. Cell Biol Toxicol. 19:299-311.

Liu DH, Kottke I. 2004. Subcellular localization of cadmium in the root cells of Allium cepa by electron energy loss spectroscopy and cytochemistry. J Biosci. 29:329-335.

Liu S, Yang C, Xie W, Xia C, Fan P. 2012. The Effects of Cadmium on Germination and Seedling Growth of *Suaeda salsa*. Procedia Environ Sci 16(0):293-298.

Liu X, Shi Q, Zou J, Wang J, Wu H, Wang J, Jiang W, Liu D. 2016. Chromosome and nucleolus morphological characteristics in root tip cells of plants under metal stress. Fresenius Environ Bull. 25:2419–2426.

Maheswari UL, Subramani A. 2017. Inhibitory effects of cadmium on seed germination characteristics of *Vigna radiata* (L.) Wilczek. Int J of Current Research. 9(03):48551-48554.

Mohanpuria P, Rana NK, Yadav SK. 2007. Cadmium induced oxidative stress influence on glutathione metabolic genes of *Camellia sinensis* (L.) O. Kuntze. Environ Toxicol. 22(4):368-374.

Mrozek E, Funicelli NA. 1982. Effect of lead and on germination of *Spartiana alterniflora* seeds at various salinities. Env Exp Bot. 22 (1):23-32.

Petrescu I., Sarac I, Chereches B, Madosa E. 2015. Effect of lead on the growth of *Coriandrum sativum* L. J of Hortic Forest and Biotechnology 19(4):93-95.

Puia M, Mihon B, Ionescu B, Butucel E, Chicinas A, Farcas E, Puskas H, Raducu C, Longodor AL, Coroian A. 2019. Assessing the level of heavy metals in different geographical areas in Romania. Banat¢s Journal of Biotechnology. X(19):5-10.

Rosculete CA, Bonciu E, Rosculete E, Olaru LA. 2019. Determination of the environmental pollution potential of some herbicides by the assessment of cytotoxic and genotoxic effects on *Allium cepa*. Int J Environ Res Public Health. 16(1):75.

Rosculete E, Olaru AL, Rosculete CA, Bonciu E. 2019. Assessment of Cytological Effects of Food Preservative Potassium Metabisulphite to *Allium cepa*. American Journal of Plant Sciences. 11(1):11-23.

Samanta A, Bandyopadhyay B. 2012. Prevention of Cadmium induced genotoxicity with *Emblica officinalis* L. (Amla) in *Allium* Test.. RJPBCS. 3(2):890-897.

Sarac I, Petrescu I, Madosa E, Antonie IF. 2015, Copper effects at seed germination of *Secale cereale* L. J of Hortic Forest and Biotechnology 19(4):84-88.

Singh P. 2015. Toxic effect of chromium on genotoxicity and cytotoxicity by use of *Allium cepa* L. IJREAS. 5(10):1-10.

Şuţan NA, Uţă G, Bărbuceanu D. 2018. Oxidative stress and cytogenetic effects in root tip cells of *Allium cepa* L. induced by alcoholic extracts of *Leptinotarsa decemlineata* (Say). Caryologia. 71(4):405-413.

Verma S, Arora K, Srivastava A. 2016. Monitoring of genotoxic risks of nitrogen fertilizers by *Allium cepa* L. mitosis bioassay. Caryologia. 69(4):343–350.

Xu P, Liu D, Jiang W. 2009. Cadmium effects on the organization of microtubular cytoskeleton in interphase and mitotic cells of *Allium sativum*. Biol Plant. 53(2):387-390.

Wójcik M, Tukiendorf A. 2014. Phytochelatin synthesis and cadmium localization in wild type of *Arabidopsis thaliana*. Plant Growth Regul. 44(1):71-80.

Caryologia
International Journal of Cytology, Cytosystematics and Cytogenetics

Firenze University Press
www.fupress.com/caryologia

OPEN ACCESS

Citation: N.A. Şuţan, A.N. Matei, E. Oprea, V. Tecuceanu, L.D. Tătaru, S.G. Moga, D.Ş. Manolescu, C.M. Topală (2020) Chemical composition, antioxidant and cytogenotoxic effects of *Ligularia sibirica* (L.) Cass. roots and rhizomes extracts. *Caryologia* 73(1): 83-92. doi: 10.13128/caryologia-116

Received: January 9, 2019

Accepted: February 22, 2020

Published: May 8, 2020

Data Availability Statement: All relevant data are within the paper and its Supporting Information files.

Competing Interests: The Author(s) declare(s) no conflict of interest.

Chemical composition, antioxidant and cytogenotoxic effects of *Ligularia sibirica* (L.) Cass. roots and rhizomes extracts

Nicoleta Anca Şuţan[1,*], Andreea Natalia Matei[1], Eliza Oprea[2], Victoriţa Tecuceanu[3], Lavinia Diana Tătaru[1], Sorin Georgian Moga[1], Denisa Ştefania Manolescu[1], Carmen Mihaela Topală[1]

[1] *University of Piteşti, Faculty of Sciences, Physical Education and Informatics, Department of Natural Sciences, 1 Targu din Vale Str., 110040 Pitesti, Romania*
[2] *University of Bucharest, Faculty of Chemistry, Department of Organic Chemistry, Biochemistry and Catalysis, Blvd. Regina Elisabeta, No. 4-12, 030018, Bucharest, Romania*
[3] *Organic Chemistry Centre of the Romanian Academy "Costin D. Nenitescu", 202B Splaiul Independentei, 78100 Bucharest, Romania*
*Corresponding author. E-mail addresses: ancasutan@yahoo.com, mateiandreeanatalia@gmail., eliza_oprea2003@yahoo.com, vichi_tecu@yahoo.com, lavinia.tataru@upit.ro, sorin.g.moga@gmail.com, stefaniamanolescu@yahoo.com, carmen.topala@gmail.com.

Abstract. Through time, in the traditional medicine *Ligularia* genus has been used as a remedy to cure several diseases and affections. The paper represents an essential step in offering more information about the antioxidant activity, chemical composition and cytogenetic activity of *L. sibirica* (L.) Cass. rhizomes and roots extracts. The antioxidant activity of the extracts has been achieved by analyzing the total phenolic content, total flavonoids, the organic chemical compound and trolox equivalent antioxidant capacity and their major polyphenolic constituents were quantified by liquid chromatography electrospray ionization-tandem mass spectrometry. The extracts were obtained by the Supercritical Fluid Extraction (SFE-CO2) technique, SFE-CO2 extraction with co-solvent and absolute ethanol extraction. The best results for the antioxidant activity have been fulfilled through the last two techniques. High Performance Liquid Cromatography (HPLC) has been applied in order to identify and quantify selected phenolic acids and flavonoids in the ethanolic extracts of *L. sibirica* (L.) Cass. The cytogenotoxic effects of the extracts completed the present study, with a furtherance of antiproliferative potential highlighted by the statmokinetic effect and an additional genoprotective effect.

Keywords. antioxidant activity, phenols, SFE extraction, HPLC, cytogenotoxic effects, Ligularia sibirica.

Abbreviation: TP - total phenols, TF - total flavonoids, DPPH - the organic chemical compound 2,2-diphenyl-1-picrylhydrazyl, TEAC - Trolox Equivalent Antioxidant Capacity, FTIR - Fourier Transform Infrared spectroscopy, HPLC - High-performance liquid chromatography, SFE - Supercritical fluid extraction, MIR - middle infrared region, ATR - Attenuated total reflection, GAE - gallic acid equivalents, ABTS - 2,2'-azino-bis(3-ethylbenzothiazoline-6-sulphonic acid), MI - mitotic index.

INTRODUCTION

The genus *Ligularia* from the *Asteracae* family has been extensively researched from phytochemical point of view especially in the last years, having a real significance in the traditional medicines as a remedy for bronchitis, asthma, tuberculosis, haemoptysis, soothing pain, rheumatoid arthritis, coughs, inflammations, jaundice, scarlet fever and hepatic diseases (Pinglin *et al*. 2008; Xie *et al*. 2010). *Ligularia* genus has many biological activities such as antibacterial activity, antifeedant and insecticidal activities, antihepatotoxicity, antioxidant, antithrombotic and anticoagulant activity (Yang *et al*. 2011). The pharmaceutical studies as well as the chemical studies on *Ligularia* species demonstrate the specific presence of constituents such aseremophilane-type sesquiterpenes (Wu *et al*. 2016).

Over the glacial and interglacial period, a large number of species migrated from the Asian continent to Europe, including the glacial relict *Ligularia sibirica* (L.) Cass. which is the target of the present study. *L. sibirica* (L.) Cass., a perennial hemicryptophyte species, has a short and thick rhizome with long lateral fasciculated roots, leaves with long petioles, and inflorescence stem straight up to 200 cm. The blooming period starts from July till the end of August (Pop, 1960; Šmídová *et al*. 2011).

An overall small number of studies have been published with regards to the chemical composition and cytogenotoxic effects of *L. sibirica* (L.) Cass. Scientific literature highlights the use of this species as a cure for treating phlegm and for reducing cough (Liao *et al*. 1002; Tori *et al*. 2008; Yuan *et al*. 2013).

It is worth to mention here that there is not a clear situation regarding the *L. sibirica* (L.) Cass. populations in Romania related to its distribution in the Natura 2000 sites (Brînzan *et al*. 2013), and the protection of the species through the Bern Convention, Annex I - Strictly Protected Flora Species (Berne Treaty No. 104), complemented by the IUCN threat status, Data Deficient (Bilz *et al*. 2011). Due to the fact that the species of community interest is protected by the Habitats Directive through Annexes IIb and IVb, GEO 57/2007 (Law 49/2011): Annexes 3, 4 A and mentioned in the Carpathian List of Endangered Species in the category Near Threatened (Mihăilescu *et al*. 2015), the material used in our study was collected after a complex survey regarding the quantitative and qualitative analysis of *L. sibirica* (L.) Cass. population in each site, as follows: Apa Roşie Peat Bog, Hărman Marsh and Zănoaga Gorges. The necessary material for study was harvested in minimum amounts, in order to preserve the existing vegetal communities.

In the present study, we analyzed the chemical composition, antioxidant activity and cytogenotoxic properties of ethanol extracts obtained from roots and rhizomes of *L. sibirica* (L.) Cass. Our study represents a first step in estimating the possible phytotherapeutic applications of *L. sibirica* (L.) Cass., and to understand to what extent this species can be incorporated into farming systems as a medicinal herb.

MATERIALS AND METHODS

Plant material

Roots and rhizomes of *L. sibirica* (L.) Cass were harvested in August 2017, from 3 distinct sites, both in terms of habitat, pedo-climatic conditions, but also with the same level of anthropogenic activity, in order to decide which of them hold a higher potential for further studies. The first sample was collected from Zănoagei Gorges (Lat N45°28', Long E25°25'), which are part of Bucegi Natural Park an interesting limestone mountain system, the studied area being characterized by a cool-wet climate type, the average annual temperature being of 4.9°C where the rainfalls varies with the altitude, covered by rendzina soils (Beldie, 1967). The second sample of *L. sibirica* (L.) Cass. was collected from Hărman Marsh (Lat N45°43', Long E25°39'), an eutrophic marsh with hydric and alluvial soils and $CaCO_3$ deposits, located in the Braşov Depression, with an annual temperature of 7°C and low rainfall. The last sample was collected from Apa Roşie Peat Bog (Lat N46°10', Long E26°15'), located in Nemira Mountains and characterized by a cool-wet climate type rich in precipitations, with an average annual temperature of 2–4°C, occupying hydric soils without $CaCO_3$ deposits (Brînzan *et al*. 2013).

After weighing the plant material, the fresh rhizomes and roots were washed in tap water to remove the soil, rinsed well in distilled water, pat dried with paper towel, and then minced at room temperature.

Reagents and Chemicals

The reagents used: gallic acid monohydrate ACS reagent ≥ 98% and Folin Ciocalteu's phenol reagent of 2M concentration, caffeic, cinnamic, ferulic, rosmarinic and syringic, catechin, myricetin, naringenin, methanol, and ethanol were from Sigma-Aldrich (USA). Chlorogenic acid and quercetin were from Alfa Aesar (Germany) and Fluka, respectively. Ethanol (HPLC degree) was obtained from Merck Co. (Darmstadt, Germany). The used water was double-distilled. The carbon dioxide (99.5% purity)

used in SFE extraction and the rest of the reagents used in the experiments were purchased from commercial sources. The weight of the samples was measured on an analytical balance of Shimadzu Corporation with a precision of 0.1 mg.

Extraction Procedures

Ethanolic extract was prepared by mixing 5 g of each type of plant material, roots and rhizomes, in 50 mL absolute ethanol stored for 8 h at room temperature (22°C). Using Whatman filter paper no. 1, the extracts were filtered and the resulted filtrates were used to indicate their cytogenotoxic potential using *Allium cepa* test.

The SFE extracts were achieved through the specific equipment, a pilot unity called SFT-110 Supercritical Fluid Extractor (Supercritical Fluid Technologies, Inc.). The temperature of the restrictor valve was adjusted to 50° or 60°C for all extraction processes. The extract was collected in a 50 mL glass vial. The output of CO_2 in the system was of 6.0 g/min. The yields of extraction were around 2%. For the co-solvent extraction (sample 4), using 1% and 2% ethanol in relation to the CO_2 the experiment was performed in conditions of 50°C, 250 bar and flow of CO_2 at 6 g/min (Erdogan *et al.* 2011). In this case the extraction yield was 2.5% from the raw material.

Five samples of extracts were prepared: Hărman Mash – **1**, Zănoagei Gorges – **2** and Apa Roşie Peat Bog – **3** through SFE extraction with CO_2, then it was added a SFE extraction with CO_2 and EtOH as cosolvent from Apa Roşie Peat Bog – **4** and the last one was the absolute ethanol extraction from Apa Roşie Peat Bog – **5**. The extracts of every single assay were individualized by studying the antioxidant activity through: TP, TF, DPPH and TEAC. The functional groups were analysed using FTIR in the region 4000–400 cm^{-1}. The ethanolic extract (sample **5**) was used to evaluate cytogenotoxic activity.

Evaluation of chemical composition of the rhizome and roots extracts FT-MIR

The extracts of *L. sibirica* (L.) Cass. were investigated for their chemical composition: extract with CO_2 (**1**, **2**, **3**), CO_2 and ethanol (**4**), ethanolic extract (**5**). For FTIR spectroscopy, was used a Jasco 6300 spectrometer. The FTIR spectroscopy of each rhizomes and roots extract was recorded in the MIR region. An ATR accessory equipped with a diamond crystal (Pike Technologies) was used for sampling. Samples were carried out at 100 scans with resolution of 4 cm^{-1} in the regions of 4000-400 cm^{-1}. Spectra Manager II software was used for processed the spectra data.

Total phenolic content

In order to assess the TP content of the material extract, it has been used the Folin-Ciocalteu method (Singleton and Rossi, 1965). The TP content was brought out by mixing 0.5 mL of sample or standard (gallic acid) with 5 mL of Folin - Ciocalteu reagent and 4 mL of 1M sodium carbonate. It was measured the absorbance at 746 nm (Shimadzu UV-1800 Spectrophotometer) and the calibration curve with standard solutions of gallic acid concentrations ranging from 0.05 to 1 mgL^{-1} was traced. Equation of standard curve was y=0.0067x+0.0105 (R2=0.9960). The results were expressed as mg of GAE in 100 g of the rhizomes and roots.

Extract constituents

The identification and quantification of selected phenolic acids and flavonoids in the plant extracts was performed by high performance liquid chromatography (HPLC) using a Varian 310-MS LC/MS/MS triple quadrupole mass spectrometer (USA) fitted with an electrospray ionization interface (ESI). A sample of each dry plant extract was dissolved in HPLC-grade methanol. The mobile phase was double distilled water/methanol, f_r = 20:80. A Varian C18 column (150 mm 9 3.0 mm; 5 mm) was used at a flow-rate of 0.6 ml/min, in an isocratic elution. The injection volume was 20 ml and triplicate injections were used for each sample. The drying gas was air at a pressure of 131 kPa and 250 °C, and the nebulizing gas was nitrogen at 276 kPa. The capillary voltage was set at the potential -4500 V for negative ionization. The resulting deprotonated molecular ion was selected by the first quadrupole; in the second quadrupole, the deprotonated molecular ion was fragmented by collision with an inert gas (argon) at a pressure of 0.2 Pa; the fragments were analyzed in the third quadrupole. Prior to these experiments, the tuning of the mass spectrometer was performed using a polypropylene glycol standard for both positive and negative modes. The determinations have been carried out in triplicate. The results are expressed as µg of selected phenolic acid or flavonoid per 1 g of dry extract.

Determination of antioxidant activity

1. **DPPH Antioxidant activity**. In order to determine the radical scavenging activity of the ethanol

extract of *L. sibirica* (L.) Cass. the Brand-Williams DPPH assay has been used (Brand-Williams *et al.* 1995). DPPH is stable organic nitrogen radical, with a purple colour solution, which reacts with the antioxidant compounds. The method it stands on the measurement of the reducing ability of antioxidants toward this radical. The ability can be evaluated by measuring the decrease of DPPH absorbance at 517 nm. The percentage of the DPPH remaining was calculated using the equation: I% = [(Ablanck-Asample)/Ablanck] x100, where: Ablank is the absorbance for the blank (ethanol - DPPH. ethanolic solution) and Asample is the absorbance for the sample mixed with 0.04 mg/mL DPPH solution.

The results were expressed as IC50 (the extract concentration which inhibits the activity of DPPH by 50%). In short, to 4 mL of extract at 1 mL of DPPH (0.04 mg/mL) ethanol solution was added. After incubating for 30 min in dark, the absorbance of the resulting solutions was measured at 517 nm using UV-VIS Jasco 730 Spectrophotometer (Kedare and Singh 2011).

2. **TEAC assay**. A stock solution of ABTS•+ was obtained after reacting the ABTS chemical compound with potassium persulfate. Then the mixture has been left at dark at room temperature for 12–16 hours before use. The ABTS•+ used solution was prepared by dilution of this solution with ethanol till the absorbance was around 0.70 (Pellegrini *et al* 2003). The absorbance was measured at 734 nm. The calibration curve was made with Trolox (with concentrations between 0.125 and 2 mM). The results were done in mmol of Trolox per 100g rhizomes and root. Equation of standard curve was y=45.432x+20.334 (R2=0.9896).

Evaluation of cytogenetic effects of L. sibirica ethanol extract

The two samples extracted with ethanol (sample **4** and **5**) showed the best antioxidant properties, taking into account a higher volume of extraction, the sample **5** was studied in order to evaluate the cytogenotoxic effects of *L. sibirica* (L.) Cass. extracts.

The cytogenotoxic effects were evaluated through the changes of the mitotic indices and through the frequency of the phases of mitosis (prophase, metaphase, anaphase, telophase), as well as through the chromosomal aberrations frequency and the nuclear anomalies induced in root tip cells of *A. cepa L.*

The onion bulbs (a local variety), about 4 cm diameter, have been checked to fit in the phytosanitary standards. In order to expose root primordia, the outer scales have been gently removed and the bulbs were placed in 30 mL containers, with the discoid stem being in contact with distilled water. The *Allium* test was performed through static exposure, initially at the action of distilled water for 24 or 48 hours as well as at various concentrations of *L. sibirica* (L.) Cass. ethanol extracts for 24 or 48 hours. Further the samples were defined by the extracts concentration, respectively 5%, 10%, and 15%, as well as by the incubation time of onion roots, 24 hours and 48 hours (L 5% 24h, L 5% 48h, L 10% 24h, L 10% 48h, L 15% 24h, L 15% 48h).

For the cytogenetic analysis roots with a length of about 10 mm were used. The roots were fixed in a mixture of absolute ethanol: glacial acetic acid 3:1 overnight and then transferred to 70° ethanol for long-term preservation. For each experimental variant, a number of 5 roots were subjected to attenuated hydrolysis with HCl 1N for 15 minutes at 60°C. Fixed and macerated roots were stained with aceto-orcein solution 1% at 60°C for 15 minutes. The root tips were cut on a glass slide, in a drop of 45% glacial acetic acid, and used to perform microscopic slides using the squash technique. The coverslips were glued with several layers of nail polish, and the resulted microscopic slides were analyzed on an Olympus CX-31 microscope, at a 400x magnification. The microscopic analysis aimed at establishing the numbers of cells at different stages of mitosis, the frequency of chromosomal and nuclear aberrations related to about 3000 cells for each experimental sample. The MI was determined as the percentage ratio between the number of cells in mitosis and the total number of analysed cells (Tedesco *et al.* 2012). Depending on the total number of cells that carry out mitosis, it was determined the percentage of the cells mitosis stages. The frequency of chromosomal aberrations and nuclear abnormalities was calculated as the percentage between the number of damaged cells and total number of cells in the appropriate stage of the cell cycle and mitosis.

The results were statistical analysed using the IBM SPSS Statistics 20 program. Significant differences among samples were determined using the analysis of variance (one-way ANOVA), as well as the Duncan multiple comparison test. The $P \leq 0.05$ values were considered statistically significant. The graphs and tables were elaborated based on average values ± the standard error (SE) of more independent experiments.

RESULTS AND DISCUSSION

Evaluation of chemical composition of the rhizome and roots extracts by FT-MIR

The ATR-MIR spectra (4000-400 cm^{-1}) of each extract was registered and the specific wavenumbers

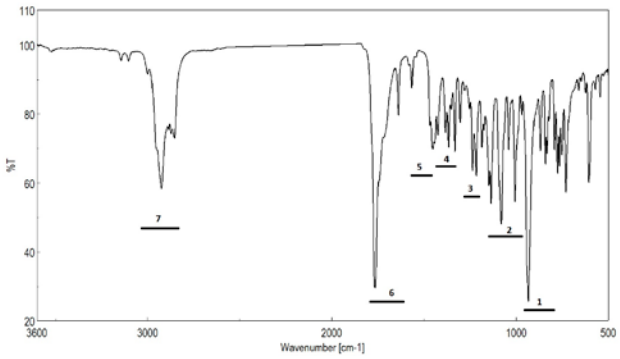

Figure 1. ATR-MIR spectra registered for sample **3** (SFE extraction with CO_2).

and intensities were considered in order to present the FTIR-ATR spectra of alcoholic and CO_2 extracts (Figure S1 in the Supplementary Material), as well as the FT-IR absorption bands for rhizomes and roots extracts (Table S1 in the Supplementary Material). The vibrational assignments for extracts were compared with literature data (Szymanska-Chargot and Zdunek 2013). The identification of the functional groups was based on the FTIR peaks attributed to stretching and bending vibrations. Eight areas were identified in the MIR domain and the fingerprint region was localized between 900 and 1760 cm^{-1} (areas 1-6) (Zavoi *et al*. 2011). Figure 1 shows the spectral regions 1-7 for sample analysis.

Area 1 (< 1000 cm^{-1}) corresponds to C-H bending vibrations from isoprenoids, area 2 (997-1140 cm^{-1}) to stretching vibrations C-O of carbohydrates, with signals at 1005, 1009, 1040, 1080 and 1136 cm^{-1}, while area 3 (1150-1270 cm^{-1}) corresponds to stretching vibrations of carbonyl C-O or O-H bendings. The intense peaks at 1040 cm^{-1} and to nearly 1080 cm^{-1} are attributed to characteristic functional groups of polyphenols. C-O (amide) and C-C stretchings vibrations appear in the region 4 (1300-1450 cm^{-1}) Region 5 (1500-1600 cm^{-1}) corresponds to aromatic group and N-H bending vibrations. Domain 6 is a complex one (1600-1760 cm^{-1}) and corresponds to bending vibrations N-H (amino acids), C=O stretchings (aldehydes and ketones, esters) as well to free fatty acids (1766 cm^{-1}) and glycerides (1738 cm^{-1}). Area 7 (2800-2900 cm^{-1}), corresponds to C-H stretching vibrations of CH_3 and CH_2 from lipids, lipid derivatives, C-H (aldehydes). Region 8 (3350-3600 cm^{-1}) is assigned to stretching vibrations of OH (from water, alcohols, phenols, carbohydrates).

The spectra show relatively more bands in the region of 400-700 cm^{-1}. The inorganic constituents can be observed in the region between 470-480 and 530-540 cm^{-1}. The variation may be due to the differences in the extraction and purification methods.

Antioxidant activity and phenol content of plant extracts

There are a few studies about compounds with antioxidant activity from the genus *Ligularia*. According to them, *L. fischeri* (Ledeb.) Turcz. showed high total phenolic contents (215.8 ± 14.2 mg gallic acid equivalent/g) with low contents of total flavonoid (86.9 ± 3.8 mg rutin equivalent/g) (Lee *et al*. 2013). Liu (2010) has reported the isolation and structural elucidation of the furanoeremophilane-type sesquiterpenes and benzofuran derivatives (part of them with phenol groups) from *L. veitchiana* (Hemsl.) Greenm., and some results about its biologic activity (Liu *et al*. 2010). *L. macrophylla* (Ledeb.) DC. has been reported to contain at least two flavonoids: 6-acetyl-8-methoxy-2,3-dimethylchromen-4-one and 4-14 (2S)-3'-hydroxy-5',7-dimethoxyflavanone in root and rhizome, while in *L. duciformis*'s root have been identified some derivatives of sinapyl alcohol and coniferyl alcohol, with known antioxidant activities (Yang *et al*. 2011). From our knowledge, phenols, flavonoids or other compounds with antioxidant activity from *L. sibirica* (L.) Cass. were not assessed. The Table 1 presents the TP and TF content of *L. sibirica* (L.) Cass. rhizome and root extracts and its TEAC. The highest concentrations of TP and TF were obtained for extracts of *L. sibirica* (L.) Cass. prepared by the co-solvent method (EtOH), as expected.

Our results have also shown that supercritical CO_2 extractions were the least efficient, predictable since phenols are polar compounds and thus are less extractible by CO_2. Something more effective than this was the extraction method at cold temperatures with ethanol (method used for extraction of phenols from vegetal matrix (Santos-Buelga *et al*. 2012).

The polyphenol constituents present in extract 5, as identified and quantified by LC–ESI–MS/MS, are listed in Table 2. Based on these results, it was concluded that the antioxidant properties of the extract originate in

Table 1. TP, TF and TEAC assay for *L. sibirica* rhizome and root extracts.

Sample	TP (mg gallic acid equivalent/100g root)	TF (mg quercetol equivalent/100g root)	TEAC assay (mmoli Tolox equivalent/100g root)
1	2.13	n. d. [a]	0.03
2	3.08	n. d.	0.04
3	10.01	n. d.	0.09
4	494.26	5.25	1.42
5	49.25	n. d.	0.47

[a] not detected.

Table 2. The phenolic profile of the plant extract-**5**, as determined by LC–ESI–MS/MS.

Class compound	Compound	Concentration (µg compounds/g dry extract)
Phenolic acids	Caffeic acid	69.778±1.0229
	Chlorogenic acid	189.114±1.7604
	Cinnamic acid	0.438±0.0177
	Ferulic acid	1.856±0.0764
	Gallic acid	7.420±0.1071
	Rosmarinic acid	25.359±0.1292
	Syringic acid	2.532±0.0955
Flavonoids	Catechin	6.901±0.0124
	Myricetin	0.343±0.0158
	Naringenin	0.704±0.0283
	Quercetin	13.032±0.6992

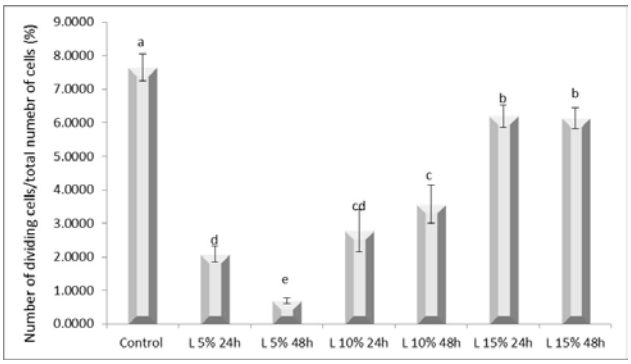

Figure 2. The influence of *L. sibirica* extracts on the mitotic index in root meristem cells of *Allium cepa* L. (The data are the averages ± SE of three repetitions; a, b, c, d, e, - the interpretation of statistical significance and of significant differences through the Duncan test, $p < 0.05$).

two main classes of compounds, namely flavonoids (catechin, myricetin, naringenin, quercetin) and, to a greater extent, phenolic acids (caffeic, chlorogenic, cinnamic, ferulic, gallic, rosmarinic, syringic acid).

Evaluation of cytogenetic effects of L. sibirica ethanol extracts

Starting with Fiskejio (1988) the *Allium* test was considerably used for the evaluation of cytotoxic and genotoxic effects, as well as for the genoprotective potential of various natural or synthetic chemical compounds. The *Allium* test follows some endpoints, such as the mitotic index, chromosomal aberrations and the nuclear anomalies (Bonciu *et al*. 2018).

For each experimental sample, the results were compared with the control. Figure 2 shows the MI variation in onion roots exposed for 24 or 48 hours at the action of *L. sibirica* (L.) Cass. extracts of 5%, 10% and 25% concentration. Statistical analyzis of the microscopic results revealed that ethanol extracts of *L. sibirica* (L.) Cass. have determined a significant decrease in the frequency of cells in various phases of mitosis. The highest MI was determined for the control for which the calculated percentage was 7.64%. *L. sibirica* (L.) Cass. extracts had a statistically important mitoinhibitory effect, when compared to the control, showing an indirect correlation with their concentration. The lowest MI (0.7%) was calculated after the roots incubation in the extract with the concentration of 5% for 48h. This decreased frequency of cells in the mitosis was followed at a statistically significant difference by that determined in the experimental sample, defined by the 5% concentration, respectively 24h. In the root tip cells incubated in *L. sibirica* (L.) Cass. extracts, the highest MI with a 6.19% value was calculated for the L 15% 24h experimental sample. The overall interpretation of the microscopic results revealed that the variation of the mitotic index was independent of the exposure time. The decrease of the MI in *A. cepa* L. meristematic root cells demonstrates the presence of bioactive substances with antiproliferative potential.

The effects of *L. sibirica* (L.) Cass. extracts on the distribution of the mitotic division phases in the onion meristem cells are summarized in Figure 3. The frequency of prophase and metaphase has significantly varied, in a concentration dependent manner. Therefore L 5% 24h has induced the highest percentage of prophases, significantly different compared to the other tested concentrations. When compared to the control, the ethanol extracts of *L. sibirica* (L.) Cass. have induced an increase and a significant increase of metaphases frequency. The

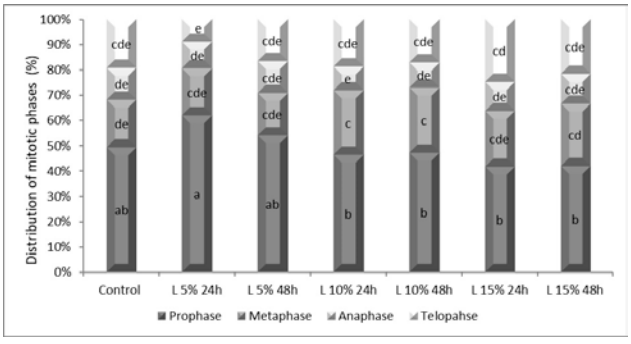

Figure 3. The influence of *L. sibirica* extracts on the distribution of mitotic division phases in the radicular meristem cells of *A. cepa* L. (the data are ± SE averages of three repetitions; a, b, c, d, e, f, g, h, i, j, k – the interpretation of statistical significance and of significant differences through the Duncan test, $p < 0.05$).

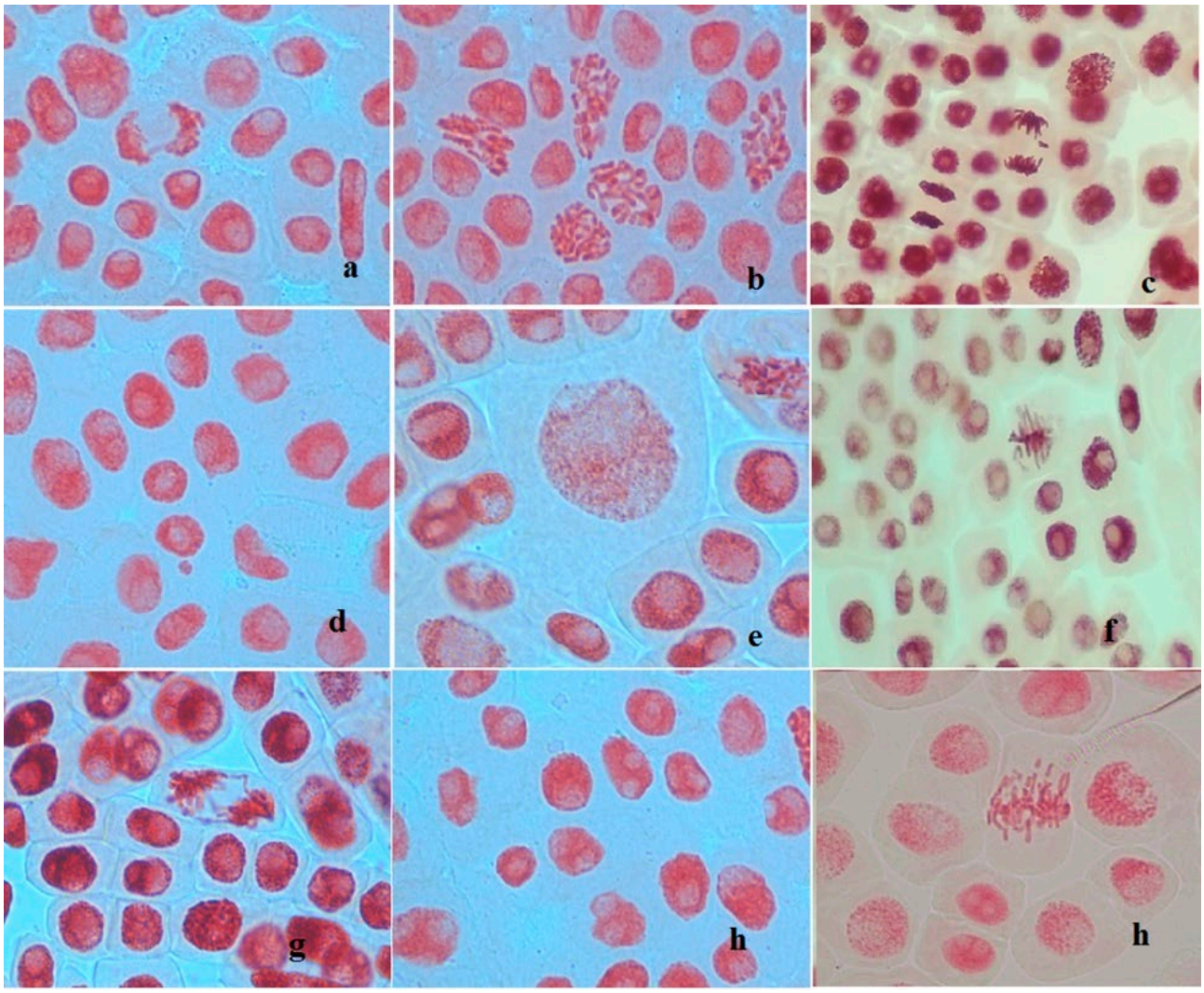

Figure 4. Chromosomal aberrations and nuclear abnormalities identified in meristematic root cells of *A. cepa L.* (a) telophase bridge – L 5% 24h; (b) C-mitosis – L 5% 48h; (c) laggards – L 5% 24h; (d) micronucleus and nuclear buds - L 5% 48h; (e) giant cell – L 10% 48h; (f) vagrant – L 10% 24h; (g) anaphase bridges – L 15% 24h; (h) altered nuclear shape – L 10% 48h; (h) fragments – L 5% 24h.

highest metaphases percentage was determined in L 10% 24h and L 10% 48h variants. The calculated percentage values for anaphase and telophase were not significantly different compared to the control.

On the basis of these observations it can be appreciated that the MI decline is due to cells arresting in the metaphase at a 5% extracts concentration. The overall interpretation of the results also reveals a global slowdown of mitotic progression at a higher concentration of the extracts. The decrease of the MI may be reflecting a cytogenotoxic effect of *L. sibirica* (L.) Cass. ethanol extracts and could be interpreted as cellular death (Yuet Ping *et al.* 2012). According to Nieva-Moreno *et al.* (2005) cited by Stojković *et al.* (2013) the main mechanisms of cancer chemoprevention are anti-mutagenesis and anti-proliferation or mitotic anti-progression.

An extensive review by Yang *et al.* in 2011, as well as other recent studies (Dong *et al.* 2015) shows that among the bioactive chemical constituents of *Ligularia* species, the most common phytochemical types are sesquiterpenes, which have demonstrated a strong cytotoxic or inhibitory activity on some tumor cell lines.

Among the volatile compounds identified by Gas chromatography with mass spectrometry detection in the *L. sibirica* (L.) Cass. extracts obtained by microwave assisted hydrodistillation, there were sabinene, limonene and terpinolene (monoterpenoids), as well as alkaloids that were most likely tussilagine and isotussilagine. In

our study, the statmokinetic effect may be attributed to these terpenoids. Many of the isolated terpenoids from natural sources have chemopreventive effects (Akihisa *et al*. 2003; Yang *et al*. 2011).

Nuclear and chromosomal aberrations observed in the root tip meristem cells of *A. cepa* L. are shown in Figure 4. Their frequency in the various experimental samples is shown in Supplementary Material (Table S2).

The average percentage value of the nuclear and chromosomal aberrations calculated for the control it was only 0.35 ± 0.07, and the percentages 1.53 ± 0.12, 3.46 ± 0.55, 3.25 ± 0.94, 1.83 ± 0.22, 1.25 ± 0.42 and 1.26 ± 0.35 for L 5% 24h, L 5% 48h, L 10% 24h, L 10% 48h, L 15 % 24h, L 15% 48h. The significant higher frequency of the chromosomal and nuclear aberrations in L 5% 48h, L 10% 24h, L 10% 48h variants, may be attributed to the potentially lower antioxidant activity as a result of the dilution of the tested extracts. This antimutagenic activity may be attributed to the secondary metabolites or to synergistic action of the antioxidant compounds. Besides that, the FT-MIR analysis has revealed the existence of OH group characteristic for phenols, to which may be due the genoprotective activity. Oxidative DNA damage can contribute to single double strand breaks formation or to oxidation of the purines or pyrimidines bases, inducing a genomic instability and also the development of cancer (Chobotokova 2009). The biologically active phenols are known for the antioxidant properties exerted by the absorption of the free radicals (Hidalgo and Almajano 2017; Shahidi *et al* 2015) as well as for the wide spectrum of biological and physiological actions (Durazzo 2017).

Mitoinhibitory effect of *L. sibirica* (L.) Cass. extracts was supported by the C-mitosis high percentage, which indicates the spindle disturbance in metaphase (Firbas and Amon 2014; Bonciu 2018). However, the nuclear aberrations identified in the meristematic root cells were much more varied and had a higher frequency compared to chromosomal aberrations. The nuclear abnormalities defined by the nuclear morphology alterations in the interphase, such as micronuclei, nuclear buds, altered nuclei shape may be an indicator of some processes such as cell death or tumorigenesis (Pellegrini 2003; Nefic *et al*. 2013).

In our study, except for the L 10% 24h experimental sample, changes in the shape of the nucleus was observed with a very low frequency. Nuclear envelope proteins ensure the nucleus rigidity to the distortion associated forces caused by the cytoplasmic microtubules. These changes may be the consequence of microtubule generated forces in the cytoplasm, if any of the membrane nuclear proteins is inactive (Nefic 2013; King *et al*. 2008). Other studies have shown that the inactivation of the associated proteins with the endoplasmic reticulum affects the nucleus form (Higashio *et al*. 2000; Matynia *et al*. 2002; Webster *et al*. 2009).

Moreover, the chromosomal aberrations and nuclear abnormalities identified by microscopic analysis are indicative of both clastogenic and aneugenic effects and of genotoxic damage. In this context, for a deeper estimation of the potential of this species additional *in vitro* and *in vivo* studies are required, aiming the extraction conditions, extract concentration and exposure time.

CONCLUSION

The paper represents an essential step in offering more information about the antioxidant activity, chemical composition and cytogenotoxic activity of ethanol extracts obtained from roots and rhizomes of *L. sibirica* (L.) Cass. The best results for phenols and flavonoids extraction from roots and rhizomes of *L. sibirica* (L.) Cass. were obtained in supercritical CO_2 extraction with cosolvent (ethanol) followed by ethanol extraction. The ethanol extracts of *L. sibirica* (L.) Cass. have demonstrated a very strong mitoinhibitory effect on *in vitro* root meristem cells of *A. cepa L*. Chromosomal aberrations and nuclear abnormalities identified by the microscopic analysis are key indicators of both clastogenic and aneugenic effects, and of genotoxic damage.

SUPPORTING INFORMATION

The version of this article contains supplementary material: vibration assignments for the rhizome and roots of *L. sibirica* (L.) Cass. extracts; the FTIR fingerprint of the studied rhizome and roots extracts, the chromosomal aberrations and nuclear anomalies observed in root meristem cells of *A. cepa* L. incubated in *L. sibirica* (L.) Cass. ethanolic extracts.

REFERENCES

Akihisa T, Yasukawa K, Tokuda H. 2003. Potentially cancer chemopreventive and anti-inflammatory terpenoids from natural sources, Studies in Natural Products Chemistry. 29:73-126. doi:10.1016/S1572-5995(03)80005-4

Beldie A. 1967. Flora şi vegetaţia Munţilor Bucegi. Ed Academiei Republicii Populare Române, Bucureşti, p.15-40

Bilz M, Kell SP, Maxted N, Lansdown RV. 2011. European Red List of Vascular Plants. Luxembourg: Publications Office of the European Union

Bonciu E, 2018 – *Evaluation of cytotoxicity of the herbicide Galigan 240 EC to plants*. Agricultural Sciences & Veterinary Medicine University, Bucharest. Scientific Papers. Series A. Agronomy, LXI(1):175-178.

Bonciu E, Firbas P, Fontanetti CS, Wusheng J, Karaismailoğlu MC, Liu D, Menicucci F, Pesnya DS, Popescu A, Romanovsky AV, Schiff S, Ślusarczyk J, de Souza CP, Srivastava A, Sutan A**,** Papini A, 2018. An evaluation for the standardization of the *Allium cepa* test as cytotoxicity and genotoxicity assay. Caryologia 71(3):191–209

Brand-Williams W, Cuvelier ME, Berset C. 1995. Use of a free radical method to evaluate antioxidant activity. Food Science and Technology. 28:25-30. doi:10.1016/S0023-6438(95)80008-5

Brînzan T, Bădărău AS, Murariu D, Staicu C, Patriche N, Ciubuc C, Hulea D. 2013. Catalog of habitats, species and Natura 2000 sites in Romania. Ed Fundația Centrul Național pentru Dezvoltare Durabilă, București; p.143-601

Chobotokova K. 2009. Aging and cancer: converging routes to disease prevention. Integr Cancer Ther. 8:115-122. doi: 10.1177/1534735409335505.

Dong LL, Xiong HY, Qi FM, Li HH, Fan GX, Che JM, Guo DD, Zhang ZX, Fei DQ. 2015. A new norsesquiterpenoid from *Ligularia virgaurea*. J Asian Nat Prod Res. 17:415-419. doi: 10.1080/10286020.2014.971018

Durazzo A. 2017. Study approach of antioxidant properties in foods: update and considerations. Foods. 6:1-7. doi:10.3390/foods6030017

Erdogan E, Ates B, Durmaz G, Yilmaz I, Seckin T. 2011. Pressurized liquid extraction of phenolic compounds from *Anatolia propolis* and their radical scavenging capacities. Food Chem Toxicol. 49:1592–1597. doi:10.1016/j.fct.2011.04.006

Firbas P, Amon T. 2014. Chromosome damage studies in the onion plant *Allium cepa* L. Caryologia 67:25–35

Hidalgo GI, Almajano MP. 2017. Red fruits: extraction of antioxidants, phenolic content and radical scavenging determination: A Review. Antioxidants. 6:1-27. doi: 10.3390/antiox6010007

Higashio H, Kimata Y, Kiriyama T, Hirata A, Kohno K. 2000. Sfb2p, a yeast protein related to Sec24p, can function as a constituent of COPII coats required for vesicle budding from the endoplasmic reticulum. J Biol Chem. 275:17900-17908. doi: 10.1074/jbc.M000751200

Kedare SB, Singh RP. 2011. Genesis and development of DPPH method of antioxidant assay. J Food Sci Technol. 48:412-422. doi: 10.1007/s13197-011-0251-1

King MC, Drivas TG, Blobel G. 2008. A network of nuclear envelope membrane proteins linking centromeres to microtubules. Cell. 134:427-438. doi: 10.1016/j.cell.2008.06.022

Lee YJ, Kim DB, Lee JS, Cho JH, Kim BK, Choi HS, Lee BY, Lee OH. 2013. Antioxidant activity and anti-adipogenic effects of wild herbs mainly cultivated in Korea. Molecules. 18:12937-12950. doi: 10.3390/molecules181012937

Liao JC, Zhu QX, Yang XP, Jia XJ. 2002. Sesquiterpenes from *Ligularia Hodgsonii*, J. Chin. Chem. Soc. 49:129-132. doi: 10.1002/jccs.200200022

Liu Q, Shen L, Wang TT, Chen CJ, Qi WY, Gao K. 2010. Novel modified furanoeremophilane-type sesquiterpenes and benzofuran derivatives from *Ligularia veitchiana*. Food Chem. 122:55–59. doi: doi.org/10.1016/j.foodchem.2010.01.069

Matynia A, Saluss SS, Sazer S. 2002. Three proteins required for early steps in the protein secretory pathway also affect nuclear envelope structure and cell cycle progression in fission yeast. J Cell Sci. 115: 421-431

Mihăilescu S, Anastasia P, Popescu A, Alexiu VF, Negrean GA, Bodescu F, Manole -Aiftimie A, Ion RG, Goia IG, Holobiuc I, Vicol I, Neblea MA, Dobrescu C, Mogîldea DE, Sanda V, Biță-Nicolae CD, Comănescu P. 2015. Ghidul de monitorizare a speciilor de plante de interes comunitar din România. Ed. Dobrogea, Constanța. p. 66-67

Nefic H, Musanovic J, Metovic A, Kurteshi A. 2013. Chromosomal and nuclear alterations in root tip cells of *Allium cepa* L. induced by Alprazolam. Med Arch. 67:388-392. doi: 10.5455/medarh.2013.67.388-392

Pellegrini N, Del Rio D, Colombi B, Bianchi M, Brighenti F. 2003. Application of the 2,2'-azinobis(3-ethylbenzothiazoline-6-sulfonic acid) radical cation assay to a flow injection system for the evaluation of antioxidant activity of some pure compounds and beverages. J Agric Food Chem. 51:260-264. doi: 10.1021/jf020657z

Pinglin L, Zhang ZX, Jia ZJ. 2008. Four new eremophilane derivatives from *Ligularia sagitta*. Chem Letters. 37:308–309. doi: 10.1246/cl.2008.308

Pop E. 1960. In mlaștinile de turbă din Republica Populară Română. Ed Academiei Republicii Populare Române, București. p.139-423

Santos-Buelga C, Gonzalez-Manzano S, Dueñas M, Gonzalez-Paramas AM. 2012. Extraction and isolation of phenolic compounds. Methods Mol Biol. 864:427-464. doi: 10.1007/978-1-61779-624-1_17

Shahidi F, Ambigaipalan P. 2015. Phenolics and polyphenolics in foods, beverages and spices: antioxi-

dant activity and health effects – A Review. J Functional Foods. 18B:820-897. doi: doi.org/10.1016/j.jff.2015.06.018

Singleton VL, Rossi JA. 1965. Colorimetry of total phenolics with phosphomolybdic phosphotungstic acid reagents. Am J Enol Viticult. 16:144-158.

Šmídová A, Münzbergová Z, Plačková I. 2011. Genetic diversity of a relict plant species, *Ligularia sibirica* (L.) Cass. (Asteraceae), Flora. 206:151-157. doi: 10.1016/j.flora.2010.03.003

Stojković DS, Davidović S, Živković J, Glamočlija J, Ćirić A, Stevanović M, Ferreira I, Soković M. 2013. Comparative evaluation of antimutagenic and antimitotic effects of *Morchella esculenta* extracts and protocatechuic acid. Frontiers in Life Science. 7: 218-223. doi: 10.1080/21553769.2014.901925

Szymanska-Chargot M and Zdunek A. 2013. Use of FT-IR spectra and PCA to the bulk characterization of cell wall residues of fruits and vegetables along a fraction process. Food Biophys. 8:29–42. doi: 10.1007/s11483-012-9279-7

Tedesco SB, Laughinghouse HD. 2012. Bioindicator of genotoxicity: the *Allium cepa* test. In: Srivastava JK (ed) Environmental Contamination, InTech Publisher. 137–156 p. doi: 10.5772/31371

Tori M, Tanio Y, Okamoto Y, Saito Y, Gong X, Kuroda C, Hanai R. 2008. Chemical constituents of *Ligularia franchetiana* collected in Yunnan province of China. Heterocycles. 75:2029-2034.

Webster M, Witkin KL, Cohen-Fix O. 2009. Sizing-up the nucleus: nuclear shape, size and nuclear-envelope assembly. J Cell Sci. 122:1477-1486. doi: 10.1242/jcs.037333.

Wu L, Liao Z, Liu C, Jia H, Sun J. 2016. Eremophilane sesquiterpenes from the genus *Ligularia*. Chem Biodivers. 13:645-671. doi: 10.1002/cbdv.201500169

Xie WD, Weng CW, Li X, Row KH. 2010. Eremophilane sesquiterpenoids from *Ligularia fischeri*. Helv Chim Acta. 93:1983 –1989. doi: 10.1002/hlca.201000010

Yang JL, Wang R, Shi YP. 2011. Phytochemicals and biological activity of *Ligularia* species. Nat Prod Bioprospect. 1:1-24. doi: 10.1007/s13659-011-0003-y

Yuan YL, Fang LZ, Bai SP, Liang HJ, Ye DD. 2013. A novel eremophilane sesquiterpenoid from *Ligularia* intermedia roots and rhizomes. Chem Nat Compd.49:258-260. doi: 10.1007/s10600-013-0575-3

Yuet Ping K, Darah I, Yusuf UK, Yeng C, Sasidharan S. 2012. Genotoxicity of *Euphorbia hirta*: an *Allium cepa* assay. Molecules. 17:7782-7791.

Zavoi S, Fetea F, Ranga F, Pop RM, Baciu A, Socaciu C. 2011. Comparative fingerprint and extraction yield of medicinal herb phenolics with hepatoprotective potential, as determined by UV-Vis and FT-MIR spectroscopy. Not Bot Horti Agrobo. 39:82-89. doi: http://dx.doi.org/10.15835/nbha3926278

Caryologia
International Journal of Cytology, Cytosystematics and Cytogenetics

Firenze University Press
www.fupress.com/caryologia

OPEN ACCESS

Citation: H.P. Shambhavi, P. Makwana, B. Surendranath, K.M. Ponnuvel, R.K. Mishra, A.N.R. Pradeep (2020) Phagocytic events, associated lipid peroxidation and peroxidase activity in hemocytes of silkworm *Bombyx mori* induced by microsporidian infection. *Caryologia* 73(1): 93-106. doi: 10.13128/caryologia-112

Received: January 9, 2019

Accepted: February 22, 2020

Published: May 8, 2020

Data Availability Statement: All relevant data are within the paper and its Supporting Information files.

Competing Interests: The Author(s) declare(s) no conflict of interest.

Phagocytic events, associated lipid peroxidation and peroxidase activity in hemocytes of silkworm *Bombyx mori* induced by microsporidian infection

Hungund P. Shambhavi[1], Pooja Makwana[2], Basavaraju Surendranath[3], Kangayam M Ponnuvel[1], Rakesh K Mishra[1], Appukuttan Nair R Pradeep[1,*]

[1] *Proteomics Division, Seribiotech Research Laboratory, CSB-Kodathi Campus, Carmelaram P.O., Bangalore-560035, Karnataka, India*
[2] *Central Sericultural Research and Training Institute, Berhampore, India*
[3] *Central Tasar Research and Training Institute, Ranchi, India*
*Corresponding author. E-mail: arpradeepnair@gmail.com

Abstract. Microbial infections induced humoral and cell- mediated immune events in hemocytes. After infection by the microsporidian *Nosema bombycis* in the commercially important silkworm, *Bombyx mori*, hemocytes exhibited deformed nucleus and degranulation of structural granules by exocytosis. Granulocytes showed signs of phagocytosis included formation of microvilli, pseudopodia, engulfment of spores, phagosome formation and membrane porosity. Association of membrane disintegration with infection – induced lipid peroxidation (LPO) was revealed by testing level of malondialdehyde, a byproduct of LPO. LPO activity enhanced significantly ($P < 0.0002$) throughout infection with peak activity in later stages of infection from day 11 accompanied by hemocyte plasma membrane disintegration. Partial increase in LPO activity coupled with increased peroxidase activity recorded in early and mid stages of infection. In later stages, peroxidase activity decreased however LPO increased accompanied by phagocytosis events. In hemocytes, phagocytic events are initiated by activation of genes encoding recognition proteins, aggregation factors and immune-associated proteins. ß-*GRP* expression was down regulated after the infection whereas *CTL-11* enhanced expression on day 10. Humoral lectin enhanced expression on day 6 whereas apolipophorin showed 2.59 fold increase on day 10 after infection. Gene encoding cytoskeletal protein, ß- Actin showed stable enhanced expression throughout infection showing positive correlation ($R^2 = 0.65$) with age after infection. Phagocytosis- associated gene *Eater* from Drosophila showed enhanced heterologous expression. Altogether phagocytic events induced by microsporidian infection are accompanied by increased LPO, decreased peroxidase activity and modulated gene activity in hemocytes of *B. mori.*

Keywords. Phagocytosis, lipid peroxidation, peroxidase activity, *Bombyx mori,* microsporidian infection, hemocytes.

INTRODUCTION

Insects have developed functionally active immune system for survival in the widespread habitat. Insect immune system comprises humoral and cellular responses as well as phenol oxidase cascade culminates in melanisation. Innate immunity components included activation of different pathways such as Toll, IMD and JAK-STAT pathways effecting in production of antimicrobial proteins (Hoffmann 2003; Govind 2008). Cell- mediated responses, facilitated instantaneously by hemocytes against pathogens (Barillas-Mury *et al*. 2000) involved nodulation, encapsulation and phagocytosis depending on size of the pathogen/ parasite (Rosales 2011). Phagocytic response of a cell is evolutionarily conserved from protozoan to mammals (Faurschou and Borregaard 2003; Nazario-Toole and Wu 2017) which involved recognition, binding and ingestion of parasites (Rosales 2011; Kwon *et al*. 2014). Phagocytic receptors evoke different signalling pathways such as Draper activated Draper/Src/Syk/CED-6 pathway (Fullard *et al*. 2009) whereas TEP (thioester containing protein) activated CSD6 pathway (Blandin *et al*. 2004). Activation of signalling leads to cytoskeletal rearrangement, insertion of new membrane for pseudopodia and microvilli formation for parasitic engulfment (Bajno *et al*. 2000). In Drosophila, plasmatocytes and granulocytes act as major phagocytic cells against bacteria (Castillo *et al*. 2006; Lamprou *et al*. 2007) whereas in lepidopterans granulocytes are modified to become phagocytic cells (Ling and Yu 2006; Rebeiro and Brehelin 2006).

Though commercially important silkworm, *Bombyx mori* (Lepidoptera) is domesticated and reared under protected conditions, worms are exposed to pathogenic attack causing major losses to silk industry. In *B. mori*, infection by the obligate intracellular microsporidian parasite *Nosema bombycis* causes devastating disease, pebrine. *N. bombycis* infects either through transovarian transmission or through secondary contamination by feeding contaminated mulberry leaves (Hukuhara 2017). On reaching midgut, spores germinate and inject sporoplasm into midgut epithelial cells (Franzen 2005) where it multiplies and spread to other host tissues including haemolymph and hemocytes. Though pathogens spread through eggs to newly hatched larvae, symptoms or presence of spores could not be identified in initial stages of infection and spores could be identified only after six days of infection (Ma *et al*. 2013).

In *B. mori,* infection by *N. bombycis* suppressed host responses, inhibited melanization events and down regulated immune genes in midgut (Pan *et al*. 2013; Ma *et al*. 2013). However hemocyte- mediated cellular responses against microsporidian infection is not known. In this investigation, cellular, biochemical and molecular immune responses of hemocytes in *B. mori* were revealed showing induction of LPO activity and peroxidase activity in association with phagocytosis events against *N. bombycis* infection.

MATERIALS AND METHODS

Infection and sample collection

B. mori larvae were reared on mulberry (*Morus* sp) leaves under standard rearing conditions of 25 ± 2°C, 70% relative humidity and natural photoregime (13L : 11D). Initially larvae were grown till third instar and separated after third moulting to fourth instar. Day 0 fourth instar larvae were collected and exposed to experimental infection by feeding spores of *N. bombycis* (standard strain: NIK-1s_mys) smeared on mulberry leaf with a dose of 1 x 10^6 spores / larva that induced 50% mortality within the lethal time LT_{50} (Rao *et al*. 2004). Non-infected *B. mori* larvae of the same age group were used as control and reared separately.

In order to analyse hemocyte responses after *N. bombycis* infection, haemolymph samples were collected from control and infected larvae on day 0, 2, 6, 8, 9, 10, 11 and 12 after the infection. Haemolymph was collected by piercing first abdominal proleg using a sterilized needle. Haemolymph of pupae were collected from newly formed pupa (14 days after infection) by puncturing leg impressions on ventral side. The hemocytes were separated by centrifugation at 880 g for 10 min at 4°C. The hemocyte pellets were washed with anticoagulant solution (0.098M NaOH, 0.186M NaCl, 0.017M EDTA, 0.041M Citric acid, pH 4.5 adjusted using NaCl) twice and stored at -80°C for protein analysis. For total RNA extraction, hemocyte pellets were stored in RNA stabilization reagent RNA later (Qiagen).

Light microscopy and transmission electron microscopy (TEM)

Hemocytes of infected and non-infected control larvae were observed under inverted tissue culture microscope (Leica) and the hemocytes and spores were counted using hemocytometer. In order to carryout TEM analysis, hemocyte samples were processed essentially as described earlier (Pradeep *et al*. 2013). Briefly, hemocytes were fixed in 3 % glutaraldehyde upto 24 h before fixation in 1% osmium tetroxide. The samples were dehydrated through alcohol series, brought to acetone and then stained with 2 % uranyl acetate. Using an embedding kit

(Araldite Embed- 812) hemocyte samples were embedded in araldite for 48h. Ultrathin sections (100nm) were cut using Ultramicrotome (Leica –EM UC6) and placed on a copper grid. The ultrathin sections were stained with uranyl acetate and lead citrate and observed under TEM. Ultrastructural variations in the hemocytes (n = 50 each) were observed at 60 kV in a Tecnai G^2 transmission electron microscope attached with Megaview Soft Imaging System and photographed (at the TEM facility in National Institute for Mental Health and Neuro Sciences (NIMHANS), Bangalore, India).

Lipid peroxidation

In order to examine lipid peroxidation in the hemocytes of *B. mori* larva infected with *N. bombycis*, hemocyte samples were collected at different time points after infection along with sample from same aged non-infected control. The assay was performed using EZAssay™ TBARS lipid peroxidation estimation kit following manufacturer's (HiMedia) protocol. Membrane lipids are destructed by phagocytes to form lipid peroxides (Mylonas and Kouretas 1999) which in turn breakdown to form a by-product malondialdehyde (MDA) which is measured by absorbance. The lipid peroxidation was estimated as malondialdehyde (MDA) equivalents (Hodges *et al.* 1999) in a 96 well microtiter plate using absorbance reading at 532 nm in a microtiter plate reader (Multiskan spectrum, Thermo). From 1- 10 µM MDA, a standard curve was obtained by using a slope of standard curve (y = 0.00457+0.00416x) and MDA concentration in the sample was calculated (Yagi 1998; Fatima *et al.* 2011).

Ascorbate peroxidase activity

In order to test whether peroxidase activity varied in hemocytes after the infection, ascorbate peroxidase (PRX) activity was determined as described earlier (Nakano and Asada 1981). Hemocyte pellet was collected from haemolymph at different time points after the infection and then lyzed in Insect cell lysis buffer and quantified the protein (Lowry *et al.* 1951). Briefly, PRX assay was performed using 750 µl 100 mM phosphate buffer (pH- 7.0), 150 µl of 5.0 mM ascorbate and 300 µl 0.5 mM of H_2O_2. The reaction was carried out in 1.5 ml Eppendorf tubes using 300 µl of hemocyte lysate sample containing 100 µg protein. The reaction mixture was transferred to 96 well plate. The rate of decrease in absorbance was read at 290 nm at every one minute interval for ten minutes duration. The enzymatic activity was calculated using a molar extinction coefficient of 2.8 mM-1 cm-1 and the result was expressed as micromoles per minute per milligram of protein (Nakano and Asada 1981).

Hydrogen peroxide activity

In order to test variation in hydrogen peroxide (H_2O_2) level after infection, assay was performed using hemocyte extract in phosphate buffered saline (PBS) buffer (pH 7.1) as described earlier (Velikova *et al.* 2000; Pooja *et al.* 2017). The absorbance was measured at 390 nm in the microplate reader and H_2O_2 content was calculated based on a standard curve.

Total RNA extraction and cDNA synthesis

Total RNA was extracted from hemocytes collected from control and *N. bombycis*- infected *B. mori* larva. Genomic DNA contamination was removed from total RNA by incubation with RNAse free – DNAse I (Takara). Complementary DNA (cDNA) was synthesized from 1 µg total RNA using oligo d(T) primer and M-MuLV (Moloney Murine Leukemia virus) reverse transcriptase using cDNA synthesis kit as per manufacturer's protocol (Primescript; Takara). RT-PCR was performed to analyse semiquantitative expression on 0, 2, 6, 8 and 10 days after infection using gene- specific primers (Table 1) which was validated by qPCR.

Quantitative PCR (qPCR)

qPCR was performed using DyNaMo SYBR GREEN qPCR Master Mix (Thermo - Finzyme) with 0.3X Rox as passive reference dye, on Agilent Stratagene Mx3005P qPCR system. A 25 µl reaction mixture contained 2.5 µl cDNA template, one pmol each of forward and reverse primers and 12.5 µl SYBR Green qPCR master mix (1X) containing 4 mM $MgCl_2$. The thermal program was set as 95°C for 15 min, followed by 40 cycles of 95°C for 30 seconds and at primer- specific annealing temperature (Tm) for a minute (Table 1).The PCR products were resolved by 1.5 % agarose gel electrophoresis and confirmed target-specific amplification. For housekeeping gene, *ribosomal protein* gene was used and fold change in expression relative to calibrator was calculated.

Cloning and sequencing

From *B. mori* genome phagocytosis- associated genes *TEP-1* and *Eater* are not reported. In order to con-

Table 1. Key to the genes and encoding proteins associated with phagocytosis induced in hemocytes of *B. mori* larva after infection with the microsporidian *N. bombycis*.

Gene name	Nucleotide Accession No.	Primer (Left (L) and right (R))	Tm (°C)	Protein Accession No.	Functions	Reference
TEP- 1	AY433751	5'GTGGCTAAGCCCAGTTTCAG3'L 5'AGTCACTCGGAAGCACTCGT3'R	59.4	ABG-0034413	Hemocyte mediated complement like protein, *Plasmodium berghei* binding and mediates killing	Blandin *et al*, 2004
Eater	NM_143276	5'ATAGCCGCTGCTGATGACTC3' 5'TCTTCGATCCGGCAAAAC3'	56.5	Q9VB78	Transmembrane protein, scavenger receptor, bacterial recognition and phagocytosis.	Kocks *et al*, 2005; Chung *et al.*, 2011
βGRP- 2	NM_001043985	5'AATGACACTGTTCGCGTTCC3' 5'TCGCACTCTCGTCTTTGTTG3'	57.3	H9JQ04	Recognition of β- 1, 3 glucan from fungi and mediate cellular responses.	Kim *et al*, 2000 Xiang-Jun Rao *et al* 2014
βGRP- 4	NM_001166142	5'ACCTTGTCGAATCCAGAGGC3' 5'CGGGTCTATTGTTGAAGCCG3'	59.4	Q9NL89	Recognition of β- 1, 3 glucan from fungi and mediate cellular responses.	Kim *et al*, 2000 Xiang-Jun Rao *et al* 2014
CTL- 11	BGIBMGA006623	5'TCTGGTCGGTCGGCTGTATA3' 5'GAGCTGCTCCGCTATGAACT3'	59.4	D2X2F7	Acts as opsonin and increase phagocytosis.	Pendland *et al*, 1988
CTL- 17	NM_001130899	5'ACGTCCTGCATACCGAAAAG3' 5'GCCTCGTCTAACGATTCAGG3'	58.3	Q06FJ6	Acts as opsonin and increase phagocytosis.	Pendland *et al*, 1988
Apolipoph-orin I/II	AB640623	5'TGGCGGATAAATGCTCGTTG3' 5'TCTTCTTCCGCGCAAATCTG3'	57.3	G1UIS8	Act as pattern recognition protein and binds to fungal β- 1, 3 glucan, aid in phagocytosis.	Whitten *et al*. 2004; Barabas and Cytryńska, 2013
Humoral lectin	NP_001104817.1	5'GGCGGTACAACGTTAAGGAG3' 5'AACGAGCACCGACACAAGTA3'	58.3	P98092	Adhesive protein and relates to hemostasis or encapsulation of foreign substances for self-defense.	Kotani *et al*. 1995
Beta Actin A4	NM_001126255	5'ATCCTGCGTCTGGACTTAGC3' 5'AAGACTTCTCGAGGGAGCTG3'	59.4	P84183	Cytoskeletal protein, helps in formation of cellular projections.	May *et al*. 2001; May and Machesk 2001
Ribosomal protein	NP_001037259.1	5'TGGAGCGCCTTACAAACTCT3' 5'GCCAGATTGCTTGGTTGACT3'	57.3	Q5UAN9	House- keeping gene	Lu *et al* 2013

firm heterologous expression of *TEP-1* and *Eater,* mRNA sequence of *TEP-1* of *Aedes aegypti* (Acc No.AY432915.1) and *Eater* of *Drosophila melanogaster* (Acc. No. HM165182) were collected from NCBI database and primers were designed (Primer 3 program) and used for qPCR (Table 1). The amplicons were resolved on 1.2 % agarose gel containing the fluorescent dye ethidium bromide. The *Eater* gene amplified at expected product size. In order to confirm the sequence identity *Eater* amplicon from RT-PCR was purified using a PCR purification kit (QIAquick, Qiagen) and cloned into a vector pJET 1.2/blunt using CloneJet PCR cloning kit (Thermo Scientific) as per manufacturer's protocol. The cloned product was transformed into JM 109 competent cells. Through colony PCR, plasmids were confirmed and the plasmid DNA was isolated using QIAprep spin miniprep kit (Qiagen). Presence of the fragment was confirmed by PCR and sequenced using Sanger method at a facility (Applied Biosystems) available at Eurofins Genomics India Pvt. Ltd., Bangalore, India.

The nucleotide sequence was used to perform BLASTN 2.8.1+ (NCBI) search against non-redundant database. The nucleotide sequence was then translated to protein sequence using Expasy – Translate tool (https://web.expasy.org/translate/). The 3'5' Frame 2 of the translated sequence was used for analysis by BLASTP 2.8.1+ (NCBI) and searched against non-redundant GenBank CDS translations, PDB, SWISSPROT, PIR and PRF.

Statistical analyses

The data were presented as Mean ± SD. Significance of difference between means was evaluated by Students' *t*- test or single factor ANOVA. Correlation between variables was analysed by linear regression (y = a + bx).

Quantitative gene expression was performed using cDNA synthesized from total RNA of hemocytes of control and infected *B. mori* larva, relative to the calibrator using Mx3500P Real Time PCR system (Agilent). Average threshold cycle (Ct) value of transcript expression was calculated from triplicates using ΔΔ Ct method (Livak and Schmittagen 2001) and normalized by housekeeping gene encoding ribosomal protein. Comparative Ct values of the genes were standardized by Ct values for the house keeping gene encoding ribosomal protein. Ct values were standardized with average control value, providing ΔCt value which is standardized to make the average control value '1' (the ΔΔ Ct values) (Gerardo *et al*. 2010). Fold change in gene expression was calculated with reference to the calibrator, which in turn presented down regulated relative quantities as negative values. The data (mean ± SD) denoted is the gene expression induced by infection after eliminating the changes in control.

RESULTS

Organismal variations

Day 0 fourth instar larvae were experimentally infected by feeding spores of *N. bombycis* smeared on mulberry leaf with LD_{50} dose of 1 x 10^6 spores / larva. After the infection, changes were not observed in larval behaviour and activity till day 2. Larval death was recorded from four days after infection. Moulting of infected larvae to fifth instar delayed by 24 h in comparison to control. Infected larvae were smaller in size and showed reduced growth from day 8. Infected larvae initiated cocoon spinning at 24 h after control larvae spun silk. Cocoons of infected larvae were smaller and flimsy with lower silk content. Infected larvae were black and showed melanization under cuticle. Infected pupae were smaller in size and acutely melanized (Fig 1 A-C).

N. bombycis spores were absent in non- infected control larval haemolymph and tissue samples. In *N. bombycis*- infected larvae (n = 30 each), spores were not found till day 6. On day 6, spore count was 0.1 x 10^5 / ml haemolymph. On day 9 the count was 0.95 x 10^5 spores/ ml showing significant ($P< 0.001$) increase in comparison to day 6. Spore count then enhanced significantly ($P < 0.001$) to 4.4 x 10^5 spores / ml on day 10 and to 5.6 x 10^5 spores / ml on day 11 after infection showing the increase in a sigmoid fashion. Within 11 days, average of 60% larval mortality was recorded after the infection.

Cellular variations in hemocytes

Total hemocyte count of control and *N. bombycis*- infected larvae did not vary significantly on day 0 of infection, however significant ($P < 0.005$; ANOVA) decrease observed in later stages (8 to 11 days) of infection. In control, total hemocyte count on day 0 fourth instar larvae was 14.4 x 10^5 cells/ml, which did not vary significantly ($P < 0.1$), on day 0 after infection. The count increased to 16.55 x 10^5 cells/ ml on day 6 however hemocyte count significantly ($P< 0.002$) increased to 17.95 x 10^5 cells/ml after infection. In control, hemocyte count significantly ($P < 0.001$) increased on day 8 to 37.05 x 10^5 cells/ ml whereas after infection it decreased to 32.35 x 10^5 cells/ ml. On day 9 the count was 49.15 x 10^5 cells / ml in control and 45.05 x 10^5 cells / ml after infection. In control on day 10 and 11, mean hemocyte count was 50.4 x 10^5 cells/ ml in comparison to 42.1x 10^5 cells/ ml after infection.

Under light microscope, four types of hemocytes *viz*., granulocytes, plasmatocytes, spherulocytes and oenocytes were observed in addition to the precursor

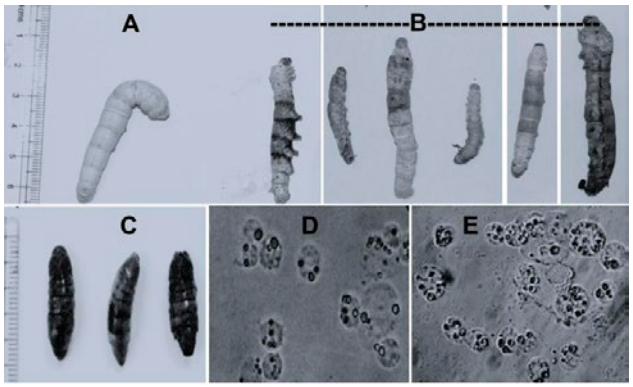

Figure 1. Organismal effects of microsporidian infection on *B. mori* larva: In comparison to control larva (A), infected larvae showed retarded growth and both larvae and pupae melanised (B – C). Control larval hemocytes illustrate clear cytoplasm and less granules (D) whereas infected larval hemocytes were with granulated cytoplasm and few showed degranulation (E).

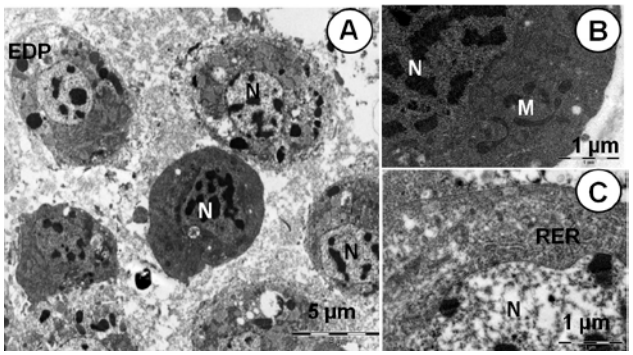

Figure 2. Transmission electron microscopy (TEM) of hemocytes of control fifth instar larvae of *B. mori* (A) showed smooth plasma membrane, clear cytoplasm and cells with few granules and electron dense particles (EDP), nucleus (N) with oval or branched nuclear membrane and evenly distributed chromatin, several mitochondria (M) with developed cristae (B) and rough endoplasmic reticulum (RER) (C).

prohemocytes. In control, hemocytes appeared intact with clear cytoplasm and less granules whereas after infection, cytoplasm becomes granulated on day 6. Many cells ruptured and degranulated from day 8 after infection (Fig.1 D - E).

In order to examine subcellular variations induced by *N. bombycis* infection, infected and control hemocytes were examined under TEM on day 6, 8 and 11 after infection. In hemocytes of control day 6 larvae, cytoplasm was clear. RER and mitochondria with well developed cristae distributed in cytoplasm (Fig. 2 A-C). In plasmatocytes, nuclei were round or ovoid and in granulocytes, smooth or branched. Chromatin was

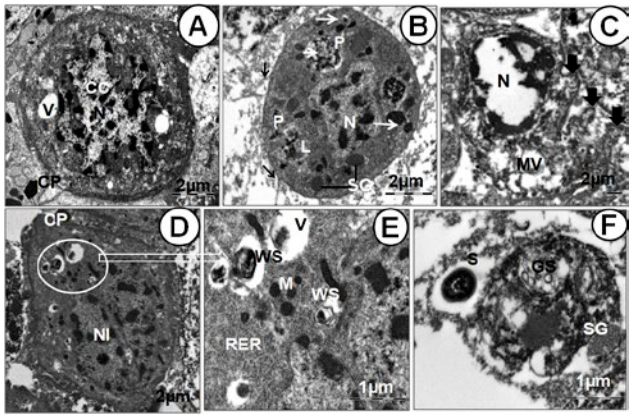

Figure 3. TEM observations on hemocytes of fifth instar larvae of *B. mori* showing subcellular variations after infection with *N. bombycis*: Granulocytes turn phagocytic on day 6 (A-B) showing highly deformed nucleus with condensed chromatin (CC), cellular projections (CP) and few vacuoles (V) in cytoplasm. On day 10 well differentiated pseudopodia (C; black arrow heads), multivesicular body (MV) and phagosomes (P) in association with lysosomes (L) were found. On day 11, hemocytes (D - F) with dense cytoplasmic contents, invaginated nucleus (NI) with condensed chromatin, packets of structured granules (SG), engulfed mature spores (S; white arrows), ghost spores (GS) and whirled sporoplasm (WS) in vacuoles found. Cytoplasm was with RER, mitochondria (M), and vacuoles with cellular remnants (E).

uniformly spread in nucleoplasm. Granulocytes showed presence of few granules and plasmatocytes with few electron dense particles (EDP). Plasma membrane was smooth and with pinocytic vesicles showing active membrane transport.

On day 6 after infection, several packs of structured granules appeared in granulocytes. Large- sized vacuoles occupied major cytoplasmic area**.** Mitochondria increased in number. Many granulocytes featured highly irregular branched nucleus with condensed chromatin. Plasma membrane showed few cellular projections (Fig. 3 A).

On day 8 after infection, granulocytes showed plasma membrane with cytoplasmic extensions, lysosomes and phagosomes with engulfed spores (Fig. 3 B). More granulocytes were with pseudopodia and microvilli (Fig. 3 C). Phagosomes enclosing spores were observed and were associated with lysosomes (Fig. 3 B).

On day 11 after infection, hemocytes showed porous plasma membrane that lost integrity. In few cells, cell membrane completely degenerated. Degranulation by exocytosis observed in close vicinity of spores (Fig. 4 A-B). Many phagocytic granulocytes were observed with cytoplasmic extensions, developed pseudopodia, whirled sporoplasm, engulfed mature spores and ghost spores (Fig. 3 D - F). Rough endoplasmic reticulum (RER) and several mitochondria were observed in

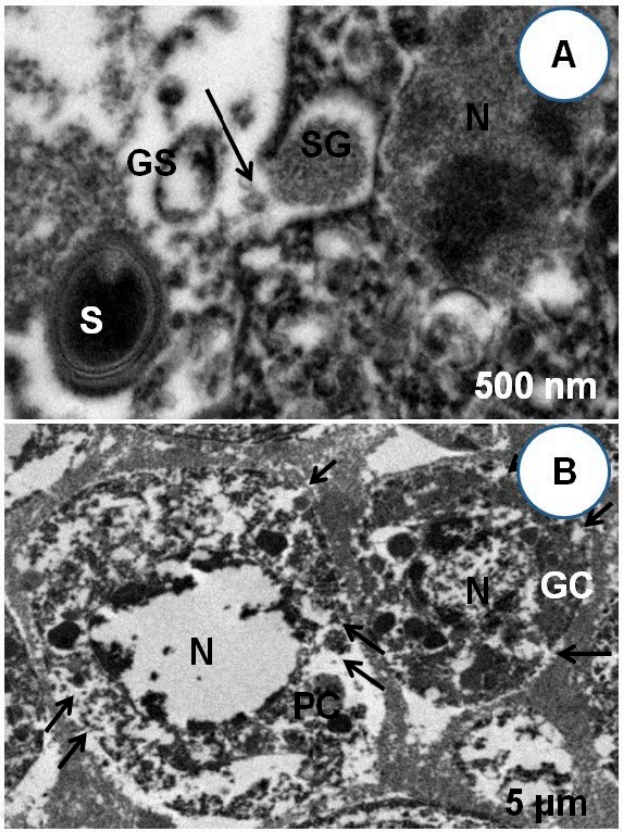

Figure 4. TEM observations on hemocytes of fifth instar larvae of *B. mori* showing subcellular variations after infection with *N. bombycis*. Hemocytes (A) showed degranulation by exocytosis (arrow) to the microsporidian infection locale; (B) Plasmatocyte (PC) and granulocytes (GC) showed membrane disintegration (arrows) after infection with *N. bombycis*. S- spore; GS- ghost spore; SG- structured granules; N- nucleus.

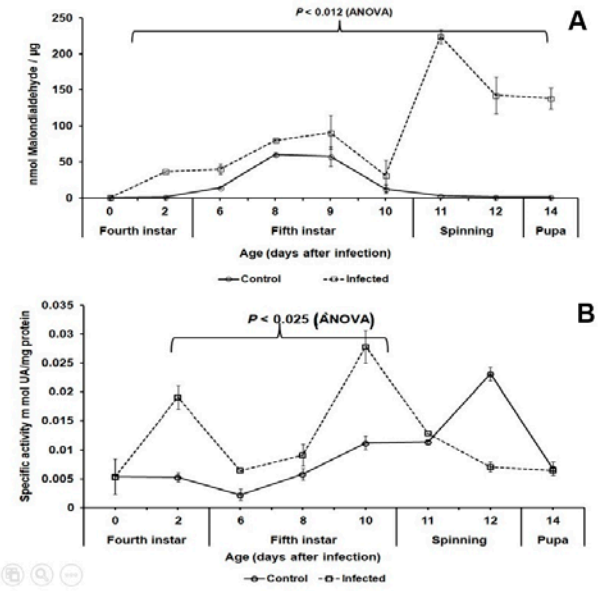

Figure 5 A-B. Lipid peroxidation in hemocytes of *B. mori* larva induced after infection by *N. bombycis* indicated by the variation in malondialdehyde which is a bye-product of lipid peroxidation (A): Lipid peroxidation was at significantly higher level from initial stages of infection and at peak level from day 11 onwards. (B): Variation in ascorbate peroxidase (PRX) activity in hemocytes of *B. mori* larva induced after infection by *N. bombycis*: PRX activity was significantly higher after infection with peak activity on day 2 and 10 followed by decline from day 11 onwards.

dense cytoplasm. Nucleus demorphed, highly intended and showed deep invagination (Fig. 3D). Number of lysosomes increased and located adjacent to spores or fused with vacuoles formed phagosomes.

Lipid peroxidation

In order to examine involvement of lipid peroxidation (LPO) in inducing membrane permeability, LPO was assayed by measuring malondialdehyde (MDA) which is a by-product of lipid peroxidation. After *N. bombycis* infection, MDA levels significantly ($P < 0.012$; ANOVA) increased from day 2 to day 14 with significantly ($P < 0.000004$) larger increase from day 11 indicating increased LPO activity after infection (Fig. 5 A). The increase in LPO activity showed positive correlation with increase in age after infection ($R^2 = 0.58$) as well as number of spores increased exponentially ($y = 0.0003e^{0.5572x}$; $R^2 = 0.80$) with increasing age. In order to verify relation between infection level and LPO increase, correlation analysis was performed which showed significant linear correlation ($R^2 = 0.65$) between increase in spore number and LPO activity.

Ascorbate peroxidase activity

In order to examine change in activity of ascorbate peroxidase (PRX) with increase in infection, PRX activity was measured in hemocytes using ascorbic acid as substrate. PRX activity significantly ($P < 0.025$; ANOVA) enhanced from day 2 to 10 after infection with peak activity on day 10 (Fig. 5 B) whereas control hemocytes showed PRX activity at basic level and increased activity on day 12, during spinning duration. Relation between increase in LPO activity (MDA level) with changes in PRX activity in infected hemocytes was analyzed by correlation- regression which showed positive linear correlation though with low correlation coefficient value ($R^2 = 0.294$) during initial ten days of infection. Notably, from day 11 after infection PRX activity significantly decreased and LPO increased.

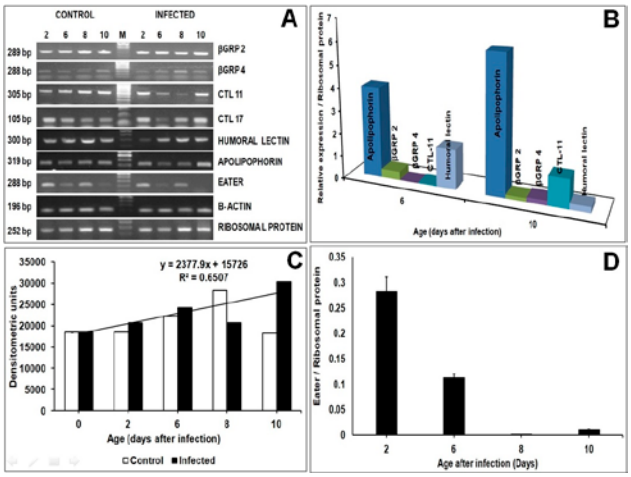

Figure 6 A-D. Modulation in expression of immune genes in hemocytes of *B. mori* larva after infection with *N. bombycis*: (A) RT-PCR profile of gene expression of different genes including cytoskeletal protein gene β- Actin and the house keeping gene encoding ribosomal protein resolved from hemocytes collected from control and infected larvae at 2, 6, 8 and 10 days after infection. M- Massruler DNA marker (Thermo). (B) qPCR showed relative expression of different immune genes in hemocytes at 6 and 10 h after infection. (C) β- Actin, the cytoskeletal protein gene showed gradual increase in expression represented by densitometric units. Increase in expression was correlated with age after infection shown by allometric line. The linear regression formula and correlation coefficient are inserted. (D) Relative expression pattern of the phagocytosis associated gene *Eater like* after standardization with expression of the house keeping gene, ribosomal protein and after elimination of control value.

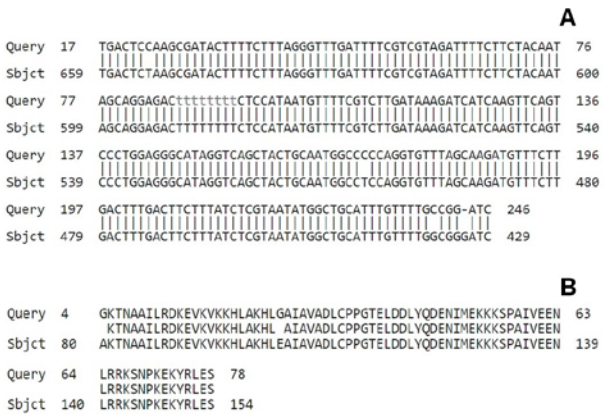

Figure 7. Alignment of nucleotide sequence (A) of amplification product from heterologous expression profile of *Eater* gene of *Drosophila* (query) with nucleotide sequence (subject) of the most similar gene, *B. mori* uncharacterized transcript variant X2 (Accession No. XM_004928120.3) revealed by NCBI-BLASTn analysis, showed 98 % similarity. (B) Protein sequence of the uncharacterized transcript variant (subject) is aligned with translated sequence of the *Eater* like gene (query) showing 97% similarity.

Hydrogen peroxide assay

In order to quantify reactive oxygen species level in hemocyte- phagocytes, level of hydrogen peroxide (H_2O_2) in the hemocytes was tested at 0, 2, 6, 8 and 10 days after the infection using hemocyte lysate extracted in PBS. In hemocytes of *N. bombycis*- infected larvae, H_2O_2 levels did not show significant variation from control (data not provided).

Expression of phagocytosis- associated genes

Humoral immune responses of hemocytes are initiated with recognition of pathogen followed by signalling and effector action. Expression of genes encoding recognition proteins β- glucan recognition proteins (*BGRP2* and *BGRP4*), opsonins C- type lectin (*CTL11 and CTL 17*), hemocyte aggregation factor humoral lectin, phagocytosis enhancer *apolipophorin,* cytoskeletal protein β- *Actin,* hemocyte mediated complement like protein that bind and kill *Plasmodium berghei* in *Aedes aegypti Thioester containing protein* (*TEP-1*) and bacterial phagocytosis associated *Eater* from *Drosophila melanogaster* was analysed by RT- PCR (Table 1) and qPCR (Fig. 6).

RT-PCR profile and qPCR revealed down regulation of βGRP2 and *BGRP4* expression after *N. bombycis* infection. *CTL* genes showed low level of expression in earlier days of *N. bombycis* infection whereas 0.334 fold increase in expression was noticed on 10^{th} day after infection (Fig. 6 B). *Humoral lectin* enhanced relative expression on day 6 (0.79 fold) after infection followed by down regulation (-1.97 fold) on day 10. After infection by *N. bombycis,* apolipophorin showed increase in expression by 1.96 fold on 6^{th} day and by 2.59 fold on 10^{th} day. Expression of β- *actin* showed stable increase from early to late stages of infection with strong positive correlation (R^2 = 0.65) with age after infection (Fig. 6 C).

In the dipterans *A. aegypti* and *D. melanogaster, TEP1* (Blandin *et al.* 2004) and *Eater* (Kocks *et al.* 2005; Juneja and Lazzaro 2010) respectively are closely associated with phagocytosis however these genes are not reported from *B. mori.* Primers derived from *TEP* of *A. aegypti* and *Eater* of *Drosophila* was used for amplification with template cDNA from hemocytes of *B. mori* after infection with *N. bombycis.* In this study *TEP* did not show expression in hemocytes of *B. mori* whereas *Eater* showed enhanced relative expression on day 2 and 6 after infection followed by significant ($P < 0.005$) decrease (Fig. 6 D).

Sequence analysis

In order to confirm presence of *Eater like* gene in *B. mori*, amplification products were ligated, cloned and sequenced. The nucleotide sequence was analysed by NCBI-BLAST. *Eater like* sequence showed 98 % similarity with *B. mori* uncharacterized transcript variant X2 (Accession No. XM_004928120.3) with an expect value 7e-110. The translated sequence of *Eater like* (3'5' frame 2) showed 97 % similarity with translated amino acid sequence of *Bm* uncharacterized protein (*Bm*UCP) *Bm*UCP LOC101736235 isoform X2 (H9JFY7_BOMMO of Uniprot; BGIBMGA008434 of *B. mori)* revealing existence of *Eater like* sequence in *B. mori* genome (Fig. 7). This sequence showed orthology in the lepidopterans *Heliconius melpomene* and *Danus plexippus* with unknown function (EggNOG 4.5.1). However complete sequencing of the gene has to be performed for gene structure confirmation.

DISCUSSION

In the initial stages of microsporidian infection in *B. mori*, spores were not detected microscopically for six days after infection. In the mid and later stages, exponential increase in spore count was recorded. In insects host responses in hemocytes initiated with activation of cell surface receptors and signal transduction (Lamprou *et al* 2007; Tsakas and Marmaras 2010). Hemocytes recognize pathogens entered in larval body with assistance from recognition proteins. The proteins that recognize *Nosema* sporoplasm / spores have not been identified in *B. mori* though microbial recognition proteins such as peptidoglycan recognition proteins (PGRPs) have role in host responses of honey bees against infection by *N. ceranae* through Toll / IMD pathways (Li *et al* 2017). β-GRP (β-1,3-glucan recognition proteins) are recognition proteins in Toll/ Dif pathway (Gobert *et al* 2003) and are associated with detection of bacterial endotoxin in Drosophila (Kim *et al*. 2000) and phenol oxidase activation in *B. mori* (Yoshida *et al*. 1986) indicating multiple role associated with immune reactions. Following recognition, hemocytes initiated cellular immune events such as cell aggregation, nodulation, cytokine release, melanization and encapsulation depend on size of the pathogen / parasite (Lavine and Strand 2002). Similarly, hemocytes initiate phagocytosis against bacteria and fungi particularly against those with size less than five microns (Pech and Strand 1996; Scapigliati and Mazzini 2009). Notably, *N. bombycis* spores infecting *B. mori* larva are of 2.6 to 3.8 microns (breadth x length) (Rao *et al*. 2007) which could be phagocytosed by hemocytes though mechanism of parasite destruction is not clearly known. Phagocytic uptake of KOH treated- or cold storaged *Nosema* spores is found in insect cell line (Cai *et al*. 2012) however phagocytosis of live *Nosema* spores by larval hemocytes *in vivo* had not been reported in *B. mori***.** After *N. bombycis* infection in *B. mori* larva, TEM observation showed symptoms of phagocytosis in granulocytes such as formation of pseudopodia and appearance of phagosomes with lysosomal bags. Spores and ghost spores were observed within phagosomes of hemocytes indicative of lysosomal activity on spores. Phagosomes enclosing spore / meront were found in granulocytes of *B. mori* as noticed in *A. aegypti* after infection by *Plasmodium gallinaceum* (Hillyer *et al*. 2003) and in the coleopteran *Rhynchophorus ferrugineus* infected with the yeast *Saccharomyces cerevisae* (Manachini *et al*. 2011). In the coleopteran flower chafers *Protaetia brevitarsis seulensis,* development of autophagic vacuoles observed in association with phagocytosis by granulocytes indicative of autophagic elimination of pathogens (Kwon *et al*. 2014). After *N. bombycis* infection, granulocytes showed cytoplasmic projections, pseudopodia, microvilli, membrane porosity and disruption as characteristics of phagocytic cells (Castillo *et al*. 2006; Williams 2007). Moreover granulocytes showed degranulation by exocytosis in spore 'locales' indicating active transportation of structural granules to the plasma membrane and degranulation in the site of infection by the spores as observed in mouse models (Dias *et al*. 2018). Hemocytes with extended pseudopodia, cytoplasmic projections and phagosomes were observed in *Anopheles quadrimaculatus* infected with nematode, *Romanomermis culicivorax* (Shamseldean *et al*. 2006), *Culex quinquefasciatus* infected by *Wuchereria bancrofti* (Brayner *et al*. 2007) and in plasmatocytes of the tick *Rhipicephalus sanguineus* infected with *Leishmania infantum* (Feitosa *et al*. 2015). Stable increase in expression of the cytoskeletal protein gene β- actin with age was noticed in hemocytes of *B. mori* after *N. bombycis* infection indicated continuous requirement of actin to redistribute the cytoskeletal protein during formation of pseudopodia and microvilli after *N. bombycis* infection and to meet rearrangement of cytoskeletal proteins for engulfment (Moore *et al*. 1992; Kwon *et al*. 2014). Variation in actin protein content and its critical role was reported in association with formation of pseudopodia in other models also (May and Machesky 2001; Baranov *et al*. 2016).

LPO and peroxidase activity associated with phagocytosis

Infection with *N. bombycis* increased malondialdehyde production in hemocytes revealed increased lipid

peroxidation (LPO). Lipoprotein structure of the membrane is disrupted by LPO, which caused membrane porosity and disintegration in association with phagocytosis. LPO activity significantly increased with age in early and mid stages of infection however it was higher in later stages of infection. Moreover spore count is increased exponentially after six days of infection and lipid peroxidation increased simultaneously showing correlated increase. During lipid peroxidation, carbon-carbon double bonds present in the polyunsaturated fatty acids of plasma membrane are attacked (Yin *et al*. 2011; Wong-ekkabut *et al*. 2007) which is initiated with oxidation of few lipid molecules and subsequently continued as a chain reaction leading to disintegration of cell membrane (Mylonas and Kouretas 1999; Ayala *et al*. 2014). Though infection induced oxidative stress caused lipid peroxidation (Milei *et al*. 2007; Pooja *et al*. 2017), increment in reactive oxygen species (H_2O_2) was not observed in hemocytes of *B. mori* larva after *N. bombycis* infection indicating a direct effect of LPO on hemocyte membrane integrity probably through accumulated toxic products (Clark *et al* 1987). Similar direct impact of lipid peroxidation on tissue damage was reported in liver of the fish *Pimephales promelas* infested by liver trematode *Ornithodiplostomum* sp (Stumbo *et al*. 2012). Accumulation of LPO toxic products could suppress the phagocytic action of hemocytes which defend parasite survival. A possibility for less H_2O_2 content observed in the infected hemocytes might be due to relatively shorter half life induced by its reactivity with biomolecules (Lennicke *et al*. 2015).

In order to protect the cells from peroxidation, enzymatic antioxidant peroxidases are activated (Brigelius-Flohe and Maiorino 2013; Jablonska *et al*. 2015). Ascorbate peroxidase removed lipid peroxides in the lepidopteran *Helicoverpa zea* (Mathews *et al*. 1997) through ascorbate recycling system (Summers and Felton 1993; Krishnan and Kodrik 2006; Lukasik *et al*. 2009). After *N. bombycis* infection, in hemocytes of *B. mori,* peroxidase activity was significantly higher in early and mid- stages of infection which regulated LPO activity to comparatively lower level. In the later stages of infection, peroxidase activity significantly reduced, in contrast, lipid peroxidation increased significantly indicating negative interaction between lipid peroxidation and ascorbate peroxidase activity, corroborating with the negative relation noticed between LPO and peorxidase activity in humans under diseased conditions (McCay *et al*. 1976; Motghare *et al*. 2001). The peroxidase regulation of LPO in association with phagocytic events is unknown in invertebrates after parasitic infection.

Modulation in gene expression after infection

In order to enhance immune reactions after *N. bombycis* infection, genes encoding proteins associated with humoral and cellular immune response were activated before eliciting the host responses (Brown and Gordon 2003; Manachini *et al*. 2011). Notably β-GRP genes did not show significant variability in expression after infection showing an ambiguity in its role in immune reactions against *N. bombycis* infection. On the other hand CTL genes showed upregulated expression on day 6 after infection and its role was suggested to be in spore recognition and signal trasnsduction (Ma *et al*. 2013). *CTL-11 and 17* implicated in opsonising blastospores of the fungus, *Beauveria bassiana* to make fungal spores susceptible to phagocytosis (Pendland *et al*. 1988). Notably, taxonomic position of *N. bombycis* is shifted from protozoan to fungus (Han and Weiss 2017) based on molecular phylogeny. CTL proteins activated during infection by other fungus could be effective during infection by *N. bombycis* probably due to activation of similar immune mechanisms against different species of fungi. Gene encoding hemocyte adhesive factor humoral lectin (Kotani *et al*. 1995) and the phagocytosis enhancer Apolipoprotein III (Whitten *et al*. 2004) enhanced expression after infection. Apolipophorin III together with I/ II help in pattern recognition as well as enhances phagocytic action of hemocytes in insects (Barabas and Cytryńska 2013; Whitten *et al*. 2004).

In the dipterans *Aedes* and *Drosophila, Thioester containing protein (TEP1)* (Blandin *et al*. 2004) and *Eater* (Kocks *et al*. 2005) respectively are associated with phagocytosis however these genes have not reported from *B. mori*. Though *TEP1* did not show expression, *Eater like* showed heterologous expression in hemocytes of *B. mori* larva on day 2 and 6 after infection. Both nucleotide sequence and translated amino acid sequence of *Eater like* amplicon showed 98% similarity with that of an uncharacterized transcript variant from *B. mori* indicating activation of *Eater like* gene in *B. mori* in association with hemocyte- mediated phagocytosis against *N. bombycis*. In *Drosophila*, Eater is a transmembrane protein involved in binding and internalization of bacteria in the phagosomes (Stuart *et al*. 2005; Kocks *et al*. 2005; Chung and Kocks 2011) however role of Eater like protein in *B. mori* immune responses is unknown.

N. bombycis infection induced subcellular variations in hemocytes of *B. mori* including demorphed nucleus, activation of phagocytosis including formation of pseudopodia, microvilli, porous plasma membrane and formation of phagosomes. In addition, lipid peroxidation was increased in hemocytes with increase in age after

infection. Simultaneous increase in peroxidase reduced the LPO activity. In the later stage, peroxidase activity reduced and LPO activity increased showing negative relation. Moreover infection by *N. bombycis* induced modulation of phagocytosis- associated genes where heterologous expression of *Eater* also observed indicating activation of phagocytic events and associated events against *N. bombycis* infection in *B. mori* larva which are potential novel targets for developing new control measures. The protein- based targets could be used to develop antibody- based mechanisms for early detection of microsporidian infection.

ACKNOWLEDGEMENTS

The authors thank anonymous reviewers for valuable suggestions, Central Silk Board, Bangalore for the facilities and Department of Biotechnology (Government of India), New Delhi for financial support in the form of a research project to ARP (BT/PR6355/PBD/19/236/2012 dated 08/01/2013). SPH and PM were supported by research fellowships from the project.

CONFLICT OF INTEREST

The authors declare no conflict of interest.

REFERENCES

Ayala A, Munoz MF, Arguelles S. 2014. Lipid peroxidation: production, metabolism, and signaling mechanisms of malondialdehyde and 4-hydroxy-2-nonenal. Oxid Med Cell Longev. Article ID 360438; http://dx.doi.org/10.1155/2014/360438

Bajno L, Peng X-R, Schreiber AD, Moore H-P, Trimble WS, Grinstein S. 2000. Focal exocytosis of Vamp3-containing vesicles at sites of phagosome formation. J Cell Biol. 149:697-706.

Baranov MV, Revelo NH, Dingjan I, Maraspini R, Beest M, Honigmann A, Bogaart G. 2016. SWAP70 organizes the actin cytoskeleton and is essential for phagocytosis. Cell Reports 17:1518–1531.

Barillas-Mury C, Wizel B, Han YS. 2000. Mosquito immune responses and malaria transmission: lessons from insect model systems and implications for vertebrate innate immunity and vaccine development. Insect Biochem Mol Biol. 30:429–442.

Blandin S, Shiao SH, Moita LF, Janse CJ, Waters AP, Kafatos FC, Levashina EA. 2004. Complement-like protein TEP1 is a determinant of vectorial capacity in the malaria vector *Anopheles gambiae*. Cell. 116:661–670.

Brayner FA, Araujo HRC, Santos SS, Cavalcanti MGS, Alves LC, Souza JRB, Peixoto CA. 2007. Haemocyte population and ultrastructural changes during the immune response of the mosquito *Culex quinquefasciatus* to microfilariae of *Wuchereria bancrofti*. Med Vet Entomol. 21:112–120.

Brigelius-Flohe R, Maiorino M. 2013. Glutathione peroxidases. Biochim Biophys Acta.1830: 3289–303.

Brown GD, Gordon S. 2003. Fungal β- glucans and mammalian immunity. Immunity. 19:311-315.

Cai S- F, Lu X- M, Qiu H- H, Li M- Q, Feng Z- Z. 2012. Phagocytic uptake of *Nosema bombycis* (Microsporidia) spores by insect cell lines. J Integr Agric. 11:1321-1326.

Castillo JC, Robertson AE, Strand MR. 2006. Characterization of hemocytes from the mosquitoes *Anophles gambiae* and *Aedes aegypti*. Insect Biochem Mol Biol. 36:891-903.

Chung YS, Kocks C. 2011. Recognition of pathogenic microbes by the Drosophila phagocytic pattern recognition receptor eater. J Biol Chem. 286:26524-26532.

Clark IA, Butcher GA, Buffinton GD, Hunt NH, Cowden WB. 1987. Toxicity of certain products of lipid peroxidation to the human malaria parasite *Plasmodium falciparum*. Biochem Pharmacol. 36:543-6.

Dias FF, Amaral KB, Malta KK, Silva TP, Rodrigues GSC *et al* (2018) Identification of piecemeal degranulation and vesicular transport of MBP-1 in liver-infiltrating mouse eosinophils during acute experimental *Schistosoma mansoni* infection. Front. Immunol. 20 https://doi.org/10.3389/fimmu.2018.03019

Fatima MN, Vivek AS, Amreeta D, Uma DP. 2011. Oxidative stress and antioxidant status in primary bone and soft tissue sarcoma. BMC Cancer 11: 382. DOI: 10.1186/1471-2407-11-382.

Faurschou M, Borregaard N. 2003. Neutrophil granules and secretory vesicles in inflammation. Microb Infect. 14:1317–1327.

Feitosa APS, Alves LC, Chaves MM, Veras DL, Silva EM, Alianca ASS, Franca IRS, Goncalves GGA, Lima-Filho JL, Brayner FA. 2015. Hemocytes of *Rhipicephalus sanguineus* (Acari: Ixodidae): Characterization, population abundance, and ultrastructural changes following challenge with *Leishmania infantum*. J Med Entomol 52:1193-1202.

Franzen C. 2005. How do microsporidia invade cells? Folia Parasitol. 52:36-40

Fullard JF, Kale A, Baker NE. 2009. Clearance of apoptotic corpses. J Apoptosis. 14: 1029-1037.

Gerardo NM, Altincicek B, Anselme C, Atamian H, Barribeau SM, de Vos M, Duncan EJ, Evans JD, Gabaldón T, Ghanim M, *et al*. 2010. Immunity and other defenses in pea aphids, *Acyrthosiphon pisum*. Genome Biology 11, R21. doi: 10.1186/gb-2010-11-2-r21.

Gobert V, Gottar M, Matskevich AA, Rutschmann S, Royet J, Belvin M, Hoffmann JA, Ferrandon D. 2003. Dual activation of the *Drosophila* toll pathway by two pattern recognition receptors. Science. 302:2126-30.

Govind S .2008. Innate immunity in *Drosophila*: Pathogens and pathways. Insect Sci. 15: 29–43.

Han B, Weiss LM. 2017. Microsporidia: obligate intracellular pathogens within the fungal kingdom. Microbiol Spectr. 5. doi:10.1128/microbiolspec.FUNK-0018-2016

Hillyer JF, Schmidt SL, Christensen BM. 2003. Hemocyte-mediated phagocytosis and melanization in the mosquito *Armigeres subalbatus* following immune challenge by bacteria. Cell Tissue Res. 313:117–127.

Hodges DM, DeLong JM, Forney CF, Prange RK. 1999. Improving the thiobarbituric acid-reactive-substances assay for estimating lipid peroxidation in plant tissues containing anthocyanin and other interfering compounds. Planta. 207:604–611.

Hoffmann JA. 2003. The immune response of *Drosophila*. Nature 426:33–38.

Hukuhara T. 2017. The epizootiology of pebrine, one of the great scourges of sericulture. J Biochem Biotech 1:1-3.

Jablonska E, Gromadzinska J, Peplonska B, Fendler W, Reszka E, Krol MB, Wieczorek E, Bukowska A, Gresner P, Galicki M, *et al*. 2015. Lipid peroxidation and glutathione peroxidase activity relationship in breast cancer depends on functional polymorphism of GPX1. BMC Cancer. 15:657; DOI 10.1186/s12885-015-1680-4

Juneja P, Lazzaro BP. 2010. Haplotype structure and expression divergence at the *Drosophila* cellular immune gene *eater.* Mol Biol Evol. 27:2284–2299.

Kim YS, Ryu JH, Han SJ, Choi KH, Nam KB, Jang IH, Lemaitre B, Brey PT, Lee WJ. 2000. Gram-negative bacteria-binding protein, a pattern recognition receptor for lipopolysaccharide and beta-1, 3-glucan that mediates the signalling for the induction of innate immune genes in *Drosophila*. J Biol Chem. 275:32721-32727.

Kocks C, Cho JH, Nehme N, Ulvila J, Pearson AM, Meister M, Strom C, Conto SL, Hetru C, Stuart LM, *et al*. 2005. Eater, a Transmembrane protein mediating phagocytosis of bacterial pathogens in *Drosophila.* Cell. 123:335-346.

Kotani E, Yamakawa M, Iwamoto S, Tashiro M, Mori H, Sumida M, Matsubara F, Taniai K, Kadono-Okuda K, Kato Y, Mori M. 1995. Cloning and expression of the gene of hemocytin, an insect humoral lectin which is homologous with the mammalian von Willebrand factor. Biochem Biophys Acta. 1260:245-58.

Krishnan N, Kodrik D. 2006. Antioxidant enzymes in *Spodoptera littoralis* (Boisduval): Are they enhanced to protect gut tissues during oxidative stress? J. Insect Physiol. 52: 11–20.

Kwon H, Bang K, Cho S. 2014. Characterization of the hemocytes in larvae of *Protaetia brevitarsis seulensis*: Involvement of granulocyte- mediated phagocytosis. PLoS ONE. 9: e103620.

Lamprou I, Mamali I, Dallas K, Fertakis V, Lampropoulou M, Marmaras VJ. 2007. Distinct signalling pathways promote phagocytosis of bacteria, latex beads and lipopolysaccharide in medfly hemocytes. Immunology. 121: 314-327.

Lavine MD, Strand MR. 2002. Insect hemocytes and their role in immunity. Insect Biochem Mol Biol. 32: 1295–1309.

Lennicke C, Rahn J, Lichtenfels R, Wessjohann LA, Seliger B. 2015. Hydrogen peroxide – production, fate and role in redox signalling of tumor cells. Cell Commun. Signal. 13:39. DOI 10.1186/s12964-015-0118-6

Li W, Evans JD, Li J, Su S, Hamilton M, Chen Y. 2017. Spore load and immune response of honey bees naturally infected by *Nosema ceranae*. Parasitol Res. 116:3265-3274.

Ling E, Yu Q- X. 2006. Hemocytes from the tobacco hornworm *Manduca sexta*have distinct functions in phagocytosis of foreign particles and self dead cells. Dev Comp Immunol. 30:301-309.

Livak, KJ, Schmittagen TD. (2001) Analysis of relative gene expression data using real time quantitative PCR and the 2–ΔΔ CT method. Methods 25:402–408.

Lowry OH, Rosebrough NJ., Farr AL, Randall RJ. 1951. Protein measurement with the folin-phenol reagent. J. Biol. Chem. 193:265–275.

Lukasik I, Golawska S, Wójcicka A. 2009. Antioxidant defense mechanisms of cereal aphids based on ascorbate and ascorbate peroxidase. Biologia. 64:994-998.

Ma Z, Li C, Pan G, Li Z, Han B, Xu J, Lan X, Chen J, Yang D, Chen Q, Sang Q, Ji X, Li T, Long M, Zhou Z. 2013. Genome-wide transcriptional response of silkworm *(Bombyx mori)* to infection by the microsporidian *Nosema bombycis.* PLoS ONE 8(12): e84137. doi:10.1371/journal.pone.0084137.

Manachini B, Arizza V, Parrinello D, Parrinello N. 2011. Hemocytes of *Rhynchophorus ferrugineus* (Olivier) (Coleoptera: Curculionidae) and their response to *Saccharomyces cerevisiae* and *Bacillus thuringiensis*. J Invertebr Pathol. 106:360-365.

Mathews MC, Summers CB, Felton GW. 1997. Ascorbate peroxidase: A novel antioxidant enzyme in insects. Arch Insect Biochem Physiol. 34:57-68

May RC, Machesky LM. 2001. Phagocytosis and the actin cytoskeleton**.** J Cell Sci. 114:1061-107.

McCay PB, Gibson DD, Fong K-A, Hornbrook KR (1976) Effect of glutathione peroxidase activity on lipid peroxidation in biological membranes. Biochim Biophys Acta - Lipids Lipid Metab. 431:459-468.

Milei J, Forcada P, Fraga CG, Grana DR *et al.* 2007. Relationship between oxidative stress, lipid peroxidation and ultrastructural damage in patients with coronary artery disease undergoing cardioplegic arrest/reperfusion. Cardiovasc Res. 73:710–719.

Moore CA, Beckmann N, Morse MP. 1992. Cytoskeletal structure of diseased and normal hemocytes of *Mya arenaria.* J Invertebr Pathol. 60:141-147.

Motghare KS, Bhutey A, Murrhar BB, Gupta M, Meshram AM, Balsubramanium Y. 2001. Lipid peroxidation and glutathione peroxidase in ischemic heart disease. Indian J Clin Biochem. 16:213–215.

Mylonas C, Kouretas D. 1999. Lipid peroxidation and tissue damage. In Vivo 13:295-309.

Nakano Y, Asada K. 1981. Hydrogen peroxide is scavenged by ascorbate- specific peroxidase in spinach chloroplasts. Plant Cell Physiol. 22:867-880.

Nazario-Toole AE, Wu LP. 2017. Phagocytosis in insect immunity. Adv Insect Physiol. 52:35-82.

Pan G, Xu J, Li T, Xia Q, Liu S-L, Zhang G, Li S, Li C, Liu H, Yang L, *et al.* 2013. Comparative genomics of parasitic silkworm microsporidia reveal an association between genome expansion and host adaptation. BMC Genomics. 14:186.

Pech LL, Strand MR. 1996. Granular cells are required for encapsulation of foreign targets by insect haemocytes. J Cell Sci. 109:2053-2060.

Pendland JC, Heath MA, Boucias DG. 1988. Function of a galactose- binding lectin from *Spodoptera exigua* larval haemolymph: Opsonization of blastospores from entomogenous hyphomycetes. J Insect Physiol. 34:533-540.

Pooja M, Pradeep ANR, Hungund SP, Chandrashekhar S, Kangayam MP, Awasthi AK, Trivedy K. 2017. Oxidative stress and cytotoxicity elicited lipid peroxidation in hemocytes of *Bombyx mori* larva infested with dipteran parasitoid, *Exorista bombycis.* Acta Parasitol. 62:1230-2821

Pradeep AR, Anitha J, Awasthi AK, Babu MA, Murthy NG, Arun HK, Sagar C, Rao GC, Vijayaprakash NB. 2013. Activation of autophagic programmed cell death and innate immune gene expression reveals immuno-competence of integumental epithelium in *Bombyx mori* infected by a dipteran parasitoid. Cell Tissue Res, 352**:**371–385.

Rao SN, Muthulakshmi M, Kanginakudru S, Nagaraju J. 2004. Phylogenetic relationships of three new microsporidian isolates from the silkworm, *Bombyx mori*. J Invertebr Pathol. 86:87-95.

Rao SN, Nath BS, Bhuvaneswari G, Urs SR. 2007. Genetic diversity and phylogenetic relationships among microsporidia infecting the silkworm, *Bombyx mori*, using random amplification of polymorphic DNA: Morphological and ultrastructural characterization. J Invertebr Pathol. 96:193–204.

Rebeiro C, Brehelin M. 2006. Insect haemocytes: What type of cell is that? J Insect Physiol. 52:417-429.

Rosales C. 2011. Phagocytosis, a cellular immune response in insects. Invertebrate Surviv J. 8:109-131.

Scapigliati G, Mazzini M 1994. *In vivo* and *in vitro* phagocytosis by hemocytes of the stick insect *Bacillus rossius*, Boll Zool. 61:115-120.

Shamseldean MM, Platzer EG, Gaugler R. 2006. Ultrastructure of the Immune Responses of *Anopheles quadrimaculatus* to *Romanomermis culicivorax* (Nematoda: Mermithidae) Infection. Nematropica. 36:243-249.

Stuart LM, Stehle T, Hoffmann JA, Reichhart JM, Ferrandon D, Rämet M, Ezekowitz RAB. 2005. Eater, a transmembrane protein mediating phagocytosis of bacterial pathogens in *Drosophila.* Cell. 123:335–346.

Stumbo AD, Goater CP, Hontela A. 2012. Parasite-induced oxidative stress in liver tissue of fathead minnows exposed to trematode cercariae. Parasitology. 139:1666-71.

Summers CB, Felton GW. 1993. Antioxidant role of dehydroascorbic acid reductase in insects. Biochim. Biophys. Acta 1156:235–238.

Tsakas S, Marmaras VJ. 2010. Insect immunity and its signalling: an overview. Invertebrate Surviv J. 7:228-238.

Velikova V, Yordanov I, Edreva A. 2000. Oxidative stress and some antioxidant system in acid rain treated bean plants: protective role of exogenous polyamines. Plant Science 151:59–66.

Whitten MMA, Tew IF, Lee BL, Ratcliffe NA. 2004. A novel role for an insect apolipoprotein (Apolipophorin III) in β-1,3- glucan pattern recognition and cellular encapsulation reactions. J Immunol. 172:2177-2185.

Williams MJ. 2007. Drosophila hemopoiesis and cellular immunity. J Immunol. 178:4711-4716.

Wong-ekkabut J., Xu Z., Wannapong T., Tang I-M., Tieleman D.P.,Monticelli L. 2007. Effect of lipid peroxidation on the properties of lipid bilayers: a molecular dynamics study. Biophysical Journal, 93:4225–4236. DOI: 10.1529/biophysj.107.112565

Yagi K. 1998. Simple assay for the level of total lipid peroxides in serum or plasma. Methods in Molecular Biology 108:101–106. DOI:10.1385/0-89603-472-0:101

Yin H., Xu L., Porter N.A. 2011. Free radical lipid peroxidation: mechanisms and analysis. *Chemical Reviews*, 111:5944–5972. DOI: 10.1021/cr200084z

Yoshida H, Ochiai M, Ashida M. 1986. β- 1,3- glucan receptor and peptidoglycan receptor are present as separate entities within insect pro-phenoloxidase activating system. Biochem Biophys Res Commun. 141:1177-1184.

Caryologia
International Journal of Cytology, Cytosystematics and Cytogenetics

Firenze University Press
www.fupress.com/caryologia

OPEN ACCESS

Citation: P. Mahditabar Bahnamiri, A. Mahmoudi Otaghvari, N. Ahmadian Chashmi, P. Azizi (2020) Electrophoretic study of seed storage proteins in the genus *Hypericum* L. in North of Iran. *Caryologia* 73(1): 107-113. doi: 10.13128/caryologia-122

Received: Januray 9, 2019

Accepted: February 23, 2020

Published: May 8, 2020

Data Availability Statement: All relevant data are within the paper and its Supporting Information files.

Competing Interests: The Author(s) declare(s) no conflict of interest.

Electrophoretic study of seed storage proteins in the genus *Hypericum* L. in North of Iran

Parisa Mahditabar Bahnamiri[1], Arman Mahmoudi Otaghvari[1,*], Najme Ahmadian Chashmi[1], Pirouz Azizi[2]

[1] *Department of Biology, Faculty of Basic Sciences, University of Mazandaran, Babolsar, Iran*
[2] *Department of Soil science, University of Guilan, Rasht, Iran*
*Corresponding author. E-mail: P.mahditabar@gmail.com, botany1347@gmail.com, najme.ahmadian@gmail.com

Abstract. In this research we studied the electrophoretic of seed storage proteins in the genus *Hypericum* L. from Iran. The plant samples were collected from various phytogeographical regions of Iran to study the seed storage proteins. The study was performed to determine the boundary among different species of genus *Hypericum* using sodium dodecyl sulfate polyacrylamide gel electrophoresis (SDS-PAGE). All samples belong to three species of *H. perforatum*, *H. tetrapterum* and *H. androsaemum*. A total of 22 protein bands were observed in the studied species. The results show that *H. perforatum, H. tetrapterum* are closely related based on seed storage proteins. A closely relationship and high protein similarity (J=0.66) were found between *H. perforatum, H. tetrapterum*. Electophoretic results compared with earlier molecular and morphological studies. The highest number of bands was observed in Kordkoy1 population (Pop12) and Gardane heyran population (Pop20) of *H. perforatum* and the lowest in Gorgan/ Naharkhoran population (Pop 25) of *H. androsaemum.* Our results showed the species of *Hypericum* were placed intermixed. The aim of this study to delimit species in the genus *Hypericum* and used these seeds storage protein for the correct identification.

Keywords. *Hypericum*, North of Iran, Species relationships, SDS-PAGE.

INTRODUCTION

The genus *Hypericum* (Guttiferae, Hypericoideae) is perennial, belonging to the Hypericaceae family, having 484 species in forms of trees, shrubs, and herbs, distributed in 36 taxonomic sections (Crockett and Robson 2011). The species of the family are distributed worldwide in the temperate zones but are absent in extreme environmental conditions such as deserts and poles. Iranian species of this genus grow mainly in north, northwest and center of Iran and form floristic elements of Hyrcanian mountainous areas, Irano-Turanian, Mediterranean and Zagros elements. They generally prefer steep slopes of rocky and calcareous cliffs and margin of mountainous forests (Robson 1968; Azadi 1999). Robson (1968) introduced 21 species in the

area covered by Flora Iranica. Robson (1977) and Assadi (1984) reported *H. fursei* N. Robson and *H. dogonbadanicum* Assadi as two endemics of North and South West of Iran. In Flora of Iran, Azadi (1999) identified 19 species, 4 subspecies arranged in 5 sections (comprising *Campylosporus* (Spach) R. Keller, *Hypericum*, *Hirtella* Stef., *Taeniocarpum* Jaub. & Spach. and *Drosanthe* (Spach) Endl.), and two doubtful species including *H. heterophyllum* Vent. and *H. olivieri* (Spach) Boiss.

Hypericum species are generally known locally in Iran with the names "Hofariqun" which Ebn Sina (or Bo Ali Sina) called it (Rechinger, 1986). Plants of the genus *Hypericum* have traditionally been used as medicinal plants in various parts of the world. *Hypericum perforatum* L. is the source to one of the most manufactured and used herbal preparations in recent years, especially as a mild antidepressant, and thus is the most studied *Hypericum* species (Mozaffarian, 1998). According to Brutovska´ *et al*. (2000), *H. perforatum* is probably originated from autopolyploidization of an ancestor closely related to diploid *H. maculatum*. The chemical composition of *H. perforatum* oil has been the subject of many researcher in recent past (Cakir *et al*. 1997; Baser *et al*. 2002; Osinska 2002; Schwob *et al*. 2002; Mockute *et al*. 2003; Smelcerovic *et al*. 2004). The methanolic extract from the aerial parts of *Hypericum* plants typically contain hypericins, hyperforins and phenolic compounds (Osinska 2002).

Proteins and enzymes, characterized as primary gene products, are important parameters in biochemical taxonomy. Storage proteins separated by electrophoretic methods are thought to undergo the process of evolution with relative slowness due to their "non-essential nature" (Margoliash and Fitch 1968), while enzymes are thought to be extremely sensitive to selection pressures in evolution and thus to survival of the organism (McDaniel 1970). Analysis of proteins and isozymes is a tool for supplementing the evidence obtained by comparative morphology, breeding experiments and cytological analysis. Seed protein electrophoresis for the study of phylogenetic relationship in *Capsicum* L. was performed by Panda *et al*. (1986).

Although phenotypic traits are important for diversity studies, they need to be supported by molecular markers to give robust genetic diversity estimates (Esfandani-Bozchaloyi *et al*. 2018a, 2018b, 2018c, 2018d). Genetic diversity studies in *Capsicum* using morphological, cytological and biochemical marker systems (Kaur and Kapoor 2001; Gopinath *et al*. 2006) are also conducted. The data on agronomic, morphological and physiological plant traits are generally used to estimate the magnitude of genetic diversity present in the germplasm. However, such data may not provide an accurate indication of genetic diversity because of environmental influences upon the expression of observed traits and also the time consuming and laborious field evaluation procedures. The introduction of biochemical techniques like Sodium dodecyl sulphate polyacrylamide gel electrophoresis (SDS-PAGE), isozyme markers has been particularly helpful in deducing systematic relationships between groups where morphological and cytological data were not corollary. SDS-PAGE is an economical, simple and extensively used technique for describing the seed protein diversity of crop germplasm (Fufa *et al*. 2005; Iqbal *et al*. 2005). Furthermore, seed proteins, used as genetic markers convey greater precision to measures of genetic diversity because they are the primary products of structural genes (Srivalli *et al*. 1999). Seed protein electrophoresis for the study of phylogenetic relationship in *Capsicum annuum* was performed by Panda *et al*. (1986) and of diploids and tetraploid hybrids of *Capsicum* was initiated by Srivalli *et al*. (1999). There is no report of SDS-PAGE in *Hypericum* species in Iran.

The present study was conducted on the genetic diversity of *Hypericum* genotypes from different locations which will be useful for breeding programmes and also for conservation of germplasm. To use genetic resources adequately, it is necessary to understand the extent and pattern of genetic diversity. Therefore, an attempt with the present investigation was undertaken to evaluate the extent of variability existing in 29 geographical populations belonging to three species of *Hypericum* of North region of Iran through seed protein analysis to provide a scientific basis for future selection and crop improvement program. The objective of this study was to assess the level of seed electrophoretic patterns of *Hypericum* taxa in Iran and used it for the correct taxonomy of the genus.

MATERIAL AND METHODS

Plant Material

Extensive field visits and collections were undertaken during 2016-2017 throughout the north of Iran. In present study 63 plant samples from 29 geographical populations belonging to three species of *Hypericum* in Iran were collected from field: *H. perforatum* L., *H. tetrapterum* Fries. and *H. androsaemum* L. Different references were used for the correct identification of species (Rechinger, 1999 , Azadi, 1999). The details of the voucher specimens and their localities are given in Table 1 and Fig 1. All materials were examined with a stereomicroscope (NIKON-SMZ1) and all voucher specimens

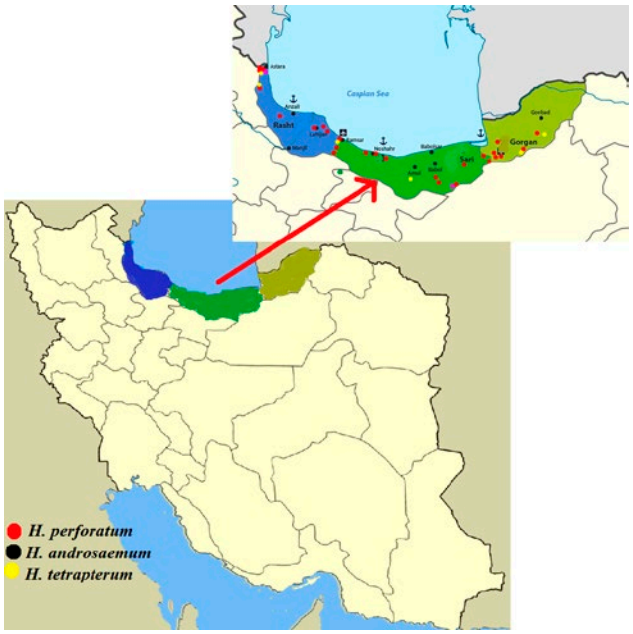

Figure 1. Distribution map of *Hypericum* populations studied.

are deposited at the University of Mazandaran Herbarium (HUMZ).

Protein extraction & Electrophoresis

An amount of 0.1 g of mature seeds were selected from each population and crushed in liquid nitrogen at low temperature. After obtaining a fine powder, proteins were extracted under cool conditions with 3 ml of Tris-Glycin buffer (pH 8). The resulting samples were centrifuged twice for 5 min at 11000 g. The protein electrophoresis was based on Laemmlis procedure (1970), using a discontinuous vertical slab gel. The separating gel comprises 12 ml of 30 % acrylamid

stock solution, 2.5 ml Tris-HCl 1.5 M (pH 8.8), 100 µl SDS 10 %, 2.3 ml water, 7 µl TEMED, and 60 µl APS (Ammonium per Sulfate). After polymerization of the separating gel, the stacking gel with 530 µl of 30 % acrylamide stock solution, l ml Tris 0.5 M (pH 6.8), 40 ml SDS 10 %, 2.37 ml water, 5µl TEMED, and 40 µl APS was polymerized on the separating gel.

The electrophoresis was carried out at a constant voltage of 100V for 7-15h. Gels were stained in Coomasie Brilliant Blue for 1-2 h and overnight distained with acetic acid and methanol (Laemmli 1970).

We used Jaccard similarity coefficient. Standard proteins (b-galactosisase, Ovalbumin, Lactate dehydrogenase, lactoglobulin-b, Lysozyme and Bovine serum albumin) were used to evaluate the molecular weight of the unknown proteins. The protein density was determined by Bradford Protocol(Bradford, 1976).

Protein banding profile analysis

Number and location of each protein band were identified and their RF (relative factor) and molecular weight were estimated. In statistical analysis, each protein band was considered as a qualitative character and coded as 1 (presence) versus 0 (absence). For grouping of the plant specimens,Ward (minimum spherical characters) were used (Podani 2000). PCA (principal components analysis) biplot was used to identify the most variable characters among the studied populations (Podani 2000). PAST version 2.17 (Hammer *et al.* 2012)

RESULTS

A total of 22 protein bands were observed for these taxa. (Fig. 2 and Table 2). All studied taxa had bands 76.12 KD and 45 KD except for Gorgan/Naharkhoran population (Pop 25) of *H. androsaemum*. The highest number of bands was observed in Kordkoy1 population (Pop12) and Gardane heyran population (Pop20) of *H. perforatum* and the lowest in Gorgan/Naharkhoran population (Pop 25) of *H. androsaemum* (Fig. 2 and Table 2).

In order to find out the most variable protein bands in the studied taxa, a Principal Component Analysis was implemented. Primitive analysis showed that three factors were responsible for 62.37 % of total studied variation in the taxa. In the first factor, with almost 37.81 % of the total variation, bands 6.12, 9.87, 34.87, 51.12 KD had the highest correlation. In the second factor, with about 14.63 % of the observed variation, bands 27.37, 30.19, 76.77 and 81.67 KD had the highest positive correlation. In the third factor, with 9.92 % of the total variation, bands 21.54, 78.14, 93.16 KD had the highest correlation.

Both clustering and PCA analyses of the *Hypericum* species studied produced similar groupings and therefore only WARD clustering characters are presented here (Fig. 3). Two major clusters were formed in WARD clustering (Fig.3). WARD clustering, of the studied populations did not entirely delimit the studied species and revealed that plants in these species are intermixed. In WARD dendrogram, a higher degree of intermixture occurred between *H. perforatum*, *H. tetrapterum* and *H. androsaemum*. Also WARD dendrogram revealed that although population of the species *H. perforatum* is more distinct than the other two species, but it showed a high degree of intraspecific genetic variability as they are positioned in different places of the dendrogram.

Table 1. Voucher details of *Hypericum* species examined in this study from Iran.

Population No.	Species	Population cod	Locality / Voucher number
1	*H. perforatum* L.	Hp1	Mazandaran , Ramsar, 1723 HUMZ
2	*H. perforatum* L.	Hp2	Mazandaran , Ramsar/Javaherde1,1724 HUMZ
3	*H. perforatum* L.	Hp3	Mazandaran , Ramsar/Javaherde2/daryache ghoo,1725 HUMZ
4	*H. perforatum* L.	Hp4	Mazandaran , Savadkoh/Alasht,1726 HUMZ
5	*H. perforatum* L.	Hp5	Mazandaran , Babolkenar1,1727 HUMZ
6	*H. perforatum* L.	Hp 6	Mazandaran , Babolkenar2,1728 HUMZ
7	*H. perforatum* L.	Hp 7	Mazandaran , Galogah1,1729 HUMZ
8	*H. perforatum* L.	Hp 8	Mazandaran , Galogah2,1730 HUMZ
9	*H. perforatum* L.	Hp9	Mazandaran , Aliabad katool,1731 HUMZ
10	*H. perforatum* L.	Hp10	Golestan , Gorgan,1732 HUMZ
11	*H. perforatum* L.	Hp 11	Golestan , Ziarat,1733 HUMZ
12	*H. perforatum* L.	Hp 12	Mazandaran ,Kordkoy1,1734 HUMZ
13	*H. perforatum* L.	Hp13	Mazandaran , Kordkoy2,1736 HUMZ
14	*H. perforatum* L.	Hp14	Mazandaran , Kelachay,1737 HUMZ
15	*H. perforatum* L.	Hp15	Guilan , Langrood,1738 HUMZ
16	*H. perforatum* L.	Hp16	Guilan , Lahijan/Bam Lahijan,1739 HUMZ
17	*H. perforatum* L.	Hp17	Guilan , Somesara,1740 HUMZ
18	*H. perforatum* L.	Hp18	Guilan , Asalem,1741 HUMZ
19	*H. perforatum* L.	Hp19	Guilan , Heyran,1742 HUMZ
20	*H. perforatum* L.	Hp20	Guilan , Gardane heyran,1743 HUMZ
21	*H. perforatum* L.	Hp21	Mazandaran , Nowshahr/Sisangan,1744 HUMZ
22	*H. perforatum* L.	Ht22	Guilan , Astara,1745 HUMZ
23	*H. tetrapterum* Fries.	Ht23	Mazandaran , Savadkoh/Alasht,1746 HUMZ
24	*H. tetrapterum* Fries.	Ha24	Guilan , Asalem,1747 HUMZ
25	*H. androsaemum* L.	Ha25	Golestan , Gorgan/Naharkhoran,1748 HUMZ
26	*H .androsaemum* L.	Ha26	Guilan , Astara,1759 HUMZ
27	*H. androsaemum* L.	Ha27	Mazandaran, Ramsar/Bam Ramsar,1750 HUMZ
28	*H. androsaemum* L.	Ha28	Mazandaran , Aliabad Katool/ Kabodval,1751 HUMZ
29	*H. androsaemum* L.	Ha29	Mazandaran , Amol/Sangchal,1752 HUMZ

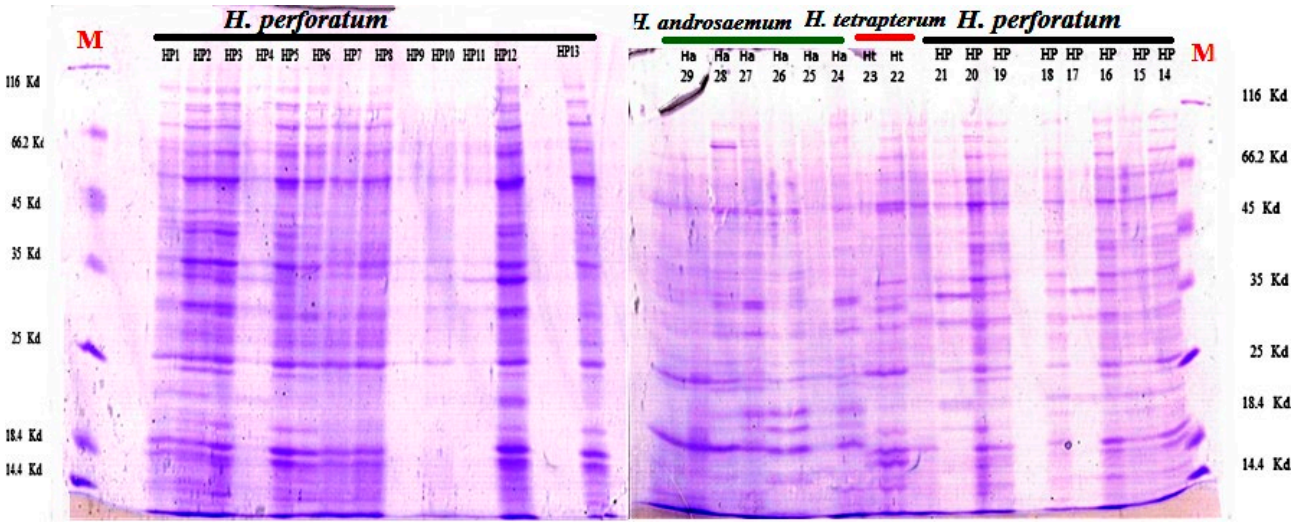

Figure 2. SDS-PAGE electrophoresis profiles of the studied population of *Hypericum*. Note: Populations abbreviations are according to Table 1.

Table 2. Band number and molecular weight for each studied population of *Hypericum*. (1- band is present in the seed sample, 0- band is absent in the seed sample).

Band No	1	2	3	4	5	6	7	8	9	10	11	12	13	14	15	16	17	18	19	20	21	22
MW(kd)	99	95	94	92	85	82	76	68	65	62	59	55	51	45	40	37	34	27	22	18	12	8
Pop																						
1	1	1	1	1	1	1	1	1	1	1	0	1	1	1	1	1	1	0	1	1	1	1
2	1	1	1	1	1	1	1	1	1	1	0	1	1	1	1	1	1	1	1	1	1	1
3	1	1	1	1	1	1	1	1	1	1	0	1	1	1	1	1	1	1	1	1	1	1
4	1	0	0	0	1	1	1	1	1	1	0	0	0	1	1	1	1	0	0	1	1	1
5	1	1	1	1	1	1	1	1	1	1	1	1	1	1	1	1	1	1	0	1	1	1
6	1	1	1	1	1	1	1	1	1	1	1	1	1	1	1	1	1	1	0	1	1	1
7	0	1	1	1	1	1	1	0	0	0	1	1	1	1	1	1	1	0	0	1	1	1
8	1	1	1	1	1	1	1	0	0	0	1	1	1	1	1	1	1	0	0	1	1	1
9	0	1	1	1	1	1	1	0	0	0	0	1	1	1	0	1	1	0	0	1	1	1
10	0	0	0	0	1	1	1	0	0	0	0	1	1	1	0	0	1	0	0	1	0	0
11	1	1	1	0	1	1	1	0	0	0	0	1	1	1	0	0	1	0	0	1	0	0
12	1	1	1	1	1	1	1	1	1	1	1	1	1	1	1	1	1	1	1	1	1	1
13	1	1	0	1	1	1	1	1	1	1	1	1	1	1	1	1	1	1	0	1	1	1
14	1	1	0	1	1	1	1	1	1	1	0	1	1	1	1	1	1	1	1	0	1	1
15	1	1	1	0	1	1	1	1	1	1	0	1	1	1	1	1	1	1	1	1	1	1
16	1	1	1	1	1	1	1	1	1	1	1	1	1	1	1	1	1	1	1	0	1	1
17	0	0	0	0	1	1	1	0	0	0	0	0	1	1	1	0	1	1	1	0	0	0
18	0	0	0	1	1	1	1	1	1	1	0	1	1	1	1	1	1	0	1	1	0	0
19	1	1	1	1	1	1	1	1	1	1	0	1	1	1	1	1	1	1	1	1	1	1
20	1	1	1	1	1	1	1	1	1	1	1	1	1	1	1	1	1	1	1	1	1	1
21	0	0	0	1	1	1	1	1	0	0	0	1	1	1	1	0	1	0	1	1	0	0
22	1	0	1	1	1	1	1	1	0	0	0	1	1	1	1	0	1	0	1	1	1	1
23	0	0	0	1	1	1	1	1	0	0	0	1	1	1	1	0	0	0	0	1	1	1
24	1	1	1	1	1	1	1	0	1	1	0	0	1	1	1	0	0	0	1	1	1	0
25	0	0	0	0	0	0	0	0	0	0	0	0	0	0	0	0	1	0	0	0	0	0
26	0	0	0	0	1	1	1	0	0	0	1	0	1	1	1	0	1	0	1	1	1	0
27	0	1	1	1	0	0	1	0	1	1	1	0	1	1	1	0	1	1	1	1	1	0
28	1	1	1	1	0	0	1	0	1	1	1	0	1	1	1	1	1	1	1	1	1	0
29	0	0	0	1	0	0	1	0	0	0	0	0	0	1	1	0	1	1	0	1	1	0

DISCUSSION

In the present study, 29 geographical populations belonging to three species of *Hypericum* of North region of Iran was examined using sodium dodecyl sulfate polyacrylamide gel electrophoresis (SDS-PAGE). Electrophoretic data of the seed storage proteins presented in this study have shown that the dendrogram obtained from the studied species is not capable of the species recognition. We found findings the seed storage was often incongruent with the result of Faghir, *et al.* (2018) and Mahmoudi Otaghvari & al, (2015) and Bayat & al., (2015) for pollen data.

In previous studies, the micromorphology of pollen grains was performed in several species and their importance in plant taxonomy was emphasized (Faghir, *et al.* 2018; Mahmoudi Otaghvari & al,2015; Bayat & al., 2015).

Faghir, *et al.* (2018) pollen grains of ten species and two subspecies of the genus *Hypericum* in Iran belonging to four sections were studied using light and scanning electron microscopy. Palynological analysis of selected species of the genus *Hypericum* revealed important pollen morphological characters, especially pollen outline, numbers and types of apertures, colpus length; presence and absence of operculum; exine sculpturing type, pore shape, size and arrangements. These traits can be used for infrageneric classification, especially at sectional and species levels (Faghir, *et al.* 2018).

Different techniques including morphological, biochemical and especially molecular markers let scien-

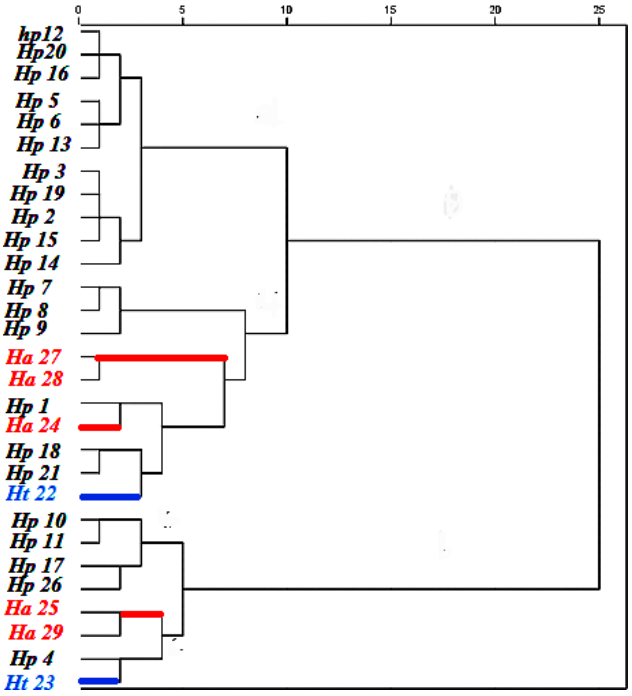

Figure 3. Phenogram by WARD method based on SDS-PAGE electrophoresis characters in *Hypericum* species. Note: Populations abbreviations are according to Table 1.

tists to study genetic variability of plants. As molecular markers present reproducible results regardless of environmental conditions, they have gained nowadays considerable attention for studies relating to the genetic diversity (Farooq and Azam 2002).

According to Morshedloo *et al.* (2015) genetic variability among ten wild populations of *H. perforatum* growing in different climatic regions of Iran via ISSR markers. They observed the studied populations were classified into four main groups which was, to the some extent, in accordance with their geographical origins. Also they recovered, ISSR markers revealed relatively a high level of genetic variability among Iranian *H. perforatum* populations suggesting that the ISSR technique is efficient and powerful for assessment of genetic diversity at the intraspecific level.

The present study also provide the way for use of molecular systematics within genus *Hypericum*. The taxa are not clearly separated on the basis of electrophoretic data of seed storage proteins. The results have revealed that *H. perforatum, H. tetrapterum* were closely related. A high Similarity Index is a reflex of genomic identity (J=0.66). The dendrogram showed close relationship and high protein similarity (J=0.66) between *H. perforatum, H. tetrapterum*. This is the first of its kind report on electrophoretic data of the seed storage proteins of three species of *Hypericum* of North region of Iran.

REFERENCES

Azadi, R. 1999. Guttiferae. In: Assadi, M. (Eds.), Flora of Iran. 27:1–62. R.I.F.R. –Tehran.

Baser KHC, Oze T, Nuriddinov HR, Demirci AB. 2002. Essential oils of two *Hypericum* species from Uzbekistan, Khim. Prir. Soedin. 38:54–57.

Bayat, M., Rahiminejad, M. & Ghaem maghami, L. 2015. The anatomical and palynological study of *Hypericum dogonbadanicum*. Journal of plant researches. 29 (1):15-30.

Bradford MM. 1976. A rapid and sensitive method for the quantitation of microgram quantities of protein utilizing the principle of protein-dye binding. Analytical biochemistry 72(1-2):248–254.

Brutovska´ R, C ˇ ella´rova´ E, Schubert I (2000) Cytogenetic characterization of three Hypericum species by in situ hybridization. Theor Appl Genet 101(1–2):46–50.

Cakir A, Duru ME, Harmandar M, Ciriminna R, Passannanti S, Piozzi F. 1997. Comparison of the volatile oils of *Hypericum scabrum* L. and *Hypericum perforatum* L. from Turkey. Flavour Fragr. J.12: 285–287.

Crockett, S.L., Robson, N.K.B. 2011. Taxonomy and chemotaxonomy of the genus Hypericum. In: MS, O., Cirak, C. (Eds.), Hypericum. Medicinal and Aromatic Plant Science and Biotechnology 5 Special Issue 1:1–13.

Esfandani-Bozchaloyi S, Sheidai M, Keshavarzi M, Noormohammadi Z. 2018a. Species Relationship and Population Structure Analysis In *Geranium* Subg. *Robertium* (Picard) Rouy With The Use of ISSR Molecular Markers. Act Bot Hung 60(1–2):47–65.

Esfandani-Bozchaloyi S, Sheidai M, Keshavarzi M, Noormohammadi Z. 2018b. Species Identification and Population Structure Analysis In *Geranium* Subg. *Geranium* (Geraniaceae). Hacquetia 17(2):235–246. DOI: 10.1515/hacq-2018-0007

Esfandani -Bozchaloyi S, Sheidai M, Keshavarzi M, Noormohammadi Z. 2018c Morphometric and ISSR-analysis of local populations of *Geranium molle* L. from the southern coast of the Caspian Sea. Cytology and genetics 52(4):309–321.

Esfandani-Bozchaloyi S, Sheidai M. 2018d. Molecular diversity and genetic relationships among *Geranium pusillum* and *G. pyrenaicum* with inter simple sequence repeat (ISSR) regions, Caryologia 71(4):1–14. DOI: 10.1080/00087114.2018.1503500

Fufa, H., P.S. Baenziger., B.S. Beecher., I. Dweikat., R.A. Graybosch, K.M. Eskridge. 2005. Comparison of phenotypic and molecular marker based classifications of hard red winter wheat cultivars. Euphytica 145:133–146.

Farooq S, Azam F. 2002 Molecular markers in plant breeding-I: concepts and characterization. Pak J Biol Sci 5(10):1135–1140.

Faghir M.B., M. Razaz, F. Attar, Z. Salehi, M. Vafadar. 2018. Palynological Survey of The Genus *Hypericum* (Hypericaceae) In Iran and Its Taxonomic Importance. Iranian Journal of Botany 24(1):1–15.

Gopinath K, Radhakrishnan NV, Jayaral J. 2006. Effect of propiconazole and difenoconazole on the control of anthracnose of chilli fruit caused by *Colletotricum capsaci*. Crop Prot 25:1024–1031.

Hammer Ø., Harper D., Ryan P.D. 2012. PAST: Paleontological Statistics software package for education and data analysis. Palaeontologia Electronica 4:1–9.

Iqbal S.H., A. Ghafoor, N. Ayub (2005). Relationship between SDS-PAGE markers and *Ascochyta* blight in chickpea. Pakistan Journal of Botany 37:87–96.

Kaur C, Kapoor HC. 2001. Antioxidants in fruits and vegetables – the millennium's health. Int J Food Sci Tech 36:703–725.

Laemmli U.K. 1970. Cleavage of structural proteins during the assembly of the head of bacteriophage T4. Nature 227:680–685.

Mockute D, Bernotiene G, Juzdentiene A. 2003. Volatile compounds of the aerial parts of wild St. John's wort (*Hypericum perforatum* L.) plants, Chemija. 14:108–111.

Margoliash E., Fitch W.M. 1968. Evolutionary variability of cytochrome (primary structures). Ann. NYAcad. Sci. 151:359–381.

Mahmoudi Otaghvari A., Alinattaj Omrani K., Fadaei F. 2015. The pollen morphology study on some species of *Hypericum* L. in the northern Iran. IJBPAS 4(11):957-967.

Morshedloo M, Ebadi A, Fatahi Moghadam M, Yazdani D. 2014. Genetic relationships of Iranian Hypericum perforatum L. wild populations as evaluated by ISSR markers. Plant Syst Evol

Mozaffarian V. 1998. A Dictionary of Iranian Plant Names, Latin, English, Persian. Published By Farhang Mo'aser.

McDaniel R.G. 1970. Electrophoretic characterization of proteins of *Hordeum*. J. Heridity 61:243–247.

Osinska E. 2002. Comparative study on essential oil content and its composition of different ecotypes of St. Johns wort (*Hypericum perforatum* L.). Herbal Pol. 48:174–177.

Panda R.C., Kumar O.A., Rao K.R. 1986. The use of seed protein electrophoresis in the study of phylogenetic relationships in chili pepper (Capsicum L.). Theoretical and Applied Genetics 72(5):665–670.

Podani J. 2000. Introduction to the Exploration of Multivariate Data [English translation]. Leide, Netherlands: Backhuyes.

Rechinger KH. 1986. Flora Iranica. No. 158, pp. 1-44. Pub. By Akademische Druck-u. Verlagsanstalt, Graz.

Rechinger KH. 1999. *Flora iranica, Vol. 175. Papilionaceae IV, Astragalus II*. Akademische Verlagsgesellschaft.

Robson NKB. 1968. *Hypericum* L. In: Rechinger K.H. (Ed), Flora Iranica. 2–20. –Graz.

Robson, N. K. B. 1977: Studies in the genus *Hypericum* L. (Guttiferae): 1. Infrageneric classification. -Bull. Brit. Mus. (Nat. Hist.) Bot. 5: 291–355.

Schwob I, Bessiere JM, Viano J. 2002. Composition of the essential oils of *Hypericum perforatum* L. from southeastern France. C. R. Biologies. 325:781–785.

Shah S.N., Ahmad M., Zafar M., Malik K., Rashid N., Ullah F., Zaman W., Ali M. 2018a. A light and scanning electron microscopic diagnosis of leaf epidermal morphology and its systematic implications in Dryopteridaceae: Investigating 12 Pakistani taxa. Micron 111:36–49.

Smelcerovic A, Mimica-Dukic N, Djordjevic S. 2004. Essential oil composition of *Hypericum perforatum* L. sp. *angustifolium* from South Serbia. J. Essent. Oil. Bear. Plants 7:275–278.

Srivalli T., N. Lakshmi, C.H.G. Gupta (1999). Analysis of seed proteins by polyacylamide gel electrophoresis (PAGE) in diploids, tetraploids and tetraploid hybrids of *Capsicum*. *Capsicum* and Eggplant Newsletter 18:48–51.

Caryologia
International Journal of Cytology, Cytosystematics and Cytogenetics

Firenze University Press
www.fupress.com/caryologia

OPEN ACCESS

Citation: H. Ahmad Ganaie, Md. N. Ali, B.A. Ganai (2020) *Melissa officinalis*: A potent herb against EMS induced mutagenicity in mice. *Caryologia* 73(1): 115-123. doi: 10.13128/caryologia-136

Received: January 9, 2019

Accepted: February 23, 2020

Published: May 8, 2020

Data Availability Statement: All relevant data are within the paper and its Supporting Information files.

Competing Interests: The Author(s) declare(s) no conflict of interest.

Melissa officinalis: A potent herb against EMS induced mutagenicity in mice

Hilal Ahmad Ganaie[1,2,*], Md. Niamat Ali[1], Bashir A Ganai[2]

[1] *Cytogenetics and Molecular Biology Research Laboratory, Centre of Research for Development (CORD), University of Kashmir, Srinagar-190 006, J & K, India*
[2] *Phytochemistry Research Laboratory, Centre of Research for Development (CORD), University of Kashmir, Srinagar-190 006, J & K, India*
*Corresponding author. E-mail: hilalganie@hotmail.com

Abstract. *Melissa officinalis* (L) is used traditionally for different medical purposes such as tonic, antispasmodic, carminative, diaphoretic, surgical dressing for wounds, sedative hypnotic, strengthening the memory and relief of stress induced headache. The methanolic extractof *Melissa officinalis* (Mo-ME) was investigated for antimutagenic activity. The extraction was done by Soxhlet extraction method and the extract was evaluated for antimutagenic assay against EMS induced mice by micronucleus and chromosomal aberration assay. Briefly, mice were treated with methanolic extract of *Melissa officinalis* (Mo-ME) (100, 200 300 & 400 mg/kgbw) for 15 days. Without the doses of EMS, no and mutagenic effects were observed in blood and bone marrow samples of the mice. Micronucleus and chromosomal aberration test revealed the protective effects of Mo-ME when administered at high doses.The reduction profiles in the MN induction of methanolic extract of *Melissa officinalis* at the concentration (100, 200, 300 and 400 mg/kgbw) with EMS were estimated as 14.5%, 28.0%, 47.7% and 81.5% respectively. The methanolic extract of *Melissa officinalis* exhibited no cytotoxic and mutagenic effects but only have antimutagenic effects, an effect that can be attributed the presence of majorital compounds, and the antimutagenic property of Mo-ME is an indication of its medicinal relevance.

Keywords. *Melissa officinalis*, GC-MS, EMS, mice, micronucleus test, chromosomal aberration, antimutagenicity.

INTRODUCTION

Medicinal plants with antioxidant and antimicrobial properties are gaining a lot of attention as these properties are commonly assumed to play an important role in preventing diseases caused by oxidative stress, such as cancer, coronary arteriosclerosis and the ageing processes (Haraguchi *et al.* 2009). Derived forms of medicinal plants (extracts, syrups, etc.) have been the basis of medical therapy for centuries. Traditionally used in the treatment of several human disorders, their pharmacological and therapeutic properties are attributed to various chemical constituents isolated from their crude extracts (Pereira *et al.* 2009, Kwak and Ju, 2015; Liu *et al.* 2015). Notwith-

standing, their correct use requires the manipulation of plants selected for their efficacy and safety, based either on folk tradition or scientific validation (Tovart, 2009). The use of herbal infusions to cure various disorders is very common in folk medicine especially to those who live in upper reaches of Kashmir Himalayas (Dutt *et al*. 2015). Although the diversity of plant species in Kashmir Himalayas is a potential source of biologically active compounds, the effects on human health and genetic material are often unknown. There are indications that the protective action on genetic material can lead, not only to its repair, but also the preservation of its integrity (Berhow *et al*. 2000; Fernandes and Vargas, 2003; Souza *et al*. 2004). Not all are harmless, some even presenting toxic and mutagenic substances in their phytochemical composition (Bresolin and Vargas, 1993; Sa-Ferreira and Vargas, 1999). Interest in such popular usage has recently gained strength, through recent knowledge that chemicals, such as proteases and antioxidants may prevent or reduce the development of cancer by blocking genetic damage (Hernandez-Ceruelos *et al*. 2002).

Melissa officinalis belongs to Lamiaceae family, a large group of medicinal plants. *M. officinalis* is native to southern Europe and northern Africa; although, over the last several centuries it has been successfully cultivated all over the world. Today it can be found growing wildly throughout North America, Europe, Asia, and in the Mediterranean. The leaves of *M. officinalis* have been used in folk medicine especially in Turkey and Iran, for the treatment of some disease (Sadraei *et al*., 2003). Also, the leaves of *M. officinalis* are often used as herbal teas. *M. officinalis* contains some phenolic and flavonoid compounds such as rosmarinic acid (Herodez *et al*., 2003). The phenolic contents in plants have some antioxidant properties (Chen *et al*., 2001). Essential oils and extracts of this plant have been reported to have antiviral (Schnitzler *et al*., 2008), antimicrobial and antioxidant properties (Dastmalchi *et al*., 2008). As little has been done on the antimutagenicity of *Melissa officinalis*, therefore, the purpose of this study was to determine the antimutagenic activities of methanolic extract of *Melissa officinalis*.

MATERIAL AND METHODS

Collection and air drying of plant material

Aerial parts of *M. officinalis* were collected from Bandzoo area of Pulwama from the garden of IIIM, Srinagar and from SKUAST-K in the month July, 2013. The plant was identified at the Centre of Biodiversity and Plant Taxonomy, Department of Botany, University of Kashmir, Srinagar, J&K and a voucher specimen (JKASH/CBT/227 Dated 08. 08. 2014) was deposited there. The parts were allowed to dry under shade (30 °C) for 8-10 days.

Preparation of extracts

After shade drying, the aerial parts were macerated to fine powder, 1 kg of leaves were extracted successively with hexane for defatenning and methanol for 16 h using Soxhlet apparatus. The extracts were filtered through a Buchner funnel using Whatman No. 1 filter paper, and all the extracts were concentrated to dryness under vacuum using a Heidolph rotary evaporator, yielding hexane, and methanol crude extracts of 65 and 48g respectively. All the extracts were stored at 4°C in air tight glass bottles before use.

GC-MS analysis

GC-MS analysis was carried out with GCMS-QP2010 Plus, Shimadzu, Japan fitted with programmable head space auto sampler and auto injector. The capillary column used was DB-1/RTX-MS (30 metre) with helium as a carrier gas, at a flow rate of 3 mL/min with 1 µL injection volume. Samples were analysed with the column held initially at 100°C for 2 min after injection, then increased to 170°C with 10°C/min heating ramp without hold and increased to 215°C with 5°C/min heating ramp for 8 min. Then the final temperature was increased to 240°C with 10°C/min heating ramp for 15 min. The injections were performed in split mode (30: 1) at 250°C. Detector and injector temperatures were 260°C and 250°C, respectively. Pressure was established as 76.2 kPa and the sample was run for 70 min. Temperature and nominal initial flow for flame ionization detector (FID) were set as 230 °C and 3.1 mL/min, correspondingly. MS parameters were as follows: scan range (*m/z*): 40-650 atomic mass units (AMU) under the electron impact (EI) ionization (70 eV). The constituent compounds were determined by comparing their retention times and mass weights with those of authentic samples obtained by GC and as well as the mass spectra from the Wiley libraries and National Institute of Standards and Technology (NIST) database.

Experimental Animals

Both sex of albino mice, Balb/c strain useful for research in cancer and immunology, age of 6 weeks, weighing 25-35 g were obtained from the Indian Institute of Inte-

grative Medicine (IIM), Canal Road Jammu-India, kept in plastic cages in an animal room under controlled conditions of temperature (22 ± 2°C), humidity (55 ± 10%), 12 h light/dark cycles and access to food and water. They were randomized at the beginning of the experiment.The study design was approved by the Institutional Animal Ethical Committee, and the experiments undertaken in accordance with the ethical principles of the CPCSEA norms.

Treatment protocol

The mice were divided into 8 groups, with 5 animals per group. Ethyl methane sulfonate (EMS, SigmaAldrich) was used to induce mutations. Just before use, the EMS was diluted in 0.9% NaCl. The exposure route was by gavage(1/4thof LD_{50} of EMS; 117.5 mg/kgbw). Evaluation of either DNA damage or protection by the methanolic extracts of *Melissa officinalis* was according to protocol developed by Azevedo *et al.* (2003), with the some adaptations. The mice in group 1 received only distilled water (10 mL/kg bw. per day by gavage) for 2 weeks and acted as negative control (Table 1). Mice in group 2 were exposed to EMS (1/4thof LD_{50}) for 24 h and this group acted as positive control. Group 3 and 4 were given different doses (100 & 400 mg/kgbw) of the extract to see the cytotoxic and mutagenic potential of *M. officinalis* and served as positive control of plant extracts. Group 5, 6, 7 and 8 were treated with dose of 100, 200, 300 and 400 mg/kgbw respectively for 15 days after treatment with EMS. The mice were killed by cervical dislocation on 16thday for evaluation of micronucleus and chromosomal aberrations.

The micronucleus test

The method of MacGregor *et al.* (1987) was used for micronucleus test. Mice were sacrificed by cervical dislocation. Slides were prepared with blood collected from the jugular vein. The slides were air-dried, fixed in absolute methanol, stained in 10% Giemsa and then coded for blind analysis. One thousand polychromatic erythrocytes (PCE) were analysed per mouse. The proportion of PCE and normochromatic erythrocytes (NCE) in 1000 erythrocytes/group was calculated, to detect possible cytotoxic effects. The slides were scored blindly, using a light microscope with a 45x and 65x objectives. Photography was done using 100x immersion objective.

Chromosomal aberration

Mice were injected intraperitoneal with 0.5 ml of 0.06% colchicine and two hours later, were sacrificed by cervical dislocation. Both the femurs were fleshed out from the muscles and kept in HBSS (Hank's balanced salt solution). The femurs were then rinsed with 3 ml 0.056% KCl solution in a centrifuge tube. The tube was then incubated at 37°C for 20 minutes. After incubation, centrifugation at 800 rpm for 4 minutes was carried out. Supernatant was discarded and fresh Carnoy's fixative was added (3:1 methanol: acetic acid). The process of centrifugation was repeated three times. Then slides were prepared, stained with 4% Giemsa, air dried and studied under compound microscope.

Statistical analysis

Variable normality was assessed using the Kolmogorov-Smirnov test. Micronucleus testing and chromosomal aberration involved multiple pair-wise comparison between experimental groups and positive and negative controls, with the Mann Whitney U test at a significance level of <0.05. Lower the Mann Whitney statistic value and Z score value, higher the difference.

Table 1. Grouping, dose (distilled water, EMS and Ab-ME in concentrations of 100, 200, 300 and 400 mg/kg bw) and duration of experiment.

Group	Dose	Purpose of group	Duration
Group 1	Distilled water	Negative control	15 days
Group 2	1/4th LD_{50} EMS	Positive control EMS	24 h
Group 3	Mo-ME 100 mg/kg bw	Positive control *Melissa officinalis*	24 h
Group 4	Mo-ME 400 mg/kg bw	Positive control *Melissa officinalis*	24 h
Group 5	Mo-ME 100 mg/kg bw + EMS	Treated Group	15 days
Group 6	Mo-ME 200 mg/kg bw + EMS	Treated Group	15 days
Group 7	Mo-ME 300 mg/kg bw + EMS	Treated Group	15 days
Group 8	Mo-ME 400 mg/kg bw + EMS	Treated Group	15 days

Mo-ME = Methanolic extract of *Melissa officinalis.*

RESULTS

GC-MS analysis

In order to find out the phytocomponents of *Melissa officinalis,* the methanolic extract was subjected to GC-MS analysis. The active principals present in the methanolic fraction of *Melissa officinalis* along with their retention time (RT), molecular formula, molecular weight (MW) and peak area (%) are presented in Table 2. The chromatograms of methanolic extract of *Melissa officinalis* (Mo-ME) showed three major peaks (Fig. 1): 2, 3-dihydro-3, 5-dihydroxy-6-methyl-4H-pyran-4-one (51.62%), 5-(hydroxymethyl)-2-furan carboxaldehyde (29.46%), hexadecanoic acid, methyl ester (8.24%), constituting 89.32% of the total peak area. The minor fractions of Mo-ME include octadecanoic acid (3.26%), stigmast-5-en-3-ol (1.44%), tetradecanoic acid (1.43%), 2, 4- cresotaldehyde (1.17), comprising 7.30% of the total peak area. The phytoconstituents identified in the methanolic fraction of *Melissa officinalis* along with their retention time (RT), molecular formula, molecular weight (MW) and peak area (%) are presented in Table 3.6.

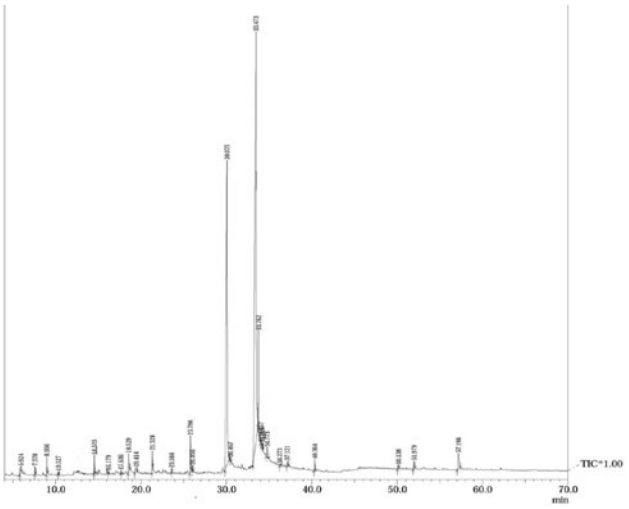

Figure 1. GC-MS chromatogram of methanolic extract of *Melissa officinalis.*

Micronucleus test

According to MN testing of mouse blood cells the low frequencies of micronucleated cells presumes the too little effects of methanolic extract of *Melissa officinalis* (Mo-ME) 100 and 400mg/kg (Table 3, Fig. 2), thereby indicating the virtual absence of mutagenic or cytotoxic effects. In other words, no statistically significant difference in the frequency of MN polychromatic erythrocytes (PCE) or the ratio of PCE to normochromatic erythrocytes (NCE), between the negative control and the groups that ingested extracts could be detected. When evaluating antimutagenicity inMo-ME, a significant decrease in the frequency of EMS-induced MNPCE was observed only in mice that had received 100, 200, 300 and 400 mg/kg ofMo-ME (p = 0.05 –Mann Whitney U test). In the present study, the methanolic extract of *M. officinalis* showed antimutagenic activities by reducing the % age of micronuclei with increase in the dose of the extract (Fig. 3).

Table 2. Phytocomponents identified in the methanolic extract of *Melissa officinalis* (Mo-ME) by GC-MS.

S. No.	Compound	RT	% Area	MF	MW
1	2,4-Cresotaldehyde	18.52	1.17	$C_8H_8O_2$	136
2	D-allose	19.41	0.56	$C_6H_{12}O_6$	180
3	Dodecanoic acid	21.32	0.58	$C_{12}H_{24}O_2$	200
4	Tetradecanoic acid	25.79	1.43	$C_{14}H_{28}O_2$	228
5	2,6,10-Trimethyl,14-ethylene-14-pentadecne	27.37	0.49	$C_{20}H_{38}$	278
6	Hexadecanoic acid, methyl ester	29.13	8.24	$C_{38}H_{68}O_8$	652
7	5- (hydroxymethyl)-2-furan carboxaldehyde	30.07	29.46	$C_6H_6O_3$	126
8	2, 3-dihydro-3, 5-dihydroxy-6-methyl-4H-pyran-4-one	33.47	51.62	$C_6H_8O_4$	144
9	Octadecanoic acid	33.76	3.26	$C_{18}H_{36}O_2$	284
10	Malonic acid, 3-hexyl tridecyl ester	34.05	0.38	$C_{22}H_{42}O_4$	370
11	9-Octadecenoic acid	34.22	0.12	$C_{18}H_{34}O_2$	282
12	9,12-Octadecadienoic acid	34.77	0.50	$C_{18}H_{32}O_2$	280
13	1,2-Benzenedicarboxylic acid	40.36	0.34	$C_{24}H_{38}O_4$	390
14	Tochopherol	51.97	0.41	$C_{29}H_{50}O_2$	430
15	Stigmast-5-en-3-ol	57.19	1.44	$C_{29}H_{50}O$	414

Table 3. Frequency profile of micronuclei induced alone by ethyl methanesulphonate and *Melissa officinalis* methanolic extract and their simultaneous exposure for different doses to evaluate antimutagenicity in *Mus musculus*.

	Treatment	Total No. of cells analysed per mice	No. of cells with micronuclei	% age of MN	% Reduction
Group 1	Negative Control (Distilled water)	1000	2.35 ± 0.12	-	-
Group 2	Positive control (EMS)	1000	7.23 ± 0.89	-	-
Group 3	Mo- ME 100 mg/kgbw	1000	2.28 ± 0.10	-	-
Group 4	Mo- ME 400 mg/kgbw	1000	2.27 ± 0.09	-	-
Group 5	Mo- ME 100 mg/kg + EMS	1000	6.52 ± 0.70	90.1	14.5
Group 6	Mo-ME 200 mg/kg + EMS	1000	5.86 ± 0.58	81.0	28.0*
Group 7	Mo-ME 300 mg/kg + EMS	1000	4.90 ± 0.50	67.7	47.7**
Group 8	Mo-ME 400 mg/kg + EMS	1000	3.25 ± 0.43	44.9	81.5***

NC: Negative control (distilled water), PC: Positive control [Ethyl methane sulfonate (EMS) 117.5 mg/kgbw; dose is 1/4th LD_{50}], Mo-ME: *Melissa officinalis* Methanolic Extract. Values with different asterisks ($^{*}p < 0.05$: significant, $^{**}p < 0.01$: highly significant, $^{***}p < 0.001$: extremely significant) differ significantly from the positive control (Mann-Whitney U test).

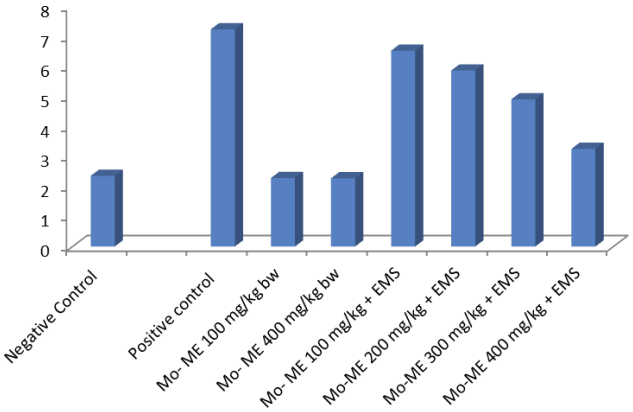

Figure 2. Graph showing number of micronucleated cells in different groups of mice treated with EMS alone, EMS + Mo-ME and Mo-ME alone in different concentrations.

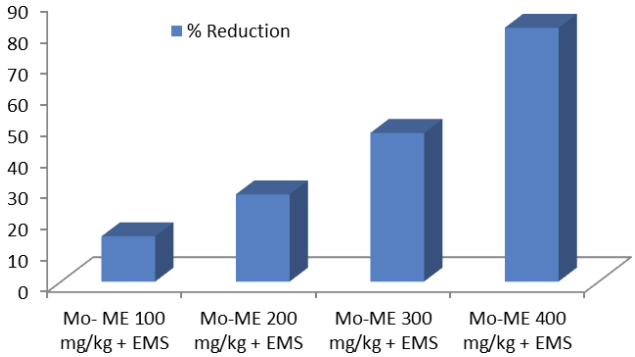

Figure 3. Bar diagram showing percentage reduction in EMS treated micronuclei with increase in concentration of Melissa officinalis methanolic extract (Mo-ME).

Chromosomal aberrations

The chromosomal aberrations induced by ethyl methanesulphonate (EMS 117.5 mg / kg body weight; positive control) were significant ($p<0.05$) to that of the control group. The frequency of breaks per cell in the EMS treated group at 24 h was 0.12 ± 0.010, which was significantly higher when compared to that of total number of breaks per cell in the control group (0.014 ± 0.002) ($p<0.05$). Our results also showed that in the Mo-ME and EMS combined treatment group, the frequency of chromosomal aberrations was significantly lower in comparison to those observed for the EMS only treated group at 24 h. The methanolic extract of *Melissa officinalis* reduced the chromosomal aberrations by 38.1%, 60.1%, 74.5% and 91.5% at 100, 200, 300 and 400 mg/kgbw (Table 4, Fig. 4). The chromosomal aberrations induced by EMS are mainly chromatid breaks, exchanges, gaps, fragments and rings (Fig. 5).

DISCUSSION

From ancient times, medicinal plants are being used as remedies for various diseases in human. In today's industrialized society, the use of medicinal plants has been traced to the extraction and development of several drugs as they were used traditionally in folk medicine (Shrikumar and Ravi, 2007). Medicinal plants have potent phytoconstituents which are important source of compounds and are responsible for the therapeutic properties (Jeeva *et al*., 2011; Florence *et al*., 2014; Sumathi*et al*., 2014, Ganaie *et al*, 2016; 2017). These phytoconstituents endow them with medicinal properties. Many plants possess antioxidant properties because of the presence of phenolic compounds (Brown and Rice-

Table 4. Frequency profile of chromosomal aberrations induced by ethyl methanesulphonate and *Melissa officinalis* methanolic extract separately and by their combination for different doses to evaluate the antimutagenicity in *Mus musculus*.

Treatments		Chromosomal Aberrations							
Concentration (mg/kgbw)	No. of cells	Rings	Fragments	Exchange	Breaks	Gaps	Total Aberrations	%age of Aberrations	% Reduction
Distilled water	500	1	3	-	7	-	11	2.2	-
EMS 117.5 mg/kgbw	500	4	18	14	62	31	129	25.8	-
Mo-ME Alone100 mg/kgbw	500	1	3	-	7	-	11	2.2	-
Mo-ME Alone400 mg/kgbw	500	1	3	-	6	-	10	2.0	-
Mo-ME 100 mg/kgbw + EMS	500	3	13	10	44	14	84	16.8	38.1*
A-ME 200 mg/kgbw + EMS	500	2	9	7	32	8	58	11.6	60.1*
Mo-ME 300 mg/kgbw + EMS	500	1	7	5	22	6	41	8.2	74.5**
Mo-ME 400 mg/kgbw + EMS	500	-	4	3	10	4	21	4.2	91.5***

NC: Negative control (distilled water), PC: Positive control [Ethyl methane sulfonate (EMS) 117.5 mg/kgbw; dose is $1/4^{th}$ LD_{50}], Mo-ME: *Melissa officinalis* Methanolic Extract. Values with different asterisks ($^{*}p < 0.05$: significant, $^{**}p < 0.01$: highly significant, $^{***}p < 0.001$: extremely significant) differ significantly from the positive control (Mann-Whitney U test).

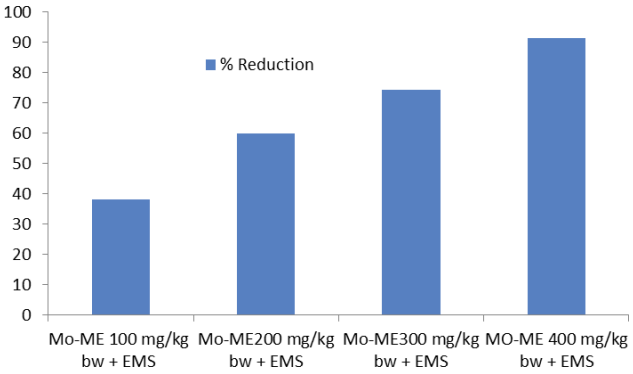

Figure 4. Bar diagram showing percentage reduction in chromosomal aberrations (CA) induced by EMS following post-treatment with methanolic extract of *Melissa officinalis* (Mo-ME).

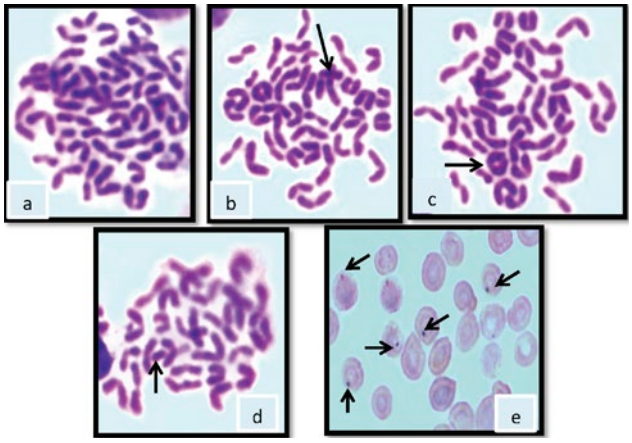

Figure 5. Photomicrograph showing metaphase chromosome preparation from bone marrow. a) Normal set of chromosomes, b) Exchanges (arrow), c) Ring (arrow), d) Fragment (arrow), e) Micronuclei (arrow).

Evans, 1998; Krings and Berger, 2001). These phenolic compounds possess biological properties such as anti-apoptosis, anti-aging, anti-carcinogen, anti-inflammation, anti-atherosclerosis, cardiovascular protection and improvement of endothelial function, as well as inhibition of angiogenesis and cell proliferation activities (Han *et al*., 2007). Tannins bind to proline rich protein and interfere with protein synthesis. Flavonoids are hydroxylated phenolic substances known to be synthesized by plants in response to microbial infection and they have been found to be antimicrobial substances against wide array of microorganisms *in vitro*. The activity is probably due to their ability to complex with extracellular and soluble proteins and to complex with bacterial cell wall (Marjorie, 1999). They are also effective antioxidant and show strong anticancer activities (Salah *et al*., 1995; Del-Rio *et al*., 1997).

Previous reports show that the essential oil of *M. officinalis* is composed of some important compounds like (E)-caryophyllene and caryophyllene oxide in addition to major constituents such as citronellal, neral and geranial (Sorensen, 2000; van de Berg *et al*., 1997). Literature reveals that the essential oil of *M. officinalis* subsp. *officinalis* contains significant amounts of citral and/or citronellal, whereas *M. officinalis* subsp. *altissima* contains only traces (van de Berg *et al*., 1997). Van de Berg *et al*. (1997) identified b-caryophyllene, germacrene-D, sabinene, and b-pinene as the main components in leaf oils of *M. officinalis* subsp. *altissima*.

Marnewick *et al*. (2000) found that the aqueous extracts of fermented and unfermented rooibos tea

(*Aspalathus linearis*) and honey-bush tea (*Cyclopia intermedia*) possess antimutagenic activity against 2-acetylaminofluorine and aflatoxin B_1. Vitamin C and E also significantly reduced the CA frequency in mouse bone marrow cells against rifampicin, an anti-tuberculosis drug, (Aly and Donia, 2002).

According to Kaur *et al*. (2010), the phytoconstituents from *Terminalia arjuna* suppressed the mutagenic effect of the aromatic amine, i.e., 2-aminofluorene (2-AF). The observed activity caused the inhibition of the metabolic activation of pro-mutagens. Hong *et al*. (2011) found that the extracts of *Acanthopanax divaricatus* were able to rapidly eliminate the mutagenic compounds from the cells before they induce the DNA damage. In a similar study, Nardemir *et al*. (2015) observed that the methanol extracts of the lichens have antimutagenic effects against sodium azide.In another study, Prakash *et al*. (2014) found that the different extracts of *Dioscorea pentaphylla* significantly inhibited the effects of methyl methanesulphonate (MMS) induced mutagenicity. They also found that the methanolic extract was highly mutagenic in comparison to Petroleum ether and chloroform. Entezari *et al*. (2014) compared the antimutagenic and anticancer activities of *Echinophora platyloba* DC on acute promyelocytic leukemia cancer cells and found that the methanolic extract of this plant prevented the reverted mutations and the hindrance was 93.4% in antimutagenic test. Akinboro *et al*. (2014) utilised the leaves of *Myristica fragrans* (Houtt.) for antimutagenic activity against benzo[a]pyrene and cyclophosphamide induced mutagenicity in *Salmonella typhimurium* and *Mus musculus* and found that the aqueous extract significantly suppressed more than 50 % of the mutations in all the tested concentrations. Sarac, (2015) utilised an edible wild plant, *Tragopogon longirostis* for the evaluation of antioxidant, mutagenic and antimutagenic properties and found that the ethanolic extract of its leaves exhibited antimutagenic properties at 2.5, 0.25, and 0.025 mg/plate concentrations. Habibi *et al*. (2014) found that the ethanolic extract of *Origanum vulgare* reduced the frequency of MN PCR from 10.52 ± 1.07 for CP to 2.17 ± 0.6 for the synergic test of CP and the ethanolic extract.

CONCLUSION

Based on the above results it can be concluded that the methanolic extractof *Melissa officinalis* possess some important phytoconstituents which possess antimutagenic activity.

The results of the present study clearly showed that the methanolic extract of *Melissa officinalis* had an antimutagenic and anticlastogenic potential against the mutagenic activity of ethyl methane sulphonate in mice. Our results suggest that there may be several ways through which *M. officinalis* extract can work against EMS. Selection of *M. officinalis* for the present study on the basis of its folklore usage seems to be justified as it is scientifically proved to have much potentiality. The extracts from such plants could be seen as a good source of useful drugs.However, further studies are needed in other test systems so that in the future *M. officinalis* can be used in reducing the occurrence of cancers or even as a coadjuvant to chemotherapy to reduce its side effects.

ACKNOWLEDGEMENTS

The authorsare highly thankful to the Director, Centre of Research for Development, University of Kashmir for providing the necessary facilities for the smooth research and also to Curator, Centre of Biodiversity and Plant Taxonomy, Department of Botany, University of Kashmir, Srinagar, J & K in proper identification of the plant.

REFERENCES

Akinboro A, Bin Mohamed K, Asmawi MZ, YekeenTA. 2014. Antimutagenic effects of aqueous fraction of *Myristica fragrans* (Houtt.) leaves on *Salmonella typhimurium* and *Mus musculus*. Acta Biochim Pol. 61(4): 779-785.

Aly FA, Donya SM. 2002. *In vivo* antimutagenic effect of vitamins C and E against rifampicin-induced chromosome aberrations in mouse bone-marrow cells. Mutation Research/Genetic Toxicology and Environmental Mutagenesis. 518(1): 1-7.

Azevedo L, Gomes JC, Stringheta PC, Gontijo AMMC, Padovani CR, Ribeiro LR, Salvadori DMF. 2003. Black bean (*Phaseolus vulgaris* L.) as a protective agent against DNA damage in mice. Food Chem Toxicol. 41: 1671-1676.

Berhow M, Wagner E, Vaughn S, Plewa M, 2000. Characterization and antimutagenic activity of *soybean saponins*. Mutat Res. 448: 11-22.

Bresolin S, Vargas VMF. 1993. Mutagenic potencies of medicinal plants screened in the Ames test. Phytother Res. 7: 260-262.

Brown JE, Rice-Evans CA (1998). Luteolin-rich artichoke extract protects low density lipoprotein from oxidation *in vitro*. Free Radical Research. 29(3): 247-255.

Chen H, Zuo Y, Deng Y. 2001. Separation and determination of flavonoids and other phenolic compounds in cranberry juice by high performance liquid chromatography. J. Chromatogr. A., 913: 387- 395

Dastmalchi K, Dorman HD, Oinonen PP, Darwis Y, Laakso I, Hiltunen R. 2008. Chemical composition and *in vitro* antioxidative activity of a lemon balm (*Melissa officinalis* L.) extract. LWT-Food Science and Technology, 41(3): 391-400.

Del-Rio A, Obdululio BG, Casfillo J, Main FG, Ortuno A. 1997.Uses and properties of citrus flavonoids. J. Agric. Food Chem. 45: 4505-4515.

Dutt HC, Bhagat N, Pandita S. 2015. Oral traditional knowledge on medicinal plants in jeopardy among Gaddi shepherds in hills of northwestern Himalaya, J&K, India. J Ethnopharmacol. 168: 337-348.

Entezari M, Dabaghian FH, Hashemi M. 2014.The comparison of antimutagenicity and anticancer activities of *Echinophora platyloba* DC on acute promyelocytic leukemia cancer cells. Journal of Cancer Research and Therapeutics. 10(4): 1004-1007.

Fernandes JBF, Vargas VMF. 2003. Mutagenic and antimutagenic potential of the medicinal plants *M. laevigata* and *C. xanthocarpa*. Phytother Res. 17: 269-273.

Florence AR, Joselin J, Brintha TSS, Sukumaran S, Jeeva S. 2014.Preliminary phytochemical studies of select members of the family Annonaceae for bioactive constituents. Bioscience Discovery. 5(1): 85-96.

Ganaie HA, Ali MN, Ganai BA, Kaur J, Ahmad M. 2016. GC-MS Analysis and evaluation of mutagenic and antimutagenic activity of ethyl acetate extract of *Ajuga bracteosa* Wall ex. Benth: An endemic medicinal plant of Kashmir Himalaya. Indian J. Clin Toxicol. 6: 288.

Ganaie HA, Ali MN, Ganai BA, Meraj M, Ahmad M. 2017. Antibacterial activity of 14, 15-dihydroajugapitin and 8-oacetylharpagide isolated from *Ajuga bracteosa* Wall ex. Benth against human pathogenic bacteria. Microbial Pathogenesis. 103: 114-118.

Habibi E, Shokrzadeh M, Ahmadi A, Chabra A, Naghshvar F, Keshavarz-Maleki R. 2014. Genoprotective effects of *Origanum vulgare* ethanolic extract against cyclophosphamide-induced genotoxicity in mouse bone marrow cells. Pharmaceutical Biology. 53(1): 92-97.

Han X, Shen T, Lou H. 2007. Dietry polyphenols and their biological significance. Int. J. Mol. Sci. 950-988.

Haraguchi FK, Pedrosa ML, de Paula H, dos Santos RC, Silva ME. 2009. Influência das proteínas do sorosobreenzimashapáticas, perfillipídico e formaçãoóssea de ratoshipercolesterolêmicos. Rev Nutr. 22: 517–525.

Hernandez-Ceruelos A, Madrigal-Bujaidadar E, De La Cruz C. 2002. Inhibitory effect of chamomile essential oil on the sister chromatid exchanges by daunorubicin and methyl methanesulfonate in mouse bone marrow. Toxicol Lett. 135: 103-110.

Herodez SS, Hadolin M, Skerget M, Knez Z. 2003. Solvent extraction study of antioxidants from Balm (*Melissa officinalis* L.) leaves. Food Chem. 80: 275-282.

Hong CE, Cho MC, Jang HA, Lyu SY. 2011. Mutagenicity and anti-mutagenicity of *Acanthopanax divaricatus* var. albeofructus. The Journal of Toxicological Sciences 36(5): 661-668.

Jeeva S, Johnson M, Aparna JS, Irudayaraj V. 2011. Preliminary phytochemical and antibacterial studies on flowers of selected medicinal plants.International Journal of Medicinal and Aromatic Plants 1(2): 107-114.

Kaur H, Kalotra R, Walia GK, Handa D. 2013. Genotoxic effects of dyeing industry effluent on a freshwater fish, *Cirrhinus mrigala* by chromosomal aberration test. International Journal of Pharmacy and Biological Sciences 3: 423-431.

Krings U, Berger RG. 2001. Antioxidant activity of roasted foods. Food Chem. 72: 23-229.

Kwak Y, Ju J. 2015. Inhibitory activities of *Perilla frutescens* britton leaf extract against the growth, migration, and adhesion of human cancer cells. Nutr. Res. Pract. 9: 11–16.

Liu HX, He MT, Tan HB, Gu W, Yang SX, Wang YH, Li L, Long CL. 2015. Xanthine oxidase inhibitors isolated from Piper nudibaccatum. Phytochem. Lett. 12: 133–137.

Marjorie MC. 1999. Plant products as antimicrobial agents. Clinical Microbiology Review 12(4): 564-582.

Marnewick JL, Gelderblom WC, Joubert E. 2000. An investigation on the antimutagenic properties of South African herbal teas. Mutation Research/ Genetic Toxicology and Environmental Mutagenesis 471(1): 157-166.

Nardemir G, Yanmis D, Alpsoy L, Gulluce M, Agar G, Aslan A. 2015. Genotoxic, antigenotoxic and antioxidant properties of methanol extracts obtained from *Peltigera horizontalis* and *Peltigera praetextata*. Toxicology and Industrial Health 31(7): 602-613.

Pereira RP, Fachineto R, Prestes AS, Puntel RL, Boschetti TK, Athayde ML, Büerguer ME, Morel AF, Morsch VM, Rocha JBT. 2009. Antioxidant effects of different extracts from *Melissa officinalis, Matricaria recutita* and *Cymbopogon citratus*. Neurochem Res. 34: 973-983.

Prakash G, Hosetti BB, Dhananjaya BL. 2014. Antimutagenic effect of *Dioscorea pentaphylla* on genotoxic effect induced by methyl methanesulfonate in the

drosophila wing spot test. Toxicology International. 21(3): 258-263.

Sadraei H, Ghannadi A, Malekshahi K. 2003. Relaxant effect of essential oil of *Melissa officinalis* and citral on rat ileum contractions. Fitoterapia 74: 445- 52.

Salah N, Miller NJ, Pagange G, Tijburg L, Bolwell GP, Rice E, Evans C. 1995. Polyphenolic flavonoids as scavenger of aqueous phase radicals as chai breaking antioxidant. Arc. Biochem. Broph. 2: 339-346.

Sarac N. 2015. Antioxidant, mutagenic, and antimutagenic activities of *Tragopogon longirostis* var. longirostis, an edible wild plant in Turkey. Indian Journal of Pharmacology 47(4): 414-418.

Schnitzler P, Schuhmacher A, Astani A, Reichling J. 2008. *Melissa officinalis* oil affects infectivity of enveloped herpesviruses. Phytomed. 15(9): 734-740.

Shrikumar S, Ravi TK. 2007.Approaches towards development and promotion of herbal drugs. Pharmacognosy Reviews 1(1): 180-184.

Sorensen JM. 2000. *Melissa officinalis*, essential oil authenticity, production and pharmacological activity. International Journal of Aromatherapy 10(1): 7-15.

Souza AC, Alviano DS, Alves PB, Alviano CS, Gattass CR. 2004. *Melissa officinalis* L. essential oil: Antitumoral and antioxidant activities. J Pharm Pharmacol. 56: 677-681.

Sumathi BM, Uthayakumari F. 2014. GC MS analysis of Leaves of *Jatropha maheswarii* Subram & Nayar. Science Research Reporter 4(1): 24-30.

Tovart RT. 2009. Clinical approach to clinical herbal toxicity. Sem Diagn Pathol. 26: 28-37.

Van den Berg T, Freundl E, Czygan FC. 1997. *Melissa officinalis* subsp. altissima: characteristics of a possible adulteration of lemon balm. Pharmazie 52(10): 802-808.

Caryologia
International Journal of Cytology, Cytosystematics and Cytogenetics

Firenze University Press
www.fupress.com/caryologia

OPEN ACCESS

Citation: R. Partovi, A. Iaranbakhsh, M. Sheidai, M. Ebadi (2020) Population genetic studies in wild olive (*Olea cuspidata*) by molecular barcodes and SRAP molecular markers. *Caryologia* 73(1): 125-132. doi: 10.13128/caryologia-147

Received: January 9, 2019

Accepted: February 23, 2020

Published: May 8, 2020

Data Availability Statement: All relevant data are within the paper and its Supporting Information files.

Competing Interests: The Author(s) declare(s) no conflict of interest.

Population genetic studies in wild olive (*Olea cuspidata*) by molecular barcodes and SRAP molecular markers

Rayan Partovi[1], Alireza Iranbakhsh[1,*], Masoud Sheidai[2], Mostafa Ebadi[3]

[1] *Department of Biology, Science and Research Branch, Islamic Azad University, Tehran, Iran*
[2] *Faculty of Life Sciences & Biotechnology, Shahid Beheshti University, Tehran, Iran*
[3] *Department of Biology, Islamic Azad University, Damghan Branch, Damghan, Semnan Province, Iran*
*Correspondign author. E-mail: iranbakhsh@iau.ac.ir

Abstract. Olive is an important horticultural plant having both cultivated and wild forms. The aim of the present study was investigating genetic diversity of 13 wild olive trees belonging four geographical populations in IRAN using SRAP neutral molecular markers as well as cp-DNA rpl intergenic sequences and ITS region. Genetic diversity parameters determined for 76 SRAP loci within the studied olive populations identified the most variable loci. Population differentiation parameters determined for SRAP loci, identified 13 SRAP loci with Gst value of 1, that means they differentiate the studied trees. PCoA analysis based on SRAP data separated olive trees from each other due to genetic difference. Distribution of the samples in PCoA plot indicated that the population 1 are more spread due to population genetic variability. However, the SRAP result reveals that these molecular markers can be used in population genetic investigations and germ plasm analysis. AMOVA showed significant genetic difference among the studied olive populations. Cp-DNA analysis produced 366 bp long sequences, out of which 224 sites were segregating among the studied plants. The mean nucleotide diversity was 0.32. TCS network based on cp-DNA separated most of the studied populations. Therefore, it seems that cp-DNA rpl sequences is a suitable barcode molecular marker for population genetic studies. Phylogenetic tree of ITS data could partially differentiate wild olive population. In conclusion, a combined use of SRAPs and cp-DNA sequences are suggested for wild olive population genetic investigation.

Keywords. SRAP, cp-DNA, ITS, Population genetic, Olive.

INTRODUCTION

Olive tree (*O. europaea* L.) of the genus Olea (*O. europaea* subsp. *europaea* var. *europaea*) is one of the most important horticultural crop plants. It is an ancient plant species with grate economic value (Zohary and Hopf 2000), and has both cultivated and wild forms. Oleaster (*O. europaea* sub-

sp. *europaea* var. *sylvestris* Miller) is the Mediterranean wild olive and is possibly the progenitor of the cultivated olive. The non-Mediterranean wild olives are geographically isolated from the oleaster and show different morphological characters. Green (2002) grouped all morphological forms of wild olive in a single aggregate i.e. *Olea europaea* subsp. cuspidata, but the other investigators consider these intra-specific forms as ecotypes both in Africa and Iran (Besnard *et al*. 2002; Sheidai *et al*. 2010).

The occurrence of natural hybridization has been reported between different sub spices within the genus *Olea*. This holds true also for *O. cuspidate* and *O. africana* (Besnard and Bervill 2000). Moreover, (Omrani-Sabbaghi *et al*. 2007) suggested hybridization of subsp. *cuspidata* and the cultivated olive in South Africa and Iran and (Sheidai *et al*. 2010) identified a population with intermediate morphological and molecular (RAPDs) characteristics.

The wild relatives of crop plants (CWRs) constitute an important resource for improving agricultural production and for maintaining sustainable agro-ecosystems. Genetic material from CWRs has been utilized by humans for to improve the quality and yield of crops. For example, wild maize (*Zea mexicana*) is routinely grown alongside maize to promote natural crossing and improve yields. More recently, plant breeders have utilized CWR genes to improve a wide range of crops like rice (*Oryza sativa*), tomato (*Solanum lycopersicum*) and grain legumes *(*Hajjar and Hodgkin 2007*).* Therefore, A CWR can be defined as "a wild plant taxon that has an indirect use derived from its relatively close genetic relationship to a crop. The CWRs comprise a wonderful gene pool for future crop breeding programs.

Since natural populations of CWRs are at risk and are threatened by habitat loss, deforestation, etc., population genetic study of these natural populations is important task as it provides insight about the genetic variability, population genetic structure, gene flow versus population fragmentation as well population genetic differentiation. The obtained information can be utilized in both breeding as well as conservation strategies of the CWRs.

Recent population genetic studies use different molecular markers to investigate the genetic diversity as well as other population genetic features. This is also true for olive (Bracci *et al*. 2011), for example, Random Amplified Polymorphic DNA (RAPDs) (Sheidai *et al*. 2010) microsatellite (simple sequence repeat; SSRs) and inter simple sequence repeat; ISSR markers, Amplified Fragments Length Polymorphic markers (AFLPs) (Baldoni *et al*. 2006), cp-DNA (Besnard *et al*. 2011).

In the present study, genetic diversity, genetic divergence and genetic structure of four populations of *O. europaea* subsp. *cuspidata* from different localities are investigated using nrDNA ITS (Internal Transcribed Spacer) and SRAP (sequence-related amplified polymorphism) markers.

Since, SRAP marker technique combines easiness, reliability, high variability, moderate throughput ratio and superficial sequencing of the selected bands, we used this technique to amplify coding regions of DNA to target open reading frames.

MATERIALS AND METHODS

Thirteen specimens belonging to four geographical populations of subspecies *Olea europaea* subsp. *cuspidata* L. were collected from different localities that were placed between three provinces Bakhtiari, Boyer-Ahmad and Khuzestan. Details of geographical populations are given in Table 1.

DNA extraction and PCR reactions

DNA was extracted from dried leaf specimens (approximately 0.5 g material per sample) using CTAB (Cetyl trimethyl-ammonium bromide) activated charcoal protocol (Krizman *et al*. 2006 and Sheidai *et al*. 2013). Extracted DNA was run on 0.8% agarose gel. PCR reactions were carried in a 25µl volume containing 10 mM Tris-HCl buffer at pH 8; 50 mM KCl; 1.5 mM MgCl2; 0.2 mM of each dNTP (Bioron, Germany); 0.2 µM of a single primer; 20 mg genomic DNA and 1 U of Taq DNA polymerase (Bioron, Germany).

Table 1. List of 13 specimens of *Olea europaea* subsp. *cuspidata* L. from four populations accompanied by their distribution, altitude, longitude and herbarium number.

No.	Localities	Altitude	Latitude	Longitude	Voucher no.
1	Chaharmahal and Bakhtiari Province, Dehedz – Lordgan, Iran	1713	31°31'18"	50°28'26"	HSBU2018700
2	Kohgiluyeh and Boyer-Ahmad Province, Khersaan Road, Iran	1380	31°26'59"	50°28'57"	HSBU2018705
3	Chaharmahal and Bakhtiari Province, Lordgan, Monj, Gachahan, Iran	1151	31°26'48"	50°32'19"	HSBU2018711
4	Chaharmahal and Bakhtiari Province, Lordgan, Monj, Gachahan, Iran	1592	35°55'41"	57°41'53"	HSBU2018712

SRAP study

Five sequences related amplified polymorphism (SRAP) primer pairs including forward primers: Me1, Me2, Me3, Me4, Me5 and reverse primers: Em1, Em2, Em3, Em4, Em5 were used (Feng *et al*. 2014). PCR reactions were carried in a 25µl volume containing 10 mM Tris-HCl buffer at pH 8; 50 mM KCl; 1.5 mM MgCl2; 0.2 mM of each dNTP (Bioron, Germany); 0.2 µM of a single primer; 20 ng genomic DNA and 1 U of Taq DNA polymerase (Bioron, Germany). Following programs used for amplification of SRAP region in a PCR reaction: 94°C, 1 min, 35°C, 1 min, and 72°C, 1 min for first five cycles then 5 min initial denaturation step 94°C, followed by 40 cycles of 1 min at 94°C; 1 min at 55°C and 2 min at 72°C and a final extension at 72°C for 7-10 mi

ITS study

The complete ITS region was amplified using forward ITS5 (5'- GGA AGT AAA AGTCGT AAC AAG G- 3') and reverse primers ITS4 (5'- TCC GCT TAT TGA TAT GC-3') (White *et al*. 1990). Following program used for amplification of nuclear region in a PCR reaction: 5 min initial denaturation step 94°C, followed by 40 cycles of 1 min at 94°C; 1 min at 53.5°C and 2 min at 72°C. The reaction was completed by final extension step of 7 min at 72°C.

Cp- DNA study

The intergenic spacer of chloroplast genome rpl16 was amplified and sequenced with universal primers following the methodology of (Shaw *et al*. 2005; Timme *et al*. 2007). Each 20 µl of PCR tube contained 10 µl of 2x PCR buffer, 0.5 mM of each primer, 200 mM of each dNTP, 1 Unit of Taq DNA polymerase (Bioron, Germany), and 1 µl of template genomic DNA at 20 ng µl-1 . The amplification reaction was performed in Techne thermocycler (Germany) with the following program: 2 min 94°C, 1 min at 94°C; 1 min at 54°C and 1min at 72°C. The reaction was completed by final extension step of 6 min at 72°C.

Data Analyses

SRAP bands were coded as binary characters (presence = 1, absence = 0) and used for genetic diversity analysis. Data obtained were analyzed for the genetic diversity parameters like, Nei's gene diversity (H), Shannon information index (I), number of effective alleles, and percentage of polymorphism (Weising *et al*. 2005; Freeland *et al*. 2011). Principal coordinate analyses (PCoA) were performed using PAST ver. 2.17 (Hammer *et al*. 2012).

Nei's genetic distance was used among populations. AMOVA (Analysis of molecular variance) test (with 1000 permutations) as implemented in GenAlex 6.4 (Peakall and Smouse 2006).

The phylogenetic methods used to investigate the species relationships were Maximum parsimony (MP), Maximum likelihood (ML), Networking and Bayesian approaches. The ITS sequences were firstly aligned and used to test the proper nucleotide substitution model as applied in MEGA 7. Program (Tamura *et al*. 2012). Networking was performed using Splits Tree 4 program (Huson and Bryant 2006) and Bayesian analysis was done using BEAST software v1.6.1 (Drummond *et al*. 2012a, b).

RESULTS

In total, 76 SRAP bands were obtained in olive trees studied. Some of these bands were common while, few bands were private in these trees. For example, SRAP bands 51, 52 and 76 occurred only in trees of population 4, while SRAP band 7 happened only in one of the trees in population 1. Similarly, SRAP band 4 was observed in the tree of population 3.

Genetic diversity parameters determined for all SRAP loci within the studied *olive* populations identified the most variable loci. The loci with highest value of gene diversity (H) and Shanon information index (I) are the most diverse SRAP loci (Table 2). The mean value obtained for H = 0.34, while I = 0.52.

Population differentiation parameters determined for SRAP loci in the studied olive trees (Table 3), identified the loci with highest migration/ exchange value (Nm) and also SRAP loci with the highest differentiation value (Gst). In total, 13 SRAP loci had Gst value = 1, that means they differentiate the studied trees. Similarly, SRAP loci with Nm>1 are considered highly migrated among the populations.

PCoA analysis of the studied olive trees after 99 times permutation, based on SRAP data is presented in Figure 1. PCoA plot clearly separates olive trees of the studied populations from each other due to genetic difference. Distribution of the samples in PCoA plot indicates that olive trees of population 1 are more spread due to within population genetic variability. However, in general, the SRAP result reveals that these molecular markers can be used in population genetic investigations and germ plasm analysis of olive.

Nei' genetic distance determined among olive trees based on SRAP data (Table 4), revealed that the genetic distance among trees of the population 1 varies from

Table 2. Genetic variability parameters for SRAP loci studied in *olive* populations.

Locus	Sample Size	Ne	H	I
5	13	1.9187	0.4788	0.6718
8	13	1.9299	0.4818	0.6749
30	13	1.9683	0.4920	0.6851
36	13	1.9882	0.4970	0.6902
39	13	1.8989	0.4734	0.6663
53	13	1.9882	0.4970	0.6902
54	13	1.8943	0.4721	0.6650
55	13	1.9928	0.4982	0.6913
57	13	1.9562	0.4888	0.6819
58	13	1.9216	0.4796	0.6726
59	13	1.8943	0.4721	0.6650
64	13	1.8943	0.4721	0.6650
65	13	1.9865	0.4966	0.6898
67	13	1.9562	0.4888	0.6819
72	13	1.8943	0.4721	0.6650
Mean	13	1.5918	0.3492	0.5242
St. Dev	0.2911	0.1268	0.1506	

Ne = Effective number of alleles.
H = Nei's (1973) gene diversity.
I = Shannon's Information index [Lewontin (1972)].

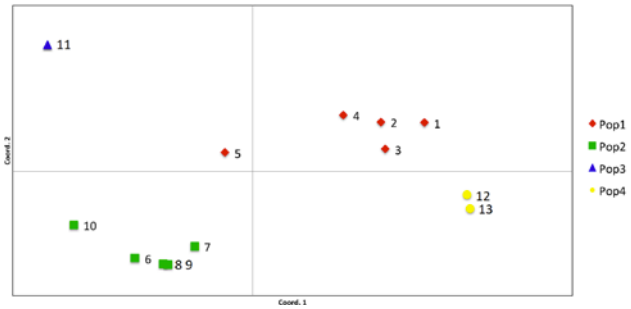

Figure 1. PCoA plot of olive trees based on SRAP data revealing genetic separation of populations.

0.30 to 0.54, while it varies from 0.46 to 0.76 in olive trees of population 2.

AMOVA showed significant genetic difference (Phipt = 0.43, P =0.01) among the studied olive populations. It also revealed that 43% of total genetic variation was due to among population genetic difference, whereas, 57% occurred due to within population genetic variability.

Cp-DNA analysis

We obtained 366 bp long sequences, out of which 224 sites were segregating among the studied plants. The

Table 3. Genetic differentiation parameters in the olive trees studied based on SRAP loci.

Locus	Sample Size	Ht	Hs	Gst	Nm
2	13	0.2633	0.2381	0.0958	4.7202
3	13	0.3921	0.3145	0.1981	2.0240
4	13	0.3750	0.0000	1.0000	0.0000
7	13	0.0514	0.0472	0.0813	5.6481
10	13	0.2633	0.2381	0.0958	4.7202
13	13	0.3750	0.0000	1.0000	0.0000
14	13	0.1669	0.1162	0.3036	1.1472
17	13	0.2000	0.1746	0.1270	3.4365
22	13	0.0514	0.0472	0.0813	5.6481
23	13	0.3750	0.0000	1.0000	0.0000
24	13	0.1064	0.0873	0.1791	2.2910
28	13	0.1794	0.1508	0.1595	2.6340
31	13	0.2086	0.1634	0.2164	1.8105
32	13	0.3750	0.0000	1.0000	0.0000
34	13	0.1000	0.0944	0.0557	8.4721
36	13	0.5000	0.0000	1.0000	0.0000
39	13	0.3750	0.0000	1.0000	0.0000
41	13	0.1064	0.0873	0.1791	2.2910
43	13	0.2086	0.1634	0.2164	1.8105
44	13	0.5000	0.0000	1.0000	0.0000
45	13	0.3750	0.0000	1.0000	0.0000
47	13	0.1794	0.1508	0.1595	2.6340
48	13	0.1669	0.1162	0.3036	1.1472
50	13	0.3750	0.0000	1.0000	0.0000
51	13	0.3750	0.0000	1.0000	0.0000
52	13	0.3750	0.0000	1.0000	0.0000
53	13	0.5000	0.0000	1.0000	0.0000
58	13	0.4226	0.3434	0.1875	2.1669
62	13	0.3625	0.2744	0.2431	1.5564
68	13	0.2086	0.1634	0.2164	1.8105
69	13	0.1000	0.0944	0.0557	8.4721
75	13	0.5000	0.0000	1.0000	0.0000
76	13	0.3750	0.0000	1.0000	0.0000
Mean	13	0.3680	0.1308	0.6445	0.2758
St. Dev	0.0172	0.0085			

mean nucleotide diversity (p) was 0.32. TCS network of the studied olive trees Figure. 2) separated most of the studied populations. For instance, trees of the population 2 and the population 4 were grouped together, while trees of population 1 were scattered in between these two populations. Therefore, it seems that cp-DNA (rpl16) sequences are a suitable barcode molecular marker for population genetic studies of olive.

There has been no report of rpl16 sequences for the cultivates olive. Therefore, we could not compare these two forms together.

Table 4. Nei genetic distance among the studied olives.

Pop	1	2	3	4	5	6	7	8	9	10	11	12
2	0.30											
3	0.39	0.42										
4	0.44	0.46	0.33									
5	0.54	0.40	0.52	0.42								
6	0.65	0.54	0.57	0.62	0.40							
7	0.56	0.62	0.66	0.64	0.65	0.54						
8	0.76	0.70	0.81	0.77	0.71	0.44	0.69					
9	0.65	0.64	0.68	0.73	0.67	0.49	0.57	0.57				
10	0.60	0.53	0.60	0.68	0.50	0.41	0.48	0.55	0.43			
11	0.60	0.55	0.73	0.60	0.57	0.65	0.80	0.82	0.69	0.53		
12	0.41	0.43	0.57	0.62	0.63	0.60	0.72	0.65	0.56	0.65	0.67	
13	0.47	0.46	0.57	0.52	0.63	0.63	0.68	0.69	0.56	0.68	0.71	0.17

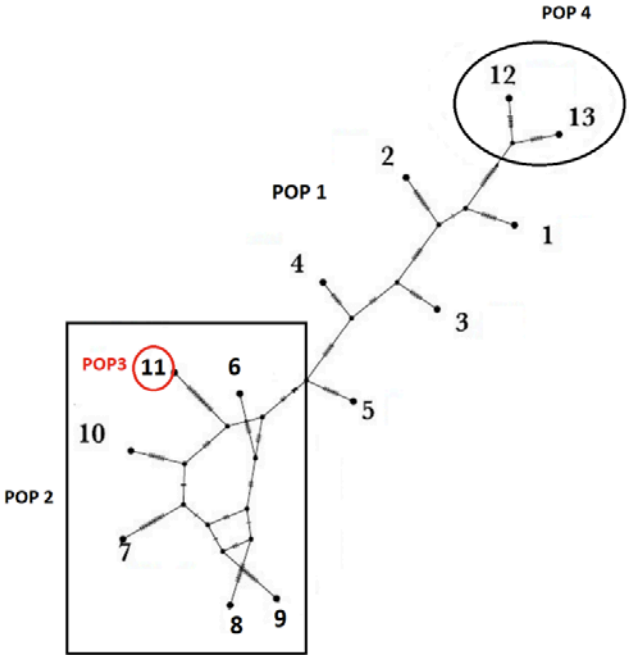

Figure 2. TCS network of olive trees based on cp-DNA sequences revealing almost separation of the studied populations.

ITS sequence analysis

We obtained 183 bp long sequences in ITS region with 150 variable sites. The analysis revealed the presence of 8 haplotypes in ITS with haplotype diversity, Hd: 0.80.

An Olive tree 7, 9, 11 and 13 had similar sequences and forms a single haplotype group.

The nucleotide distance (p distance) of the studied trees (Table 5), revealed that p distance among olive trees of population 1 varied from 0.36 to 0.54, while the same value in population varied from 0.01 to 0.49.

Maximum likelihood phylogenetic tree (ML) (Figure 3) of the studied olive trees based on ITS sequences revealed that, trees of population 1, differ in their ITS sequences and were grouped in a separate clade. However, trees of populations 2, 3, and 4 were placed together in a single unresolved clade. This result indicates that ITS sequences can be used along with cp-DNA barcodes in olive population genetic studies.

Comparing phylogenetic trees of SRAP markers, Cp-DNA and ITS sequences produced quart let distance = 0.56 and test performed based on the most agreeable sub-trees (MAST) (Figure. 4) revealed that, these markers do differentiate some of the olive trees and place them in distinct clades.

Joint phylogenetic ITS analysis of wild populations and randomly selected cultivated olives (Figure. 5) revealed the genetic separation of these olives from each other. ITS sequences could differentiate different olive trees of wild populations but not the cultivars from each other.

DISCUSSION

Genetic structure analysis of both cultivated and wild olive is important for breeding and conservation purposes (Baldoni *et al.* 2006). Olive cultivars can be considered as varieties of unknown origin, currently propagated vegetative by cutting or grafting. Analysis of nuclear and cytoplasmic DNA polymorphisms in Mediterranean oleaster populations has shown that eastern oleaster populations differ greatly from those of the west Mediterranean (Besnard *et al.* 2001), while the genet-

Table 5. P nucleotide distance among olive plants based on ITS sequences.

	1	2	3	4	5	6	7	8	9	10	11	12	13
1	-												
2	0.53	-											
3	0.52	0.43	-										
4	0.56	0.50	0.36	-									
5	0.54	0.51	0.46	0.45	-								
6	0.49	0.36	0.25	0.36	0.33	-							
7	0.48	0.35	0.24	0.35	0.32	0.01	-						
8	0.48	0.35	0.24	0.35	0.33	0.01	0.00	-					
9	0.48	0.35	0.24	0.35	0.33	0.01	0.00	0.00	-				
10	0.48	0.35	0.24	0.35	0.33	0.01	0.01	0.01	0.01	-			
11	0.48	0.35	0.24	0.35	0.33	0.01	0.00	0.00	0.00	0.01	-		
12	0.48	0.35	0.24	0.35	0.32	0.01	0.00	0.00	0.00	0.01	0.00	-	
13	0.48	0.35	0.24	0.35	0.32	0.01	0.00	0.00	0.00	0.01	0.00	0.00	-

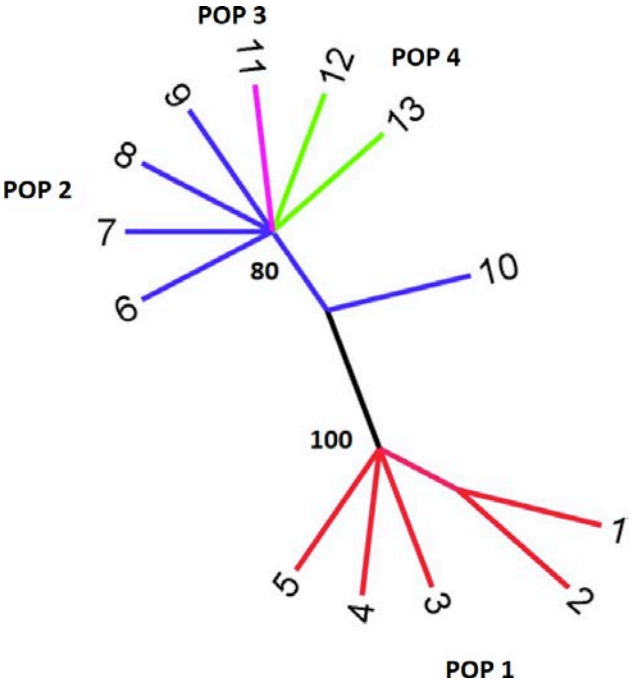

Figure 3. ML phylogenetic tree of the studied olive trees based on ITS sequences.

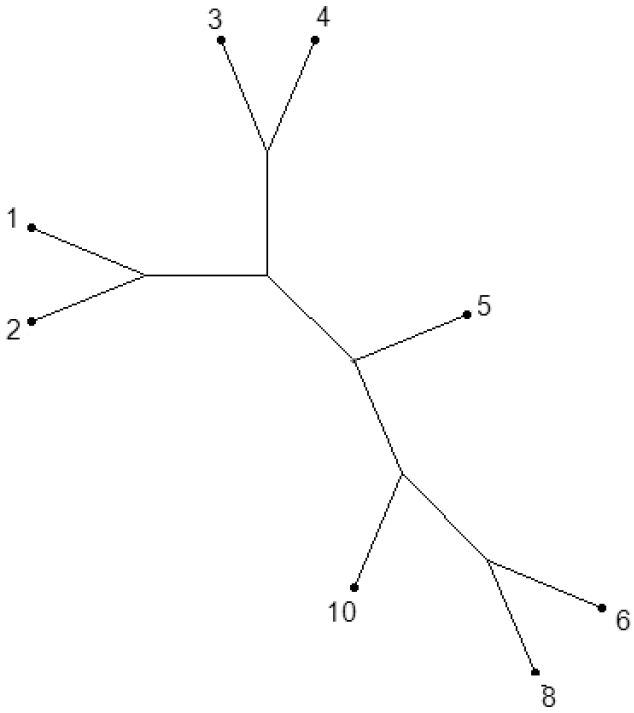

Figure 4. Most agreeable sub-trees (MAST) plot showing the common clades differentiated by ITS, Cp-DNA and ISSR trees.

ic diversity of cultivated populations shows a complex patchy pattern (Owen *et al.* 2005). The present investigation also revealed genetic difference between Iranian wild populations and the cultivated olive forms.

Based on the frequency and distribution of polymorphisms, several authors suggested that many olive cultivars have been produced from naturally cross-bred genotypes (Besnard *et al.* 2001), while, others, due to the great genetic distance between populations of wild olives and cultivars, suggested that many local cultivars may have an allochthonous origin (Angiolillo *et al.* 1999; Bronzini de Caraffa *et al.* 2002).

Genetic diversity of both cultivated and wild olives has been investigated by using different molecular markers (Bracci *et al.* 2011), revealing the genetic structure of these olive forms. In the present study, SRAP and cp-DNA rpl sequences could be used in wild olive dif-

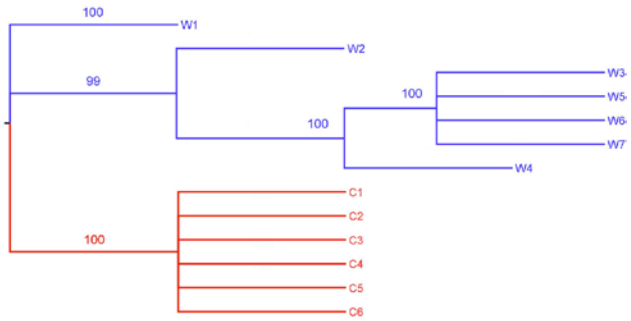

Figure 5. Maximum parsimony phylogenetic tree of wild and cultivated olives based in ITS sequences, revealing genetic distinctness of the two groups.

ferentiation. Cp-DNA polymorphisms is used for phylogeographic, population genetic and forensic analyses in plants, but detecting cp-DNA variation is sometimes challenging, limiting the applications of such an approach (Besnard *et al.* 2011). According to our knowledge rpl16 sequences were only used in genetic variability assessment of tissue culture regenerated olive plants (Kangarloo *et al.* 2016) and not in olive population genetic investigation. Therefore, our study is the first time report on application of the cp-DNA sequences for wild olive population differentiation.

Besnard *et al.* (2001) used eight complete sequences of cp-DNA genomes of *Olea* in their study. The reported low nucleotide divergence between olive cp-DNA lineages, not exceeding 0.07%. Based on these sequences, markers were developed for studying two single nucleotide substitutions and length polymorphism of 62 regions (with variable microsatellite motifs or other indels). They used these markers to study the cp-DNA variation in cultivated and wild Mediterranean olive trees. The discriminating power of cp-DNA variation was particularly low for the cultivated olive tree with one predominating haplotype, but more diversity was detected in wild populations. This is almost in agreement with present study findings. Besnard *et al.* (2001) and Pérez-Jiménez *et al.* (2013) suggested that cp-DNA markers will have applications for a comparative study of the dynamic of wild olive tree populations in different environments, such as archipelagos and Saharan mountains. Such information may be relevant for defining appropriate strategies of prospection and *in situ* conservation of the wild olive tree.

In conclusion, the present study revealed that a combination of neutral molecular markers, like SRAPs and cp-DNA sequences are powerful markers to differentiate wild olive populations.

ACKNOWLEDGMENTS

This work was funded by Islamic Azad University, Science and Research Branch and Shahid Beheshti university for providing the laboratory equipment for this investigation.

REFERENCES

Angiolillo A, Mencuccini M, Baldoni L. 1999. Olive genetic diversity assessed using amplified fragment length polymorphisms. Theoretical and Applied Genetics. 98: 411–421.

Azadi R. 2005. Family Oleaceae. Flora of Iran, No. 48. 1st ed. Tehran, IRAN: Research Institute of Forest and Range Lands, pp. 36.

Baldoni L, Tosti N, Ricciolini C (2006) Genetic Structure of Wild and Cultivated Olives in the Central Mediterranean Basin. Annals of Botany. 98(5):935-942.

Besnard G, Baradat P, Berville´ A .2001. Genetic relationships in the olive (Olea europaea L.) reflect multilocal selection of cultivars. Theoretical and Applied Genetics. 102: 251–258.

Besnard G, Hernández P, Khadari B, Dorado G, Savolainen V .2011. Genomic profiling of plastid DNA variation in the Mediterranean olive tree. BMC Plant Biology 11:80.

Bracci TM, Busconi M, Fogher C, Sebastiani L .2011. Molecular studies in olive (Olea europaea L.): overview on DNA markers applications and recent advances in genome analysis. Plant Cell Reports. 30: 449-462.

Bronzini de Caraffa V, Maury J, Gambotti C, Breton C, Berville´ A, Giannettini J .2002. Mitochondrial DNA variation and RAPD mark oleasters, olive and feral olive from Western and Eastern Mediterranean. Theoretical and Applied Genetics. 104: 1209–1216.

Drummond AJ, Rambaut A, Suchard MA .2010. BEAST (v1.6.1). http://beast.bio.ed.ac.uk . Accessed 15 October 2010.

Drummond AJ, Rambaut A, Xie W (2010) BEAUti (v1.6.1) [computer program]. http://beast.bio.ed.ac.uk. Accessed 15 October 2010.

Green PS .2002. A revision of *Olea* L. (Oleaceae). Kew Bull 57: 91-140.

Hajjar R, Hodgkin T .2007. The use of wild relatives in crop improvement: a survey of developments over the last 20 years. Euphytica. 156: 1–13.

Hammer Ø, Harper DAT, Ryan PD .2012. PAST: Paleontological Statistics software package for education and data analysis. Palaeontol Electronica 4: 9.

Huson DH, Bryant D .2006. Application of Phylogenetic Networks in Evolutionary Studies. Molecular Biology and Evolution. 23: 254-267.

Kangarloo B, Noormohammadi, Z, Farahani F, Ghasemzadeh-Baraki S, Sheidai M. 2016. An assessment of tissue culture-induced genetic variability in olive (*Olea europaea* L.) using chloroplast *rpl16* intron sequences and single primer amplification reaction (SPAR) markers. The Journal of Horticultural Science and Biotechnology. 90: 719-723.

Križman M, Jakse J, Baricevic D, Javornik B, Prošek M .2006. Acta Agri Slov, 87, 427.

Owen CA, Bita EC, Banilas G, Hajjar SE, Sellianakis V, Aksoy U. 2005. AFLP reveals structural details of genetic diversity within cultivated olive germplasm from the Eastern Mediterranean. Theoretical and Applied Genetics. 110: 1169–1176.

Pérez-Jiménez M, Besnard G, Dorado G, Hernandez P .2013. Varietal Tracing of Virgin Olive Oils Based on Plastid DNA Variation Profiling. PLOS.

Omrani-Sabbaghi A, Shahriari M, Falahati-Anbaran M, Mohammadi SA, Nankali A, Mardi M, Ghareyazie B .2007. Microsatellite markers based assessment of genetic diversity in Iranian olive (Olea europaea L.) collections. Scientia Horticulturae 112: 439–447

Sheidai M, Zanganeh S, Haji-Ramezanali R, Nouroozi M, Noormohammadi Z, Ghsemzadeh-Baraki S .2013. Genetic diversity and population structure in four Cirsium (Asteraceae) species. Biológia 68: 384-397.

Shaw J, Small RL (2005) Chloroplast DNA phylogeny and phylogeography of the North American plums (Prunus subgenus Prunus section Prunocerasus, Rosaceae). American Journal of Botany. 92: 2011-2030.

Timme RE, Kuehl JV, Boore JL, Jansen RK. A .2007. Comparative analysis of the *Lactuca* and *Helianthus* (Asteraceae) plastid genomes: identification of divergent regions and categorization of shared repeats. American Journal of Botany. 94:302–312. [PubMed]

Tamura K, Peterson D, Peterson N, Stecher G, Nei M, Kumar S (2011) MEGA5: Molecular Evolutionary Genetics Analysis using Maximum Likelihood, Evolutionary Distance, and Maximum Parsimony Methods. Molecular Biology and Evolution. 28: 2731-2739.

White TJ, Bruns T, Lee S, Taylor J .1990. Amplification and direct sequencing of fungal ribosomal RNA genes for phylogenetics. In: Innis M A (ed) PCR protocols: a guide to methods and applications. New York, US: Academic Press, Inc. pp. 315–322.

Zohary D, Hopf M .2000. Domestication of plants in the Old Word. 3rd edn. Oxford, UK: Clarendon Press.

Caryologia
International Journal of Cytology, Cytosystematics and Cytogenetics

Firenze University Press
www.fupress.com/caryologia

OPEN ACCESS

Citation: S. Tarkesh Esfahani, G. Karimzadeh, M. Reza Naghavi (2020) *In Vitro* Polyploidy Induction in Persian Poppy (*Papaver bracteatum* Lindl.). *Caryologia* 73(1): 133-144. doi: 10.13128/caryologia-169

Received: February 15, 2019

Accepted: February 23, 2020

Published: May 8, 2020

Data Availability Statement: All relevant data are within the paper and its Supporting Information files.

Competing Interests: The Author(s) declare(s) no conflict of interest.

In Vitro Polyploidy Induction in Persian Poppy (*Papaver bracteatum* Lindl.)

Saeed Tarkesh Esfahani[1], Ghasem Karimzadeh[1,*], Mohammad Reza Naghavi[2]

[1] *Department of Plant Breeding and Biotechnology, Faculty of Agriculture, Tarbiat Modares University (TMU), P. O. Box. 14115-336, Tehran, Iran*
[2] *Department of Agronomy and Plant Breeding, College of Agricultural and Natural Resources, University of Tehran, Karaj, Iran*
*Corresponding author. E-mail: karimzadeh_g@modares.ac.ir

Abstract. *Papaver bracteatum* Lindl. grows as a wild perennial medicinal plant in Northern Iran and is known mainly for its high amounts of the pharmaceutically valuable alkaloid of thebaine. In vitro production of tetraploid *P. bracteatum* through colchicine treatment of imbibed seeds is reported. Resulted tetraploid and mixoploid plants were effectively identified by chromosome counting and flow cytometry technique. The chromosome number in diploid and successfully induced tetraploids were confirmed to be $2n=2x=14$ and $2n=4x=28$, where their calculated 2C DNA values were 6.15±0.03 and 11.95±0.07 pg, respectively. The highest induction efficiency was obtained by colchicine concentration of 0.05% and the treatment duration of 24 h. The effects of colchicine toxicity on plant survival and growth were proportional mainly to its concentration rather than duration of exposure to colchicine. Tetraploid plants possessed significantly larger and less frequent leaf stomata as well as a larger cell size. These attributes may serve as criteria for preliminary screening of *P. bracteatum* populations for ploidy level.

Keywords. Persian poppy, seed, tetraploid, colchicine, flow cytometry, 2C DNA value.

INTRODUCTION

Persian poppy (*Papaver bracteatum* Lindl.; $2n=2x=14$) is a wild perennial medicinal plant belonging to the Papaveraceae family, section *Oxytona* that grows natively in the Alborz Mountains in the North of Iran in altitudes higher than 1800 m on the slopes facing the Caspian Sea (Sharghi and Lalezari 1967). It is mainly known for the high amounts of the valuable isoquinoline alkaloid thebaine as the main secondary metabolite in different organs particularly in roots and capsules (Nyman and Bruhn 1979; Madam 2011) while some 20 other alkaloids are reported to be present in this species only in trace amounts (Wu and Dobberstein 1977). Persian poppy seeds contain 45-48% oil rich in nutritionally valuable unsaturated fatty acids, so the other important usage of the plant is in the food industry (Madam 2011).

Seddigh *et al*. (1982) reported mean seed yield and seed-oil yield of *P. bracteatum* to be 90 and 40 kg ha^{-1}, respectively.

Successful polyploidy induction has been reported in various medicinal and ornamental plants with the aim of producing plants with improved agronomical, phytochemical or economically important characteristics. Application of anti-mitotic agents such as colchicine (Chen and Gao 2007; Sakhanokho *et al*. 2009; Majdi *et al*. 2010; Omidbaigi *et al*. 2010a, b; Kaensaksiri *et al*. 2011; Wu *et al*. 2011; Marzougui *et al*. 2011; Tavan *et al*. 2015; Javadian *et al*. 2017; Sadat Noori *et al*. 2017), oryzalin (Bouvier *et al*. 1994; Thao *et al*. 2003; Kermani *et al*. 2003; Lehrer *et al*. 2008; Sakhanokho *et al*. 2009), amiprophosmethyl (Rodrigues *et al*. 2011) and trifluralin (Eeckhaut *et al*. 2002) has been reported as the most common procedure for *in vitro* polyploidy induction in plants with colchicine being the most commonly used anti-mitotic agent.

Polyploid plants have been found to be valuable genetic resources due to possession of superior agronomic and phytochemical traits over their diploid progenitors. They have therefore attracted increasing attention in breeding programs, agriculture and medicinal plants industries. Some of the more frequently reported advantages of induced polyploid plants include larger vegetative and reproductive organs such as leaves and flowers (Chen and Gao 2006; Majdi *et al*. 2010; Tang *et al*. 2010; Gantait *et al*. 2011; Miller *et al*. 2012), darker green leaves with a higher chlorophyll content and photosynthesis capacity (Kulkarni and Borse 2010; Gantait *et al*. 2011), increased tolerance to environmental stresses (Natuli and Zobolo 2008), increased production of secondary metabolites (Dhawan and Lavania 1996; Kaensaksiri *et al*. 2011; Xu *et al*. 2013; Tavan *et al*. 2015; Javadian *et al*. 2017), increased expression of important genes and enzymes (Adams *et al*. 2003; Mishra *et al*. 2010; Miller *et al*. 2012; Xu *et al*. 2013) and delayed florescence time (Gu *et al*. 2005). On the other hand, decreased fertility, increased level of mitotic disruptions and pollen sterility (Liu *et al*. 2012) and facilitated biological invasion (Beest *et al*. 2012) are reported as the most important unfavorable consequences of induced polyploidy. *In vitro* polyploidy induction in several Papaveraceae plants has been previously studied mainly with the aim of obtaining an increased content of medicinal alkaloids. Mishra *et al*. (2010) successfully induced tetraploidy in *Papaver somniferum* L. and reported a significant enhancement in the morphine content and increased expression level of important genes involved in alkaloid biosynthesis pathway in tetraploid plants. Milo *et al*. (1987) reported the induction of tetraploidy in *P. bracteatum* through colchicine treatment of apical meristems and subsequent production of triploid plants by crossing induced tetraploids to diploid plants. They suggested the ploidy breeding and tetraploidy induction as the most promising approach for development of thebaine-rich poppy lines. In their studies, they selected the plants with different ploidy levels through chromosome counting and cytological techniques. So an effective, easy and clearly described method for *in vitro* polyploidy induction in *P. bracteatum* and effective discrimination of tetraploid and mixoploid results based on flow cytometric (FCM) technique and 2C DNA value is not reported yet. Consequently, we report for the first time the *in vitro* production of autotetraploid *P. bracteatum* by colchicine treatment of imbibed seeds followed by FCM identification of polyploidy. The differences in the DNA C-value, anatomical and morphological traits between diploid and induced tetraploid plants were also measured and their capability for being employed as reliable indicators of ploidy level in the plant populations was described.

MATERIAL AND METHODS

Plant material

Seeds of mature Persian endemic *Papaver bracteatum* plants were collected in Polour region (Latitude 35° 52' 16.99" N, Longitude 52° 04' 38.62" E, Altitude 2489 ± 50 m) from hillsides of Alborz Mountains in northern Iran. The seeds from each individual plant were collected separately and kept in small plastic bags. Since *P. bracteatum* is a self-incompatible totally cross-pollinating plant (Nyman and Bruhn 1979), the seeds which originated from each individual plant were considered as progenitors for future colchicine-treated plants. The seeds of each maternal plant were collected separately so that the eventual comparisons between different ploidy levels could be conducted between two half-sib plants rather than two plants with completely different genetic backgrounds. For this purpose, all treated seeds in polyploidy induction assay were selected from the seeds of an individual maternal plant.

Polyploidy induction

Seeds obtained from one capsule from an individual *P. bracteatum* plant were sterilized by immersing in ethanol 70% (v/v) for three 30 s times, followed by sodium hypochlorite 5% (v/v) for 7 min. The seeds were then rinsed with distilled water for 5 min and transferred on

two layers of moistened filter papers in glass petri dishes and irrigated regularly with distilled water to allow water imbibition. Germination process progressed up to the radicle emergence. After 8-10 days, the imbibed seeds (swollen seeds without a well-defined radicle apex) were transferred to tubular penicillin vials containing 1000 µl of colchicine solutions (Sigma-Aldrich Corporation, MO, USA) with different concentrations comprising 0.00, 0.025, 0.050, 0.075, 0.10 and 0.20% (w/v). The vials were placed on a shaker with a rotation speed of 95 rpm and shaken for predetermined durations, including 4, 8, 12, 24, 36, 48, 72, and 168 h. At the end of treatment duration, the treated seeds were washed thoroughly with distilled water for 3 × 3-min and transferred to a 250-ml glass baby food jars containing 40 ml of ½ Murashige and Skoog (1962) medium with 1 g l^{-1} charcoal. The latter was used in order to prevent the seed phenolic compounds from interfering with the emergence and growth of new seedlings. Seven treated seeds were cultured in each jar (representing one replication for a given treatment in data analysis). The seedlings were re-cultured once a month on a new medium with the above-mentioned composition and conditions. After three months, the plants with 6-7 true developed leaves were transferred to 500 g pots containing sand, commercial potting soil and vermiculite as the main components mixed with a ratio of 2:2:1 orderly.

Flow cytometry analysis

One cm^2 of young, healthy and fully green developed leaf material from each examined Persian poppy plant together with about 1/3-1/2 in area of leaf material from *Pisum sativum* cv. 'Citrad' (2C DNA = 9.09 pg; Doležel *et al*. 1998) as an internal reference standard, were chopped into small pieces by a sharp razor blade in a 100 mm glass petri dish, containing one ml of Woody Plant Buffer (WPB; Loureiro *et al*. 2007). The resultant nuclear suspension was filtered through a Partec (Partec, Münster, Germany) 30 µm-nylon mesh, followed by treating with 50 µg ml^{-1} RNase (Sigma-Aldrich Corporation, MO, USA) and 50 µg ml^{-1} Propidium Iodide (PI, Fluka) as DNA staining agent, and then incubated for two min at room temperature. To determine nuclear 2C DNA amount, the nuclei suspension was analysed by a BD FACSCanto II flow cytometer (BD Biosciences, Bedford, MA, USA), using BD FACSDiva™ Software. Output data were then transferred to a Flowing Software version 2.5.0 to be editable in Partec FloMax ver. 2.4e (Partec, Münster, Germany). The measurements of relative fluorescence intensity of stained nuclei were performed on a linear scale, analysing at least 5,000 nuclei for each sample. The absolute DNA amount of a sample was calculated based on the values of the G1 peak means (Doležel *et al*. 2003, 2007; Doležel and Bartoš 2005; Mahdavi and Karimzadeh 2010; Karimzadeh *et al*. 2010, 2011; Abedi *et al*. 2015) as follows:

Sample 2C DNA (pg) = (Sample G_1 peak mean/Standard G_1 peak mean) × Standard 2C DNA (pg)

The analysed samples were classified based on the FCM results into diploid (2*x*), tetraploid (4*x*) and mixoploid (2*x* and 4*x*) samples.

Chromosome counting

The ploidy status of the induction results were additionally confirmed by microscopic chromosome, counting in 10 randomly sampled plants from each class of ploidy level. Root tips from confirmed diploid and tetraploid plants were pretreated with α-bromonaphthalene for 1 h at 24 °C, followed by rinsing with distilled water for 3 × 3 min. The pretreated roots were then fixed in Carnoy solution (3:1 ethanol:glacial acetic acid) and stored at 4 °C followed by washing in distilled water, hydrolyzing with 1 N HCl for 8 min at 65 °C and staining with 1% (w/v) aceto-orcein for 1 h. Treated 1-2 mm long root tips were excised and squashed on slide glass, with a drop of 45% (v/v) acetic acid, and protected with a cover slip. Chromosome counts were analysed by observation under a BX51 Olympus light microscope (Olympus Optical Co., Tokyo, Japan), equipped with an Olympus DP12 digital camera (Olympus Optical Co., Tokyo, Japan) using WH10X (FN22) eyepiece and 100x objective lens.

Anatomical and morphological analysis

To assess any possible relations between anatomical traits and ploidy level in *P. bracteatum*, leaf cell size as well as the dimensions and the frequency of leaf stomata were measured on the lower epidermis of 20 fully developed leaves each taken from an individual plant in each confirmed class of ploidy. Data on stomata dimensions were measured on 60 stomata from leaves of the plants in each class of ploidy level. The stomata were visualized by the impression method (Majdi *et al*. 2010; Tavan *et al*. 2015). The density of the stomata was counted at 200x and the area of stomata were measured at 1000x magnification, using high resolution microscopic digital photographs taken with an Olympus DP12 digital camera (Olympus Optical Co., Tokyo, Japan) interfaced to

an Olympus BX50 (Olympus Optical Co., Tokyo, Japan) microscope. The stomata and the cells in three random microscopic fields per each leaf were counted and measured. The measurements of stomata dimensions, including area and large diameter (length) as well as the cell area were determined, using the captured images and the UTHSCSA ImageTool program (University of Texas Health Science Center at San Antonio, Texas, USA).

Data analysis

The data regarding the effect of time and concentration of the colchicine treatment on survival rate and polyploidy induction were analysed through a Completely Randomized Design (CRD) with three replications. Mean comparison was carried out by using Least Significant Difference (LSD) test at $P<0.05$. Seeds germination percentage was calculated as GP = (number of germinated seeds / total planted seeds) * 100. Tetraploidy induction efficiency was assessed using the method reported by Bouvier *et al*. (1994) and Majdi *et al*. (2010) as follows:

Induction efficiency = % Seedling survival × % Tetraploidy induction

For induction efficiency calculation, a seedling was considered as survived if it persisted for three months after being treated with colchicine and had enough green leaf area to be analysed by FCM. The resultant data were first tested for normality with the Kolmogorov-Smirnov test. The logarithmic transformation was then used for both stomata area and stomata frequency data. Mean comparisons between two different ploidy levels for anatomical traits were conducted, using Student's *t* test. All statistical analysis were conducted, using SPSS 18 (Chicago: SPSS Inc., 2009).

RESULTS

Survival and the growth of colchicine-treated seeds

The toxic effects of colchicine on the treated Persian poppy (*Papaver bracteatum* Lindl.) plants were different in terms of their survival and consecutive growth. Some treated seeds could no longer survive colchicine treatment, as they remained as dark necrotic non-emerging seeds without any root appearance. Whereas some others could survive in the colchicine and remained alive initially at the time of transferring to the medium, but their seedlings could not keep normal growing and turned to dark brown-colored necrotic tissues during later three weeks after being transferred. The degree of mortality caused by different colchicine either concentrations or durations were variable. The toxic effects of colchicine treatment on the survival and on the growth of the seeds were therefore assessed 30 days after treatment induction. The general colchicine-induced mortality was divided and expressed as two different criteria including seed mortality and seedling mortality (Table 1). Seed mortality was calculated based on non-emerging seeds which could not survive in the colchicine treatment, while seedling mortality was reflected by the emerged seedlings with inhibited successive growth. The results showed that increased colchicine concentration significantly increased the level of lethal effects (Table 1, Fig. 1), so that only 4.76±2.38% seed survival but no subsequent growth was observed in the seeds treated with the 0.2% (w/v) colchicine solution. While no seedling growth was identified in the 0.2% colchicine treatment, the survival and the growth in the seeds treated with other concen-

Table 1. Results of the analysis of variance (ANOVA) for the effect of colchicine concentration and treatment duration on the mortality of *Papaver bracteatum* seeds.

Source of Variation	Mean Squares	
	Seed mortality	Seedling mortality
Colchicine concentration (C)	13097.26**	13173.03**
Treatment duration (D)	126.22n.s.	162.97*
C*D interaction	116.51*	70.15n.s.

**, * and n.s. indicate significant at 1%, 5% level and and not significant, respectively.

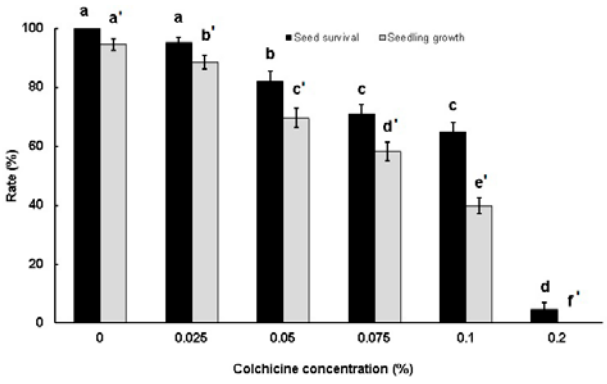

Figure 1. Effect of colchicine concentration on seed survival and seedling growth of treated *Papaver bracteatum* explants. All values are in percentage. Mean values specified by the same latter are not significantly different at $P<0.05$ by LSD test. Letters with a prime symbol designate mean differences in seedling growth.

Table 2. Effect of colchicine concentration and treatment duration on the percentage (mean ± standard error) of seed mortality, seedling mortality, diploid (2*x*), mixoploid (2*x*+4*x*), and tetraploid (4*x*) explants in *Papaver bracteatum*.

Colchicine concentration (%)	Exposure duration (h)	Seed mortality (%)	Seedling mortality (%)	2*x* (%)	2*x* + 4*x* (%)	4*x* (%)
0.000	4	0.00 ± 0.00	4.76 ± 4.76	95.24 ± 4.76	0.00 ± 0.00	0.00 ± 0.00
	8	0.00 ± 0.00	0.00 ± 0.00	100.00 ± 0.00	0.00 ± 0.00	0.00 ± 0.00
	12	0.00 ± 0.00	4.76 ± 4.76	95.24 ± 4.76	0.00 ± 0.00	0.00 ± 0.00
	24	0.00 ± 0.00	4.76 ± 4.76	95.24 ± 4.76	0.00 ± 0.00	0.00 ± 0.00
	36	0.00 ± 0.00	9.52 ± 9.52	90.48 ± 9.52	0.00 ± 0.00	0.00 ± 0.00
	48	0.00 ± 0.00	0.00 ± 0.00	100.00 ± 0.00	0.00 ± 0.00	0.00 ± 0.00
	72	0.00 ± 0.00	4.76 ± 4.76	95.24 ± 4.76	0.00 ± 0.00	0.00 ± 0.00
	168	0.00 ± 0.00	14.29 ± 8.25	85.71 ± 8.25	0.00 ± 0.00	0.00 ± 0.00
0.025	4	4.76 ± 4.76	4.76 ± 4.76	90.48 ± 4.76	0.00 ± 0.00	0.00 ± 0.00
	8	14.29 ± 8.25	0.00 ± 0.00	85.71 ± 8.25	0.00 ± 0.00	0.00 ± 0.00
	12	0.00 ± 0.00	9.52 ± 9.52	90.48 ± 9.52	0.00 ± 0.00	0.00 ± 0.00
	24	14.29 ± 8.25	4.76 ± 4.76	80.95 ± 4.76	0.00 ± 0.00	0.00 ± 0.00
	36	0.00 ± 0.00	4.76 ± 4.76	95.24 ± 4.76	0.00 ± 0.00	0.00 ± 0.00
	48	0.00 ± 0.00	14.29 ± 8.25	85.71 ± 8.25	0.00 ± 0.00	0.00 ± 0.00
	72	0.00 ± 0.00	4.76 ± 4.76	95.24 ± 4.76	0.00 ± 0.00	0.00 ± 0.00
	168	4.76 ± 4.76	9.52 ± 4.76	85.71 ± 8.25	0.00 ± 0.00	0.00 ± 0.00
0.050	4	9.52 ± 4.76	14.29 ± 8.25	33.33 ± 17.17	19.05 ± 4.76	23.81 ± 12.60
	8	28.57 ± 8.25	4.76 ± 4.76	19.05 ± 4.76	23.81 ± 12.60	23.81 ± 12.60
	12	28.57 ± 14.29	9.52 ± 4.76	0.00 ± 0.00	23.81 ± 4.76	38.10 ± 9.52
	24	4.76 ± 4.76	4.76 ± 4.76	23.81 ± 17.17	33.33 ± 4.76	33.33 ± 17.17
	36	23.81 ± 9.52	9.52 ± 9.52	19.05 ± 12.60	19.05 ± 4.76	28.57 ± 16.50
	48	19.05 ± 9.52	19.05 ± 12.60	38.10 ± 12.60	14.29 ± 0.00	9.52 ± 9.52
	72	0.00 ± 0.00	19.05 ± 4.76	57.14 ± 0.00	23.81 ± 4.76	0.00 ± 0.00
	168	28.57 ± 8.25	19.05 ± 4.76	28.57 ± 16.50	14.29 ± 0.00	9.52 ± 9.52
0.075	4	28.57 ± 14.29	14.29 ± 0.00	9.52 ± 9.52	33.33 ± 4.76	14.29 ± 8.25
	8	9.52 ± 4.76	19.05 ± 4.76	14.29 ± 8.25	23.81 ± 4.76	33.33 ± 4.76
	12	42.86 ± 8.25	4.76 ± 4.76	14.29 ± 0.00	28.57 ± 8.25	9.52 ± 9.52
	24	9.52 ± 4.76	9.52 ± 4.76	23.81 ± 4.76	23.81 ± 4.76	33.33 ± 9.52
	36	38.10 ± 4.76	9.52 ± 4.76	4.76 ± 4.76	23.81 ± 4.76	23.81 ± 12.60
	48	33.33 ± 4.76	14.29 ± 8.25	9.52 ± 4.76	19.05 ± 4.76	23.81 ± 4.76
	72	38.10 ± 4.76	14.29 ± 8.25	19.05 ± 9.52	19.05 ± 4.76	9.52 ± 4.76
	168	33.33 ± 9.52	14.29 ± 0.00	19.05 ± 12.60	9.52 ± 4.76	23.81 ± 4.76
0.100	4	33.33 ± 9.52	19.05 ± 4.76	0.00 ± 0.00	23.81 ± 9.52	23.81 ± 4.76
	8	33.33 ± 4.76	19.05 ± 12.60	9.52 ± 4.76	14.29 ± 0.00	23.81 ± 9.52
	12	47.62 ± 4.73	14.29 ± 4.25	0.00 ± 0.00	14.29 ± 0.00	23.81 ± 4.76
	24	23.81 ± 9.52	28.57 ± 8.25	4.76 ± 4.76	19.05 ± 4.76	23.81 ± 4.76
	36	28.57 ± 8.25	33.33 ± 12.60	9.52 ± 9.52	14.29 ± 0.00	14.29 ± 8.25
	48	28.57 ± 14.29	28.57 ± 8.25	14.29 ± 8.25	14.29 ±0.00	14.29 ± 8.25
	72	38.10 ± 9.52	28.57 ± 8.25	4.76 ± 4.76	9.52 ± 4.76	19.05 ± 4.76
	168	47.62 ± 9.52	28.57 ± 0.00	9.52 ± 4.76	4.76 ± 4.76	9.52 ± 4.76
0.200	4	76.19 ± 12.60	23.81 ± 12.60	0.00 ± 0.00	0.00 ± 0.00	0.00 ± 0.00
	8	90.48 ± 9.52	9.52 ± 9.52	0.00 ± 0.00	0.00 ± 0.00	0.00 ± 0.00
	12	95.24 ± 4.76	4.76 ± 4.76	0.00 ± 0.00	0.00 ± 0.00	0.00 ± 0.00
	24	100.00 ± 0.00	0.00 ± 0.00	0.00 ± 0.00	0.00 ± 0.00	0.00 ± 0.00
	36	100.00 ± 0.00	0.00 ± 0.00	0.00 ± 0.00	0.00 ± 0.00	0.00 ± 0.00
	48	100.00 ± 0.00	0.00 ± 0.00	0.00 ± 0.00	0.00 ± 0.00	0.00 ± 0.00
	72	100.00 ± 0.00	0.00 ± 0.00	0.00 ± 0.00	0.00 ± 0.00	0.00 ± 0.00
	168	100.00 ± 0.00	0.00 ± 0.00	0.00 ± 0.00	0.00 ± 0.00	0.00 ± 0.00

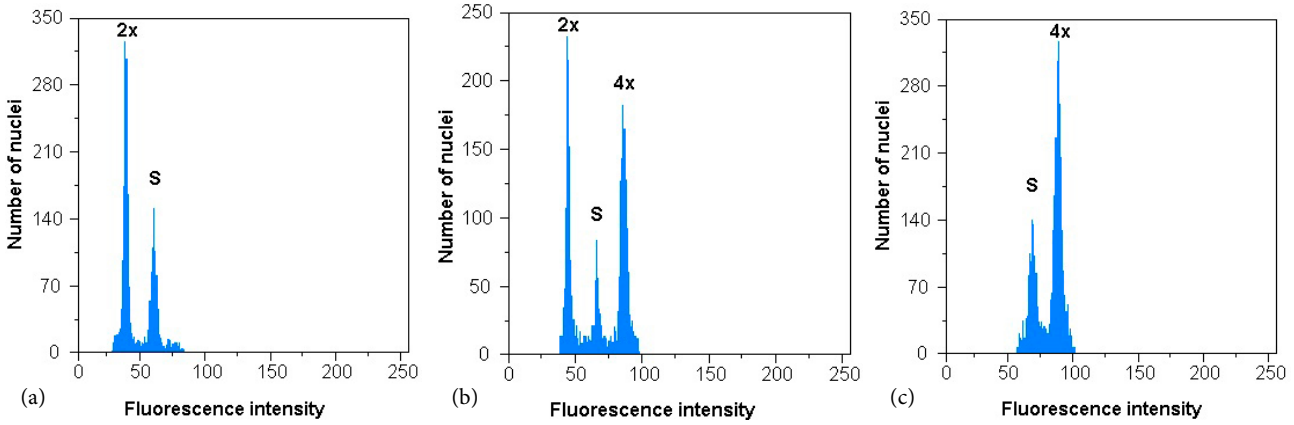

Figure 2. Flow cytometric histogram of the relative fluorescence intensity of nuclei isolated from *Papaver bracteatum* plants. Histograms show the nuclei isolated form diploid (a), mixoploid (b), and induced tetraploid (c) plants. The S in each histogram indicates the peak resulted by the cells of the *Pisum sativum* cv. 'Citrad' (2C DNA=9.09 pg) used as the internal standard.

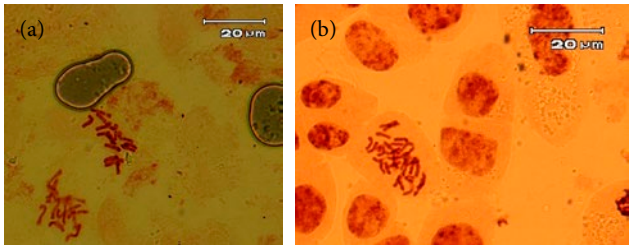

Figure 3. Chromosome numbers of surveyed *Papaver bracteatum* plants. Number of chromosomes in diploid ($2n=2x=14$) (a) and artificially induced tetraploid ($2n=4x=28$) (b) plants are compared.

Table 3. Results of the analysis of variance (ANOVA) for the effect of colchicine concentration and treatment duration on the polyploidy induction rate in *Papaver bracteatum*.

Source of Variation	Mean Squares
Colchicine concentration (C)	16.98**
Treatment duration (D)	2.57*
C*D interaction	1.11n.s.

**, * and n.s. indicate significant at 1%, 5% level and and not significant, respectively.

trations varied widely, where the mean germination percentage and the mean percentage of developed seedlings in the 0.1% treatment were 64.88±3.22 and 39.88±2.72, respectively (Table 2). These values were 95.24 ± 1.86 and 88.69 ± 2.27 in the 0.025% treatment, respectively (Fig. 1).

Flow cytometry analysis of ploidy level

The ploidy level of colchicine-treated plants was determined by FCM analysis. All treated plants with apparently normal growth and development were classified into three main classes including diploids ($2x$), mixoploids ($2x+4x$) and tetraploids ($4x$). As shown in related histograms (Fig. 2), diploid and tetraploid plants revealed a peak at the position of channels 50 and 95 of the relative fluorescent intensity respectively, while mixoploids revealed two peaks with variable heights at both channels 50 and 95.

The 2C DNA contents of the diploid and induced tetraploid plants were estimated as 6.15±0.03 (Fig. 2a) and 11.95±0.07 pg (Fig. 2c), respectively. The ploidy status of the resultant events was additionally confirmed by microscopic chromosome counting in plants with different ploidy levels. It was indicated that all diploid plants had a chromosome number of $2n=2x=14$ (Fig. 3a), whereas all tetraploids had $2n=4x=28$ (Fig. 3b). In the present study, significant differences between induction treatments were seen based on the induction efficiency data. The results showed that both higher concentrations of colchicine and longer durations of exposure to colchicine resulted in a significantly larger percentage of tetraploid plants (Table 3). The highest induction efficiency (31.29) was yielded by 0.05% (w/v) colchicine concentration at exposure duration of 24 h. The next two most efficient treatments were 0.75% (w/v)-24 h and 0.05% (w/v)-12 h with induction efficiency values of 27.89 and 25.85 respectively (Figs. 4, 5).

Anatomical and morphological characteristics

Stomata data measured on the leaves of plants in each class of ploidy showed that the stomata size in

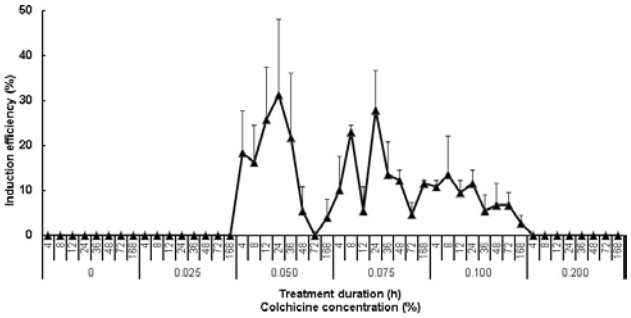

Figure 4. Effect of colchicine concentration and treatment duration on tetraploidy induction efficiency in *Papaver bracteatum*. Bars show standard errors.

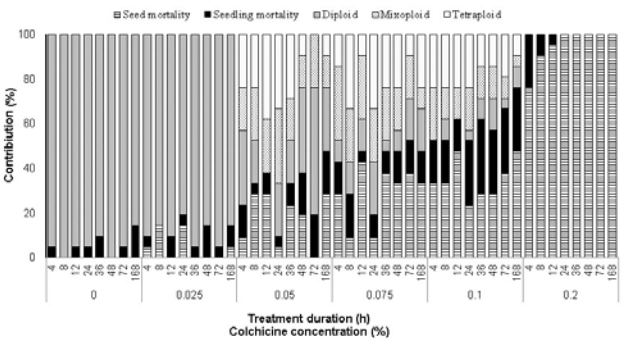

Figure 5. Effect of colchicine concentration and treatment duration on the contribution (%) of seed mortality, seedling mortality, diploid, mixoploid, and tetraploid explants produced during polyploidy induction in *Papaver bracteatum*.

tetraploid plants was larger than that in diploids (P<0.01; Figs. 6a, 6b). The average stomata area for the diploid and tetraploid (Figs. 7a, b, respectively) plants was 531.44±24.02 and 868.98±55.66 μm^2 respectively indicating a 63.51% increase in stomata area of tetraploid plants. It was also included that the stomata length in tetraploid plants (40.46±1.33 μm) was 30.06% larger than that in diploids (31.10±0.89 μm).

In addition, a significant difference was identified between diploid and polyploid plants in the stomatal density (P<0.01), where the average number of stomata per square millimetre in the leaves of diploid and tetraploid (Figs. 7c, d, respectively) plants was 236.18±10.54 and 157.14±3.78, respectively (Fig. 6c). In other words, tetraploidy induction caused a 50.3% decrease in sto-

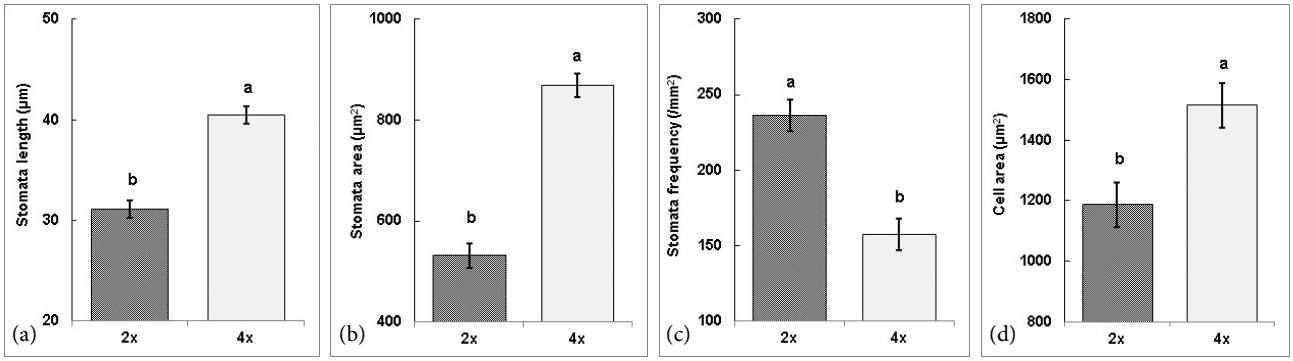

Figure 6. Comparison of anatomical traits between diploid and tetraploid plants of *Papaver bracteatum* at the cellular level. The stomata length (a), stomata area (b), stomata frequency (c), and stomata cell area (d) are significantly changed in induced tetraploid plants. Mean values specified by different letters are significantly different at P<0.05 by Students's *t* test. Bars show standard errors.

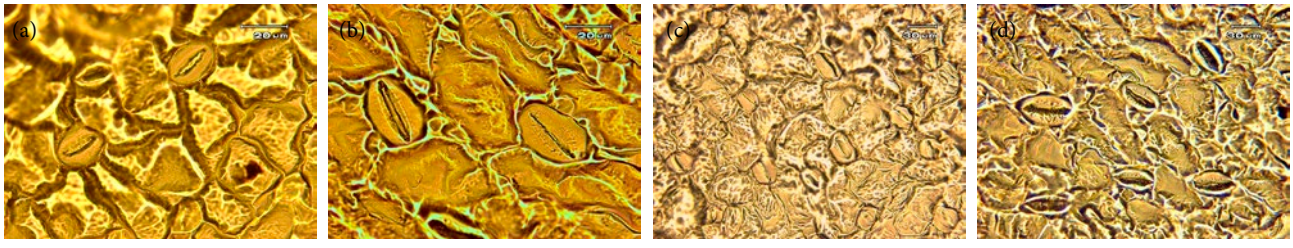

Figure 7. Impressions illustrating the size and density of the stomata in the leaf lower epidermis of *Papaver bracteatum* plants. The smaller stomata size in diploid (a) than in induced tetraploid (b) plants and the lower stomata density in diploid (c) than in tetraploid (d) plants are illustrated.

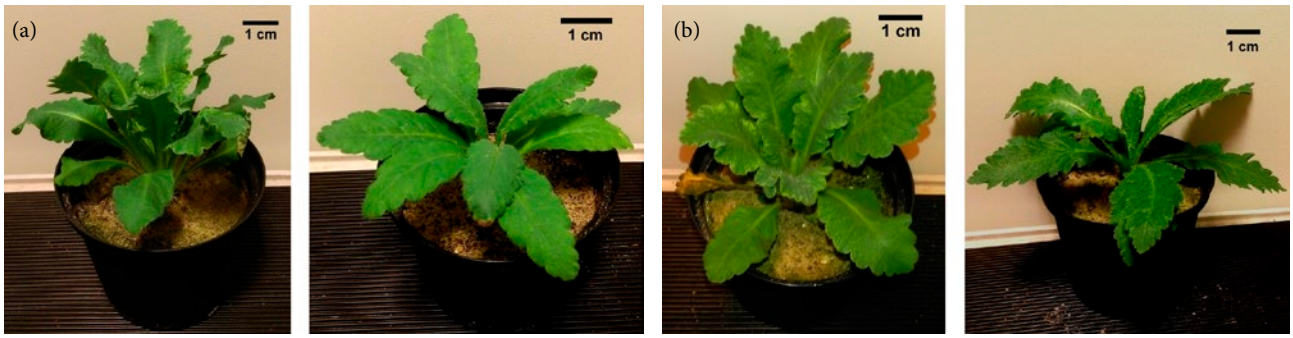

Figure 8. Comparison of visible morphological traits at the whole plant level. The illustrated diploid (a) and tetraploid (b) *Papaver bracteatum* plants are all at the same age (195 d) and acclimated under similar environmental condition.

mata density in studied *P. bracteatum* plants. Data regarding the cell size showed that the average leaf cell area in diploid and tetraploid *P. bracteatum* plants was 1187.20±73.93 and 1515.12±118.31, respectively indicating a 27.62% increase in epidermal cell area of tetraploid plants ($P < 0.05$; Fig. 6d). Unlike in the stomatal morphology, tetraploid plants exhibited no remarkable differences in visible morphological traits such as plant height, shoot or leaf thickness and growth rate compared to their diploid counterparts (Fig. 8).

DISCUSSION

The results regarding the colchicine effects on survival of seeds and seedlings are in agreement with those reported in various plant species e.g. *Berberis thunbergii* (Lehrer *et al.* 2008), *Tanacetum parthenium* (Majdi *et al.* 2010) and *Thymus persicus* (Tavan *et al.* 2015), indicating that the toxic effects of colchicine as an anti-mitotic chemical is largely influenced by the colchicine concentration (Table 1). The toxic effects of colchicine on the treated Persian poppy were expressed as two different criteria including seed mortality and seedling mortality. The results showed that increased colchicine concentration significantly increased the level of both lethal effects and decreases the ability of treated plants to survive and grow (Table 2).

The C-value index defined as the DNA content of an unreplicated haploid chromosome complement (i.e. a gamete) is highly useful in systematics, genome size estimation and many other biological fields related to eukaryotic organisms (Doležel and Bartoš 2005). During normal mitosis two daughter cells each with 2C DNA content is formed (Doležel *et al.* 2003). Therefore, the 2C DNA content of a tetraploid cell which is resulted by mitotic arrest is expected to be about two times that of the progenitor diploid cells. In the present study, the calculated 2C DNA contents of the diploid and tetraploid plants were estimated as 6.15±0.03 (Fig. 3a) and 11.95±0.07 pg (Fig. 3b), respectively, indicating the successful induction of tetraploidy. Furthermore, these results suggest the effectiveness of FCM-based analysis as a rapid and reliable strategy for discriminating *P. bracteatum* from other identified or unidentified *Papaver* species with similar morphological traits and different 2C DNA values.

Tetraploid induction efficiency has frequently been used in previous studies (Bouvier *et al.* 1994; Lehrer *et al.* 2008; Majdi *et al.* 2010) as a measure for identifying the most effective treatments capable of inducing complete and stable polyploidy. It is known as reliable index because it takes into account not only the rate of conversion of diploidy tetraploidy, but the survival rate of successful tetraploid events (Lehrer *et al.* 2008). Our results showed that both higher concentrations of colchicine and longer durations of exposure to colchicine resulted in a significantly larger percentage of tetraploid seedlings, but their interaction effect was non-significant (Table 3). There are several reports about the evaluation of the effects by the concentration of the anti-miotic agent and treatment duration as the two main determining factors in polyploidy induction efficiency in different plant types. For instance, Stanys *et al.* (2006) working on *Chaenomeles japonica* reported that with both colchicine and oryzalin as the anti-mitotic agents, the efficiency of ploidy induction was mainly dependent on the concentration of anti-mitotic agent rather than its exposure duration. On the other hand, several authors suggested that the polyploidy induction efficiency is associated with both optimum concentration and the duration of anti-miotic (Gu *et al.* 2005; Tang *et al.* 2010; Tavan *et al.* 2015).

The results of FCM analysis showed that mixoploid plants could be expected to form a large contribution of polyploids sometimes as high as 33% of induc-

tion results obtained by *in vitro* polyploidy induction in *P. bracteatum* (Table 2; Fig. 5). In polyploidy induction works, high percentage of mixoploid results are generally known as a drawback of the procedure because their unstable polyploidy state often reverts partially or totally to the diploid condition after successive cell division cycles. It occurs mainly because the remaining diploid cells proliferate at higher rates than the tetraploid ones (Mergen and Lester 1971). During artificial polyploidy induction, colchicine influences actively dividing cells in the treated tissues and polyploidization therefore occurs unequally among explant cells, leading to the occurrence of mixoploids and chimeras (Wan *et al*. 1989). Accordingly, a low growth rate and intrinsically stunted development in treated plants are expected to aggregate these effects particularly in short exposure durations leading to a higher proportion of mixoploid events among polyploidy induction results. Chakraborti *et al*. (1998) suggested that in *in vitro* induction methods, the occurrence of mixoploids may have been minimized by growing the treated plants under more favorable conditions. They stated that the uniformity of environmental factors like temperature and photoperiod may favor the synchronous division of meristematic cells and help minimize the mixoploid events leading to a high tetraploidy rate (Chakraborti *et al*. 1998).

The ratio of tetraploid to diploid cells based on the analysed FCM data can be calculated as a measure of the contribution of tetraploid cells within a mixoploid event. The values higher than one indicate a higher percentage of tetraploid cells than the diploids. In the present study, the obtained values indicated a high degree of variability in polyploidy induction capability of colchicine in *P. bracteatum* (detailed data not shown because of the large number of hits and lack of a significant interaction). In addition, it was interestingly observed that varying values of the ratio of tetraploid to diploid cells might be obtained by the same concentration-duration combination. For example, both values of 0.19 and 1.75 which indicate a low and a high contribution of tetraploid cells respectively, were seen in the mixoploid events resulted by the 0.05%- 24h treatment combination. So despite of favorable and controlled environmental factors within *in vitro* induction and growth environments, large differences between induction capabilities of certain concentration-duration combinations were revealed by the variable degrees of mixoploidy obtained by the same treatment combination. These results indicate that the effectiveness of anti-mitotic agent in polyploidy induction in *P. bracteatum* can be determined mainly by the explant and cell-related factors rather than those related to the induction environment. However, the rather high percentage of mixoploid events yielded by *in vitro* colchicine treating of *P. bracteatum* explants as well as the wide range of the ratio of tetraploid to diploid cells within mixoploid events can be explained by the incomplete effects of colchicine on meristematic cells in the treated explants. These incomplete effects could be aggravated by the intrinsically stunted growth of *P. bracteatum*. Indeed, short exposure times and lower concentrations of the anti-mitotic agent during polyploidy induction may in turn decrease the chance for complementation of polyploidization process leading to a higher degree of mixoploidy (Wan *et al*. 1989).

A recent study by Tavan *et al*. (2015) on *Thymus persicus* has showed that the mixoploid events which were produced during polyploidy induction in *Thymus persicus* had a considerable capability for producing pharmaceutically important compounds. They reported significantly increased production of medicinal triterpenoids in both tetraploid and mixoploid results as compared to their diploid progenitors, where mixoploid plants interestingly yielded significantly higher contents of Betulinic acid, Oleanolic acid and Ursolic acid even than successfully induced tetraploids (Tavan *et al*. 2015). Additionally, successful generation of tetraploid plants from mixoploid progenitors using tetraploid cells of leaf callus through callus-based techniques and tissue culture strategies has been previously reported in various plant species such as *Humulus lupulus* L. (Roy *et al*. 2001), *Astragalus membranaceus* (Chen and Gao 2007) and *Echinacea purpurea* L. (Dahanayake *et al*. 2010). Likewise Shao *et al*. (2003) reported that further subculture of mixoploid events resulted by *in vitro* colchicine treatment of shoots in *Punica granatum* L. resulted in their separation to tetraploid and diploid progenies. This strategy has been recommended to be employed when an anti-mitotic agent generates a high degree of mixoploid events during tetraploidy induction. In general, the mixoploids can therefore be considered as valuable sources of genetic material in ploidy breeding programs. They particularly can be employed for certain plant species which are expected to produce high numbers of mixoploid events during polyploidy induction works. Application of tissue culture techniques in *P. bracteatum* has been well established, where successful *in vitro* regeneration pf this species using callus derived from seedlings (Ilahi and Ghauri 1994), roots, seeds and cotyledons (Rostampour *et al*. 2010) as well as through cell suspension culture (Farjaminezhad *et al*. 2013) and hairy roots (Sharafi *et al*. 2013) have previously been reported. Therefore, it allows combination polyploidy induction strategies and tissue culture techniques to achieve higher goals in *P. bracteatum* breeding programs.

These obtained results indicating increased stomata size (Fig. 6a) and decreased stomata frequency (Fig. 6c) in tetraploid plants as compared to their diploid progenitors are in agreement with those of several previous reports in different plant types. Furthermore, differences in stomata size and density are frequently reported to successfully discriminate plants with different ploidy levels, where polyploid plants are often known to have, on average, a lower stomata number per leaf area unit and increased size of the stomata and guard cells (de Carvalho 2005; Tang *et al*. 2010; Gantait *et al*. 2011; Aina *et al*. 2012) as well as an increased number of chloroplasts in stomatal guard cells (Ewald *et al*. 2009). Gantait *et al*. (2011) suggested that the lower density of stomata in polyploid plants was due to the larger stomata and epidermal cell size, as well as reduced stomata differentiation.

The cell size is also reported to be related to polyploidy level and to be significantly different between induced tetraploid plants and their diploid progenitors (Melaragno *et al*. 1993). It is suggested as a potential anatomical indicator of ploidy level being capable of discriminating plants in a mixed population of tetraploid and diploids (Zeng *et al*. 2006). The results regarding the cell size in the plants with different ploidy levels showed that the tetraploid *P. bracteatum* plants had significantly larger leaf epidermal cells than diploid plants (Figs. 6b, 6c). These results confirm previous reports where larger cell dimensions were reported for tetraploid plants as compared to their diploid progenitors in various plant species such as *Fortunella crassifolia*, *Citrus sinensis* (Zeng *et al*. 2006), *Tanacetum parthenium* (Majdi *et al*. 2010) and *Thymus persicus* (Tavan *et al*. 2015).

The results obtained in this study indicated that certain anatomical traits such as leaf epidermal cell and stomata size and frequency may serve as reliable criteria for screening of *P. bracteatum* plants for ploidy level. However, other routinely suggested anatomical, morphological or physiological charachteristics such as chlorophyll florescence, flower size and morphology, pollen grain size, chloroplast density, enzymatic activity, etc. have to be evaluated precisely before being employed as potential indicators of ploidy level in quick evaluation and successful screening of large numbers of *P. bracteatum* plants. Because in the present study, unlike in the stomatal morphology, the colchicine-treated plants did not exhibit any remarkable differences in visible morphological traits such as plant height, shoot or leaf thickness and growth rate (Fig. 8). These observations were in agreement with those reported by Milo *et al*. (1987) who stated that there were no significant differences between *P. bracteatum* plants with different ploidy levels in the morphological traits such as plant height, flower size or in the height of the flowering stem. However, the artificially induced tetraploid plants of *P. bracteatum* were reported to flower later than diploid plants. Their capsules also matured significantly later than their diploid plants (Milo *et al*. 1987).

The lack of visible morphological distinctions between diploid and tetraploid *P. bracteatum* plants might be attributed to the high morphological variation observed in this species particularly in its natural habitat. Wild *P. bracteatum* plants naturally exhibit high variation in plant size, growth rate and other visible characteristics. So, the new polyploid variants are likely to still fall within the wide variation range that already exists in wild *P. bracteatum* populations. Consequently, like their diploid progenitors, tetraploid plants are expected to reveal a wide range of morphological variation. Hence, ploidy statuses of the induction results need to be confirmed by quick, easy and reliable criteria such as flow cytometry techniques rather than morphological measures.

In conclusion, polyploidy was successfully induced in diploid Persian poppy (*Papaver bracteatum* Lindl.) through colchicine treatment of newly germinated seeds. Tetraploid and mixoploid progenies were quickly and effectively recognized by FCM technique and the 2C DNA content. Both colchicine concentration and exposure duration were known as determining factors in success of *in vitro* tetraploidy induction. Morphological traits like stomata size and frequency and cell size were significantly associated with ploidy level in Persian poppy and were known as reliable criteria for preliminary screening of mixed populations based on ploidy level. Further research works are in progress to study the ploidy level dependent secondary metabolites and potentially major candidate gene expressions particularly of those of great importance in biosynthesis and production of pharmaceutically valuable alkaloids.

ACKNOWLEDGMENT

The authors gratefully acknowledge the support provided for this project by the Tarbiat Modares University (TMU).

REFERENCES

Abedi R, Babaei A and Karimzadeh G. 2015. Karyological and flow cytometric studies of Tulipa (Liliaceae) species from Iran. Plant Syst Evol. 301(5):1473-1484.

Adams KL, Wendel JF. 2005. Polyploidy and genome evolution in plants. Curr Opin Plant Biol. 8(2):135-141.

Aina O, Quesenberry K, Gallo M. 2012. *In vitro* induction of tetraploids in *Arachis paraguariensis*. Plant Cell Tiss Organ Cult. 111(2):231-238.

Beest M, Le Roux JJ, Richardson DM, Brysting AK, Suda J, Kubesova M, Pysek P. 2012. The more the better? The role of polyploidy in facilitating plant invasions. Ann Bot. 109(1):19-45.

Bouvier L, Fillon FR, Lespinasse Y. 1994. Oryzalin as an efficient agent for chromosome doubling of haploid apple shoots *in vitro*. Plant Breed. 113(4):343-346.

Chakraborti SP, Vijayan K, Roy BN, Qadri SMH. 1998. *In vitro* induction of tetraploidy in mulberry (*Morus alba* L.). Plant Cell Rep. 17(10):799-803.

Chen L, Gao S. 2007. *In vitro* tetraploid induction and generation of tetraploids from mixoploids in *Astragalus membranaceus*. Sci Hortic. 112(3):339-344.

Dahanayake N, Chen XL, Zhao FC, Yang YS, Wu H. 2010. Separation of trtraploid and diploid plants from chimeras in *in vitro* cultures of purple coneflower (*Echinacea purpurea* L.). Trop Agr Res Ext. 13(1):11-15.

de Carvalho JFRP, de Carvalho CRDP, Otoni WC. 2005. *In vitro* induction of polyploidy in annatto (*Bixa orellana*). Plant Cell Tiss Organ Cult. 80(1):69-75.

Dhawan OP, Lavania UC. 1996. Enhancing the productivity of secondary metabolites via induced polyploidy: a review. Euphytica. 87(2):81-89.

Doležel J, Bartoš J. 2005. Plant DNA flow cytometry and estimation of nuclear genome size. Ann Bot. 95(1):99-110.

Doležel J, Greilhuber J, Suda J. 2007. Estimation of nuclear DNA content in plants using flow cytometry. Nat Protocols. 2(9):2233-2244.

Doležel J .2003. Nuclear DNA content and genome size of trout and human. Cytometry. 51:127-129.

Doležel J, Greilhuber J, Lucretti S, Meister A, Lysak MA, Nardi L, Obermayer R. 1998. Plant genome size estimation by flow cytometry: Inter-laboratory comparison. Ann Bot. 82(suppl_1):17-26.

Duke JA. 1973. Utilization of papaver. Econ Bot. 27(4):390-400.

Ewald D, Ulrich K, Naujoks G, Schröder MB. 2009. Induction of tetraploid poplar and black locust plants using colchicine: chloroplast number as an early marker for selecting polyploids *in vitro*. Plant Cell Tiss Organ Cult. 99(3):353-357.

Farjaminezhad R, Zare N, Asghari Zakaria S, Farjaminezhad M. 2013. Establishment and optimization of cell growth in suspension culture of *Papaver bracteatum*: a biotechnology approach for thebaine production. Turk J Biol. 37(6):689-697.

Gantait S, Mandal N, Bhattacharyya S, Das PK. 2011. Induction and identification of tetraploids using *in vitro* colchicine treatment of *Gerbera jamesonii* Bolus cv. Sciella. Plant Cell Tiss Organ Cult. 106(3):485-493.

Gu XF, Yang AF, Meng H, Zhang JR. 2005. *In vitro* induction of tetraploid plants from diploid *Zizyphus jujube* Mill. cv. Zhanhua. Plant Cell Rep. 24(11):671-676.

Ilahi I, Ghauri EG. 1994. Regeneration in cultures of *Papaver bracteatum* as influenced by growth hormones and temperature. Plant Cell Tiss Organ Cult. 38(1):81-83.

Javadian N, Karimzadeh G, Sharifi M, Moieni A, Behmanesh M. 2017. *In vitro* polyploidy induction: changes in morphology, podophyllotoxin biosynthesis, and expression of the related genes in *Linum album* (Linaceae). Planta. 245(6):1165-1178.

Kaensaksiri T, Soontornchainaksaeng P, Soonthornchareonnon N, Prathanturarug S. 2011. *In vitro* induction of polyploidy in *Centella asiatica* (L.) Urban. Plant Cell Tiss Organ Cult. 107(2):187-194.

Karimzadeh G, Danesh-Gilevaei M, Aghaalikhani M. 2011. Karyotypic and nuclear DNA variations in *Lathyrus sativus* (Fabaceae). Caryologia. 64(1):42-54.

Karimzadeh G, Mousavi SH, Kermani MJ, Jalali-Javaran M. 2010. Karyological and nuclear DNA variation in Iranian endemic muskmelon (*Cucumis melo* var. Inodorus). Cytologia. 75(4):451-461.

Kermani MJ, Sarasan V, Roberts AV, Yokoya K, Wentworth J, Sieber VK. 2003. Oryzalin-induced chromosome doubling in *Rosa* and its effect on plant morphology and pollen viability. Theor Appl Genet. 107(7):1195-1200.

Kulkarni M, Borse T. 2010. Induced polyploidy with gigas expression for root traits in *Capsicum annuum* (L.). Plant Breeding. 129(4):461-464.

Lehrer JM, Brand MH, Lubell JD. 2008. Induction of tetraploidy in meristematically active seeds of Japanese barberry (*Berberis thunbergii* var. *atropurpurea*) through exposure to colchicine and oryzalin. Sci Hortic. 119(1):67-71.

Liu Y, Hui RK, Deng RN, Wang JJ, Wang M, Li ZY. 2012. Abnormal male meiosis explains pollen sterility in the polyploid medicinal plant *Pinellia ternata* (Araceae). Genet Mol Res. 11(1):112-120.

Loureiro J, Rodriguez E, Doležel J. Santos C. 2007. Two new nuclear isolation buffers for plant DNA flow cytometry: a test with 37 species. Ann Bot. 100(4):875-888.

Madam PRK. 2011. Aspects of the biology of *Papaver bracteatum* Lind, a new crop for Tasmania [dissertation]. Tasmania: University of Tasmania.

Majdi M, Karimzadeh G, Malboobi M, Omidbaigi R, Mirzaghaderi G. 2010. Induction of tetraploidy to feverfew (*Tanacetum parthenium* Schulz-Bip.): mor-

phological, physiological, cytological, and phytochemical changes. HortScience. 45(1):16-21.

Marzougui N, Boubaya A, Thabti I, Elfalleh W, Guasmi F, Ferchichi A. 2011. Polyploidy induction of Tunisian *Trigonella foenumgreaum* L. populations. Afr J Biotechnol. 10(43):8570-8577.

Miller M, Zhang C, Chen ZJ. 2012. Ploidy and hybridity effects on growth vigor and gene expression in *Arabidopsis thaliana* hybrids and their parents. G3 (Bethesda). 2(4):505-513.

Milo J, Levy A, Palevitch D, Ladizinsky G. 1987. Thebaine content and yield in induced tetraploid and triploid plants of *Papaver bracteatum* Lindl. Euphytica. 36(2):361-367.

Mishra BK, Pathak S, Sharma A, Trivedi PK, Shukla S. 2010. Modulated gene expression in newly synthesized auto-tetraploid of *Papaver somniferum* L. S Afr J Bot. 76(3):447-452.

Melaragno JE, Mehrotra B, Coleman AW. 1993. Relationship between endopolyploidy and cell size in epidermal tissue of *Arabidopsis*. Plant Cell. 5(11):1661-1668.

Murashige T, Skoog F. 1962. A revised medium for rapid growth and bio-assays with tobacco tissue cultures. Physiol Plant. 15(3):473-497.

Ntuli NR, Zobolo AM. 2008. Effect of water stress on growth of colchicine induced polyploid *Coccinia palmata* and *Lagenaria sphaerica* plants. Afr J Biotechnol. 7(20):3648-3652.

Nyman U, Bruhn JG. 1979. *Papaver bracteatum*-a Summary of Current Knowledge. Planta Med. 35(2):97-117.

Omidbaigi R, Mirzaee M, Hassani, ME, Sedghi Moghadam M. 2010. Induction and identification of polyploidy in basil (*Ocimum basilicum* L.) medicinal plant by colchicine treatment. Int J Plant Prod. 4(2):87-98.

Omidbaigi R, Yavari S, Hassani, ME, Yavari S. 2010. Induction of autotetraploidy in dragonhead (*Dracocephalum moldavica* L.) by colchicine treatment. J Fruit Ornam Plant Res. 18(1):23-35.

Rodrigues FA, Rodrigues Soares JD, Rocha dos Santos R, Pasqual M, Oliveira e Silva S. 2011. Colchicine and amiprophos-methyl (APM) in polyploidy induction in banana plant. Afr J Biotechnol. 10(62):13476-13481.

Rostampour S, Hashemi Sohi H, Dehestani A. 2010. *In vitro* regeneration of Persian poppy (*Papaver bracteatum*). Biologia. 65(4):647-652.

Roy AT, Leggett G, Koutoulis A. 2001. *In vitro* tetraploid induction and generation of tetraploids from mixoploids in hop (*Humulus lupulus* L.). Plant Cell Rep. 20(6):489-495.

Sadat Noori SA, Norouzi M, Karimzadeh G, Shirkool Kh, Niazian M. 2017. Effect of colchicine-induced polyploidy on morphological characteristics and essential oil composition of ajowan (*Trachyspermum ammi* L.). Plant Cell Tiss Organ Cult. 130(3):543-551.

Sakhanokho HF, Rajasekaran K, Kelley RY, Islam-Faridi N. 2009. Induced polyploidy in diploid ornamental ginger (*Hedychium muluense* R. M. Smith) using colchicine and oryzalin. HortScience. 44(7):1809-1814.

Seddigh M, Jolliff GD, Calhoun W, Crane JM. 1982. *Papaver bracteatum*, potential commercial source of codeine. Econ Bot. 36(4):433-441.

Shao J, Chen C, Deng X. 2003. *In vitro* induction of tetraploidy in pomegranate (*Punica granatum*). Plant Cell Tiss Organ Cult. 75(3):241-246.

Sharafi A, Hashemi Sohi H, Mousavi A, Azadi P, Razavi K, Ntui VO. 2013. A reliable and efficient protocol for inducing hairy roots in *Papaver bracteatum*. Plant Cell Tiss Organ Cult. 113(1):1-9.

Sharghi N, Lalezari I. 1967. *Papaver bracteatum* Lindl., a highly rich source of thebaine. Nature. 213(5082):1244-1244.

Stanys V, Weckman A, Staniene G, Duchovskis P. 2006. *In vitro* induction of polyploidy in Japanese quince (*Chaenomeles japonica*). Plant Cell Tiss Organ Cult. 84(3):263-268.

Tavan M, Mirjalili MH, Karimzadeh G. 2015. *In vitro* polyploidy induction: changes in morphological, anatomical and phytochemical characteristics of *Thymus persicus* (Lamiaceae). Plant Cell Tiss Organ Cult. 122(3):573-583.

Tang ZQ, Chen DL, Song ZJ, He YC, Cai DT. 2010. *In vitro* induction and identification of tetraploid plants of *Paulownia tomentosa*. Plant Cell Tiss Organ Cult. 102(2):213-220.

Thao NTP, Ureshino K, Miyajima I, Ozaki Y, Okubo H. 2003. Induction of tetraploids in ornamental *Alocasia* through colchicine and oryzalin treatments. Plant Cell Tiss Organ Cult. 72(1):19-25.

Wan Y, Petolin JF, Widholm JM. 1989. Efficient production of doubled haploid plants through colchicine treatment of anther-derived maize callus. Theor Appl Genet. 77(6):889-892.

Wu FF, Dobberstein RH. 1977. Quantitative determination of thebaine in *Papaver bracteatum* by high-pressure liquid chromatography. J Chromatogr. 140(1):65-70.

Xu CG, Tang TX, Chen R, Liang CH, Liu XY, Wu CL, Yang YS, Yang DP, Wu H. 2014. A comparative study of bioactive secondary metabolite production in diploid and tetraploid *Echinacea purpurea* (L.) Moench. Plant Cell Tiss Organ Cult. 116(3):323-332.

Caryologia
International Journal of Cytology, Cytosystematics and Cytogenetics

Firenze University Press
www.fupress.com/caryologia

OPEN ACCESS

Citation: H. Nemat Farahzadi, S. Arbabian, A. Majd, G. Tajadod (2020) Long-term Effect Different Concentrations of Zn $(NO_3)_2$ on the Development of Male and Female Gametophytes of *Capsicum annuum* L. var California Wonder. *Caryologia* 73(1): 145-154. doi: 10.13128/caryologia-174

Received: February 26, 2019

Accepted: February 23, 2020

Published: May 8, 2020

Data Availability Statement: All relevant data are within the paper and its Supporting Information files.

Competing Interests: The Author(s) declare(s) no conflict of interest.

Long-term Effect Different Concentrations of Zn $(NO_3)_2$ on the Development of Male and Female Gametophytes of *Capsicum annuum* L. var California Wonder

Helal Nemat Farahzadi, Sedigheh Arbabian*, Ahamd Majd, Golnaz Tajadod

Department of Biology, Faculty of Sciences, Islamic Azad University, North-Tehran Branch, Tehran, Iran
*Corresponding author. E-mail: helalfarahzadi@yahoo.com, arbabias@gmail.com, ahmad_majd2005@yahoo.com, tajadodg@gmail.com

Abstract. Pepper is one of the most important crop plants. Recently, the global need for this plant has been widely increased due to its use in the food and pharmaceutical industry. we invested the effects of different concentrations of zinc on the development of male and female gametophytes of bell pepper (*Capsicum annuum* L. var California Wonder). The plants were cultivated with different concentrations of zinc nitrate (0 (control), 2.5, 5, 7.5, 10 and 15 mM) in a greenhouse under experimental conditions. Buds and Flowers are harvested at different stage of development (in 6 sizes) from May to Jun. They were fixed in FAA and maintained in 70% alcohol, then embedded in paraffin, sliced with a microtome and analyzed using a light microscope. Microscopic studies showed that developmental process of ovule, gynoecium and pollen grain in bell pepper plants was taking to ordinary process in dicotyledonous plants. According to the results, increased zinc concentration resulted in a disorder in the reproductive phase, which caused the treatment 1 to enter the reproductive phase with a 4-week delay. In addition, the other of the treatments did not enter the reproductive phase and were wilt during the growth period. The developmental stages of gynoecium and anther in treatment 1 were similar to the control. However, a number of abnormalities and irregularities wereo bserved including signs of nuclei disintegration, deformation of embryo sac, accumulation of dark materials and deformation of pollen grains.

Keywords. Bell pepper, male gametophyte, female gametophyte, zinc.

INTRODUCTION

Heavy metals refer to a group of elements with a density of more than 5 gr cm^{-3}. A few of them (Co, Fe, Mn, Mo, Ni, Zn and Cu) are essential micronutrients, which are necessary for normal growth, oxidation and reduction reactions, electron transferring, and other important metabolic processes in plants (Rai *et al*., 2004). Increase in zinc occurs mainly due to the environ-

mental pollution following industrial and agricultural activities such as smelter and incinerator emissions, spreading from mine wastes, excessive use of chemical fertilizers and zinc-containing insecticides, using sewage (waste water), sludge or other industrial and mineral fertilizers contaminated with zinc (Pedler *et al*., 2004; Giuffré *et al*., 2012). As it is rapidly absorbed by plants, it can be very toxic. Growth inhibition is a common phenomenon attributable to poisoning with zinc in plants. The more poisoning occurs, the less the product will become, and it eventually overcomes the growth and inhibits it (Broadley *et al*., 2007; Marschner, 2012), which is mainly because of the degradation of the photosynthesis activity. This affects photochemical reactions (Assche and Clijsters, 1986), carbonic anhydrase activity (Ló pez-Millán *et al*., 2005) biosynthesis of chlorophyll (Assche and Clijsters, 1986) and the integrity of the cell membrane (Wissemeier and Horst, 1987). If the concentration of zinc becomes higher than the critical level, it will lead to a decrease in growth and no flower production (Rout and Das, 2003). Pepper is one of the most important crop plants. The need for pepper cultivation has doubled over the past 20 years (FAO, 2017). Given the excessive increase in chemical fertilizers in agriculture, the increase in the amount of heavy metals in the environment, and the economic and nutritional importance of the pepper in recent decades in the world, the study aimed to examine the effect of zinc nitrate on anther and gynoecium development in this plant.

MATERIALS AND METHODS

Seeds from *Capsicum annuum* L. var California Wonder were provided from the plant gene bank of Seed and Plant Improvement Institute of Karaj, Iran. After sterilizing the seeds, they were cultured in a sterilized soil (obtained from Behkam Company). Six treatment groups with different concentrations of zinc (0 (control), 2.5, 5, 7.5, 10 and 15 mM) were selected and used for irrigation from the first irrigation until the end of the growth period. During the propagation stage, temperature was 25 ± 2 ° C, humidity 75-80%, and 16 h day light. Buds and flowers in all stages of development (in 6 sizes) were collected every week from May to Jun, 2017. The collected plant materials were fixed in a FAA (37% Formalin- Glacial Acetic Acid-70%Alcohol, 2:1:17 v/v) for 12 hours, then were stored in 70% alcohol and dehydration in an ethanol series and embedding in paraffin, specimens were sliced by Shandon AS325 rotary microtome. Staining of serial sections of 6-7 µm was carried out Hematoxylin- Eosine. Specimens were viewed with a OLYMPUS model BX43 light microscope connected to OLYMPUS digital camera. At least 15 flowers were observed for each developmental stage and the best samples were chosen for photographs.

RESULTS

Generative meristem and flowering

From the fifteenth to sixteenth weeks from the first day of cultivating, the generative meristems started their activity in the control plants and the buds emerged. In order to study the stages of flower development, the buds were considered in six stages: developmental stage 1: 1 to 2 mm diameter; developmental stage 2: 3 to 4 mm diameter; developmental stage 3: 3 to 5 mm diameter with the corolla hidden in calyx; developmental stage 4: 9 to 10 mm diameter corolla is in calyx; developmental stage 5: semi-open corolla with a 10-15 mm diameter; and development stage 6: approximately 20 mm in diameter the mature flower was considered with distinct corolla (Figure 1).

After the plant reaching the stage of flowering, the vegetative meristem is transformed into a generative meristem. Figure (2A-E) shows the developmental stages of generative meristem and the formation of different part of the flower. The generative meristem has a greater volume and densely stained compared to the vegetative meristem, which is the result of increased of mitosis activity in the apical meristem, tonica and corpus regions. Microscopic studies of generative meristem show that this meristem is enlarged and expanded and its stainability is almost homogeneous in different parts. Their cells are homogeneous, dense and more stainable compared to vegetative meristem. The terminal part of this meristem is sporogenous meristem (Sp.m) and its

Figure 1. Flower bud sizes: Stage 1: 1-2 mm diameter (St1). Stage 2: 3-4 mm diameter (St2). Stage 3: 3-5 mm diameter (St3). Stage 4: 9-10 mm diameter (St4). Stage 5: 10-15 mm diameter (St5). Stage 6: 20 mm diameter (St6).

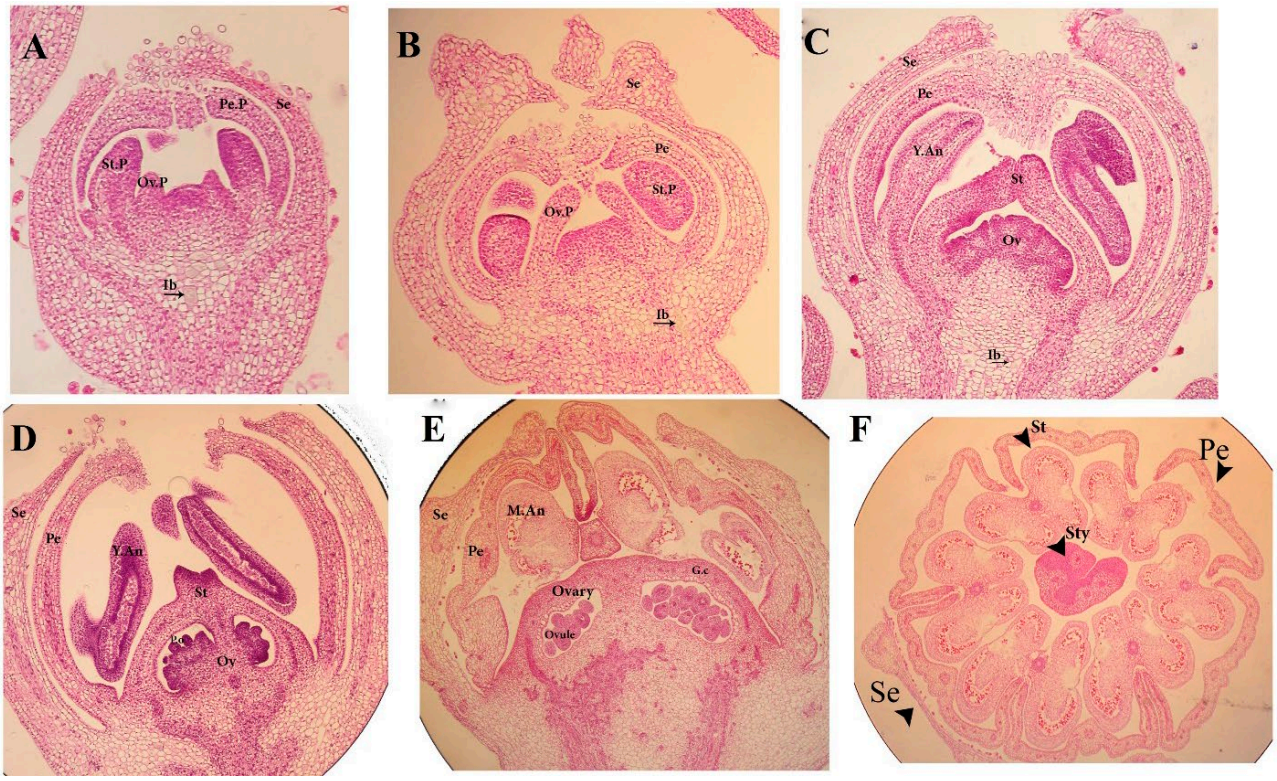

Figure 2. Longitudinal section of floral bud in different stages of flower development: (A): Stage 1. (B): Stage 2. (C): Stage 3. (D): Stage 4. (E): Stage 5; (F) Transverse section of floral bud (Ib – Idioblast; M.An – mature anther; Ov.p – ovary primordium; P – Petal; Pe.P – Petal Primordium; P.o – ovule primordium; Se – Sepal; St.p – stamen Primordium; St - stigma; St: stamen; sty – style; Y.An – young anther).

lower part, which is less stainable, is called receptacle meristem (Re.m). With the formation of generative meristem, the structural components of the flower such as Sepals (Se), stamen primordia (St.P), and petal primordia (Pe.P) gradually become distinct (Figure 2A). Simultaneous to the formation of stamen, petals (Pe) are formed, as a result of the activity of the peripheral part of sporogenous meristem against the stamen, and in the final stage, the ovary primordium (Ov.p) is formed (Figure 2B). Sepals (Se) appear with the activity and the remaining divisions of the initial ring (Figures 2A-B).

In the next steps, from the outside to inside, Sepals (Se), petals (Pe), stamen primordia (St.P) and ovary primordium (Ov.P), can be distinguished, respectively. The proliferated and deformed mass of the ovary primordium indicate the beginning of the ovary (Ov) and style (St) organization (Figure 2 B-C). Style, ovary, and ovules primordia were formed in the gynoecium. Following the mentioned changes and with gradual development of flower, sepals, petals, stamens, gynaecium, and ovules primordia can be detected (Figure 2D), and the full flower structure with mature stamen and carpel is shown in Figure 2E.

Microsporogenesis and pollen grains development

Bell pepper (*Capsicum annuum* L.) flowers are bisexual (Figure 2C-E). The flower is hexamerous (Figure 2F). All the stamens are equal in size, and they surround the style and the stigma. In addition, the anthers are tetrasporagiate and contain four pollen sacs (Figure 3 A-D). First, the stamens primordia are formed, then in the middle part, the pistil primordium is formed. As seen in Figure 2B, the development of the stamens is faster than the gynoecium and ovule. When the pistil primordium is still seen in form of cell masses without any differentiation, the stamens (filament, anther, and various layers of the anther wall and the cells of the sporogenous tissue) (Figure 2A-B) are observed and recognized clearly.

The young anther cell wall contains an epidermis, endothecium, two middle layers and tapetum from the outside to the inside (Figure 4A). Young anther layers wall cells have the same size and their large nuclei occupy most of the cell volume (Figure 4A). A series of rectangular cells form a row of single nucleus epidermis (Figure 4A). Before maturation, endothecium forms a row of single-nucleus rectangular cells (Figure 4B).

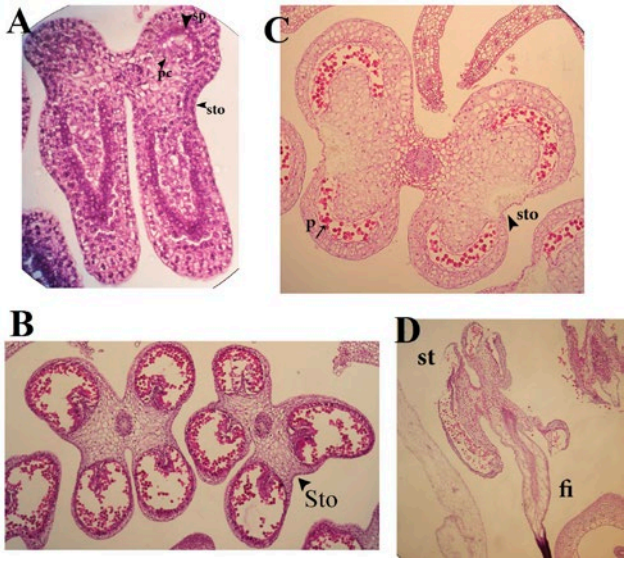

Figure 3. Transverse section of anther in different stages of development. (A) Young anther; (B) Second meiotic division in anther; (C) Anther at the binucleate pollen grain stage; (D) Longitudinally dehiscent anther in cross section (fi – filament; p – pollen; pc – placentoids; sp – primary sporogenous layer; st – stamen; sto – stomium).

During maturity, these cells are radially divided, and the single- double outer endostium form up to 3 layers of cells towards the connective tissue (Figure 4C-D). At this time, these cells form thick fibrous and the middle layers are decomposed (Figure 4C-D). First, the tapetal cells are secretive single-cellular (Figure 4A). The nuclear division in these cells usually occurs before the onset of meiosis in the pollen mother cells (PMCs) and they become bi-nuclei (Figure 4C-E). During development of the anther, these cells develop radially and they are filled with dense materials (Figure 4C). Tapetal cells differ in the morphology characteristics: on the outer surface of anther wall, they are stretched, rectangular and relatively uniform, whereas they become longer radially towards the connective tissue and are hypertrophied (Figure 4F). Sporogenous cells of anther have a dense stainable cytoplasm their large nuclei occupy most of the cell volume (Figure 5A). First, they are placed next to each other, then separated from each other and differentiated into PMCs (Figure 4A-B). First, to create pollen grains, these cells have to undergo a meiosis, but before initiation of the division process of PMCs, secrete a spe-

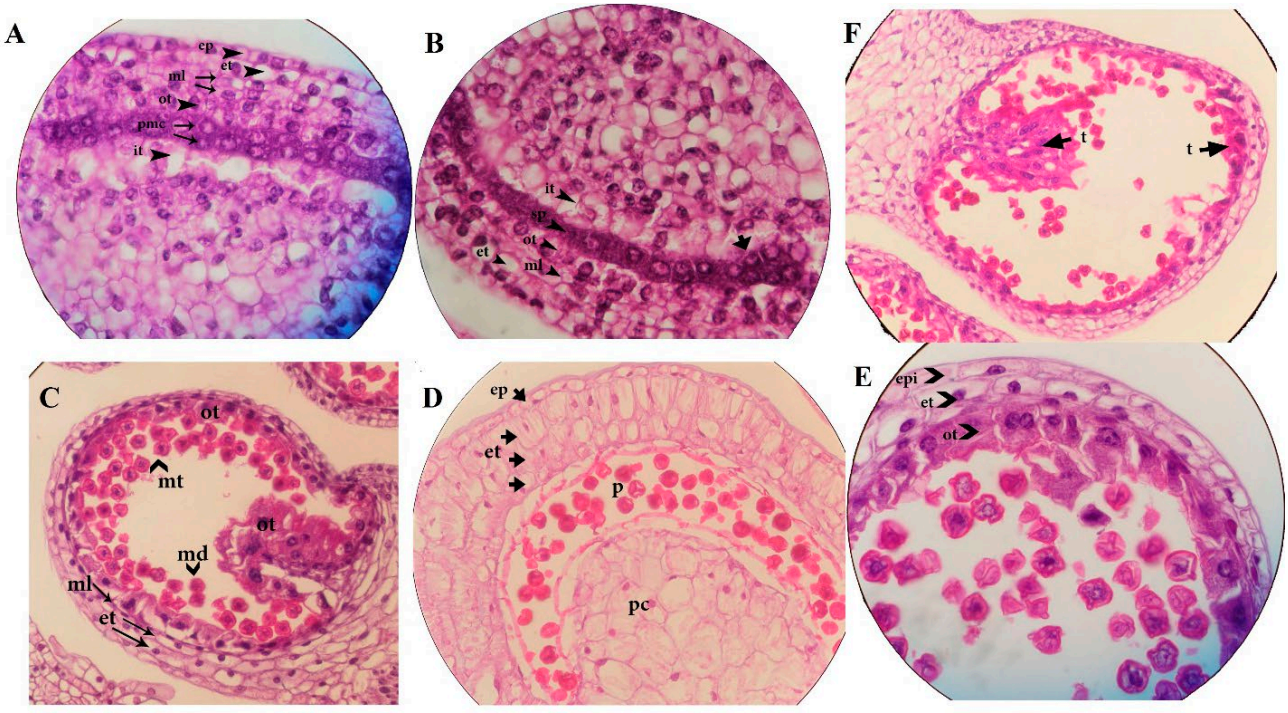

Figure 4. (A) The young anther wall layers and bilayer sporogenous tissue; (B) Anther sporogenous tissue is forming; (C) Degenerating middle layers and dividing endothecium cells at a single locule of anther. (D) Transverse section of a single locule of mature anther before dehiscence showing degenerating intersporangial septum and anther wall with only epidermis and endothecium; (E) Two-nucleated glandular tapetal cells on the outer side of anther wall; (F) Transverse section of microsporangium showing outer and inner binucleate tapetal cells, disintegrating callose in microspores tetrads and anther wall layers (et – endothecium; ep – epidermis; it – inner tapetum; ml – middle layer; mt – microspore tetrads; md – microspore diad; ot – outer tapetum; pmc – pollen mother cell; p – pollen grain; pc – placentoids; t – tapetum).

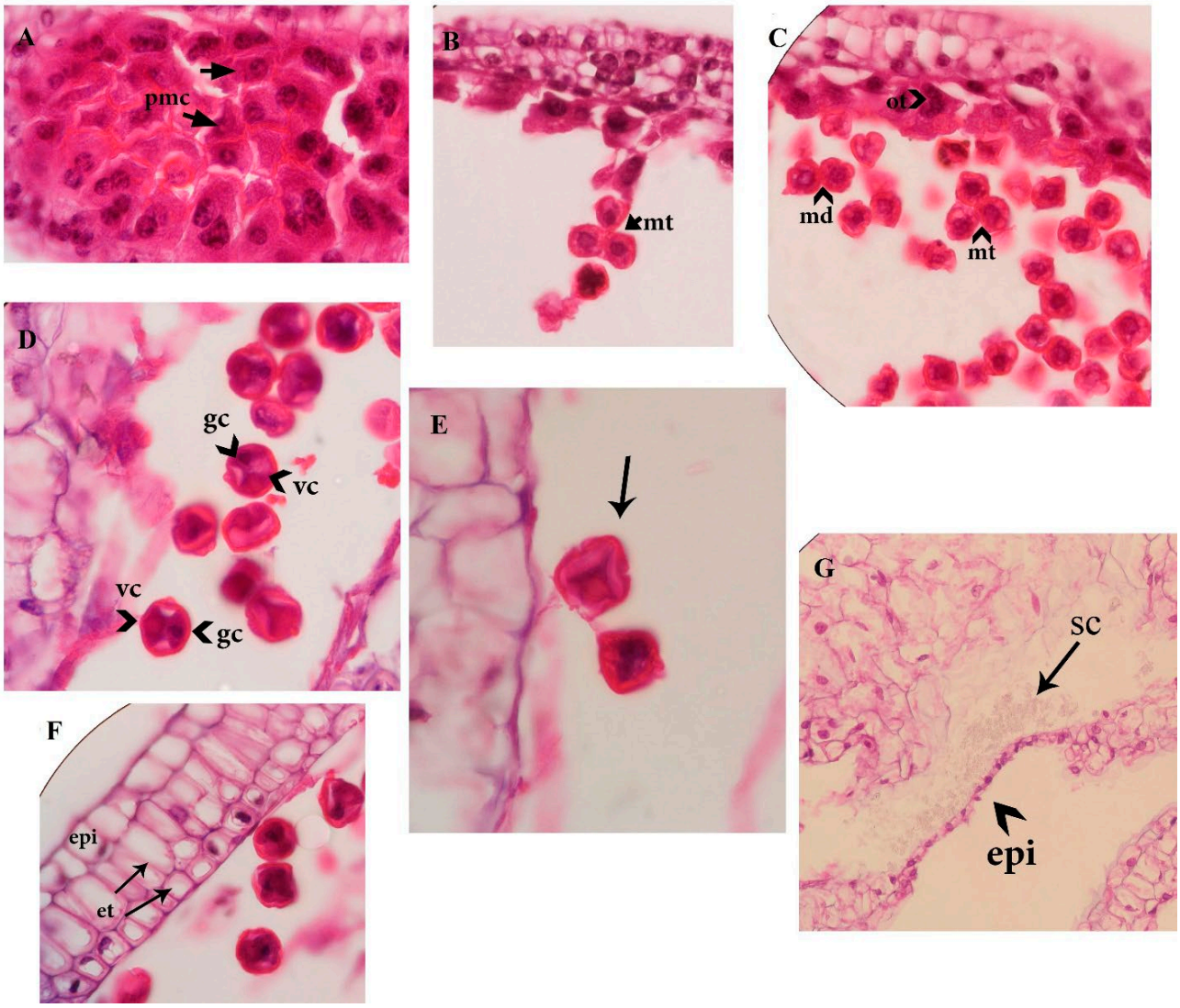

Figure 5. (A) pollen mother cell; (B) Transverse section of anther with microspore tetrahedral tetrads; (C) Microspore tetrads and diads stages. (D) Binucleate pollen grains. (E) Tricolporate pollen grains. (F) mature anther before dehiscence showing anther wall with only epidermis and endothecium; (G) Stomium degenerating epidermis cells and anther dehiscence (ep – epidermis; et – endothecium; gc – generative cell; md – microspore diad; mt – microspore tetrads; ot – outer tapetum; pmc - pollen mother cell; sc – sand crystal; vc – vegetative cell).

cial callose wall around them, surrounding the whole cell (Figure 5A). After the meiosis and the formation of the dyad (Figure 4C) and then the tetrad (Figure 4C, 5B), when the callose is decomposed, all microspores are released from tetrad into the lucule (Figure 5C). They have dense cytoplasm and thin cell walls (Figure 5C-E). At the end of the single nucleus stage, the microspore nucleus is pushed to one side. Following the expansion of microspore, the nucleus is divided and two dissimilar nuclei (generative and vegetative) are produced (Figure 5D). Mature pollen grains normally have the large vegetative cell and a small generative cell (Figure 5D). At this stage, only the epidermis and endostium exist in the anther wall (Figure 5F). Anthers dehiscence occurs through a longitudinal gap in the stomium (Figure 5G). It is formed by a layer of at most 20 cells under the epidermis, which is highly stainable and contains calcium crystals (shown with an arrow on Figure 5G).

Gynoecium, ovule and embryo development

In bell pepper (*Capsicum annuum* L.) the gynoecium is syncarpous, and the ovary is superior and

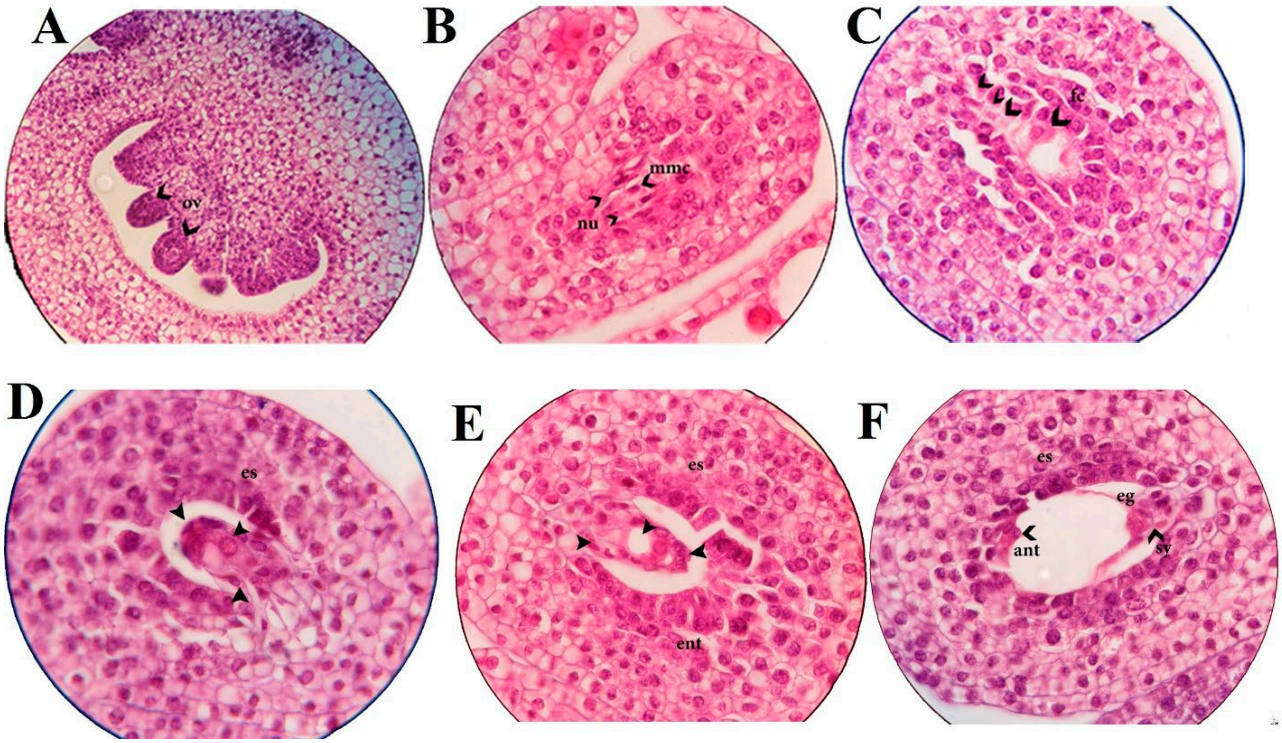

Figure 6. (A)Section of a single locule of ovary; (B) Megaspore mother cell (mmc) beneath the apical epidermis of the nucellus; (C) End of the mmc second meiosis and linear arrangement of the megaspores; (D) Eight-nucleate immature embryo sac; (E) Eight-nucleate immature embryo sac; (F) Eight-nucleate and seven-celled mature embryo sac (ant – antipodal; eg – egg cell; ent – endothelium; es – embryo sac; fc – functional megaspore; mmc – megaspore mother cell; nu – nucellus; ov – ovule; sy – synergid).

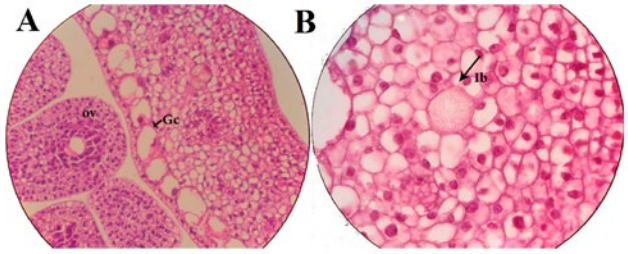

Figure 7. (A) Transverse sections of ovary wall with giant cell; (B) Transverse sections of ovary tissue with idioblast (Gc – giant cell; Ib – idioblast; ov- ovule).

ring shaped. The ovary is trilocular and consists of two carpels. Each carpel has a large number of ovules on the placenta axis (Figure 6A). The ovule is unitegmic, hemianatropous and tenuinucellate (Figure 6B). The embryo sac in the ovule is of polygonum type. The uninucleate archeospore is developed under the apical epidermis of the ovules and acts directly as a primary sporogenous cell. Thus, the meiosis in the megasporcyte initially forms as dyad and eventually as a linear tetrad (Figure 6B). In the tetrads, the sister megaspores are gradually decomposed, and the development of the embryo sac begins with the chalazal megaspore (Figure 6B). Three mitosis divisions continuously produce functional megaspore in the embryonic sac of two, four, and eight nuclei (Figure 6C). Thus, the development of the embryonic sac confirms the polygonum type (Figure 6E). For the formation of an embryo sac, the megaspore volume increases and its nucleus is divided into two nuclei, migrating to each pole of the cell (chalaza, micropyle) (Figure 6D). Then large vacuole is created between the nuclei. The nuclei are divided two times, and four nuclei of haploid are formed on each pole of the embryo sac (Figure C-D). A nucleus migrates to the middle part of the embryo sac from each pole, polar nuclei are formed, and the remaining three nuclei evolve into three cells at each pole (chalaza, micropyle). There are three adjacent cells to the micropyle which are formed, the middle is called egg cell (oosphere), and the two symmetric lateral cells which are called synergid opposite to the chalaza, as well as three cells opposite to the micropyle which are called antipodal (Figure 6F). These cells have a short life and die before fertilization in the embryo sac. The giant cells underneath the inner epi-

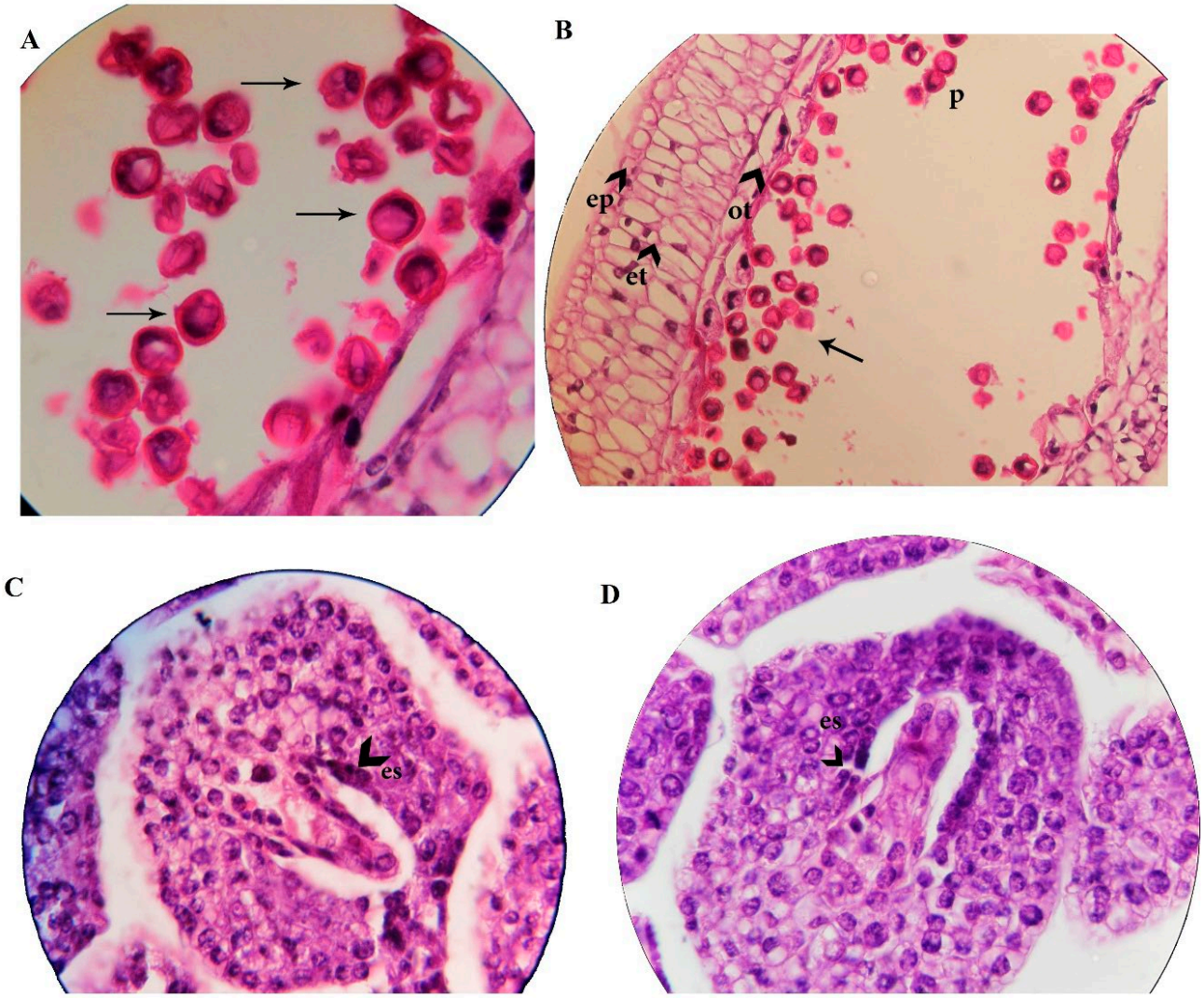

Figure 8. (A-B) Transverse sections of anther from treatment 1. abnormalities in pollen grains and collected black materials in pollen grain; (C-D) Transverse sections of ovule from treatment 1**.** Change of the shape of embryo sac and also degradation of egg apparatus in plants (et – endothecium; ep – epidermis; es – embryo sac; ot – outer tapetum; p – pollen grain).

dermis of the ovary wall are observed in developmental stages. During the developmental stages of the ovary, they enlarge (Figure 7A). Idioblasts containing calcium crystals are found in the ovule and ovary parenchyma cells (Figure 7B).

Changes pollen grain and embryo sac in treatments

In treatment 1 (2.5 mM), the plants entered the reproductive phase in the 19th to the 20th week with a 4-week delay. The plants in other treatment groups did not enter the generative phase (the number of culture periods was repeat three times, and no generative phase was observed). The process of male gametophyte development in this treatment was similar to the control. Pollen grains from zinc-treated plants showed that the shape of pollen grains was changed from the normal spherical state to a smaller shape, and a large number of pollen grains had irregular shapes. A large number of pollen grains showed the accumulation of dark materials (Figure 8A-B).

In the development of female gametophyte, the examination of microscopic slides in the plants under treatment showed signs of nuclear degradation and embryo sac changes (Figure 8C-D).

DISCUSSION

The studies on the structural characteristics of male and female gametophytes and the details of microsporogenesis and macrosporogenesis in various genera of solanaceace showed that bisexual are common in this family and dioecy are relatively rare (Davis, 1966), Hunzikera, 2001, Talebi *et al*., 2016, Ramezani *et al*., 2018). Microscopic studies showed that developmental process of ovule, gynoecium and pollen grain in bell pepper plants was taking to ordinary process in dicotyledonous plants. The differentiation of the various parts of the floral from the vegetative meristem was consistent with the results of Munting (1974) on *C.annuum*. The stamens in *C.annuum* are composed of relatively large anthers equal throughout the filaments. These stamens are tetrasporangiate and contain four pollen sacs (Dharmadhaj and Prakash, 1978), a distinct state in potato family (Endress, 1996). The taptum is glandular and its cells are binuclear. Secretive tapetum is observed in some Solanacease, such as *A. belladonna* (Yurukova-Grancharova *et al*., 2011), *W. somnifera* (Ghimire and Heo, 2012), *P. hybrida* (Chehregani and Ramezani, 2016), *S.tuberosum* (Talebi *et al*., 2016). In our observations, the structural characteristics of the tapetum cell layer were different from that of the outer surface of the anther wall and to the connective tissue in the bell pepper (*C.annuum*), that was consistent with the results of Yurukova-Grancharova *et al*. (2011) on *A. Belladonna*, Chehregani and Ramezani (2016)) on *P. hybrid* and Ramezani *et al*. (2018) on *C.annuum*. Although in these plants, the tapetal cells are different not only in structural but also in the number of nuclei, the number of nuclei in the tapetal cells is inconsistent in all families of Solanaceace (Tobe, 1989). As stated, for *A.belladonna* (Yurukova-Grancharova *et al*., 2011) it has four nuclei, for *W. somnifera* (Ghimire and Heo, 2012) two nuclei, for *P. hybrid* (Chehregani and Ramezani, 2016) four nuclei, and for *S.tuberosum* (Talebi *et al*., 2016) it has several nuclei.

Our results showed that tapetal cells of *C.annuum* had two nuclei, similar to *W. somnifera* (Ghimire and Heo, 2012) and *C.annuum* (Ramezani *et al*., 2018), whereas Dharmadhaj and Prakash (1978) reported three nuclei for *C.annuum*. At the time of maturation, each pollen grain of pepper has two nuclei; the presence of two-nucleus pollen grains is commonly found in Solanaceace (Davis, 1966, Dharamadhaj and Prakash, 1978, Poddubnaya-Arnoldi, 1976, Talebi *et al*., 2016, Ramezani *et al*. 2018). The sandy crystals accumulate in the anther cells of *C.annuum*. Crystals appear in the early stages of flower development in most solanaceace anthers (D'Arcy and Averett, 1996). When the *C.annuum* pollen grains are matured, the anther wall breaks down, and these calcium oxalate crystals are released (Ramezani *et al*., 2018). Our results confirmed the previous studies by the authors for different speices of Solanaceace (D'Arcy and Averett, 1996; Rezanejad, 2006; Chehregani and Ramezani, 2016, Ramezani *et al*., 2018). The released calcium crystals stick to the pollen and dissolve in the style mucous, and calcium ions can generate pollen for germination and pollen tube growth (Iwano *et al*., 2004).

The differentiation of male gametophyte in bell pepper (*C.annuum*) happens early from the female gametophytes, which is consistent with the results of Munting (1974) and Ramezani *et al*. (2018). The development of the embryo sac is done as a common pattern in all Solanaceace (Davis, 1966). In some *C.annuum* samples, we observed bilocular or trilocular ovary. Indeed, the bilocular ovary is a characteristic feature of Solanaceace (Ghimire and Heo, 2012, Ramezani *et al*., 2018). *C. annuum* ovule is hemiantropous that is consistent with the results of some varieties of *C. annuum* (Munting, 1974) and Ramezani *et al*. 2018 on the same variety. The present study showed that the development of the female gametophyte *C. annuum* L. var. California Wonder is of polygonum type. Polygonum type is typically known as Solanaceace (Mohan and Kamini, 1964, Mohan, 1966, Munting, 1974, Dharmadhaj and Prakash, 1978, Yurukova-Grancharova *et al*., 2011, Ghimire and Heo, 2012, Brito *et al*. 2015, Ramezani *et al*., 2018).

According to Van Assche (1986), high doses of zinc inhibit many metabolic activities in the plant by damaging the mitochondrial structure in cells (Rout and Das, 2003). The high accumulation of zinc in the cytosol of the plant cell also results in impaired cellular function and inhibition of respiration and energy responses associated with cell growth that might reduce the growth and development of the whole plant (Bonnet *et al*., 2000). This element affects the process of cell division by interrupting the interphase, prolonging the stage of prophase, G2, and stopping the synthesis of the synthesized proteins required by the cell cycle and nucleic acid synthesis (El-Ghamery *et al*., 2003). The continuity, integrity and permeability of the membrane are impaired due to toxicity of zinc. At the molecular level, it also affects the expression of many genes (Wang *et al*., 2009). Nutritional conditions play an important role in flower formation (Taiz & Zeiger, 2010). The zinc stress and increase in its concentration disrupt the plant's balance nutrition. On the other hand, the concentration of zinc affects hormonal balance and causes a disruption in hormonal balance and because hormones act as genetic regulators in inducing expression of the involved genes (Rout and Das, 2003). According to Aloni reports in 2006, delayed

flowering is due to a hormonal disorder such as auxin, which is due to gene disruption.

In treatment 1, the flowering began with delay and the rest of the treatments did not enter the reproductive phase, although stresses such as heavy metals typically cause premature aging of plants, and from the developmental perspective one of the symptoms of aging is flowering. However, in the interpretation of latency and lack of flowering in *C.annuum* seen under the influence of zinc stress in our study, one can state that the nutritional conditions of the plant plays an important role in the formation of the flower. Studying the C/N ratio in different plants has shown that each time a plant prepares for flower formation, this ratio goes higher (Taiz & Zaiger, 2010). Increase in the concentration of zinc causes disruption of absorption in other elements, including iron (Zeng *et al*., 2011), which causes a delay or lack of flowering.

Studies on microscopic sections of control and treatment samples showed that the general trend of ovule and pollen formation in plant treatment 1 and control was the same. However, for the plants in treatment 1, a large number of pollen grains smaller than the normal size were found. The results were consistent with Mohsenzadeh (2011) on *Reseda lutea* L., Yousefi (2011) about the effect of heavy metals pollution on *Chenopodium botrys* L., Albooghobaish *et al*. (2011) about the effect of lead toxicity on *Matricaria Chamomilla*, Rezanejad *et al*. (2003, 2007, 2008, and 2009) on the effects of air pollution on various plants, and Wolters and Martens (1987) on the effect of air pollution on pollen grains. Moreover, it was seen that in pollen grains that accumulated dark materials, which was also consistent with Chehregani *et al*. (2006) on the effect of acid rain on *Phaseolus vulgaris*. In treatment 1, a large number of ovules have deformed embryo sacs, so that compared to the control group, where embryo-sac has a spindle and stretched form, they have changed in their shape, which was consistent with the results of Hosseini (2006) on *Phaseolus vulgaris*.

REFERENCE

Albooghobaish, N., Zarinkamar, F., 2012, Study of inflorescence development under lead toxicity in *Matricaria Chamomilla*. International Conference on Environment, Energy and Biotechnology., IACSIT Press, Singapore. Vol. 33, PP. 253-258.

Aloni, R., Aloni, E., Langhns.M., Ullrich, C.I., 2006, Role of Cytokinin and Auxin Shaping Root Architecture: Regulating Vascular Differentiation, Lateral Root Initiation, Root Apical Dominance and Root Gravitropism.

Bonnet, M., Camares, O., Veisseire, P., 2000, Effect of zinc and influence of *Acremonium lolii* on growth parameters, chlorophyll a fluorescence and antioxidant enzyme activities of ryegrass (*Lolium perenne* L. cv Apollo). J. Exp. Bot., 51(346): 945-953.

Brito, M.S., Bertolino L.T., Cossalter, V., Quiapim, A.C., DePaoli, H.C., Goldman, G.H., Teixeira, S.P., Goldman, M.H.S., 2015, Pollination triggers female gametophyte development in immature *Nicotiana tabacum* flowers. Frontiers in Plant Science, doi: 10.3389/fpls.2015.00561

Broadley, M.R., White, P. J. J., Hammond, P., Zelko, I., Lux, A., 2007, Zinc in plants. New Phytol. 173:677–702.

Chehregani A, Ramezani H. 2016. The study of anther and pollen developmental stages in *Petunia hybrida* juss. Iran J Plant Biol 29(1):95– 105 (in Persian).

Chehregani, A., malayeri, B.E., kavianpour, F., Lari-yazdi, H., 2006, Effect of acid rain on the development, structure and viability of pollen grains in Bean plants (*Phaseolus vulgaris)*, Pakistan Journal of Biological Science 9: 1033-1036.

D'Arcy WG, Averett JE. 1996. Recognition of tribes Capsiceae and Physaleae, subfamily Solanoideae, Solanaceae. Phytologia 80:273–275.

Davis G. 1966. Systematic embryology of the angiosperms. New York (NY): Wiley

Dharamadhaj, P., and Prakash, N., 1987, Development of the Anther and Ovule in *Capsicum* L. Aust. J. Bot. 26:433-439.

El-Ghamery, A.A., El-Kholy, M.A., El-Yousser, M.A., 2003. Evaluation of cytological effects of Zn2+ in relation to germination and root growth of *Nigella sativa* L. and *Triticum aestivum* L. Mutation Research 537:29-41.

Endress PK. 1996. Diversity and evolutionary trends in angiosperm anthers. In: D'Arcy WG, Keeting R, editors. The anther: form, function and phylogeny. London: Cambridge University Press, p. 92–110.

FAO ,2017, FAOSTAT Database. Food and Agriculture Organization, Roma, Italy. Available online at URL: www.fao.org.

Ghimire B, Heo K. 2012. Embryology of *Withania somnifera* (L.) Dunal (Solanaceae). Acta Biol Cracov Ser Bot 54(2):69–78.

Giuffré, L., Romaniuk, R.I., Marbán, L., Ríos, R.P., García, T.P., 2012, Public health and heavy metals in urban and periurban horticulture. Emir. J. Food Agric. 24(2):148-154.

Hunzikera AT. 2001. Genera Solanacearum: the genera of the Solanaceae illustrated, arranged according to a new system. Ruggell: Gantner Verlag. p. 500.

Iwano M, Entani T, Shiba H, Takayama S, Isogai A. 2004. Calcium crystals in the anther of Petunia: the existence and biological significance in the pollination process. Plant Cell Physiol 45:40–47.

Ló pez-Millán, A.F., Ellis, D.R., Grusak, M.A., 2005, Effect of zinc and manganese supply on the activities of superoxide dismutase and carbonic anhydrase in *Medicago truncatula* wild type and raz mutant plants, Plant Sci. 168:1015-1022.

Marschner, H., 2012, Mineral Nutrition of Higher Plants (3rd edition). Academic Press, London.

Mohan K. 1966. The ovule and embryo sac development in *Browallia demissa* Linn. Proc Indian Acad Sci (Plant Sci) 64:26–31.

Mohan R, Kamini I. 1964. Embryology and fruit development in *Withania somnifera*. Phytomorphology 14:574–587.

Mohsenzadeh, F., Chehregani, A., Yousefi, N., 2011, Effect of the heavy metals on developmental stages of ovule, pollen, and root proteins in *Reseda lutea* L. (Resedaceae), Biological Trace Element Research 143:1777-1788.

Munting, A.J.,1974, Development of flower and fruit of *Capsicum annuum* L. Acta Bot. 23:415-432.

Pedler, J.F., Kinraide T.B., Parker, D.R., 2004, Zinc rhizotoxicity in wheat and radish is alleviated by micromolar levels of magnesium and potassium in solution culture, Plant Soil. 259:191–199.

Poddubnaya-Arnoldi VA. 1976. Cytoembryology of Angiosperms. Basics and Perspectives. Moskva: Nauka. (in Russian).

Rai, V., Vaypay E.E.P., Singh, S.N., Mehrotra, S., 2004, Effect of chromium accumulation on photosynthetic pigments, oxidative stress defence system, nitrate reduction, proline level and eugenol content of *Ocimum tenuiflorum* L. Plant Sci. 167(5):1159-1169.

Ramezani, H., Chehregani Rad, A., Karamian, R.,2018, Development of the male and female gametophyte in *Capsicum annuum* L. var. California Wonder. Plant Biosystems - An International Journal Dealing with all Aspects of Plant Biology, DOI:10.1080/11263504.2018.1435568.

Rezanejad F. 2006. Differentiation of crystal-containing cells during anther development and crystal types in the anther of *Petunia hybrid* grandiflora. Thaiszia – J Bot Košice 16:41–46.

Rezanejad, F., 2007, The effect of air pollution on microsporogenesis, pollen development and soluble pollen proteins in *Spartium junceum* L. (Fabaceae), Turkish Journal of Botany 31:183-191.

Rezanejad, F., 2009, Air pollution effects on structure, proteins and flavonoids in pollen grains of *Thuja orientalis* L. (Cupressaceae). Grana. 48:205-213.

Rezanejad, F., Majd, A., Shariatzadeh, S. M.A., Moein, M., Aminzadeh, M., Mirzaeian, M., 2003, Effect of air pollution on soluble proteins, structure and cellular material release in pollen of *Lagerstroemia indica* L. (lytraceae). Acta Biologica Cracoviensia Series Botanica 45:129–132.

Rezanejad, F.,2008, The structure and ultrastructure of anther epidermis and pollen in *Lagerstroemia indica* L. (Lythraceae) in Response to Air Pollution. Turkish Journal of Botany 32:35-42.

Rout, G.R., Das, P., 2003, Effect of metal toxicity on plant growth and metabolism: I. Zinc. Agronomie 23:3–11.

Taiz, L., Zeiger, E., 2010, Plant Physiology, Sinauer Assoc, Inc, Publ, Massachusetts., pp. 35-348.

Talebi, sh., Majd, A., Mirzai, M., Jafari, S., Abedini, M., 2016, The study of anther development, microsporogenesis and formation of male gametophyte in potato (*Solanum tuberosum* L.). Research journal of biological sciences 11(1):34-37.

Tobe H. 1989. The embryology of angiosperms: its broad application to the systematic and evolutionary study. Bot Mag Tokyo 102:351–367.

Van Assche F., Clijsters H., 1986, Inhibition of photosynthesis in Phaseolus vulgaris by treatment with toxic concentration of zinc: effect on ribulose – 1,5-bisphosphate carboxylase/oxygenase. J. Plant Physiol. 125:355–360.

Wang, C., Zhang, S.H., Wang, P.F., Hou, J., Zhang, W.J., Li, W., Lin, Z.P., 2009, The effect of excess Zn on mineral nutrition and antioxidative response in rapeseed seedlings. Chemosphere 75(11):1468–1476.

Wissemeier, A.H., Horst, W.J., 1987, Callose deposition in leaves of cowpea as a sensitive response to high Mn supply. Plant Soil. 102:283–286.

Wolters, J.H.B., Martens, M.J.M., 1987, Effects of air pollutants on pollen. The Botanical Review 53:372-414.

Yousefi, N., Chehregani, A., Malayeri, B., Lorestani, B., Cheraghi, M., 2011, Investigating the effect of heavy metals on developmental stages of anther and pollen in *Chenopodium botrys* L. (Chenopodiaceae). Biological Trace Element Research 140:368-376.

Yurukova-Grancharova P, Yankova-Tsvetkova E, Baldjiev G, Barragan MC. 2011. Reproductive biology of *Atropa belladonna*: embryological features, pollen and seed viability. Phytologia balcanica 17(1):101–112.

Zeng, X.W., Ma, L.Q., Qiu, R.L., Tang, Y.T., 2011, Effects of Zn on plant tolerance and non-protein thiol accumulation in Zn hyperaccumulator *Arabis paniculata* Franch. Environ Exp. 70:227-232.

Caryologia
International Journal of Cytology, Cytosystematics and Cytogenetics

Firenze University Press
www.fupress.com/caryologia

Citation: H. Sharghi, M. Azizi, H. Moazzeni (2020) A karyological study of some endemic *Trigonella* species (Fabaceae) in Iran. *Caryologia* 73(1): 155-161. doi: 10.13128/caryologia-184

Received: March 8, 2019

Accepted: February 23, 2020

Published: May 8, 2020

Data Availability Statement: All relevant data are within the paper and its Supporting Information files.

Competing Interests: The Author(s) declare(s) no conflict of interest.

A karyological study of some endemic *Trigonella* species (Fabaceae) in Iran

Hamidreza Sharghi[1,2], Majid Azizi[1,*], Hamid Moazzeni[2]

[1] *Department of Horticultural Sciences, Faculty of Agriculture, Ferdowsi University of Mashhad, P.O.Box: 917751163, Mashhad, Iran*
[2] *Department of Botany, Research Center for Plant Sciences, Ferdowsi University of Mashhad, P.O.Box 91779-48974, Mashhad, Iran*
*Corresponding author. E-mail: azizi@um.ac.ir

Abstract. Karyotypes of nine populations belonging to six endemic species of the genus *Trigonella* (Trifolieae/Fabaceae) studied in this survey. All studied species are perennial and recorded only from Northeast of Iran. Excluding the karyotype of *Trigonella subenervis*, which was previously reported, all of the other species studied here (six species) for the first time. Our results present that all assessed genotypes are diploid with 2n=2x=16 and the chromosomal basis of x=8. In addition to the chromosome counts, length of long and short arms of the chromosome and their ratios analyzed and presented in this study.

Keywords. Chromosome number, Cytogenetic, Karyotype, Khorassan, Trifolieae, *Trigonella*.

INTRODUCTION

The genus *Trigonella* L. is a member of the tribe Trifolieae of the family Fabaceae, with about 135 species worldwide, most of which distributed in the dry regions around the Mediterranean region extended to West Asia, and naturalized in North America. Only two species being present in South Australia (Mabberley 1997).

Trigonella consists of annual or perennial herbs with pinnately trifoliate leaves, a campanulate or tubular calyx with two large and three small equal lobes, diadelphous stamens, uniform anthers, terminal stigma and ovary with numerous ovules (Širjaev 1928-1932; Hutchinson 1964; Dangi *et al.* 2016). According to Rechinger (1984), the genus represented by 58 species in to Flora Iranica area. This number has increased to about 66 species as a result of recent researches (Hamzeh'ee 2000; Janighorban 2004; Badrzadeh and Ghafarzadeh-Namazi 2009; Ranjbar, Karamian, and Hajmoradi 2012; Ranjbar and Hajmoradi 2012, 2015, 2016). Of which, 48 taxa (15 endemics (32%)) accommodated in 12 sections growing in Iran; 14 of those are perennial species of *Trigonella* sect. *Ellipticae* (Boiss.) Sirj.

In Flora Iranica account (Rechinger 1984), section *Ellipticae* is represented with seven perennial species in Iran. The characteristics of the section

Ellipticae are: perennial species with entire or dentate stipules, calyx campanulate, petals yellow or rarely white with violet veins, sometimes completely dark violet, standard without interlocking projection, fruit a legume which is different in shape and size, elliptic or lanceolate to oblong, beakless, generally transversely veined, wingless or with thin wing and smooth seeds.

Several cytological investigations have been conducted on approximately a hundred *Trigonella* species (Agarwal and Gupta 1983; Ahmad *et al*. 1999; Astanova 1981; Aykut *et al*. 2009; Bal 1990; Bidak and Amin 1996; Darlington and Wylie 1955; Dundas *et al*. 2006; Ghosh 1980; Kumari and Bir 1990; Ladizinsky and Vosa 1986; Martin *et al*. 2006, 2008, 2010, 2011a, 2011b; Pavlova 1996; Ranjbar *et al*. 2011a, 2011b, 2015; Singh and Roy 1970; Singh and Singh 1976; Tutin and Heywood 1964; Yilmaz *et al*. 2009). The reported chromosome numbers of the genus *Trigonella* are 2n=14, 16, 18, 24, 28, 30, 32, 42, 44, 46 and 48.

To contribute to the karyological study of the genus, we carried out a karyological study on some perennial endemic species collected from different regions in East and Northeast of Iran. This study aimed to verify the chromosome numbers of some endemic *Trigonella* species recently reported in Iran. In this contribution, we report the somatic chromosome numbers of six taxa (nine populations), that five species are determined for the first time.

MATERIAL AND METHODS

The chromosome number were analyzed in nine population of *Trigonella*. The nomenclature of taxa, collection data, and vouchers are given in Table 1. The mitotic chromosome numbers were studied in three populations of *T. subenervis* Rech. f., two populations of *T. binaloudensis* and one population from each of *T. lasiocarpa*, *T. stipitata*, *T .heratensis* and *T. Torbatejamensis*. Seed materials were collected between the years of 2016 and 2018 from natural habitats. Voucher specimens were deposited at the Ferdowsi University of Mashhad Herbarium (FUMH), Iran.

For karyological observation, to accelerate germination, the seed surfaces were abraded with emery paper. Seeds were sown on wet filter paper in Petri dishes at room temperature. The seeds germinated after 2-3 days. One cm fresh root tip cells were used to study the somatic chromosomes. The root tips pretreated in an ice-water mixture for 24 hours. Afterward, they fixed in Carnoy's fixative (ethanol: acetic acid 3:1) for 24 h at 4 °C (Fukui and Nakayama 1996). The root tips were washed in distilled water to remove the fixative, then hydrolyzed in 1N HCl for 13–15 minutes at room temperature, and finally stained with 2% aceto-orcein for two hours.

The slides were created using the squash method. The prepared slides were slightly heated under an alcohol frame for 1–2 s before observation. Photographs of chromosomes were taken using a Nikon Eclipse Ni-u (Tokyo, Japan) photomicroscope equipped with Nikon Ds-Fi3 digital camera. Chromosome counts were made from well-spread metaphases in intact cells, by direct observation, and from photomicrographs. To ensure for chromosome number, a minimum of five cells, at somatic metaphase, observed (Figure 1). Karyotypic analyses were conducted on IdeoKar software (version 1.2) to calculate karyotypic parameters and generate ideograms (Mirzaghaderi and Marzangi 2015). Karyotype formulae and nomenclature followed Levan *et al*. (1964), and karyotype asymmetry followed Stebbins (1971).

Table 1. Iranian endemic species of *Trigonella* analyzed in this study, their locations, and voucher specimens data.

Taxa	Location	Collection Date	Elevation (m)	Herbarium number
T. binaloudensis*				
population 1	SW Chenaran, Ferizi towards Binaloud mountains	2016/05/30	1730	46443
population 2	NW Sabzevar, W Jalambadan, in Mnts. near Chromite mine	2018/05/29	1770	46323
T .heratensis	S Fariman, between Torbate-Heydariyeh & Fariman	2016/06/06	1685	45959
T. lasiocarpa*	NE Birjand, Now-Qand towards Bidesk	2016/05/24	2320	46442
T. stipitata*	N Mashhad, E Chenaran, Mian-Marq	2016/05/25	1420	25771
T. subenervis*				
population 1	N Torbate-Heydariyeh, Khomari pass	2016/05/23	1851	46441
population 2	N Kashmar, NE hills of Chalpu village	2017/06/06	1879	46446
population 3	N Shirvan, 12 km from Lowjalli toward Namanlu village	2017/06/24	1820	45844
T. torbatejamensis*	NE Torbate-Jam, between Saleh-Abad & Gush-Laqar,	2016/05/04	750	45958

RESULTS

Our investigations comprised nine populations belonging to 6 species of the genus *Trigonella*, of which data for five species reported here for the first time. The chromosomes of these taxa at mitotic metaphase shown in Figure 1. Detailed karyotypic parameters, formulae, and asymmetry are summarized in Table 2. In this study, the basic chromosome number of all taxa is x=8, and all of them are diploid.

Trigonella binaloudensis Ranjbar & Karamian

Population 1 (SW Chenaran):

The chromosome number was 2n=2x=16 (Figure 1e1). Haploid chromosome length was 27.73 µm. Chromosome length varied from 2.75 to 4.83 µm, and arm ratio from 1.06 to 1.88. The chromosome complement at mitotic metaphase consisted of 14 median region and two submedian region chromosomes. Karyotypic asymmetry was 1A.

Population 2 (NW Sabzevar):

The chromosome number was 2n=2x=16 (Figure 1e2). Haploid chromosome length was 24.03 µm. Chromosome length varied from 2.15 to 3.72 µm, and arm ratio from 1.030 to 1.82. The chromosome complement at mitotic metaphase consisted of 14 median region and two submedian region chromosomes. Karyotypic asymmetry was 1A.

Trigonella heratensis Rech.f

The chromosome number of *T. heratensis* was 2n=2x=16 (Figure 1c). Haploid chromosome length was 22.98 µm. Chromosome length varied from 2.46 to 3.40

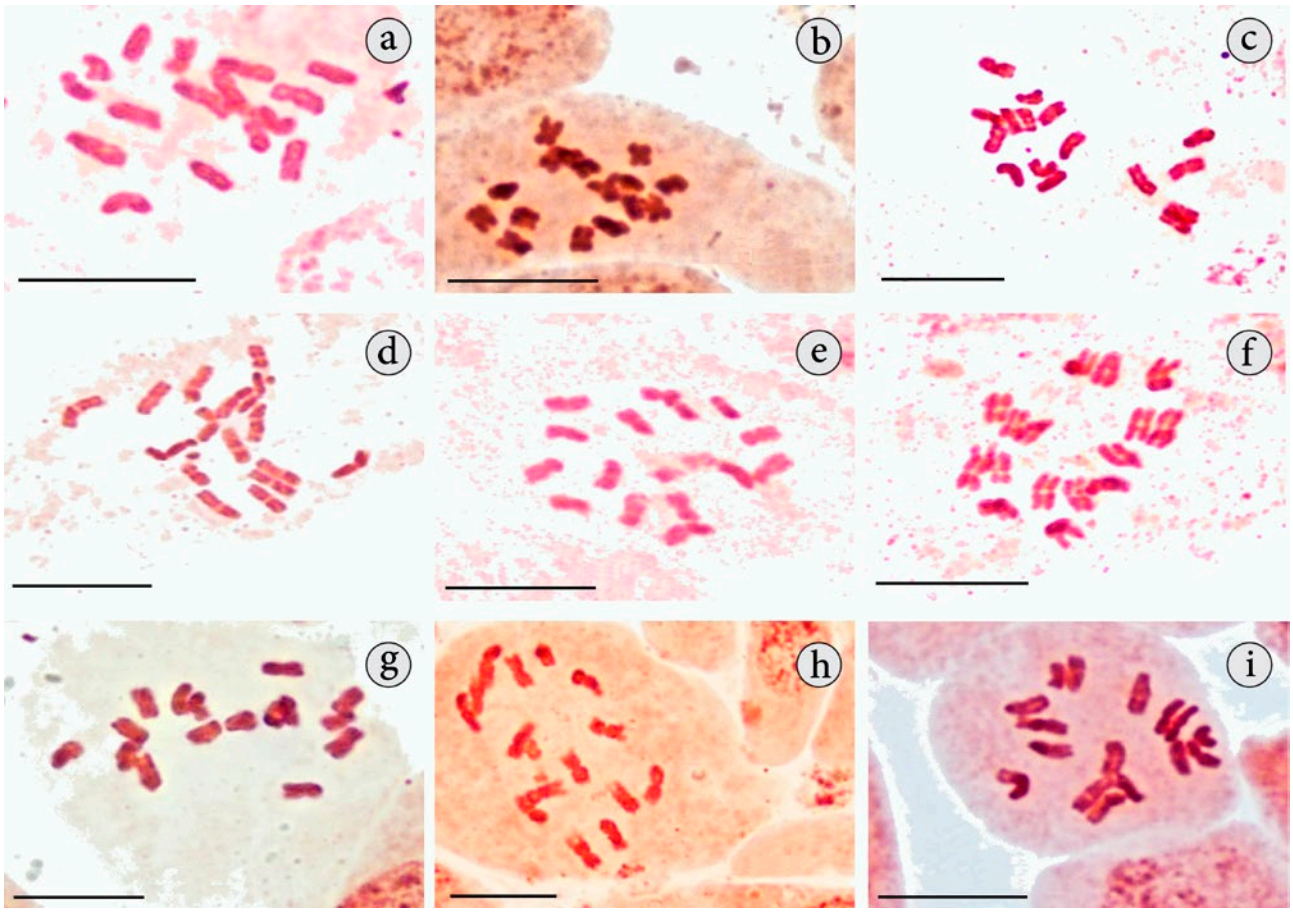

Figure 1. Photographs of somatic metaphase chromosomes of nine populations belonging to six species of the genus *Trigonella* collected from northeast of Iran. (a, b) *T. binaloudensis* from two locality; (c) *T. heratensis*; (d) *T. lasiocarpa*; (e) *T. stipitata;* (f, g, h) *T. subenervis* from three locality; (i) *T. torbatejamensis*. Scale bars = 10 µm.

μm, and arm ratio from 1.02 to 1.69. The chromosome complement at mitotic metaphase consisted of 16 median region chromosomes, and karyotypic asymmetry was 1A.

Trigonella lasiocarpa Ranjbar & Z.Hajmoradi

The chromosome number of *T. lasiocarpa* was 2n=2x=16 (Figure 1a). Haploid chromosome length was 28.9 μm. Chromosome length varied from 2.44 to 4.44 μm, and arm ratio from 1.09 to 1.51. The chromosome complement at mitotic metaphase consisted of 16 median region chromosomes, and karyotypic asymmetry was 1A.

Trigonella stipitata Ranjbar & Joharchi

The chromosome number of *T. stipitata* was 2n=2x=16 (Figure 1b). Haploid chromosome length was 19.17 μm. Chromosome length varied from 1.92 to 3.13 μm, and arm ratio from 1.02 to 1.44. The chromosome complement at mitotic metaphase consisted of 16 median region chromosomes, and karyotypic asymmetry was 1A.

Trigonella subenervis Rech.f

Population 1 (N Torbate-Heydariyeh):

The chromosome number was 2n=2x=16 (Figure 1f1). Haploid chromosome length was 19.87 μm. Chromosome length varied from 1.94 to 3.00 μm, and arm ratio from 1.01 to 1.94. The chromosome complement at mitotic metaphase consisted of 14 median region and two submedian region chromosomes. Karyotypic asymmetry was 1A.

Population 2 (N Kashmar):

The chromosome number was 2n=2x=16 (Figure 1f3). Haploid chromosome length was 20.68 μm. Chromosome length varied from 2.03 to 3.04 μm, and arm ratio from 1.01 to 1.52. The chromosome complement at mitotic metaphase consisted of 16 median region chromosomes, and Karyotypic asymmetry was 1A.

Population 3 (N Shirvan):

The chromosome number was 2n=2x=16 (Figure 1f3). Haploid chromosome length was 28.04 μm. Chromosome length varied from 2.67 to 4.18 μm, and arm ratio from 1.01 to 1.44. The chromosome complement at mitotic metaphase consisted of 16 median region chromosomes, and Karyotypic asymmetry was 1A.

Trigonella torbatejamensis Ranjbar

The chromosome number of *T. torbatejamensis* was 2n=2x=16 (Figure 1d). Haploid chromosome length was 26.77 μm. Chromosome length varied from 2.42 to 4.50 μm, and arm ratio from 1.05 to 2.21. The chromosome complement at mitotic metaphase consisted of 14 median region and two submedian region chromosomes. Karyotypic asymmetry was 2A.

DISCUSSION

All taxa in the present study showed the same basic chromosome number x=8 and same polyploidy level, which is congruent with those previously reported by Ranjbar *et al.* (2016) in *Trigonella subenervis* and six other species of the section. *Ellipticae*. This section comprises most of the perennial species of the genus *Trigonella* and widely distributed in Iran, Afghanistan and Middle Asia.

Table 2. Somatic chromosome numbers and Karyotypes of nine *Trigonella* taxa. HCl: haploid chromosome length, Cl: chromosome length, AR: arm ratio(L/S), RL%: relative length of the chromosome, CI: centromeric index.

Species	2n	X	HCL (μm)	CL μm)	AR	RL%	CI	Karyotype formulae	Karyotypic asymmetry (Stebbins)
*T. binaloudensis** (1)	16	8	27.73	2.75-4.83	1.06-1.88	4.96-8.70	0.35-0.49	14m+2sm	1A
*T. binaloudensis** (2)	16	8	24.03	2.15-3.72	1.03-1.82	4.48-7.74	0.35-0.49	14m+2sm	1A
T. heratensis	16	8	22.98	2.46-3.40	1.02-1.69	5.36-7.39	0.37-0.50	16m	1A
*T. lasiocarpa**	16	8	28.90	2.41-4.44	1.09-1.51	4.17-7.68	0.40-0.48	16m	1A
*T. stipitata**	16	8	19.17	1.92-3.13	1.02-1.44	5.00-8.15	0.41-0.49	16m	1A
*T. subenervis** (1)	16	8	19.87	1.94-3.00	1.01-1.94	4.88-7.54	0.34-0.50	14m+2sm	1A
*T. subenervis** (2)	16	8	20.68	2.03-3.04	1.01-1.52	4.91-7.34	0.40-0.50	16m	1A
*T. subenervis** (3)	16	8	28.04	2.67-4.18	1.01-1.44	4.75-7.45	0.41-0.50	16m	1A
*T. torbatejamensis**	16	8	26.77	2.42-4.50	1.05-2.21	4.51-8.41	0.31-0.49	14m+2sm	2A

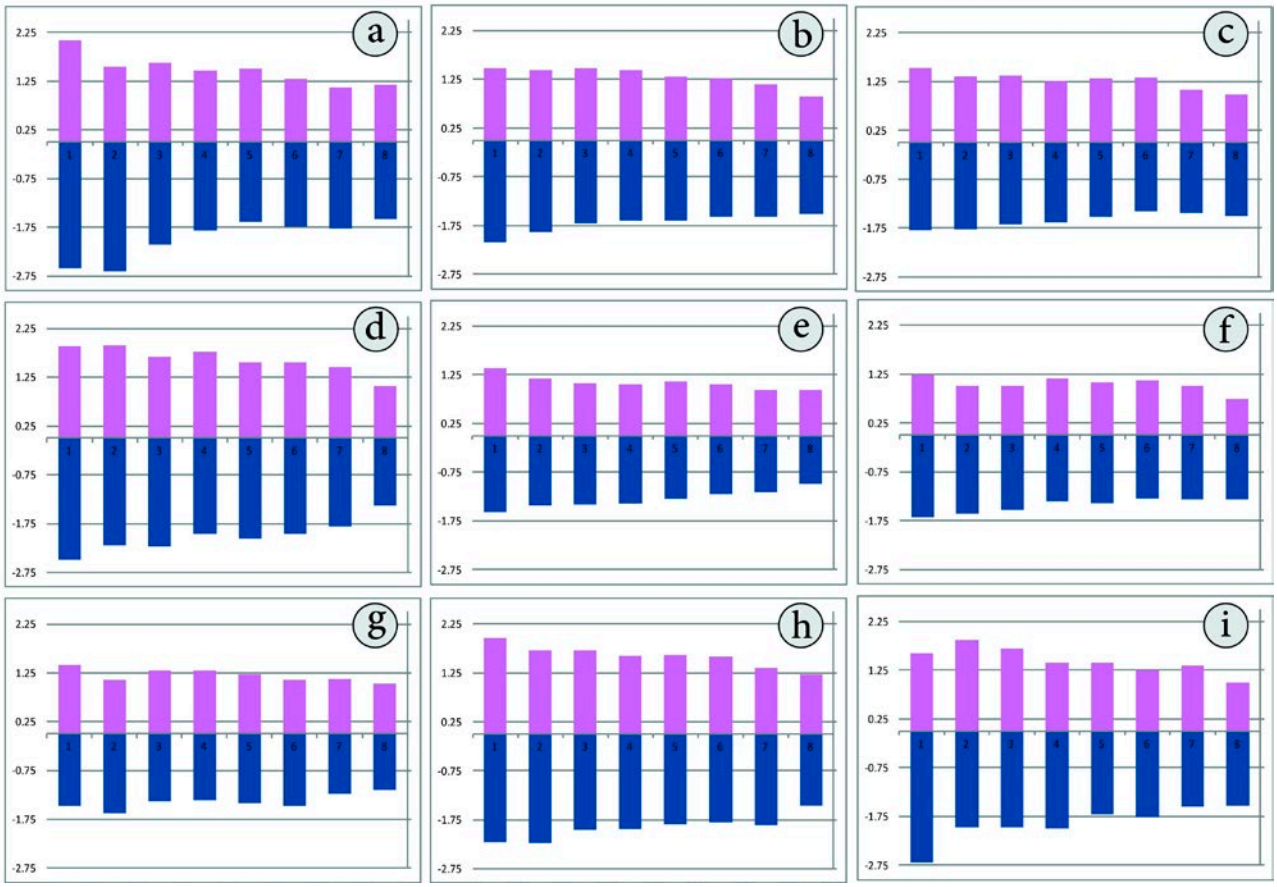

Figure 2. Haploid ideograms of *Trigonella* taxa. (a, b) *T. binaloudensis* from two locality; (c) *T. heratensis*; (d) *T. lasiocarpa*; (e) *T. stipitata;* (f, g, h) *T. subenervis* from three locality; (i) *T. torbatejamensis*. in all of studied taxa 2n=16.

All of the studied taxa in this study, analyzed karyotypically for the first time, covering chromosome length, karyotype formulae, and asymmetry (Table and Figure 2). In term of karyotypic parameters, Our results support the results reported by Riasat (2015) about *Trigonella elliptica*, a perennial species from section *Ellipticae*. In later study, the karyotype formulae reported as 14m+2sm, 16m, 8m+8sm, and 12m+4sm in different genotypes. We found the same variations in karyotype formulae and asymmetry among different species and populations that are shown in Table 2.

Karyotypic asymmetry in most of the studied taxa, was as A1 but in *T. torbatejamensis* which is A2. Karyotype formulae in most of the specimens were as 16m and in four specimens (*T. torbatejamensis*, two populations of *T. binaloudensis* and one population of *T. subenervis*) was as 14m+2sm. The incongruences may result from variations among different populations and chromosome preparation treatments. It seems that chromosome variation and evolution of *Trigonella* species need more comparative cytological studies based on more collections from different populations.

ACKNOWLEDGMENTS

This work was partly supported by the Research Center for Plant Science, Ferdowsi University of Mashhad. The authors would like to thank the staff assistance of FUMH in field and herbarium. We are grateful to Miss. S. Hosseini for technical assistance.

REFERENCES

Agarwal K, Gupta PK. 1983. Cytological studies in the genus *Trigonella* Linn. Cytologia. 48(4):771-779.

Ahmad F, Acharya S, Mir Z, Mir P. 1999. Localization and activity of rRNA genes on fenugreek (*Trigonella foenum-graecum* L.) chromosomes by fluorescent in

situ hybridization and silver staining. Theoretical and Applied Genetics. 98(2):179-185.

Aksoy H, Berber AA, Çelik S, Başer B, Karavelioğullari FA. 2016. Karyological study on 12 *Centaurea* (Asteraceae) species from Turkey. Caryologia. 69(4):285-294.

Aksu N, Inceer H, Hayırlıoğlu-Ayaz S. 2013. Karyotype analysis of six *Achillea* L.(Asteraceae, Anthemideae) taxa from Turkey. Caryologia. 66(2):103-108.

Altınordu F, Peruzzi L, Yu Y, He X. 2016. A tool for the analysis of chromosomes: KaryoType. Taxon. 65(3):586-592.

Astanova SB. 1981. Chromosome numbers of Leguminosae flora in Tajikistan. Dokl Akad Nauk

Tadziksk SSR. 24:61-63.

Avtar S, Roy R. 1970. Karyological studies in *Trigonella*, Indigofera and Phaseolus. Nucleus. 13(1):41-54.

Aykut Y, Martin E, Ünal F, Akan H. 2009. Karyological study on six *Trigonella* L. species (Leguminosae) in Turkey. Caryologia. 62(2):89-94.

Badrzadeh M, Ghafarzadeh-Namazi L. 2009. *Trigonella caerulea* (Fabaceae), an aromatic plant from Ardabil province, Iran. Iranian Journal of Botany. 15(1):82-84.

Bal Ş. 1990. *Trigonella foenum graecum* L.'da Karyotip Analizler. Gazi Üniversitesi Fen Bilimleri Enstitüsü, Yüksek Lisans Tezi.

Behroozian M, Vaezi J, Reza Joharchi M. 2012. A karyological study of some *Dianthus* L. species (Caryophyllaceae) in Northeast of Iran. Feddes Repertorium. 123(4):265-272.

Biddak L. 1996. Inter-and intraspecific chromosomal variations in four species of *Trigonella* L. Journal of Union of Arab Biologists (Cairo). 3:203-215.

Braselton JP. 1997. Microscopic procedures for plant meiosis. American Biology Teacher. 59(8):502-506.

Dangi R, Tamhankar S, Choudhary RK, Rao S. 2016. Molecular phylogenetics and systematics of *Trigonella* L.(Fabaceae) based on nuclear ribosomal ITS and chloroplast trnL intron sequences. Genetic resources and crop evolution. 63(1):79-96.

Darlington CD, Wylie AP. 1955. Chromosome atlas of flowering plants. London: Allen and Unwin Press.

Dolatyari A, Kamrani A. 2015. Chromosome number and morphology of some accessions of four *Lallemantia* Fisch. & CA Mey.(Lamiaceae) species from Iran. Wulfenia. 22:127-135.

Dundas IS, Nair RM, Verlin DC. 2006. First report of meiotic chromosome number and karyotype analysis of an accession of *Trigonella balansae* (Leguminosae). New Zealand Journal of Agricultural Research. 49(1):55-58.

Eroğlu HE. 2015. Which chromosomes are subtelocentric or acrocentric? A new karyotype symmetry/asymmetry index. Caryologia. 68(3):239-245.

Esra M, Akan H, Ekici M, Aytaç Z. 2008. Karyomorphological studies on section *Bucerates* Boiss. of *Trigonella* L.(Leguminosae) from Turkey. Caryologia. 61(3):225-236.

Fukui K, Nakayama S. 1996. Plant chromosomes: laboratory methods. CRC press.

Ghosh AK. 1980. Chromosome number of *Trigonella spinosa*. Current Science. 49(4):154-155.

Hamzeh'ee B. 2000. Some new and noteworthy plant records from Iran. Iranian Journal of Botany. 8(2):271-277.

Hu G-X, Xiang C-L, Liu E-D, Dong H-J, Funamoto T. 2016. Karyotypic study of eighteen taxa of *Salvia* (Lamiaceae) from China. Caryologia. 69(1):50-57.

Hutchinson J. 1964. Order Leguminales. The genera of flowering plants. 1:339-341.

Janighorban M. 2004. A new record of the genus *Trigonella* (Fabaceae) for the flora of Iran. Iranian Journal of Botany. 10(2):177-179.

Keshavarzi M, Abbasian S, Sheidai M. 2014. Cytological studies of the genus *Clypeola* L. (Brassicaceae) in Iran. Iranian Journal of Botany. 20(2):201-210.

Keshavarzi M, Bozchaloyi SE. 2014. Chromosome numbers for some *Stellaria* L. (Caryophyllaceae) species and related taxa in Iran. Iranian Journal of Botany. 20(1):36-40.

Kumari S. 1990. Karyomorphological evolution in Papillionaceae. Journal of Cytology and Genetics. 25:173-219.

Kursat M, Emre I, Gedik O, Kiran Y. 2018. Karyological reports for some *Salvia* taxa from Turkey. Caryologia. 71(2):120-127.

Ladizinsky G, Vosa CG. 1986. Karyotype and C-banding in *Trigonella* section *Foenum-graecum* (Fabaceae). Plant systematics and evolution. 153(1-2):1-5.

Levan A, Fredga K, Sandberg AA. 1964. Nomenclature for centromeric position on chromosomes. Hereditas. 52(2):201-220.

Mabberley DJ. 1997. The plant-book: a portable dictionary of the vascular plants. Cambridge university press.

Martin E, Akan H, Ekici M, Aytac Z. 2010. Karyology of ten Turkish *Trigonella* L. (Leguminosae) species from section *Cylindricae* Boiss. Turkish Journal of Botany. 34(6):485-494.

Martin E, Akan H, Ekici M, Aytac Z. 2011. Karyotype analyses of ten sections of *Trigonella* (Fabaceae). Comparative Cytogenetics. 5(2):105.

Martin E, Akan H, Ekici M, Aytac Z. 2011. New chromosome numbers in the genus *Trigonella* L. (Fabace-

ae) from Turkey. African Journal of Biotechnology. 10(2):116-125.

Melahat O, Hayırlıoglu-Ayaz S, Inceer H. 2011. Chromosome reports in some *Cirsium* (Asteraceae, Cardueae) taxa from north-east Anatolia. Caryologia. 64(1):55-66.

Mirzaghaderi G. 2010. Simple metaphase chromosome preparation from meristematic root tip cells of wheat for karyotyping or in situ hybridization. African Journal of Biotechnology. 9(3).

Mirzaghaderi G, Marzangi K. 2015. IdeoKar: an ideogram constructing and karyotype analyzing software. Caryologia. 68(1):31-35.

Mosaferi S, Sheidai M, Keshavarzi M, Noormohammadi Z. 2018. Karyological study of some annual *Polygonum* species in Iran. Botany Letters, 165(2):280-285

Paszko B. 2006. A critical review and a new proposal of karyotype asymmetry indices. Plant Systematics and Evolution. 258(1-2):39-48.

Pavlova D. 1996. Mediterranean chromosome number reports 6 (762–766). Flora Mediterranea. 6:323-328.

Peruzzi L, Bedini G. 2014. Online resources for chromosome number databases. Caryologia. 67(4):292-295.

Peruzzi L, Eroğlu HE. 2013. Karyotype asymmetry: again, how to measure and what to measure? Comparative cytogenetics. 7(1):1.

Ranjbar M, Hajmoradi Z. 2015. A new species of *Trigonella* sect. *Ellipticae* (Leguminosae-Papilionoideae) from Iran, including cytogenetic and anatomical notes. Phytotaxa. 202(1):26-34.

Ranjbar M, Hajmoradi Z, Karamian R. 2012. Cytogenetic study and pollen viability of four populations of *Trigonella spruneriana* Boiss.(Fabaceae) in Iran. Journal of Cell and Molecular Research. 3(1):19-24.

Ranjbar M, Karamian R, Hajmoradi Z. 2011. Cytomorphological study of *Trigonella disperma* (Fabaceae) in Iran. Cytologia. 76(3):279-294.

Ranjbar M, Karamian R, Hajmoradi Z. 2012. A new species and taxonomic studies in *Trigonella* sect. *Ellipticae* (Fabaceae) in Iran. Annales Botanici Fennici. 49(4): 279-287.

Ranjbar M, Karamian R, Hajmoradi Z, Joharchi M. 2012. A revision of *Trigonella* sect. *Ellipticae* (Fabaceae) in Iran. Nordic Journal of Botany. 30(1):17-35.

Ranjbar M, Hajmoradi Z. 2016. Chromosome numbers and biogeography of the genus *Trigonella* (Fabaceae). Caryologia. 69(3):223-234.

Rechinger K. 1984. Flora iranica: no. 157. Papilionaceae: 2 (Tabulae). Graz, Akademische Druck-und Verlagsanstalt. 424.

Riasat M. 2015. A cytogenetic study on some perennial *Trigonella* (fenugreek) in Iran. Research Journal of Recent Sciences. 4(5):10-13.

Sadeghian S, Hesamzadeh HSM, Hatami A, Jafari E. 2017. Karyotypic variation in two species of the genus *Cercis* in Iran. Iranian Journal of Botany. 23(1):56-59.

Singh A, Singh D. 1976. Karyotype studies in *Trigonella*. Nucleus. 19(1):13-16.

Širjaev GI. 1931. Generis *Trigonella* L. revisio critica. 4 (1931). Přírodověd. Fak.

Stebbins GL. 1971. Chromosomal evolution in higher plants. London: Edward Arnold Ltd.

Tutin TG, Heywood VH, Burges NA, Valentine D. 1976. Flora Europaea: Plantaginaceae to Compositae (and Rubiaceae). Vol. 4. Cambridge University Press.

Wagh M, Dakhore S, Agrawal P, Paliwal L. 2016. Comparative cytological study of *Trigonella foenum graecum* and *Brassica compestries*. Journal of Chemical and Pharmaceutical Research. 8(5):208-213.

Caryologia
International Journal of Cytology, Cytosystematics and Cytogenetics

Firenze University Press
www.fupress.com/caryologia

OPEN ACCESS

Citation: K. Saha, R.K. Sinha, S. Sinha (2020) Karyological studies in thirteen species of Zingiberacaeae from Tripura, North East India. *Caryologia* 73(1): 163-178. doi: 10.13128/caryologia-186

Received: March 11, 2019

Accepted: February 23, 2020

Published: May 8, 2020

Data Availability Statement: All relevant data are within the paper and its Supporting Information files.

Competing Interests: The Author(s) declare(s) no conflict of interest.

Karyological studies in thirteen species of Zingiberacaeae from Tripura, North East India

Kishan Saha*, Rabindra Kumar Sinha, Sangram Sinha

Cytogenetics and Plant Biotechnology Laboratory, Department of Botany, Tripura University, Suryamaninagar-799022, Tripura, India
*Corresponding author. E-mail: saha.kshn@gmail.com

Abstract. Tripura being a state in North East India belongs to Indo-Burma bio-diversity hotspot and is considered as a centre of origin of many species of Zingiberaceae. *Alpinia calcarata*, *Alpinia malaccensis*, *Alpinia nigra*, *Amomum aromaticum*, *Amomum koenigii*, *Amomum maximum*, *Curcuma amada*, *Curcuma caesia*, *Curcuma longa*, *Curcuma picta*, *Hedychium coccineum, Hedychium coronarium* and *Hedychium thyrsiforme* are found in wild state in different geographical locations of Tripura. Their karyotypes were analyzed both at interspecific and intraspecific levels. The somatic chromosome number of *Alpinia* spp. and *Amomum* spp. was found to be 2n = 4X = 48. The *Curcuma* spp. represented by *C. amada* had 2n = 42 chromosomes and three other species *viz*., *C. caesia*, *C. longa* and *C. picta* had 2n = 63 chromosomes having X=21, indicating that polyploidy is a common feature in this genus. The somatic chromosome number of *Hedychium* spp. was found to be 2n = 34 chromosomes having a basic no. X = 17. Chromosomal data based clustering pattern and their sub-grouping at intra-specific level validates the taxonomic status of these species. Gower's similarity matrix is an indicator of cryptic changes leading genus specific karyotype conservatism.

Keywords. Indo-Burma bio-diversity hotspot, Zingiberaceae, Karyotype, Polyploidy, Cryptic changes.

INTRODUCTION

The State of Tripura (20°56'-24°34' North latitude and 91°10'-92°21' East longitude) is situated in the Sub-Himalayan region of North East India and belongs to Indo-Burma biodiversity hotspot of the world (Myers *et al.* 2000; Mao *et al.* 2009). The diverse vegetation of this region includes a good number of plants, which are endemic either to the state or to the North-Eastern region of India (Deb 1981). In India, the Zingiberaceae family includes 22 genera and about 200 species which are distributed in Andaman and Nicobar Island, Western Ghats and Eastern Himalaya region including North-Eastern India (Jain and Prakash 1995; Sabu 2006). Many natural useful products such as food, dyes, medicines, spices and condiments are obtained from the members of this family (Nayak 2002; Arambewela *et al.* 2004; Sahoo *et al.* 2014; Rahman and Islam 2015). The local people of South Asian countries also use

several plant products of Zingiberaceae in traditional medicines (Jayaweera 1982; Prakash and Mehrotra 1996; Gupta *et al.* 1999; Kala 2005; Bhuiyan *et al.* 2010; Roy *et al.* 2012; Sarangthem *et al.* 2013; Rajkumari and Sanatombi 2018). Some species of Zingiberaceae are also highly valued as ornamental plants because of their showy scented flowers (Jatoi *et al.* 2007; Gao *et al.* 2008). Deb (1983) recorded nine genera having 24 different species of this family from this phyto-geographical region. However, *Alpinia galanga*, *Hedychium ellipticum* and *Hedychium marginatum* could not be found in specific localities as was earlier reported by Deb (1983). Probably, these species have eventually perished due to anthropological disturbances. In-spite of such habitat destruction, five more species *viz*., *Curcuma caesia*, *Curcuma picta*, *Hedychium coccineum*, *Amomum aromaticum* (Syn. *A. jainii* S. Tripati & Vedprakash), *Amomum koenigii* (Syn. *Amomum corynostachyum*. Wall.) and *Amomum maximum* are found in different locations which were not reported by Deb (1983). Thus, 13 different species belonging to four genera *viz., Alpinia*, *Amomum*, *Curcuma* and *Hedychium* of Zingiberaceae are now available in Tripura. These are *Alpinia calcarata* (Haw.) Roscoe, *Alpinia malaccensis* (Burm.f.) Roscoe, *Alpinia nigra* (Gaertn.) Burtt, *Amomum aromaticum* Roxb. (Syn. *Amomum jainii* S. Tripati and Vedprakash), *Amomum koenigii* J.F.Gmel. (Syn. *Amomum corynostachyum* Wall.), *Amomum maximum* Roxb., *Curcuma amada* Roxb., *Curcuma caesia* Roxb., *Curcuma longa* L., *Curcuma picta* Roxb. ex Skornick, *Hedychium coccineum* Buch.-Ham. ex Sm., *Hedychium coronarium* J. Koenig. and *Hedychium thyrsiforme* Sm. Morphologically these species are quite distinct in their rhizome, floral and fruit characters (Deb 1983; Vanchhawng and Lalramnghinglova 2016). Delineation of plant species based on morphological characters alone is not adequate (Larsen and Smith 1978) and so, for characterization of species at inter- and intra-specific levels cytological tools are now effectively used to understand the taxonomic relationship and evolutionary patterns between and within species (Yoshikane and Naohiro 1991; Joseph *et al.* 1999). Previously, cytological works on Zingiberaceae were mainly focussed on *Curcuma* spp. and various researchers from time to time (Raghavan and Venkatasubban 1943; Chakraborti 1948; Sato 1948; Sharma and Bhattacharya 1959; Sato 1960; Ramachandran 1961,1969; Fedorov 1969; Prana 1977; Prana *et al.* 1978; Nambiar 1979; Mandi 1990; Ardiyani 2002; Skornickova *et al.* 2007; Bhadra and Bandhyopadhyay 2015; Lamo and Rao 2017; Bhadra *et al.* 2018) reported the existence of different ploidy levels, ranging from diploid (2n = 42) to tetraploid (2n=84), having a basic number X=21. In addition, aneuploid cytotypes in *Curcuma* spp. had also been reported (Das *et al.* 1999, Sugiura (1931, 1936), Sato 1960). Cytological studies previously carried out in *Alpinia* spp. and *Amomum* spp. were mainly concentrated on the determination of somatic chromosome numbers having 2n = 4X= 48 chromosomes (Raghavan and Venkatasubban 1943; Chakravorti 1948; Sharma and Bhattacharya 1959; Ramachandran 1969). But, from the literature it is evident that the detailed karyotype analysis in different species of *Alpinia* and *Amomum* was very meagre (Chen *et al.* 1988; Joseph 1998). In *Hedychium* spp. the occurrence of different ploidy levels (2n=34, 51 and 68) was reported in various cytological studies (Sharma and Bhattacharyya 1959; Bhattacharyya 1968; Ramachandran 1969; Mukherjee 1970; Mahanty 1970; Khoshoo 1979; Gao *et al.* 2008). Tripura being a part of Indo- Burma hotspot is considered as a centre of origin of many Indian species of Zingiberaceae but till date, cytological investigation of these species have not been carried out from this region. The present study is the first attempt to assess the karyotypic relationship in different species of Zingiberaceae at inter- and intra- specific level from the sub – Himalayan region of Tripura and for providing additional information to the chromosomal database of Zingiberean plants of Indian origin.

MATERIALS AND METHODS

Plant materials

We examined two populations (described as Pop-I and Pop-II) of 13 different wild species of Zingiberaceae *viz*., *Alpinia calcarata* (Haw.) Roscoe, *Alpinia malaccensis* (Burm.f.) Roscoe, *Alpinia nigra* (Gaertn.) Burtt, *Amomum aromaticum* Roxb. (Syn. *Amomum jainii* S. Tripati and Vedprakash), *Amomum koenigii* J. F. Gmel. (Syn. *Amomum corynostachyum* Wall.), *Amomum maximum* Roxb., *Curcuma amada* Roxb., *Curcuma caesia* Roxb., *Curcuma longa* L., *Curcuma picta* Roxb. ex Skornick, *Hedychium coronarium* J. Koenig., *Hedychium coccineum* Buch.-Ham. ex Sm. and *Hedychium thyrsiforme* Sm. growing in different locations in Tripura. They were grown in the experimental garden, Department of Botany, Tripura University for future research. All the plant species were independently authenticated by the taxonomy experts. Herbarium of each species has been submitted in Tripura University Herbarium with respective voucher numbers (Table S1).

Preparation of somatic chromosomes

The somatic chromosome preparation was carried out with modified aceto-orcein staining technique

(Sharma and Sharma 1980). Young healthy root tips of each species were pre-treated in a mixture of saturated solution of para dichloro-benzene (p-DB) and 0.002M 8- hydroxyquinoline (1:1) at 12-15^{0}C for 6 hrs. The root tips were then washed with distilled water and kept in acidulated alcohol (mixture of 1NHCl and absolute ethyl alcohol in 1:1 ratio) for 1 hour. Thereafter, root tips were kept in 45% acetic acid for 20 minutes. After a thorough wash with distilled water, root tips were treated with 5% cellulase (Sigma Cat. No. 22178) and 5% pectinase (Sigma Cat. No. 17389) mixture (1:1) in citrate buffer (pH - 4.8) for 3 hours at 37^{0}C. Enzyme treated root tips were then washed with double distilled water and stained with 2% aceto-orcein : 1NHCl (9:1) mixture for overnight and finally squashed in 45% acetic acid. The well spread metaphase plate was captured using Zeiss make AXIO (Lab.A1) Microscope and Zen software was used for determining the length of short and long arm of individual chromosome of the species studied.

Study of nucleoli in somatic cells

Nucleolar staining was carried out following the technique of Fernandez-Gomez *et al*. (1969). Initially root tips were fixed in 10% Formol :1% Hydroquinone (1:1) solution for 2 hrs. These were thoroughly washed in distilled water and immersed in 2% silver nitrate solution at 60°C in dark for overnight. $AgNO_3$ treated root tips were again kept in Formol-Hydroquinone (1:1) solution for 1 hour and finally squashed in 45% acetic acid.

Data analysis

In preparing the numerical data of karyotype, three well spread metaphase plates of each species were compared. In cases, where the length and the arm ratio varied the mean was taken to calculate the value of centromeric Index (F%). The centromeric Index, TF%, Inter-chromosomal asymmetry index (A_2), Coefficient of variation of chromosome length (CV_{CL}), and Mean Centromeric Asymmetry (M_{CA}) were calculated by the following formulae:Centromeric Index (F%) = S/(L+S)×100 (Levan *et al*. 1964);TF% = (ΣS/ΣCL) × 100 (Huziwara 1962);Inter-chromosomal asymmetry index (A_2) = s_{CL}/X_{CL} (Zarco 1986); Degree of karyotype asymmetry (A) = [Σ (L-S)/(L+S)]/n (Watanabe *et al*. 1999); Coefficient of variation of chromosome length (CV_{CL}) = A_2×100 (Paszko 2006); Mean Centromeric Asymmetry (M_{CA}) = A×100 (Peruzzi and Eroglu 2013); (S = Length of short arm, L = Length of long arm, CL = Chromosome length, s_{CL}- Standard deviation of chromosome length, X_{CL}- Mean of chromosome length, n – haploid number of chromosome complement).

Along with Stebbins asymmetry indices, the inter- and intra-chromosomal asymmetry indices were measured statistically (Zarco 1986; Watanabe *et al*. 1999) and the relationship among the species was explained by means of bi-dimensional scattered plot (Peruzzi and Eroglu 2013).To determine the karyological relationship among taxa UPGMA mediated dendrogram was constructed using the software Past 3.03 (Hammer 2013). In addition, multivariate Principal Co-ordinate Analysis (PCA) was also performed using different parameters of numerical data of karyotypes (Table 1) of the respective species and their populations (Peruzzi and Altinordu 2014).

RESULTS

Due to difficulty in obtaining suitable metaphase chromosome spreads with the conventional aceto-orcein staining technique, a new protocol has been developed to determine the somatic chromosome number and to analyze the detailed karyotype of all the taxa studied. The somatic chromosomes of *Alpinia* spp., *Amomum* spp., *Curcuma* spp. and *Hedychium* spp. could be classified into three distinct morphological types.

Type A**:** Short chromosomes (1.33 µm – 2.66 µm) bear two constrictions, primary and secondary, one is nearly median (m) to sub-median (sm) and the other is terminal (t) in position.

Type B**:** Chromosomes are short in size and their length range from 0.96 µm – 2.79 µm. The position of centromere is sub-median (sm) to median (M) (F% >33.33%).

Type C**:** Chromosomes are short in size and their length range from 1.86 µm – 2.13µm. The position of centromere is sub-median (sm) (F% <33.33%).

Analysis of karyotypes

Except in *Alpinia nigra*, which had two pairs of C type of submetacentric chromosomes, karyograms (Figure S1) of rest of the 12 species showed the presence of different combinations of A and B types chromosomes as classified in the present study. The detailed analyses of the karyotypes of Pop-I and Pop-II of *Alpinia* spp., *Amomum* spp., *Curcuma* spp. and *Hedychium* spp. reveal the following data:

Alpinia calcarata-Pop-I:

Somatic chromosome number 2n=48 (Figure 1a); Number of chromosomes bearing secondary constric-

Table 1. Karyological parameters for cluster analysis and Gower's similarity coefficient matrix.

Name of the species and Population	SCN	HCL (µm)	BCN	TF%	M_{CA}	CV_{CL}
Alpinia calcarata, Pop-I	48	45.22	12	42.61	30.00	28.44
Alpinia calcarata, Pop-II	48	45.60	12	42.44	30.23	27.71
Alpinia malaccensis, Pop-I	48	41.05	12	43.57	26.00	18.17
Alpinia malaccensis, Pop-II	48	42.87	12	43.65	25.41	17.79
Alpinia nigra, Pop-I	48	44.06	12	40.29	38.83	23.00
Alpinia nigra, Pop-II	48	44.14	12	40.27	38.91	22.45
Amomum maximum, Pop-I	48	33.06	12	44.75	20.76	18.61
Amomum maximum, Pop-II	48	32.93	12	44.79	20.84	17.82
Amomum aromaticum, Pop-I	48	30.61	12	45.39	18.45	21.75
Amomum aromaticum, Pop-II	48	30.57	12	45.52	17.94	20.93
Amomum koenigii, Pop-I	48	39.50	12	44.56	23.67	26.46
Amomum koenigii, Pop-II	48	39.32	12	44.28	22.87	26.48
Hedychium coronarium, Pop-I	34	20.72	17	47.32	10.72	15.91
Hedychium coronarium, Pop-II	34	20.78	17	47.24	11.06	15.11
Hedychium coccineum, Pop-I	34	26.40	17	46.68	13.27	15.51
Hedychium coccineum, Pop-II	34	26.46	17	46.47	14.11	15.40
Hedychium thyrsiforme, Pop-I	34	19.13	17	46.60	13.56	15.24
Hedychium thyrsiforme, Pop-II	34	19.70	17	46.61	13.69	14.88
Curcuma amada, Pop-I	42	31.05	21	47.02	11.91	12.52
Curcuma amada, Pop-II	42	32.35	21	46.96	12.17	12.77
Curcuma caesia, Pop-I	63	34.29	21	47.98	12.05	12.08
Curcuma caesia, Pop-II	63	34.37	21	48.11	11.35	12.08
Curcuma picta, Pop-I	63	44.67	21	47.96	12.23	13.16
Curcuma picta, Pop-II	63	44.43	21	47.94	12.34	12.66
Curcuma longa, Pop-I	63	44.16	21	47.01	16.78	11.18
Curcuma longa, Pop-II	63	44.04	21	47.13	17.23	11.01

SCN – Somatic chromosome number; HCL-Total chromosome length of the haploid complement; BCN- Basic chromosome number; TF% - Total Form percentage; M_{CA} - Mean Centromeric Asymmetry; CV_{CL} - Coefficient of variation of chromosome length.

tion - 2; Range of chromosome length – (1.06 µm – 2.79 µm); Total chromosome length – 90.43 µm; Ratio of largest and smallest chromosome – 2.63:1; Mean arm ratio (L/S) –1.38; Karyotype formula - $A_{2\ (2m)}\ B_{46\ (6M+30m+10sm)}$; Stebbins category – 1B; TF% - 42.61; Coefficient of variation of chromosome length (CV_{CL}) – 28.44; Mean centromeric asymmetry (M_{CA}) – 30.00.

Alpinia calcarata-Pop-II:

Somatic chromosome count 2n=48 (Figure 1b); Number of chromosomes bearing secondary constriction - 2; Range of chromosome length – (1.06 µm – 2.79 µm); Total chromosome length – 91.20 µm; Ratio of largest and smallest chromosome – 2.63:1; Mean arm ratio (L/S) –1.39; Karyotype formula - $A_{2\ (2m)}\ B_{46\ (6M+34m+6sm)}$ Stebbins category – 1B; TF% – 42.44; CV_{CL} – 27.71; M_{CA} – 30.23.

Alpinia malaccensis-Pop-I:

Somatic chromosome count 2n=48 (Figure 2a); Number of chromosomes bearing secondary constriction - 2; Range of chromosome length – (1.16 µm – 2.14 µm); Total chromosome length – 82.10 µm; Ratio of largest and smallest chromosome – 1.84:1; Mean arm ratio (L/S) – 1.33; Karyotype formula - $A_{2\ (2m)}\ B_{46\ (36m+10sm)}$; Stebbins category – 1A; TF% – 43.57; CV_{CL} – 18.17; M_{CA} – 26.00.

Alpinia malaccensis-Pop-II:

Somatic chromosome number 2n=48 (Figure 2b); Number of chromosomes bearing secondary constriction - 2; Range of chromosome length – (1.16 µm - 2.26 µm); Total chromosome length – 85.74µm; Ratio of largest and smallest chromosome – 1.95:1; Mean arm ratio (L/S) –1.33; Karyotype formula - $A_{2\ (2m)}\ B_{46\ (4M+36m+6sm)}$; Stebbins category – 1A; TF% – 43.65; CV_{CL} – 17.79; M_{CA} – 25.41.

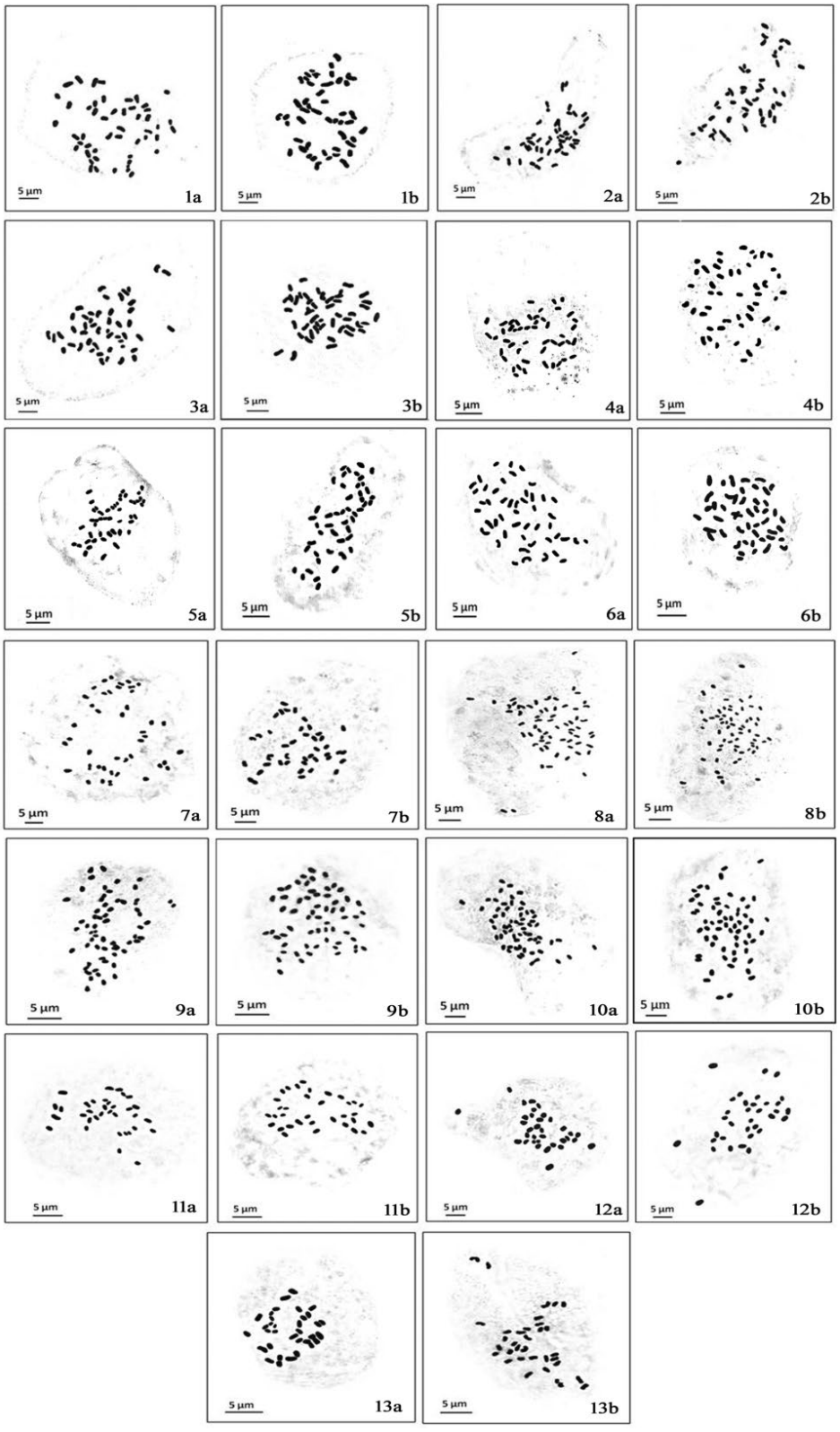

Figures. 1a-13b. Mitotic metaphase chromosomes of thirteen Zingiberaceae species from Tripura. 1- *Alpinia calcarata*; 2- *A. malaccensis*; 3- *A. nigra*; 4- *Amomum maximum*; 5- *A. aromaticum*; 6- *A. koenigii*; 7- *Curcuma amada*; 8- *C. caesia*; 9- *C. picta*; 10- *C. longa*; 11- *H. coronarium*; 12- *H. coccineum*; 13- *H. thyrsiforme* (a – Pop - I; b – Pop - II); scale bars = 5µm.

Alpinia nigra-Pop-I:

Somatic chromosome number 2n=48 (Figure 3a); Number of chromosomes bearing secondary constriction - 2; Range of chromosome length – (1.09 µm – 2.80 µm); Total chromosome length – 88.12 µm; Ratio of largest and smallest chromosomes – 2.57:1; Mean arm ratio (L/S) – 1.57; Karyotype formula – $A_{2\ (2sm)}\ B_{42\ (4M+26m+12sm)}\ C_{4\ (4sm)}$; Stebbins category – 2B; TF% – 40.29; CV_{CL} – 23.00; M_{CA} – 38.83.

Alpinia nigra-Pop-II:

Somatic chromosome number 2n=48 (Figure 3b); Number of chromosomes bearing secondary constriction - 2; Range of chromosome length – (1.09 µm – 2.72 µm); Total chromosome length – 88.28 µm; Ratio of largest and smallest chromosome – 2.50:1; Mean arm ratio (L/S) – 1.57; Karyotype formula - $A_{2\ (2sm)}\ B_{42\ (4\ M+26\ m+\ 12\ sm)}\ C_{4\ (4\ sm)}$; Stebbins category – 2B; TF% – 40.27; CV_{CL} – 22.45; M_{CA} – 38.91.

Amomum maximum-Pop-I:

Somatic chromosome number 2n=48 (Figure 4a); Number of chromosomes bearing secondary constriction - 2; Range of chromosome length – (1.06 µm – 1.94 µm); Total chromosome length – 66.12 µm; Ratio of largest and smallest chromosome – 1.83:1; Mean arm ratio (L/S) –1.27; Karyotype formula - $A_{2\ (2m)}\ B_{46(14M+26m+6sm)}$; Stebbins category – 1A; TF% – 44.75; CV_{CL} – 18.61; M_{CA} – 20.76.

Amomum maximum-Pop-II:

Somatic chromosome number 2n=48 (Figure 4b); Number of chromosomes bearing secondary constriction - 2; Range of chromosome length – (1.06 µm – 1.94 µm); Total chromosome length – 65.86 µm; Ratio of largest and smallest chromosome – 1.83:1; Mean arm ratio (L/S) –1.26; Karyotype formula - $A_{2\ (2m)}\ B_{46(16M+24m+6sm)}$; Stebbins category – 1A; TF% – 44.79; CV_{CL} – 17.82; M_{CA} – 20.84.`

Amomum aromaticum-Pop-I:

Somatic chromosome number 2n=48 (Figure 5a); Number of chromosomes bearing secondary constriction - 2; Range of chromosome length – (1.06 µm – 2.10 µm); Total chromosome length – 61.22 µm; Ratio of largest and smallest chromosome – 1.98:1; Mean arm ratio (L/S) – 1.22; Karyotype formula - $A_{2\ (2m)}\ B_{46\ (16M+30m)}$; Stebbins category – 1A; TF% – 45.39; CV_{CL} – 21.75; M_{CA} – 18.45.

Amomum aromaticum-Pop-II:

Somatic chromosome number 2n=48 (Figure 5b); Number of chromosomes bearing secondary constriction - 2; Range of chromosome length – (1.06 µm – 2.10 µm); Total chromosome length – 61.14 µm; Ratio of largest and smallest chromosome – 1.98:1; Mean arm ratio (L/S) –1.21; Karyotype formula - $A_{2\ (2m)}\ B_{46(16M+30m)}$; Stebbins category – 1A; TF% – 45.52; CV_{CL} – 20.93; M_{CA} – 17.94.

Amomum koenigii-Pop-I:

Somatic chromosome number 2n=48 (Figure 6a); Number of chromosomes bearing secondary constriction - 2; Range of chromosome length – (1.06 µm – 2.39 µm); Total chromosome length – 79.00 µm; Ratio of largest and smallest chromosome – 2.25:1; Mean arm ratio (L/S) – 1.27; Karyotype formula - $A_{2\ (2m)}\ B_{46(12M+28m+6sm)}$; Stebbins categorization – 1B; TF% – 44.56; CV_{CL} – 26.46; M_{CA} – 23.67.

Amomum koenigii-Pop-II:

Somatic chromosome number 2n=48 (Figure 6b); Number of chromosomes bearing secondary constriction - 2; Range of chromosome length – (1.06 µm – 2.39 µm); Total chromosome length – 78.64 µm; Ratio of largest and smallest chromosome – 2.25:1; Mean arm ratio (L/S) –1.28; Karyotype formula - $A_{2\ (2m)}\ B_{46(8M+32m+6sm)}$; Stebbins category – 1B; TF% – 44.28; CV_{CL} – 26.48; M_{CA} – 22.87.

Curcuma amada-Pop-I:

Somatic chromosome number 2n=42 (Figure 7a); Number of chromosomes bearing secondary constriction - 2; Range of chromosome length – (1.35 µm – 1.91 µm); Total chromosome length – 62.10 µm; Ratio of largest and smallest chromosome – 1.41:1; Mean arm ratio (L/S) –1.13; Karyotype formula - $A_{2\ (2m)}\ B_{40\ (10M+30m)}$; Stebbins category – 1A; TF% – 47.02; CV_{CL} – 12.52; M_{CA} – 11.91.

Curcuma amada-Pop-II:

Somatic chromosome number 2n=42 (Figure 7b); Number of chromosomes bearing secondary constriction - 2; Range of chromosome length – (1.37 µm – 1.91 µm); Total chromosome length – 64.70 µm; Ratio of largest and smallest chromosome – 1.39:1; Mean arm ratio (L/S) – 1.14; Karyotype formula - $A_{2\ (2m)}\ B_{40(10M+30m)}$; Stebbins category – 1A; TF% – 46.96; CV_{CL} – 12.77; M_{CA} – 12.17.

Curcuma caesia-Pop-I:

Somatic chromosome number 2n=63 (Figure 8a); Number of chromosomes bearing secondary constriction - 3; Range of chromosome length – (0.96 µm –

1.33 µm); Total chromosome length – 68.58 µm; Ratio of largest and smallest chromosome – 1.39:1; Mean arm ratio (L/S) –1.09; Karyotype formula – $A_{3\ (3m)}$ $B_{60(30M+30m)}$; Stebbins category – 1A; TF% – 47.98; CV_{CL} – 12.08; M_{CA} – 12.05.

Curcuma caesia-Pop-II:

Somatic chromosome number 2n=63 (Figure 8b); Number of chromosomes bearing secondary constriction - 3; Range of chromosome length – (0.96 µm – 1.33 µm); Total chromosome length – 68.73 µm; Ratio of largest and smallest chromosome – 1.39:1; Mean arm ratio (L/S) – 1.08; Karyotype formula – $A_{3\ (3m)}$ $B_{60(33M+27m)}$; Stebbins category – 1A; TF% – 48.11; CV_{CL} – 12.08; M_{CA} – 11.35.

Curcuma picta-Pop-I:

Somatic chromosome number 2n=63 (Figure 9a); Number of chromosomes bearing secondary constriction - 3; Range of chromosome length – (1.10µm – 1.67 µm); Total chromosome length – 89.34 µm; Ratio of largest and smallest chromosome – 1.52:1; Mean arm ratio (L/S) – 1.10; Karyotype formula – $A_{3\ (3m)}$ $B_{60\ (42M+18m)}$; Stebbins category – 1A; TF% – 47.96; CV_{CL} – 13.16; M_{CA} – 12.23.

Curcuma picta-Pop-II:

Somatic chromosome number 2n=63 (Figure 9b); Number of chromosomes bearing secondary constriction - 3; Range of chromosome length – (1.10 µm – 1.63 µm); Total chromosome length – 88.86 µm; Ratio of largest and smallest chromosome – 1.48:1; Mean arm ratio (L/S) – 1.10; Karyotype formula – $A_{3\ (3m)}$ $B_{60\ (42M+18m)}$; Stebbins category – 1A; TF% – 47.94; CV_{CL} – 12.66; M_{CA} – 12.34.

Curcuma longa-Pop-I:

Somatic chromosome number 2n=63 (Figure 10a); Number of chromosomes bearing secondary constriction - 3; Range of chromosome length – (1.17 µm – 1.70 µm); Total chromosome length – 88.32 µm; Ratio of largest and smallest chromosome – 1.45:1; Mean arm ratio (L/S) –1.13; Karyotype formula – $A_{3\ (3m)}$ $B_{60\ (15M+45m)}$; Stebbins category – 1A; TF% – 47.01; CV_{CL} – 11.18; M_{CA} – 16.78.

Curcuma longa-Pop-II:

Somatic chromosome number 2n=63 (Figure 10b); Number of chromosomes bearing secondary constriction - 3; Range of chromosome length – (1.18 µm – 1.70 µm); Total chromosome length – 88.08 µm; Ratio of largest and smallest chromosome – 1.44:1; Mean arm ratio (L/S) – 1.13; Karyotype formula – $A_{3\ (3m)}$ $B_{60\ (15M+45m)}$; Stebbins category – 1A; TF% – 47.13; CV_{CL} – 11.01; M_{CA} – 17.23.

Hedychium coronarium-Pop-I:

Somatic chromosome number 2n=34 (Figure 11a); Number of chromosomes bearing secondary constriction - 2; Range of chromosome length – (1.06 µm – 1.65 µm); Total chromosome length – 41.14 µm; Ratio of largest and smallest chromosome – 1.56:1; Mean arm ratio (L/S) –1.18; Karyotype formula - $A_{2\ (2m)}$ $B_{32(18M+14m)}$; Stebbins category – 1A; TF% – 47.32; CV_{CL} – 15.91; M_{CA} – 10.72.

Hedychium coronarium-Pop-II:

Somatic chromosome number 2n=34 (Figure 11b); Number of chromosomes bearing secondary constriction - 2; Range of chromosome length – (1.06 µm – 1.60 µm); Total chromosome length – 41.56 µm; Ratio of largest and smallest chromosome – 1.51:1; Mean arm ratio (L/S) –1.18; Karyotype formula - $A_{2\ (2m)}$ $B_{32\ (16M+16m)}$; Stebbins category – 1A; TF% – 47.24; CV_{CL} – 15.11; M_{CA} – 11.06.

Hedychium coccineum-Pop-I:

Somatic chromosome number 2n=34 (Figure 12a); Number of chromosomes bearing secondary constriction - 2; Range of chromosome length – (1.32 µm – 2.08 µm); Total chromosome length – 52.80 µm; Ratio of largest and smallest chromosome – 1.58:1; Mean arm ratio (L/S) –1.22; Karyotype formula - $A_{2\ (2m)}$ $B_{32\ (18M+14m)}$; Stebbins category – 1A; TF% – 46.68; CV_{CL} – 15.51; M_{CA} – 13.27.

Hedychium coccineum-Pop-II:

Somatic chromosome number 2n=34 (Figure 12b); Number of chromosomes bearing secondary constriction - 2; Range of chromosome length – (1.32 µm – 2.08 µm); Total chromosome length – 52.92 µm; Ratio of largest and smallest chromosome – 1.58:1; Mean arm ratio (L/S) – 1.22; Karyotype formula - $A_{2\ (2m)}$ $B_{32\ (18M+14m)}$; Stebbins category – 1A; TF% – 46.47; CV_{CL} – 15.40; M_{CA} – 14.11.

Hedychium thyrsiforme-Pop-I:

Somatic chromosome number 2n=34 (Figure 13a); Number of chromosomes bearing secondary constriction - 2; Range of chromosome length – (0.96 µm – 1.44 µm); Total chromosome length – 38.26 µm; Ratio of largest and smallest chromosome – 1.50:1; Mean arm ratio (L/S) –1.21; Karyotype formula - $A_{2\ (2m)}$ $B_{32\ (12M+20m)}$; Stebbins category – 1A; TF% – 46.60; CV_{CL} – 15.24; M_{CA} – 13.56.

Hedychium thyrsiforme-Pop-II:

Somatic chromosome number 2n=34 (Figure 13b); Number of chromosomes bearing secondary constriction - 2; Range of chromosome length – (0.96 µm – 1.44 µm); Total chromosome length – 39.40 µm; Ratio of largest and smallest chromosome – 1.50:1; Mean arm ratio (L/S) –1.21; Karyotype formula - $A_{2\ (2m)}\ B_{32\ (12M+20m)}$; Stebbins category – 1A; TF% – 46.61; CV_{CL} – 14.88; M_{CA} – 13.69.

DISCUSSION

Somatic chromosome number 2n=48 having a basic number X=12 was found to be constant in *Alpinia calcarata*, *Alpinia malaccensis* and *Alpinia nigra* as was reported by earlier researchers (Raghavan and Venkatasubban 1943; Chakravorti 1948, 1952; Ramachandran 1969; Chen 1988; Joseph 1998). The different proportions of metacentric and submetacentric chromosomes present in the somatic chromosome complements of these three species are in partial agreement with the reports of Joseph (1998). At intra-specific (Pop-I and Pop-II) level, the karyotype of each species is more or less homogeneous having one pair of chromosomes bearing secondary constriction, a characteristic of the karyotype itself. On the contrary, at inter-specific level, their karyotypes differ though the chromosomes are mostly metacentric and submetacentric in nature. According to Stebbins categorization, the karyotype of *A. malaccensis, A. calcarata* and *A. nigra* falls under category 1A, 1B and 2B, respectively. Therefore, the reduction in size of some of the chromosomes in relation to other has occurred in chromosome complements of *A. calcarata* and *A. nigra*. Moreover, the presence of two pairs of submetacentric chromosomes having F% < 33.33 in Pop-I and Pop-II of *A. nigra* indicates that their karyotypes are slightly asymmetric. Thus, in *Alpinia* spp. a tendency from symmetric to asymmetric karyotype is observed. The somatic chromosome count 2n=48 is the distinctive character of *Amomum* species which corroborates previous findings (Sharma and Bhattacharya 1959; Chen *et al*. 1988). Due to limited cytological studies in these three species, little information was available regarding the detailed chromosomal architecture. In general, chromosomes are short in size where one pair of metacentric chromosomes possessed secondary constriction. The karyotype of *A. aromaticum*, *A. koenigii* and *A. maximum* at inter-specific and intra-specific levels exhibit gross similarity in the types of chromosomes present, number of chromosomes bearing secondary constriction, TF%, total chromosome length and L/S arm ratio. The arm ratio L/S and TF% are the indicators of symmetric type of karyotype. According to Stebbins (1971) categorization, the karyotype of *A. aromaticum* and *A. maximum* falls under 1A while that of *A. koenigii* belonging to category 1B indicates minor deviation in the size of largest to smallest chromosome ratio. The identical karyotype formula A_2B_{46} without any pair of acrocentric or telocentric chromosomes having arm ratio L/S >2:1 suggests accentuated chromosomal homology. In *Curcuma* complex, the somatic chromosome number of *C. amada* was found to be 2n=42 with a basic number X=21 which corroborates previous reports (Sharma and Bhattacharya 1959; Ramachandran 1961, 1969; Islam 2004; Joseph 1998; Bhadra and Bandhyopadhyay 2015; Lamo and Rao 2017). At intra-specific level, the karyotype of Pop-I and Pop-II of *C. amada* is almost identical and symmetrical (1A) in nature indicating the absence of acrocentric or telocentric chromosomes. Based on asymmetry index value, Bhadra and Bandyopadhyay (2015, 2018) reported that the karyotype of *C. amada* falls under Stebbins category 1B which may be due to its occurrence in different eco-climatic zone. The somatic chromosome number 2n=63 of *C. caesia* and *C. longa* is in agreement with previous reports (Ramachandran 1961, 1969; Joseph *et al*. 1999; Nair and Sasikumar 2009; Nair *et al*. 2010; Lamo and Rao 2014; Bhadra and Bandyopadhyay 2015; Lamo and Rao 2016, 2017). The karyotype of these two species are identical both at inter- and intra-specific levels. According to Stebbins formula, their karyotypes belong to category 1A which is not in agreement with the report of Bhadra and Bandyopadhyay (2015, 2018). The somatic chromosome count of 2n=63 chromosomes of *C. picta* is a first report and the karyotypes of Pop-I and Pop-II of *C. picta* exhibit gross similarity in the types of chromosomes present, number of chromosomes with secondary constriction, TF%, total chromosome length and mean arm ratio (L/S). According to the degree of asymmetry, the karyotype of *C. picta* belongs to the category 1A. There are different views regarding the basic number of *Curcuma* spp. According to one school, the different species of *Curcuma* have a basic number X=21 (Sharma and Bhattacharya 1959; Ramachandran 1961, 1969; Islam 2004; Joseph 1998; Chen *et al*. 2013; Bhadra and Bandhyopadhyay 2015; Lamo *et al*. 2016) which has been derived from a combination of X=12 and X=9 (Ramachandran 1961; Lamo and Rao 2017). The other group (Sato 1960; Skornickova *et al*. 2007) proposed that the basic number of *Curcuma* is X=7 suggesting, thereby, all the species of *Curcuma* studied, having somatic chromosome number 2n=63 are nonaploid and *C. amada* with 2n=42 chromosomes is a hexaploid species. Apparently, there is no conflict between X=7 and X=21 in *Curcuma* complex. But the absence of cytotypes

in multiple of X such as 2X, 3X, 4X and 5X in natural populations and/or cultivars of *Curcuma* species suggests that the basic number X=21 is deep seated in *Curcuma* spp. from which the diploid and triploid species have eventually evolved in the due course of evolution. The occurrence of 2X, 3X, 4X, 5X and 6X cytotypes is not uncommon in flowering plants and in the monocot genus *Dioscorea*, valid cytotypes having 2X, 3X, 4X, 5X etc. are found in the natural population (Muthamia *et al.* 2014). In the light of this knowledge, the acceptance of X=7 in *Curcuma* complex is questionable. Moreover, if X= 7 is accepted as basic number in *Curcuma* spp., then their natural cytotypes having 9X, 12X and 15X chromosomes would have more copy number of genes. In such a situation, the regulation of dosage compensation having excess copy of genes in their cytotypes is beyond any elucidation. The somatic chromosome count 2n=34 chromosomes found in Pop-I and Pop-II of *Hedychium coccineum* and *H. coronarium* having a basic number X=17 supports previous findings (Mukherjee 1970; Mahanty 1970; Gao *et al.* 2008). Sharma and Bhattacharya (1959) reported a cytotype of *H. thyrsiforme* having 2n = 24 chromosomes with basic number X=12. In the present investigation, the presence of 34 chromosomes recorded in most of the somatic cells (modal number) of *H. thyrsiforme* indicates that the diploid chromosome number is, indeed 2n=34 as was reported by Mahanty (1970). This also suggests that all the three *Hedychium* species growing in this region are stabilized with a basic chromosome number X=17. It is imperative that the karyotypes of the six individuals studied are almost identical and have the same karyotype formula A_2B_{32}, but the absence of acrocentric and telocentric chromosomes infers the symmetric nature of karyotypes justifying their inclusion under Stebbins category 1A. Karyotype conservatism without any structural alteration leading to the formation of acrocentric or telocentric chromosomes in these species having a basic number X=17 reveals a karyotype stasis. Information regarding the number of chromosomes having secondary constriction in all the taxa of Zingiberaceae studied by previous researchers is minimum (Bhattacharyya 1957; Mandi 1990; Joseph *et al.* 1999; Islam 2004) and in some of the previous investigations there was no reference with regard to the number of chromosomes possessing secondary constriction. For resolving this problem, Ag-NOR study (Figure S2) has been carried out for the first time. There are different views regarding the maximum number of nucleoli per cell and the number of chromosomes bearing secondary constriction present in somatic chromosome complements of flowering plants (Sharma and Ghosh 1954; Sato 1980). However, the coincidence between the number of chromosomes possessing secondary constriction and the maximum number of nucleoli per cell indicates the relationship between the presence of secondary constriction and the ability of those chromosomes to form the maximum number of nucleoli in all the taxa studied. The presence of three nucleoli in triploid species of *Curcuma* is also an indicator of such a relationship. The inter- and intra chromosomal asymmetry based on Stebbins quali-quantitative method reveals that the karyotypes of most of the species are symmetrical in nature. A progressive asymmetry is, however, observed in *Amomum koenigii* (1B), *Alpinia calcarata* (1B) and *Alpinia nigra* (2B). Undoubtedly, Stebbins (1971) quali-quantitative method is the determinant of evaluation of the karyotype asymmetry index but based on this data alone, it would not be possible to ascertain the genetic relationship between different taxa of the same family. The bi-dimensional (Figure 14) scatter plot (Peruzzi and Eroglu 2013) drawn against Mean Centromeric Asymmetry (M_{CA}) and Coefficient of Variation of Chromosome Length (CV_{CL}) clearly indicates that the two tribes Alpinieae (represented by *Alpinia* spp. and *Amomum* spp.) and Zingibereae (represented by *Curcuma* spp. and *Hedychium* spp.) of Zingiberaceae (Angiosperm Phylogeny Group – 2009) have distinct karyotypes in which *Alpinia* spp. and *Amomum* spp. show comparatively high inter-chromosomal and intra-chromosomal asymmetry indices (Zarco 1986; Watanabe *et al.*1999; Paszko 2006) than those of *Curcuma* spp. and *Hedychium* spp. The dendrogram reveals that *Alpinia spp.*, *Amomum spp.*, *Curcuma spp.* and *Hedychium* spp. with their respective populations formed four separate clusters (Figure 15).

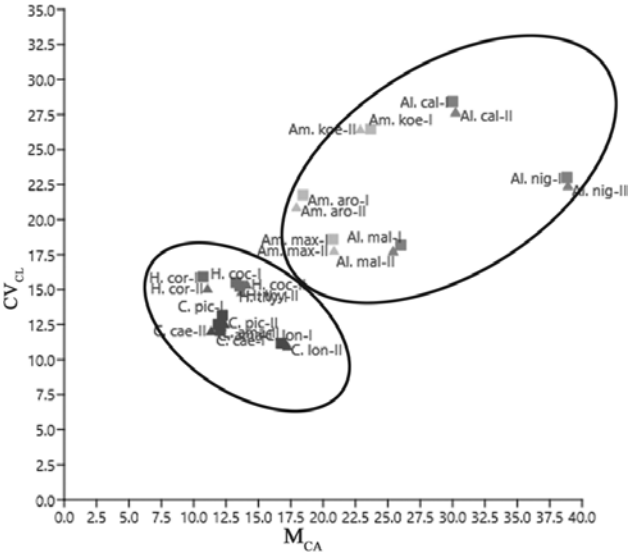

Figure 14. Bi-dimensional scattered plot against M_{CA} (x axis) and CV_{CL} (y axis).

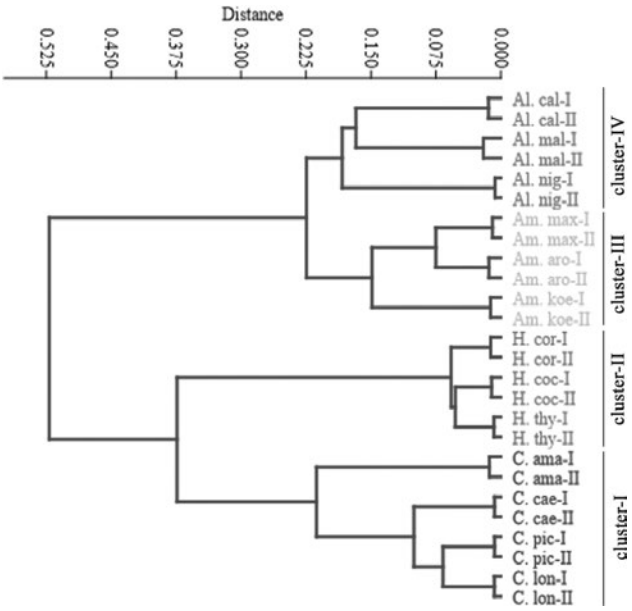

Figure 15. UPGMA dendrogram based on Gower's similarity matrix of six karyological parameters.

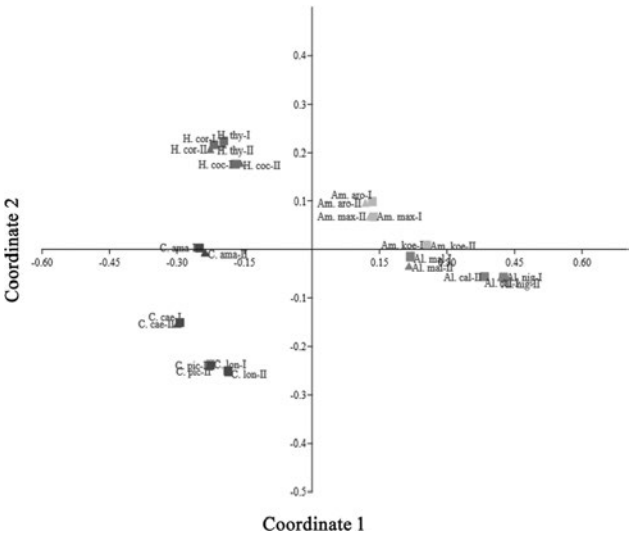

Figure 16: Principle Coordinate Analysis of selected species in 2D Plot.

The PCA illustrates no overlap and thus, the distinctive position of each genus with respect to other is evident (Figure 16). The karyotype data, therefore, validates the taxonomic position of *Alpinia* spp., *Amomum* spp., *Curcuma* spp. and *Hedychium* spp. The chromosomal data of *Alpinia* spp., *Amomum* spp., *Curcuma* spp., and *Hedychium* spp. suggest that they might have originated from a common ancestry but eventually through gradual changes, evolved as separate species in the due course of time. Gower's (1971) similarity matrix points towards a possible rearrangement of the chromosomal architectures in 13 different taxa studied. Such chromosomal rearrangements are possibly associated with cryptic changes maintaining a high syntenic value.

CONCLUSION

The present study has been focussed on the detailed karyotype analysis of two populations of *Alpinia calcarata*, *A. malaccensis*, *A. nigra*, *Amomum aromaticum*, *A. koenigii*, *A. maximum*, *Curcuma amada*, *C. caesia*, *C. longa*, *C. picta*, *Hedychium coccineum*, *H. coronarium*, and *H. thyrsiforme* of Zingiberaceae, collected from different geographical locations of Tripura. The somatic chromosome number of *Alpinia* and *Amomum* is found to be 2n = 48 having a basic number of X=12 chromosomes. In *Hedychium* spp. the diploid chromosome number is 2n=34 with basic number X=17 chromosomes. The present findings reveal that in majority of the somatic cells of *Curcuma caesia*, *Curcuma longa* and *Curcuma picta*, 63 chromosomes are present indicating their triploid nature. In contrast, diploid somatic chromosome number (2n=42) is recorded in *Curcuma amada*. Stebbins quali-quantitative analysis indicates that except in *Alpinia nigra*, the karyotype of other 12 species is symmetric in nature. The accentuated chromosome homology at intra-species level is the intrinsic characteristic of their karyotypes. The inter-chromosomal and intra-chromosomal asymmetry indices, based on statistically based method, suggest that *Alpinia* spp. and *Amomum* spp. have higher inter- and intra-chromosomal asymmetry in comparison to *Curcuma* spp. and *Hedychium* spp. The dendrogram and PCA derived data clearly validate the taxonomic position of these four genera investigated. Gower's similarity matrix endorses the cryptic changes leading to karyotype conservatism at species level of each genus.

ACKNOWLEDGEMENTS

KS is grateful to UGC, New Delhi for providing BSR Fellowship.

DISCLOSURE OF STATEMENT

The authors declare that they have no conflict of interest.

REFERENCES

Angiosperm Phylogeny Group. 2009. An update of the Angiosperm Phylogeny Group classification for the orders and families of flowering plants: APG III. Bot J Linean Soc. 161 (2): 105–121.

Arambewela LSR, Arawwawala LDAM, Ratnasooriya WD. 2004. Antinociceptive activities of aqueous and ethanolic extracts of *Alpinia calcarata* rhizomes in rats. J Ethnopharmacol. 95 (2-3):311–316.

Ardiyani M. 2002. Systematic study of *Curcuma* L.: turmeric and its allies. [Dissertation]. Scotland: University of Edinburgh.

Bhadra S, Bandyopadhyay M. 2015. Karyomorphological investigations on some economically important members of Zingiberaceae from Eastern India. Caryologia 68:(3) 184-192.

Bhadra S, Maity D, Bandyopadhyay M. 2018. Correlating karyomorphology and molecular marker analyses in turmeric: a case study. Journal of Crop Improvement 32 (5): 657-680.

Bhattacharyya NK. 1957. Some experimental aspects on the cytogenetics of species and some fundamental studies on the chromosomes of plants. [Dissertation]. India:University of Calcutta.

Bhattacharyya R. 1968. Systematic status of the family Zingiberaceae. Nucleus 39-41.

Bhuiyan MNI, Chowdhury JU, Begum J, Nandi NC. 2010. Essential oils analysis of the rhizomes of *Alpinia conchigera* Griff. and leaves of *Alpinia malaccensis* (Burm. f.) Roscoe from Bangladesh. Afr J Plant Sci. 4:197–201.

Chakravorti AK (1952) Cytogenetical studies in Zingiberaceae. Proceedings of 39th Indian Science Congress; Kolkata, India.

Chakravorti AK. 1948. Multiplication of chromosome numbers in relation to speciation in Zingiberaceae. Science and Culture 14:137-140.

Chen J, Xia N, Zhao j, Chen J, Henny RJ. 2013. Chromosome numbers and ploidy levels of chinese *Curcuma* species. Hortscience. 48(5):525–530.

Chen ZY, Chen SJ, Huang XX, Huang SP. 1988. A report on chromosome numbers on Chinese Zingiberaceae. Guihaia 8:143–147.

Das AB, Rai S, Das P. 1999. Karyotype analysis and cytophotometric estimation of nuclear DNA content in some members of the Zingiberaceae. Cytobios 97: 23–33.

Deb DB. 1981. The Flora of Tripura. Vol I. New Delhi. Today and tomorrow's publishers.

Deb DB. 1983. The Flora of Tripura. Vol II. New Delhi. Today and tomorrow's publishers.

Fedorov AA. 1969. Chromosome Number of Flowering Plants. The Academy of Sciences of USSR. 926.

Fernandez-Gomez E, Stockert JC, Lopez-Safz JF, Gimenez-Martin G. 1969. Staining plant cell nucleoli with $AgNO_3$ after formalin hydroquinone fixation. Staining Technique 44(1):48-49.

Gao L, Liu N, Huang B, Hu X. 2008. Phylogenetic analysis and genetic mapping of Chinese *Hedychium* using SRAP markers. Sci Hort. 117:369-377.

Gower JC. 1971. A General coefficient of similarity and some of its properties. Biometrics 27:857-871.

Gupta AP, Gupta MM, Kumar S. 1999. Simultaneous determination of curcuminoids in *Curcuma* samples using high performance thin layer chromatography. Journal of Liquid Chromatography and Related Technologies 22: 1561–1569.

Hammer Ø. 2013. PAST Version 3.03. (accessed October 2014). http://folk.uio.no/ohammer/past

Huziwara Y. 1962. Karyotype analysis in some genera of Compositae. VIII. Further studies on the chromosome of *Aster*. Am J Bot. 49: 116-119.

Islam MA. 2004. Genetic diversity of the genus *Curcuma* in Bangladesh and further biotechnological approaches for *in vitro* regeneration and long-term conservation of *C. longa* germplasm. [Dissertation] Germany: University of Hannover.

Jain SK, Prakash V. 1995. Zingiberaceae in India: Phytogeography and Endemism. Rheedea 5(2):154-169.

Jatoi SA, Kikuchi A, Watanabe KN. 2007. Genetic diversity, cytology and systematic phylogenetic study in Zingiberaceae. Genes, Genome and Genomics 1(1):56-62.

Jayaweera DMA. 1982. Medicinal Plants (Indigenous and Exotic) used in Ceylon. Srilanka. Colombo: The National Science Foundation.

Joseph R, Joseph T, Jose J. 1999 Karyomorphological studies in the genus *Curcuma* Linn. Cytologia 64: 313–317.

Joseph R. 1998. Karyomorphometrical analysis and exploration of major essential oil constituents in Zingiberaceae. [Dissertation]. India: Mahatma Gandhi University.

Kala CP. 2005. Ethnomedicinal botany of the Apatani in the Eastern Himalayan region of India. J Ethnobiol Ethnomed. 1: 1–8.

Khoshoo TN. 1979. Cytogenetics in relation to plant evolution and improvement. In: Khoshoo TN, Nair PKK, editors. Progress in plant research. India: NBRI. p. 1-74.

Lamo JM, Rao SR. 2014. Chromosome counts in two species of *Curcuma* Linnnaeus (Zingiberaceae) from North-East India. Pleione 8(2): 435–438.

Lamo JM, Rao SR. 2017. Chromosome counts in wild and cultivated species of *Curcuma* Linn. Cytologia 82(2):141–144.

Lamo JM, Rao SR. 2017. Meiotic behaviour and its implication on species inter-relationship in the genus *Curcuma* (Linnaeus, 1753) (Zingiberaceae). Comp Cytogenet. 11(4): 691-702.

Lamo JM, Wahlang DR, Rao SR. 2016. Comparative analysis of heterochromatin distribution pattern in wild and cultivated species of *Curcuma* L. Medicinal and Aromatic Plants S3:006.

Larsen K, Smith RM. 1978. A New Species of *Curcuma* from Thailand. Notes from the Royal Botanical Garden, Edinburgh 30:269-272.

Levan A, Fredga K, Sandbery AA. 1964 Nomenclature for centromeric position on chromosome. Heriditas 52:201-220.

Mahanty HK. 1970. A cytological study of the Zingiberales with special reference to their taxonomy. Cytologia 35:13-49.

Mandi KK. 1990. Studies on chromosomes, DNA estimation and chemical constituents of different members of Scitaminae. [Dissertation]. India: University of Calcutta.

Mao AA, Hynniewta TM, Sanjappa M. 2009. Plant wealth of northeast India with reference to ethnobotany. Indian Journal of Traditional Knowledge 8:96-103.

Mukherjee I. 1970. Chromosome studies of some species of *Hedychium*. The Botanical Magazine 83:237-241.

Muthamia ZK, Nyende AB, Mamati EG, Ferguson ME, Wasilwa J. 2014 Determination of ploidy among Yam (*Dioscorea* spp.) landraces in Kenya by flow cytometry. Afr J Biotechnol. 13(3):394-402.

Myers N, Mittermier RA, Mittermier CG, Fonseca GABda, Kent J. 2000. Biodiversity hotspots for conservation priorities. Nature 40:853-858.

Nair RR, Sasikumar B. 2009. Chromosome number variation among germplasm collections and seedling progenies in turmeric, *Curcuma longa* L. Cytologia 74(2):153–157.

Nair RR, Shiva KN, Anchu S, Zachariah TJ. 2010. Characterization of open-pollinated seedling progenies of turmeric (*Curcuma longa* L.) based on chromosome number, plant morphology, rhizome yield and rhizome quality. Cytologia 75(4):443–449.

Nambiar MC. 1979. Morphological and cytological investigations in the genus *Curcuma* L. [Dissertation]. India:University of Bombay.

Nayak S. 2002. High-frequency *in vitro* production of microrhizomes of *Curcuma amada*. Indian J Exp Biol. 40(2):230-232.

Paszko A. 2006. A critical review and a new proposal of karyotype asymmetry indices. Plant Syst Evol. 258: 39-48.

Peruzzi L Altınordu F. 2014. A proposal for a multivariate quantitative approach to infer karyological relationships among taxa. Comp Cytogenet. 8(4): 337–349.

Peruzzi L, Eroğlu HE. 2013. Karyotype asymmetry: again, how to measure and what to measure? Comp Cytogenet. 7:1-9.

Prakash V, Mehrotra BN. 1996. Zingiberaceae of northeast India: diversity and taxonomic status. Proceedings of the 2nd symposium on the family Zingiberaceae. Guangzhou, China.

Prana MS, Sastrapradja S, Hawkes JG, Lubis I. 1978. A cytological study of some Indonesian *Curcuma* species. J Root Crops. 4: 31–35.

Prana MS. 1977. Studies on some Indonesian Curcuma species. [Dissertation] England:University of Birmingham.

Raghavan TS, Venkatasubban KR. 1943. Cytological studies in the family Zingiberaceae with special reference to chromosome number and cytotaxonomy. Proceedings of Indian Academy Science, Section B. 174: 118-132.

Rahman M, Islam M. 2015. *Alpinia calcarata* Roscoe: A potential phytopharmacological source of natural medicine. Pharmacogn Rev. 9:55-62.

Rajkumari S, Sanatombi K. 2018. Genetic diversity analysis of *Hedychium* species based on RAPD and ISSR markers. Proc Natl Acad Sci India Sect B Biol Sci. 1-7.

Ramachandran K. 1961. Chromosome numbers in the genus *Curcuma* Linn. Current Science 30:194-196.

Ramachandran K. 1969. Chromosome numbers in Zingiberaceae. Cytologia 34: 213-221.

Roy B, Swargiary A, Giri BR. 2012. *Alpinia Nigra* (Family Zingiberaceae): an anthelmintic medicinal plant of north-east India. Advances in Life Sciences 2(3): 39–51.

Sabu M. 2006. Zingiberaceae and Costaceae of South India. Kerala, India: Indian Association for Angiosperm Taxonomy.

Sahoo S, Singh S, Nayak S. 2014. Chemical composition, antioxidant and antimicrobial activity of essential oil and extract of *Alpinia malaccensis* Roscoe (Zingiberaceae). Int J Pharm Pharm Sci. 6:183–188.

Sarangthem N, Talukdar NC, Thongam B. 2013. Collection and evaluation of *Hedychium* species of Manipur, Northeast India. Genetic Resour Crop Ev. 60:13-21.

Sato D. 1948. Karyotype and systematics of Zingiberales. Jpn J Genet 23: 44-45.

Sato D. 1960. The karyotype analysis in Zingiberales with special reference to the protokaryotype and stable karyotype. Scientific Papers 10:225–243.

Sharma AK, Bhattacharyya NK. 1959. Cytology of Several members of Zingiberaceae. La cellule 59:297-346.

Sharma AK, Sharma A. 1980. Chromosome technique theory and practical, Third edition London: Butterworth and Co Publishers Ltd.

Skornickova J, Sida O, Jarolimova V, Sabu M, Fer T, Travnicek P, Suda J. 2007. Chromosome numbers and genome size variation in Indian species of *Curcuma* (Zingiberaceae). Ann Bot. 100: 505–526.

Stebbins GL. 1971 Chromosomal evolution in higher plants. London: Edward Arnold Ltd.

Suguira, T. 1931. A list of chromosome numbers in angiospermous plants. The Botanical Magazine Tokyo. 45: 353–355.

Suguira, T. 1936. Studies on the chromosome numbers in higher plants, with special reference to cytokenesis I. Cytologia. 7: 544–595.

Vanchhawng L, Lalramnghinglova H. 2016. Notes on the Genus *Hedychium J. Koen.* (Zingiberaceae) in Mizoram, North East India. International Journal of Waste Resources 6 (3): 234.

Watanabe K, Yahara T, Denda T, Kosuge K. 1999. Chromosomal evolution in the genus *Brachyscome* (Asteraceae, Astereae): Statistical tests regarding correlation between changes in karyotype and habit using phylogenetic information. J Plant Res. 112:145-161.

Yoshikane I, Naohiro N. 1991. Karyotypes of *Fragaria nubicola* and *F. daltoniana*. Cytologia 56:453-457.

Zarco CR. 1986. A new method for estimating karyotype asymmetry. Taxon 35: 526–530.

SUPPLEMENTARY FILE (APPENDICES)

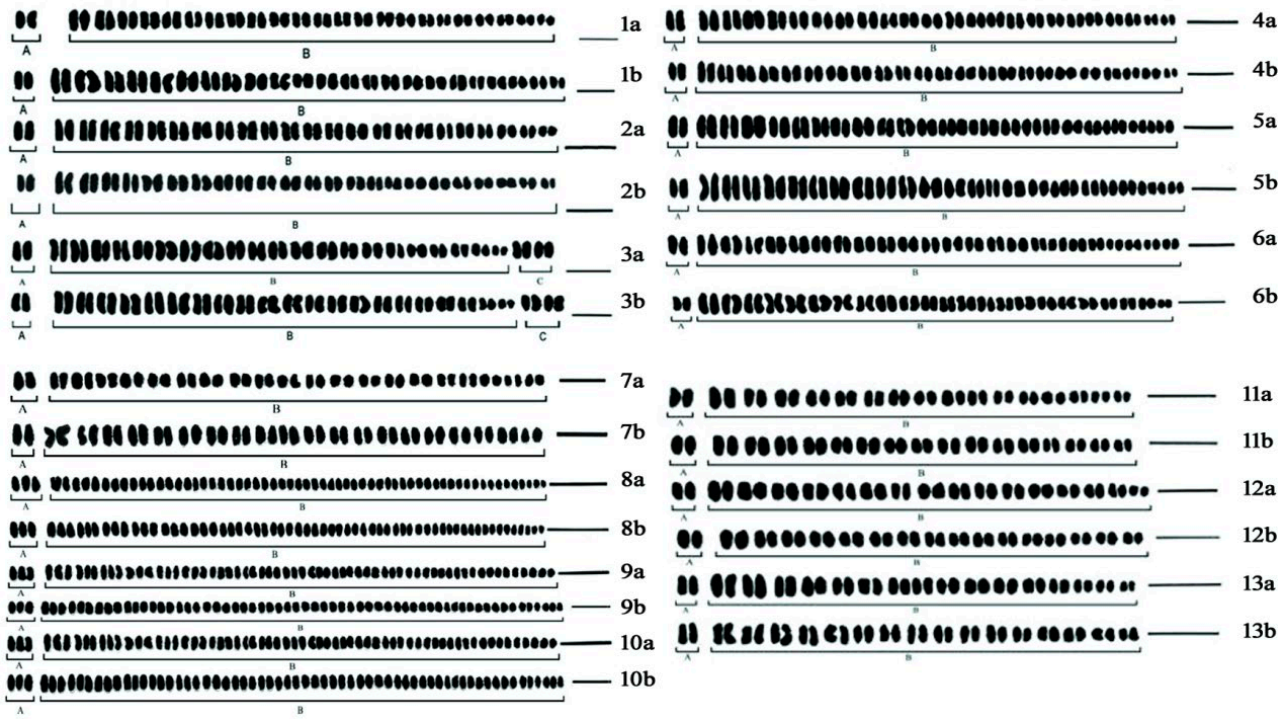

Figure S1. Karyogram of thirteen Zingiberaceae species from Tripura. 1- *Alpinia calcarata*; 2- *A. malaccensis*; 3- *A. nigra*; 4- *Amomum maximum*; 5- *A. aromaticum*; 6- *A. koenigii*; 7- *Curcuma amada*; 8- *C. caesia*; 9- *C. picta*; 10- *C. longa*; 11- *H. coronarium*; 12- *H. coccineum*; 13- *H. thyrsiforme* (a – Pop - I; b – Pop - II); scale bars = 5μm.

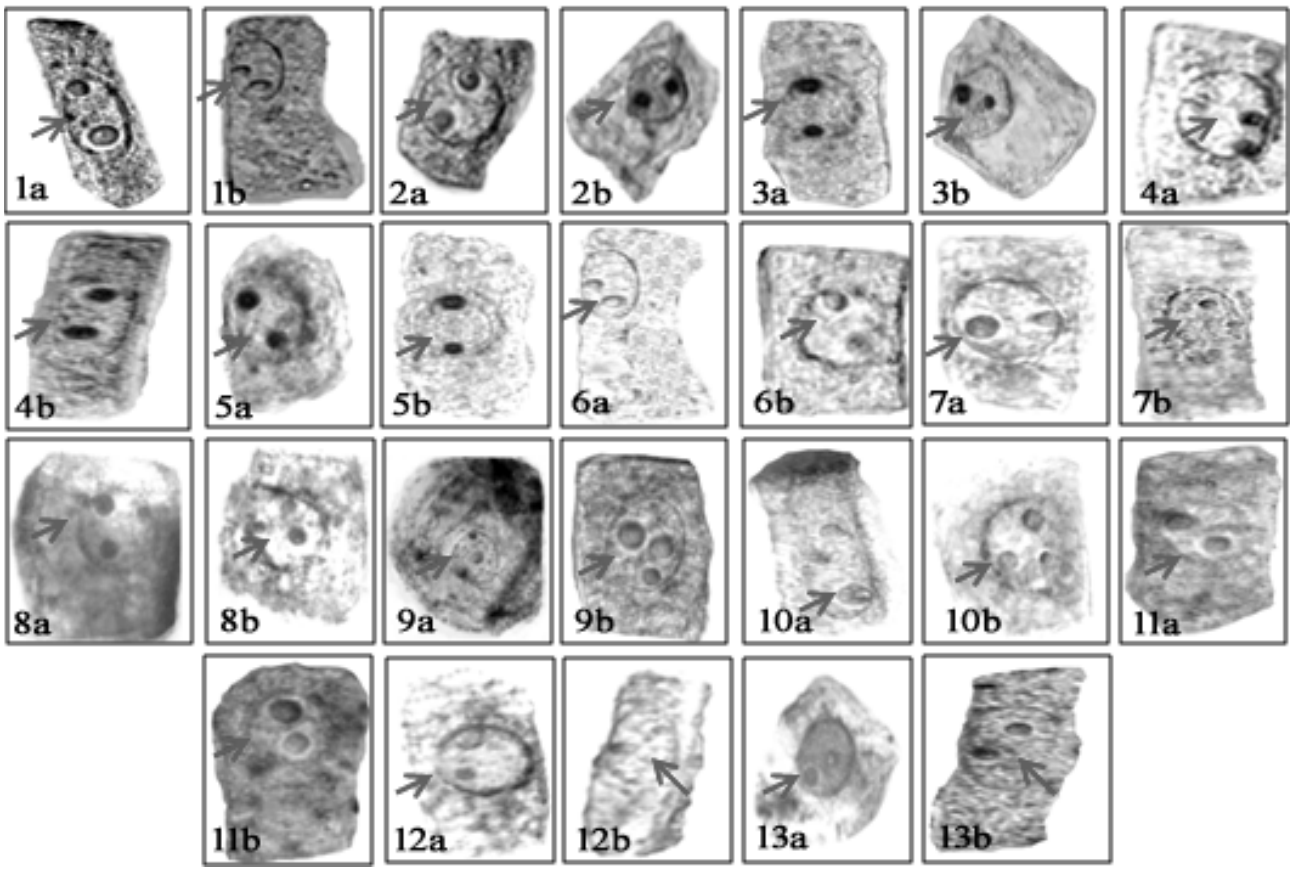

Figure S2. Ag- impregnated somatic cells of thirteen Zingiberaceae species. 1- *Alpinia calcarata*; 2- *A. malaccensis*; 3- *A. nigra*; 4- *Amomum maximum*; 5- *A. aromaticum*; 6- *A. koenigii*; 7- *Curcuma amada*; 8- *C. caesia*; 9- *C. picta*; 10- *C. longa*; 11- *H. coronarium*; 12- *H. coccineum*; 13- *H. thyrsiforme* (a – Pop - I; b – Pop - II).

Table S1. Details of plant samples collected from different geographical locations of Tripura.

Name of the species	Herbarium Voucher No.	Locations and altitudes
Alpinia calcarata	TUH – 460 (Pop-I)	Suryamaninagar, (34 mt.) 23045.0'44.74" N, 91015.0'54.29"E
	TUH – 2001 (Pop-II)	Baramura, (110 mt.) 23049.0'0.70" N, 91031.0'2.33"E
Alpinia malaccensis	TUH – 466 (Pop-I)	Debtamura, (48.0 mt.) 23033.0'2.50"N, 91038.0'5.40"E
	TUH – 2002 (Pop-II)	Atharamura, (134 mt.) 23029.0'54.10"N, 91037.0'34.30"E
Alpinia nigra	TUH – 2049 (Pop-I)	Mohanpur, (30.0 mt.) 23049.0'28.50"N, 91026.0'45.0"E
	TUH – 2003 (Pop-II)	Chabimura, (110 mt.) 23033.0'18.20"N, 91037.0'0.98"E
Amomum aromaticum	TUH – 2055 (Pop-I)	Tulamura,(46 mt.) 23023.0'11.3"N, 91026.0'10.7"E
	TUH – 2004 (Pop-II)	Unakoti, (200 mt.) 24023.0'11.3" N, 9204.0'13.0"E
Amomum maximum	TUH – 1407 (Pop-I)	Atharamura foot Hills, (45 mt.) 23053.0'2.10"N, 91042.0'12.5"E
	TUH – 2005 (Pop-II)	Jampui Hills, (191 mt.) 23059.0'4.63" N, 92017.0'50.6"E
Amomum koenigii	TUH- 470 (Pop-I)	Dhuptali, (40 mt.) 23023.0'11.3" N, 91026.0'15.1"E
	TUH- 2006 (Pop-II)	Baramura,(120 mt.) 23050.0'4.0" N, 91036.0'38.96"E
Curcuma amada	TUH – 465 (Pop-I)	Suryamaninagar, (21 mt.) 23045.0'44.27" N, 91015.0'53.38"E
	TUH – 2007 (Pop-II)	Howaibari,(105 mt.) 23049.0'0.60" N, 91034.0'04.61"E
Curcuma longa	TUH – 1407 (Pop-I)	Belkum Para, (48 mt.) 23053.0'2.1" N, 91043.0'13"E
	TUH – 2008 (Pop-II)	Jampui Hills, (163 mt.) 2402.0'30.21" N, 92016.0'42.34"E
Curcuma caesia	TUH- 466 (Pop-I)	Suryamaninagar, (30 mt.) 23045.0'43.13" N, 91015.0'52.17"E
	TUH- 2009 (Pop-II)	Sepahijala, (30 mt.) 23039.0'35.74" N, 91018.0'8.54"E
Curcuma picta	TUH – 459 (Pop-I)	Kamarikhala, (47 mt.) 23033.0'3.0" N, 91038.0'5.30"E
	TUH – 2010 (Pop-II)	Baramura foot Hills (102 mt.) 23048.0'41.24" N, 91030.0'54.24"E
Hedychium coronarium	TUH – 458 (Pop-I)	College Tilla, (25 mt.) 23049.0'46.72" N, 91017.0'36.28"E
	TUH – 2011 (Pop-II)	Baramura, (105 mt.) 23049.0'0.10" N, 91033.0'3.54"E
Hedychium coccineum	TUH – 461 (Pop-I)	Paikhola, (45 mt.) 23022.0'27.8" N, 91030.0'48.30"E
	TUH – 2012 (Pop-II)	Karbook, (106 mt.) 23021.0'38.90" N, 91042.0'12.15"E
Hedychium thyrsiforme	TUH- 507 (Pop-I)	Jampui Hills, (120 mt.) 23059.0'4.7" N, 92017.0'56.0"E
	TUH- 2013 (Pop-II)	Manpui, (290 mt.) 2408.0'5.9" N, 92016.0'39.0"E

Finito di stampare da
Logo s.r.l. – Borgoricco (PD) – Italia

OPEN ACCESS POLICY

Caryologia provides immediate open access to its content. Our publisher, Firenze University Press at the University of Florence, complies with the Budapest Open Access Initiative definition of Open Access: By "open access" , we mean the free availability on the public internet, the permission for all users to read, download, copy, distribute, print, search, or link to the full text of the articles, crawl them for indexing, pass them as data to software, or use them for any other lawful purpose, without financial, legal, or technical barriers other than those inseparable from gaining access to the internet itself. The only constraint on reproduction and distribution, and the only role for copyright in this domain is to guarantee the original authors with control over the integrity of their work and the right to be properly acknowledged and cited. We support a greater global exchange of knowledge by making the research published in our journal open to the public and reusable under the terms of a Creative Commons Attribution 4.0 International Public License (CC-BY-4.0). Furthermore, we encourage authors to post their pre-publication manuscript in institutional repositories or on their websites prior to and during the submission process and to post the Publisher's final formatted PDF version after publication without embargo. These practices benefit authors with productive exchanges as well as earlier and greater citation of published work.

PUBLICATION FREQUENCY

Papers will be published online as soon as they are accepted, and tagged with a DOI code. The final full bibliographic record for each article (initial-final page) will be released with the hard copies of *Caryologia*. Manuscripts are accepted at any time through the online submission system.

COPYRIGHT NOTICE

Authors who publish with *Caryologia* agree to the following terms:

- Authors retain the copyright and grant the journal right of first publication with the work simultaneously licensed under a Creative Commons Attribution 4.0 International Public License (CC-BY-4.0) that allows others to share the work with an acknowledgment of the work's authorship and initial publication in Caryologia.
- Authors are able to enter into separate, additional contractual arrangements for the non-exclusive distribution of the journal's published version of the work (e.g., post it to an institutional repository or publish it in a book), with an acknowledgment of its initial publication in this journal.
- Authors are permitted and encouraged to post their work online (e.g., in institutional repositories or on their website) prior to and during the submission process, as it can lead to productive exchanges, as well as earlier and greater citation of published work (See The Effect of Open Access).

PUBLICATION FEES

Open access publishing is not without costs. *Caryologia* therefore levies an article-processing charge of € 150.00 for each article accepted for publication, plus VAT or local taxes where applicable.

We routinely waive charges for authors from low-income countries. For other countries, article-processing charge waivers or discounts are granted on a case-by-case basis to authors with insufficient funds. Authors can request a waiver or discount during the submission process.

PUBLICATION ETHICS

Responsibilities of *Caryologia*'s editors, reviewers, and authors concerning publication ethics and publication malpractice are described in *Caryologia*'s Guidelines on Publication Ethics.

CORRECTIONS AND RETRACTIONS

In accordance with the generally accepted standards of scholarly publishing, *Caryologia* does not alter articles after publication: "Articles that have been published should remain extant, exact and unaltered to the maximum extent possible".

In cases of serious errors or (suspected) misconduct *Caryologia* publishes corrections and retractions (expressions of concern).

Corrections

In cases of serious errors that affect or significantly impair the reader's understanding or evaluation of the article, *Caryologia* publishes a correction note that is linked to the published article. The published article will be left unchanged.

Retractions

In accordance with the "Retraction Guidelines" by the Committee on Publication Ethics (COPE) *Caryologia* will retract a published article if:

- there is clear evidence that the findings are unreliable, either as a result of misconduct (e.g. data fabrication) or honest error (e.g. miscalculation)
- the findings have previously been published elsewhere without proper crossreferencing, permission or justification (i.e. cases of redundant publication)
- it turns out to be an act of plagiarism
- it reports unethical research.

An article is retracted by publishing a retraction notice that is linked to or replaces the retracted article. *Caryologia* will make any effort to clearly identify a retracted article as such.

If an investigation is underway that might result in the retraction of an article *Caryologia* may choose to alert readers by publishing an expression of concern.

COMPLYNG WITH ETHICS OF EXPERIMENTATION

Please ensure that all research reported in submitted papers has been conducted in an ethical and responsible manner, and is in full compliance with all relevant codes of experimentation and legislation. All papers which report in vivo experiments or clinical trials on humans or animals must include a written statement in the Methods section. This should explain that all work was conducted with the formal approval of the local human subject or animal care committees (institutional and national), and that clinical trials have been registered as legislation requires. Authors who do not have formal ethics review committees should include a statement that their study follows the principles of the Declaration of Helsinki

ARCHIVING

Caryologia and Firenze University Press are experimenting a National legal deposition and long-term digital preservation service.

ARTICLE PROCESSING CHARGES

All articles published in *Caryologia* are open access and freely available online, immediately upon publication. This is made possible by an article-processing charge (APC) that covers the range of publishing services we provide. This includes provision of online tools for editors and authors, article production and hosting, liaison with abstracting and indexing services, and customer services. The APC, payable when your manuscript is editorially accepted and before publication, is charged to either you, or your funder, institution or employer.

Open access publishing is not without costs. *Caryologia* therefore levies an article-processing charge of € 150.00 for each article accepted for publication, plus VAT or local taxes where applicable.

FREQUENTLY-ASKED QUESTIONS (FAQ)

Who is responsible for making or arranging the payment?

As the corresponding author of the manuscript you are responsible for making or arranging the payment (for instance, via your institution) upon editorial acceptance of the manuscript.

At which stage is the amount I will need to pay fixed?

The APC payable for an article is agreed as part of the manuscript submission process. The agreed charge will not change, regardless of any change to the journal's APC.

When and how do I pay?

Upon editorial acceptance of an article, the corresponding author (you) will be notified that payment is due.

We advise prompt payment as we are unable to publish accepted articles until payment has been received. Payment can be made by Invoice. Payment is due within 30 days of the manuscript receiving editorial acceptance. Receipts are available on request.

No taxes are included in this charge. If you are resident in any European Union country you have to add Value-Added Tax (VAT) at the rate applicable in the respective country. Institutions that are not based in the EU and are paying your fee on your behalf can have the VAT charge recorded under the EU reverse charge method, this means VAT does not need to be added to the invoice. Such institutions are required to supply us with their VAT registration number. If you are resident in Japan you have to add Japanese Consumption Tax (JCT) at the rate set by the Japanese government.

Can charges be waived if I lack funds?

We consider individual waiver requests for articles in Caryologia on a case-by-case basis and they may be granted in cases of lack of funds. To apply for a waiver please request one during the submission process. A decision on the waiver will normally be made within two working days. Requests made during the review process or after acceptance will not be considered.

I am from a low-income country, do I have to pay an APC?

We will provide a waiver or discount if you are based in a country which is classified by the World Bank as a low-income or a lower-middle-income economy with a gross domestic product (GDP) of less than $200bn. Please request this waiver of discount during submission.

What funding sources are available?

Many funding agencies allow the use of grants to cover APCs. An increasing number of funders and agencies strongly encourage open access publication. For more detailed information and to learn about our support service for authors.

APC waivers for substantial critiques of articles published in OA journals

Where authors are submitting a manuscript that represents a substantial critique of an article previously published in the same fully open access journal, they may apply for a waiver of the article processing charge (APC).

In order to apply for an APC waiver on these grounds, please contact the journal editorial team at the point of submission. Requests will not be considered until a manuscript has been submitted, and will be awarded at the discretion of the editor. Contact details for the journal editorial offices may be found on the journal website.

What is your APC refund policy?

Firenze University Press will refund an article processing charge (APC) if an error on our part has resulted in a failure to publish an article under the open access terms selected by the authors. This may include the failure to make an article openly available on the journal platform, or publication of an article under a different Creative Commons licence from that selected by the author(s). A refund will only be offered if these errors have not been corrected within 30 days of publication.

2020
Vol. 73 – n. 1

Caryologia

International Journal of Cytology, Cytosystematics and Cytogenetics

Table of contents

€ 25,00